SOLAR CONCENTRATOR TECHNOLOGY DEVELOPMENT FOR SPACE BASED APPLICATIONS

ENGINEERING REPORT ER-1001
VOLUME II

FINAL REPORT

SOLAR CONCENTRATOR TECHNOLOGY DEVELOPMENT FOR SPACE BASED APPLICATIONS

ENGINEERING REPORT, ER-1001

Dr. A. Pintz
Principal Investigator
Cleveland State University
Advanced Manufacturing Center
Cleveland, Ohio 44114

Prepared by:
C.H. Castle, and R.R. Reimer

December 31, 1992

Project work performed under grant NCC 3-77
NASA Lewis Resesrch Center
Solar Dynamics and Thermal Systems Branch
J.E. Calogeras: Chief
Project Managers: Dr. J.M. Savino and T.S. Mroz

<u>Appendixes</u>

A. Selected Five Foot Diameter Concentrator Data

B. Selected Sunflower Concentrator Data

C. Selected 9.5 Foot Diameter Antenna Photographs

D. Two Panel Test Rig

E. Two Meter Concentrator Assembly Dwg. 9001250

F. Two Meter Concentrator Panel Dwg. 9001250-1

G. EN-1020 "Panel Fabrication Procedure"

H. EN-1022 "Slope Error Deviations of Panel No. 6"

I. EN-1001 "Fabrication of Stretch Forming Tool"

Volume 2. Final.....

Appendix A

NASA CR-66069
TRW ER-6819

STRETCH-FORMED ALUMINUM SOLAR CONCENTRATOR

Prepared under Contract No. NAS 1-4684 by
TRW Equipment Laboratories
TRW INC.
Cleveland, Ohio

for

NATIONAL AERONAUTICS AND SPACE ADMINISTRATION

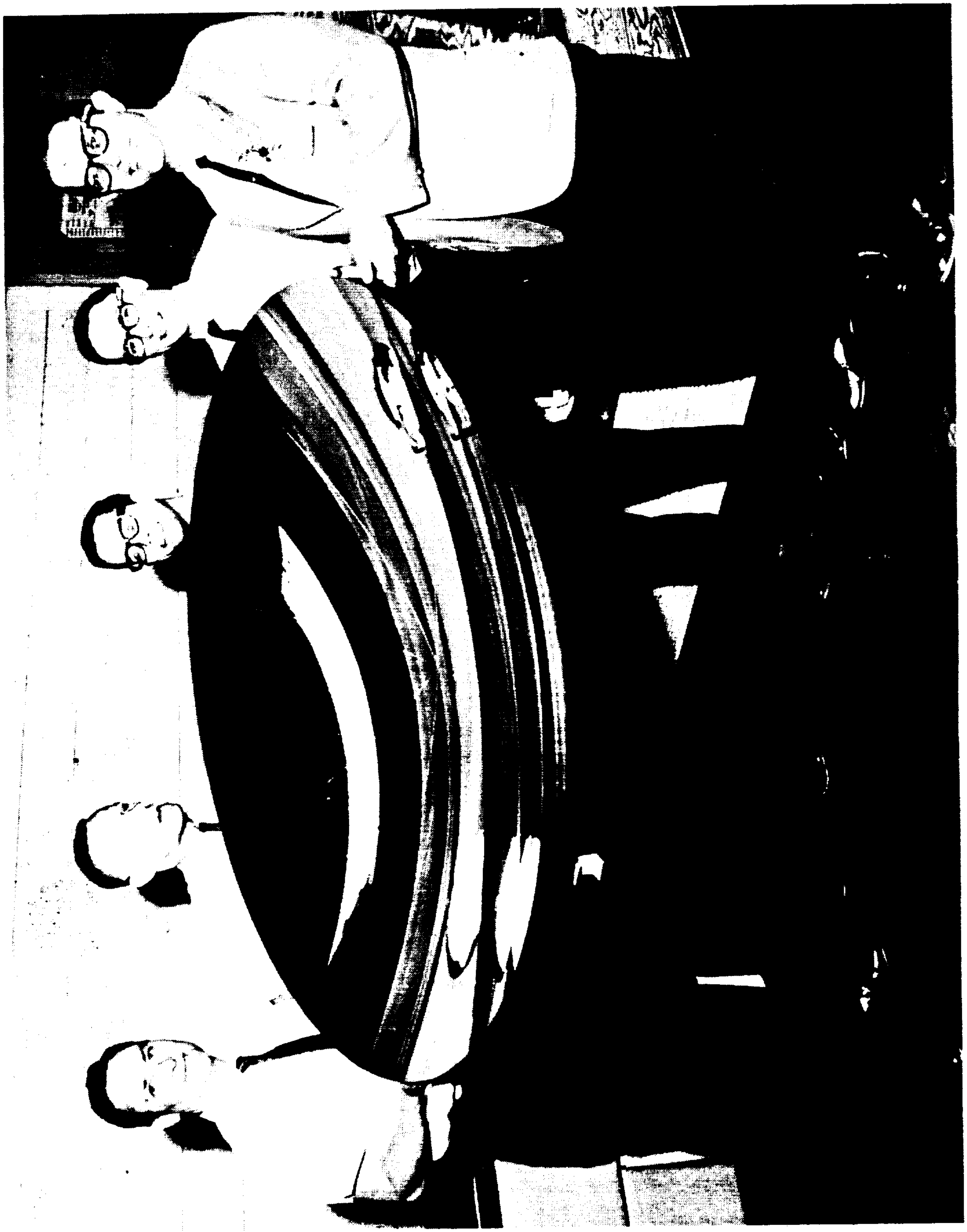

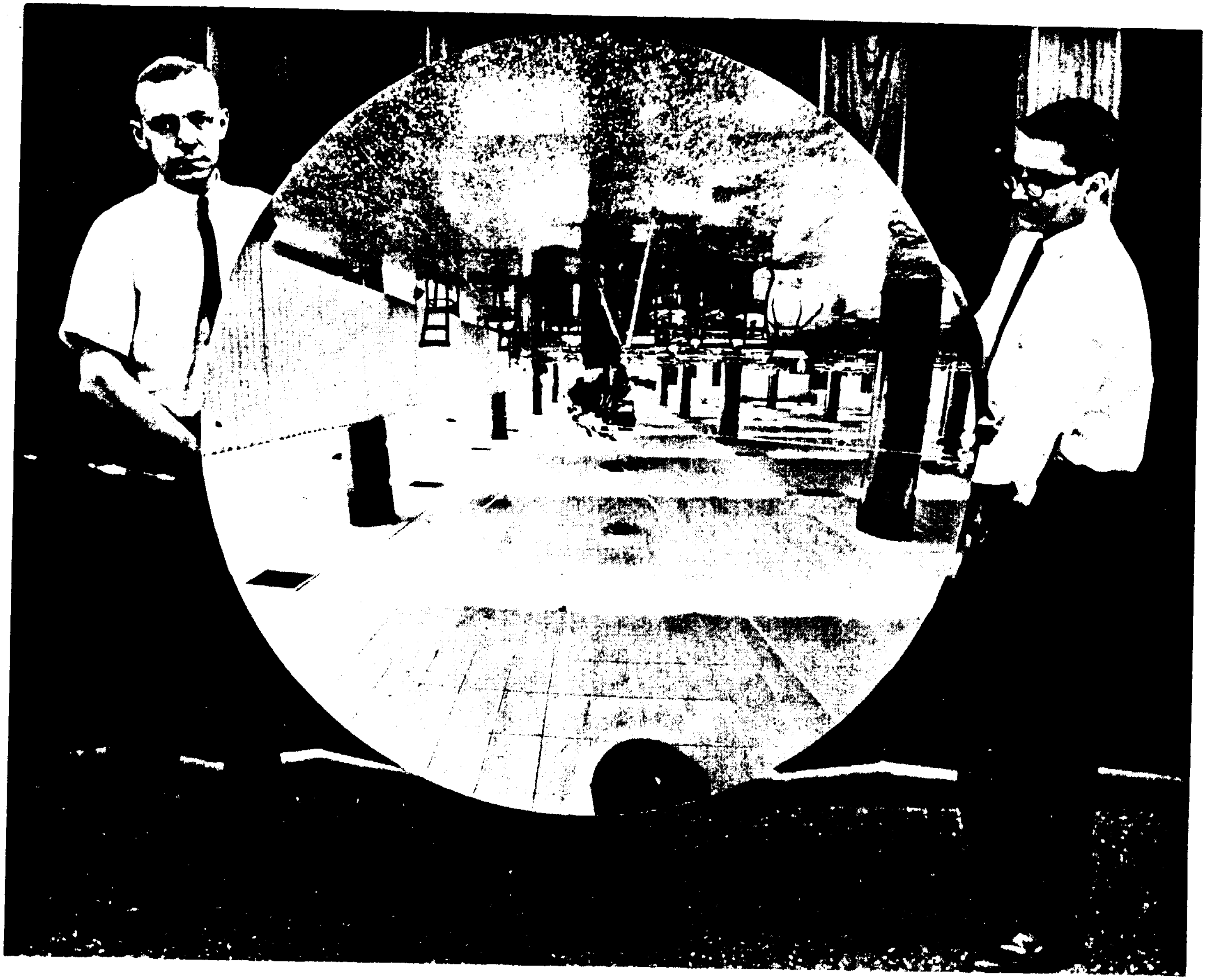

60 INCH DIAMETER SOLAR CONCENTRATOR

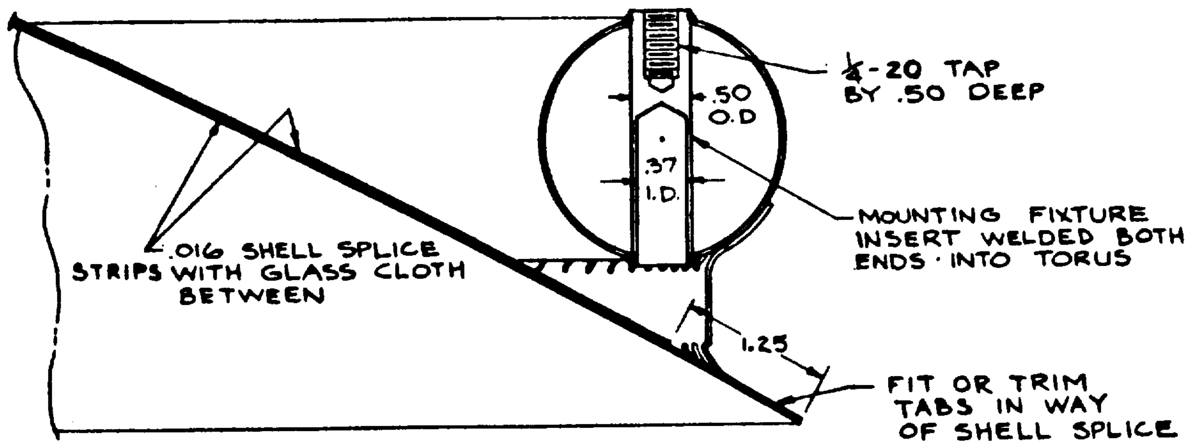

SECTION B-B
THROUGH SPLICE & MOUNTING FIXTURE

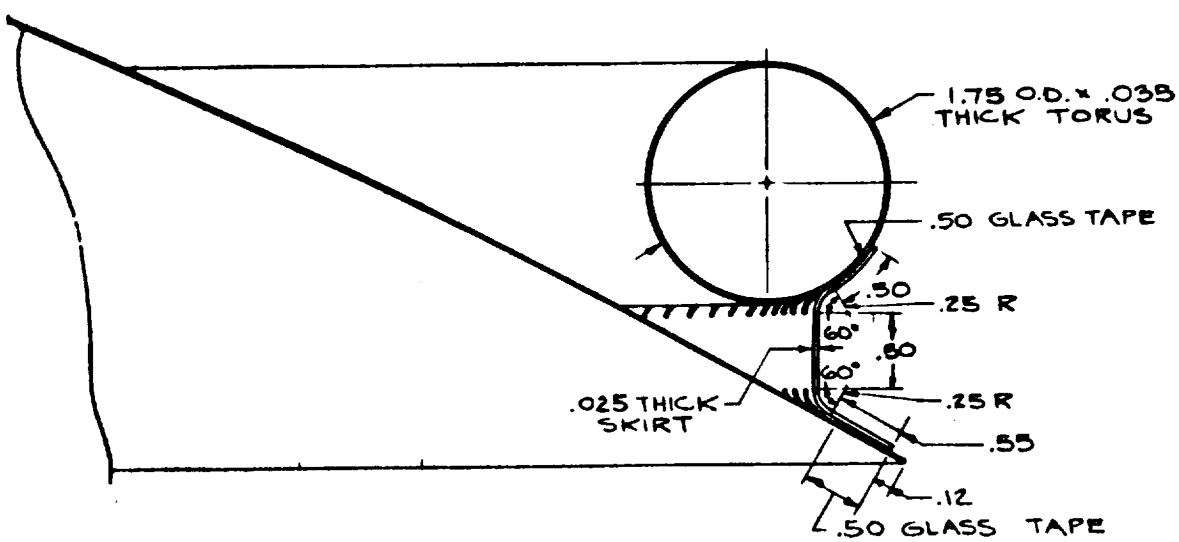

SECTION C-C
THROUGH CONCENTRATOR SHELL

FINAL CONCENTRATOR DESIGN

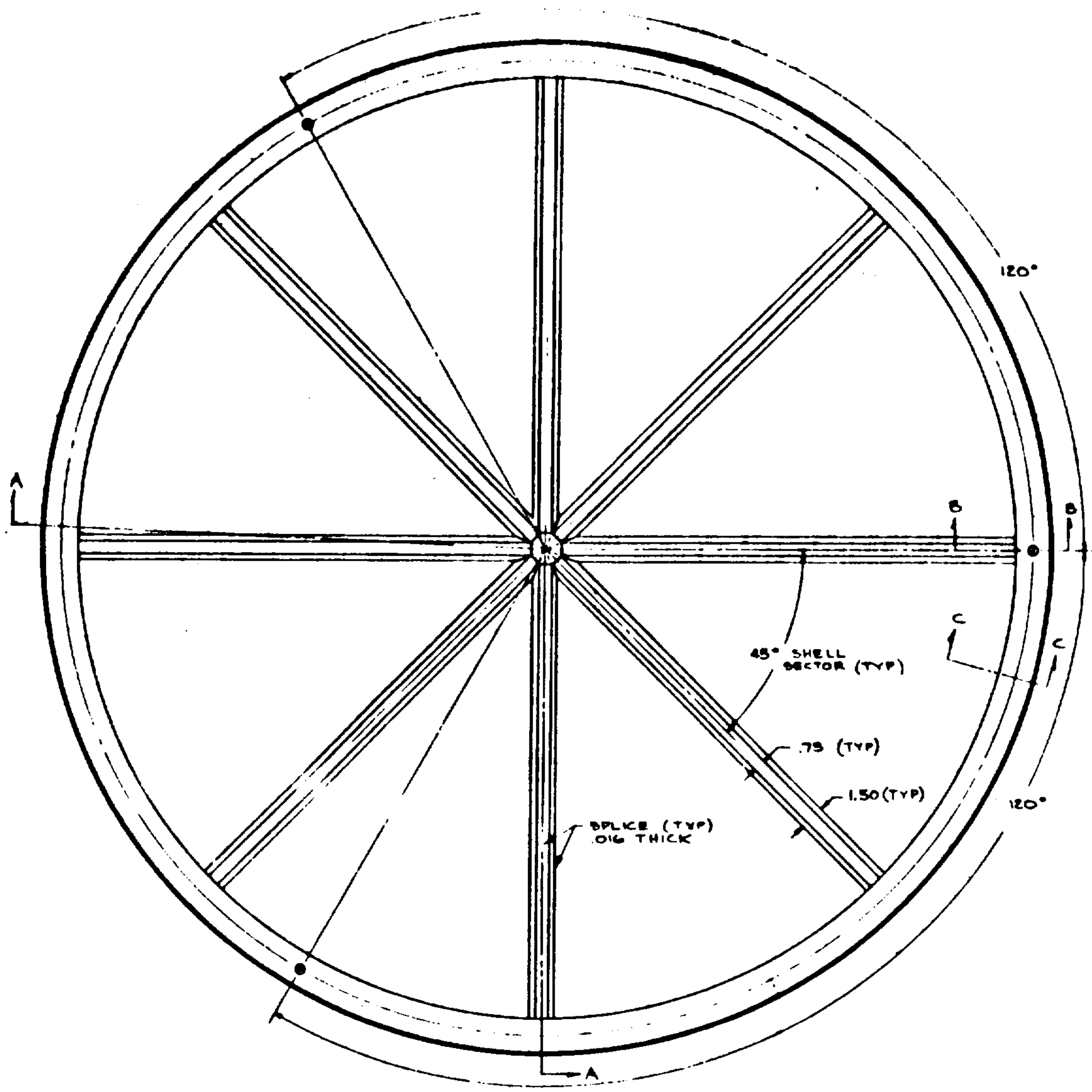
A
B
B
C
C
120°
120°
45° SHELL SECTOR (TYP)
.75 (TYP)
1.50 (TYP)
SPLICE (TYP) .016 THICK
A

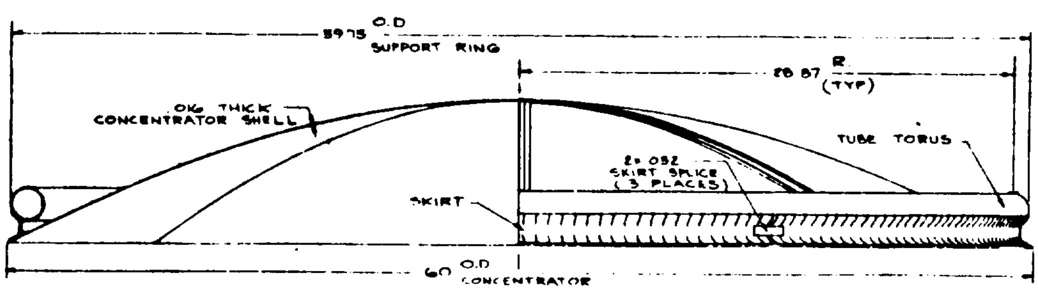
59.75 O.D SUPPORT RING
28.87 R (TYP)
.016 THICK CONCENTRATOR SHELL
TUBE TORUS
SKIRT
SKIRT SPLICE (3 PLACES)
60 O.D CONCENTRATOR

VIEW A A

CONCENTRATOR OPTICAL QUALITY

The optical quality of a solar reflector can be represented by the geometric accuracy of the general surface with respect to a paraboloid and by the solar reflectivity. The 60-inch diameter solar concentrator which was fabricated under this contract is shown in figure 24, and the measured optical quality of this reflector will now be presented.

Geometric Quality

As discussed previously, the geometric quality of the reflector is obtained from the full size inspection photographs shown at reduced scale in figure 23. The mismatch of the grid patterns determines the surface error deviations while the completely white areas along the radial joints indicates surface area which may be optically lost - especially for high concentration ratio requirements. The majority of the white area at the outer diameter is due to the oversize photographic paper. The outer diameter edge distortion can be seen as the waviness around the exposure diameter.

Standard deviation of surface slope errors. -The mismatch data at discrete points on the inspection photographs were tabulated for the radial and circumferential errors. Although a cartesian grid is most apparent in figure 23, the fine radial reference lines were used to establish the center of the reflector, and the radial and circumferential components of error were read directly by pivoting a reference scale from this center.

Histograms for both directions are shown in figures 25 and 26, and as observed with previous solar concentrators, the normal distribution characteristic is apparent. The statistically determined mean values and standard deviations are tabulated below and compared with the values which were achieved on previously fabricated stretch-formed solar reflectors.

Concentrator Description	Radial Mean	Radial Std. Dev.	Circumferential Mean	Circumferential Std. Dev.	Reference
TRW S/N 2	3.7'	8.2'	-3.6'	11.0'	Ref. 6
TRW S/N 4	0.81'	2.86'	0.40'	3.77'	Ref. 7
Present	-0.45'	1.59'	0.50'	2.08'	Figure 23

The mean or average values may indicate that the reference system for measuring errors did not correspond to the best optical fit paraboloid. However, it is seen that these mean values are small and therefore they have a small effect upon the computed standard deviations.

Edge distortions. -The range of edge distortions in the free trimmed edges of the final hardware sectors was presented previously (figure 8). The degree to which this distortion was restrained by the radial splices can be seen in figure 23 by observing the white areas along the radial joints. From the full

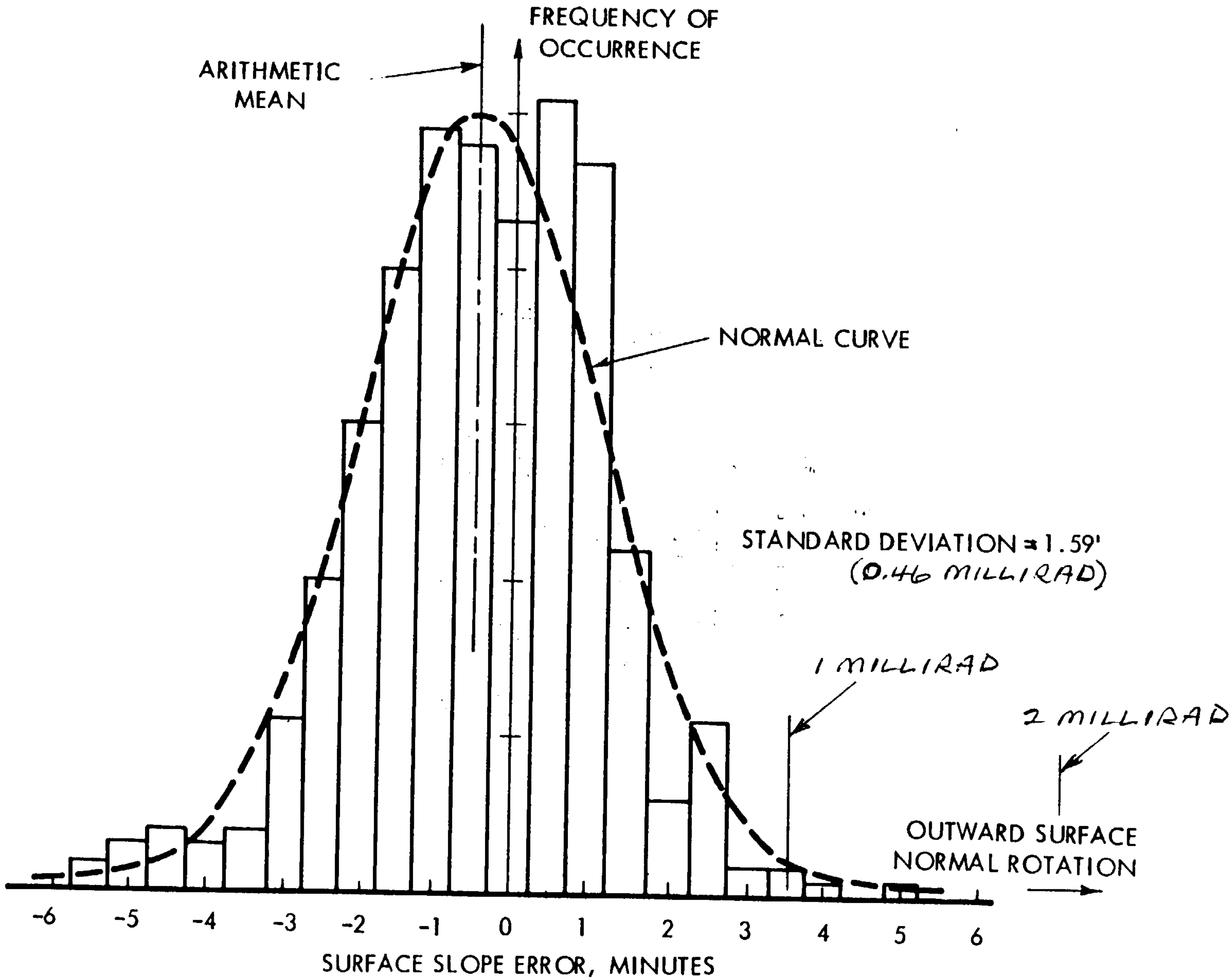

RADIAL ERROR FREQUENCY DISTRIBUTION

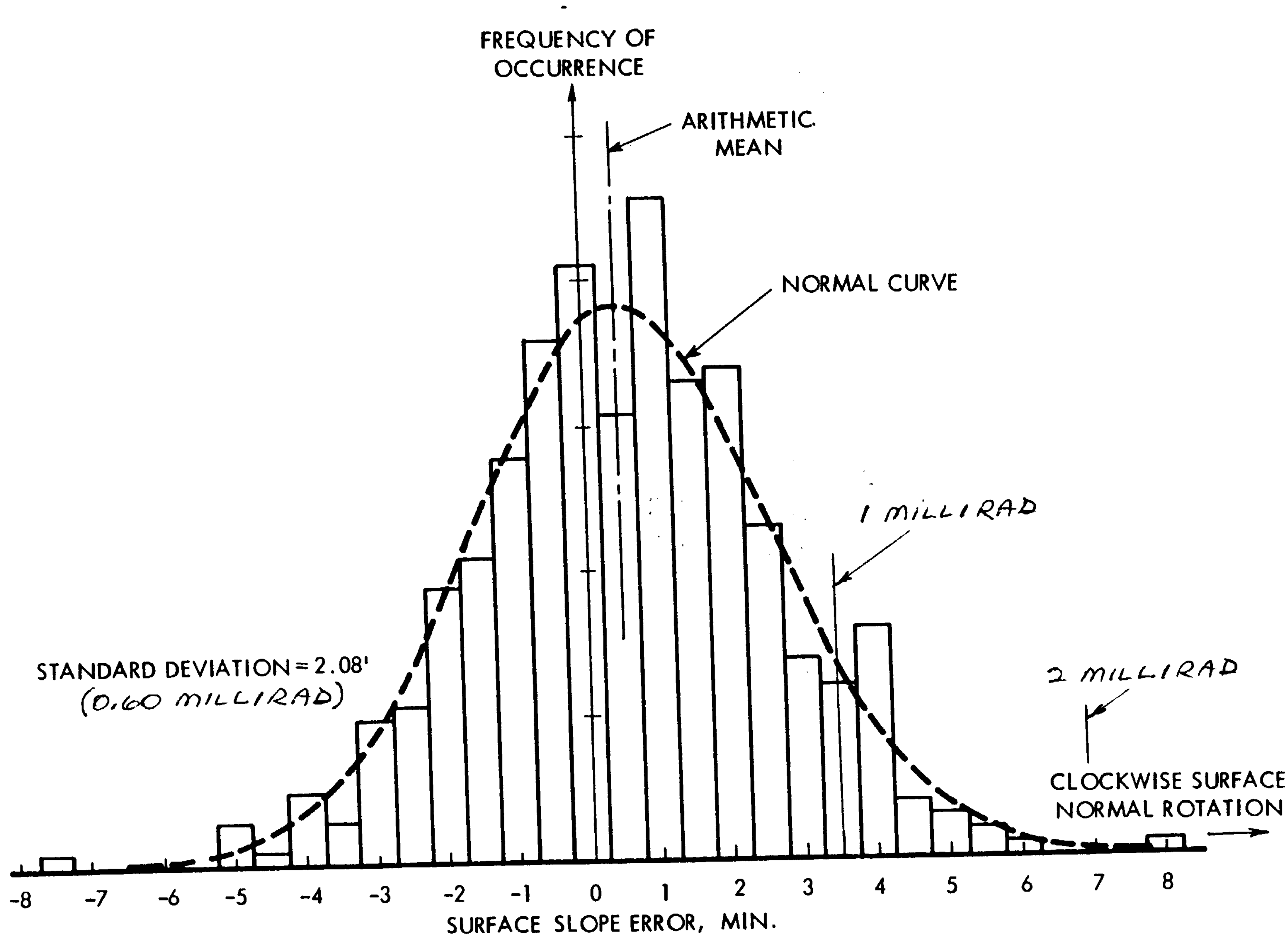

CIRCUMFERENTIAL ERROR FREQUENCY DISTRIBUTION

REVIEW OF SOLAR CONCENTRATOR TECHNOLOGY

By Atwood R. Heath, Jr., and Edward L. Hoffman

NASA Langley Research Center
Langley Station, Hampton, Va.

Presented at the Intersociety Energy Conversion
Engineering Conference

Los Angeles, California
September 26-28, 1966

REVIEW OF SOLAR CONCENTRATOR TECHNOLOGY

By Atwood R. Heath, Jr., and Edward L. Hoffman
Aerospace Engineers
NASA Langley Research Center
Langley Station, Hampton, Va.

Abstract

Continuing development of solar concentrator technology has been directed toward the improvement of methods and materials of construction to satisfy the particular design requirements of various space power conversion devices. Descriptions of fabrication techniques as well as a brief discussion of recent results from investigations made on concentrators are presented. In the area of one-piece concentrators, the stretch-formed aluminum process has been developed to the point where concentrator accuracy compares favorably with the high quality formerly obtained only by electroforming nickel. The aluminum electroforming process has been scaled up to the point where 0.76-meter-diameter concentrators have been fabricated. Two accurate 2.90-meter-diameter plastic spin castings have been fabricated, however, the concentrators subsequently electroformed of nickel were not of comparable quality. In the area of expandable concentrators, a modified model of the whirling membrane concept has given improved concentration of energy, however, the design parabolic cross section has not been attained. A 1.52-meter-diameter inflatable concentrator has been rigidized with a polyurethane foam in a simulated space environment. The concentrator gave an efficiency within 0.20 of a Rankine cycle design efficiency of 0.85.

Introduction

In the past solar energy concentrators or models of concentrators have been fabricated that are capable of generating the temperatures required for the operation of space power systems. Continuing development of solar concentrator technology has been aimed at improving the methods and materials of construction to satisfy the particular design requirements of various conversion devices. Thermionic devices with their high operating temperatures require concentrator surface accuracies that at present can only be met by the one-piece designs. Development of one-piece concentrators is continuing in order to (1) improve construction methods by the use of lightweight nonmagnetic materials, and (2) adapt present construction methods to larger diameter concentrators. Dynamic conversion devices with their lower operating temperatures and higher power levels can utilize less accurate, large diameter, expandable concentrators. Development in this area is continuing in order to improve surface accuracy (increased efficiency) as well as construction methods so that size, mass, and packaging volume may be reduced.

The status of solar energy concentrator technology was reported in 1964 at the AIAA Space Power Systems Conference.[1] Since then a continuing program has been supported by NASA to develop the technology of solar concentrators by both in-house and contractual research and development. Some recent results from investigations made on concentrators by the Lewis Research Center, the Jet Propulsion Laboratory, and the Langley Research Center are presented in this paper.

One-Piece Concentrators

Development of one-piece concentrator technology has been directed in general towards the fabrication of small (1.5 meters or less in diameter) highly accurate paraboloids suitable for thermionic conversion systems. An effort has also been directed towards the development of paraboloidal masters to be used in the fabrication of larger one-piece concentrators with surface geometries of comparable quality. In addition, work has continued on large (6.10 to 9.14 m) diameter concentrators with lower accuracies for dynamic systems. A discussion of the various fabrication techniques with the results of investigations made on several concentrators fabricated by these techniques follows.

Stretch-Formed Aluminum Concentrators

The stretch-formed aluminum approach to solar concentrator fabrication has been investigated and three 1.52-meter-diameter concentrators representing various stages in the development have been made[2,3,4] under contract. Figure 1 shows a sketch of the third model which consists of a shell made up of eight stretch-formed aluminum sectors bonded together and attached to a rear-mounted torus by a cylindrical transition strip. The design of the first two models differed from the third only in the shape and attaching scheme of the torus. The 0.4-mm-thick aluminum sectors were stretch-formed over a 1.52-meter-diameter glass searchlight mirror, given an epoxy plastic surface coating to cover the grainy surface resulting from the forming and then aluminized before assembly.

All three models have been solar tested at the Langley Research Center and the results of the calorimeter measurements are shown in figure 2. The calorimetric efficiency is defined as the ratio of the energy reflected from a concentrator and collected by a cavity-type cold calorimeter to the energy incident on the concentrator as measured by a pyrheliometer. Concentration ratio also known as area ratio is the ratio of the net projected reflective area of the concentrator to the area of the aperture of the cavity calorimeter. The data are identified by the numerals I, II, and III to indicate in which phase of the program each concentrator was built. Also shown is a theoretical maximum efficiency curve for a perfect concentrator with a solar specular reflectance of 0.91.

At concentration ratios above 5,000, a definite improvement in efficiency has been obtained with each suceeding phase of the program. For example, at a concentration ratio of about 14,000, which corresponds to that needed for thermionic operation, the efficiency has been increased from 0.42 to 0.80. The value of 0.80 is only about 0.07 below the curve for a theoretically perfect concentrator with a reflectance of 0.91. At the lower concentration ratios (below 1,000) the curves tend to reach a limiting value of efficiency. This value of efficiency is usually assumed to be the value of solar specular reflectance for the concentrator surface.

For concentrator III, a high value of reflectance of 0.91 is obtained which is 0.02 higher than the value of 0.89 measured with a spectrophotometer[4] on flat samples cut from trimmed portions of the stretched and coated panels. Spectrophotometer measurements on the flat samples at LRC verified the value of 0.89 so that it may be assumed that the calorimetric measurements are about 0.02 high possibly due to experimental error. It is also noted that a different reflectance was obtained for each model. Part of these differences may be attributed to the different coatings on each model (concentrators I and II had silicon oxide coatings over the vacuum deposited aluminum while concentrator III had aluminum only) and part may be due to the ability of the epoxy surface improvement coating to provide a specular surface.

To provide an indication of the improvements that have been made in the geometric accuracy, the efficiency data curves of figure 2 have been divided by their respective values of specular reflectance to give geometric efficiency which is shown in figure 3 as a function of concentration ratio. A definite gain has been made in geometric efficiency with each succeeding concentrator. These gains have been substantiated by optical measurements[4] which show that the standard deviation of error in the radial direction of the mirror surface has been reduced from 0.137° for I to 0.048° for II and to 0.017° for III. The value of geometric efficiency of 0.88 at a concentration ratio of 14,000 approaches closely the geometric efficiencies obtained on high quality solar concentrators fabricated by the nickel electroforming process.[1]

Electroformed Aluminum Concentrators

The fabrication of solar concentrators by the method of electroforming has been shown to give highly accurate, specular surfaces especially when nickel is used as the electroforming material. As a consequence, the electroforming of aluminum has been investigated as a possible method for forming lightweight nonmagnetic concentrators.[5] Several 0.76-meter-diameter concentrators have been electroformed from a solution of aluminum chloride, lithium aluminum hydride, and ether using the cell arrangement shown in figure 4.

The cell consists of two tanks; a bath mixing tank and a plating tank. Glove boxes are included on top of the tanks to allow access to the tanks which must be operated under a nitrogen atmosphere to prevent explosions. The operation of the electroforming cell generally followed this procedure. The mixing tank was purged with argon and ether was then transferred to the tank. Aluminum chloride was then added in small increments with the mixer running constantly. Continuous cooling of the solution was necessary to control the exothermic reaction. The lithium aluminum hydride was added next and the solution was filtered. In the meantime the conforming aluminum anode was installed in the plating tank and the tank purged with argon. The ether solution was then transferred to the plating tank, the convex nickel master was lowered into the tank and the plating was started. A paraboloidal shell was then electroformed to a thickness of 0.5 mm. The resulting deposits were a soft aluminum with a modulus of about 55 GN/m² (8 x 10⁶ psi) and a tensile strength of about 76 MN/m² (11,000 psi). Three concentrators were fabricated and all have been solar tested.

The results of the tests are shown by a typical efficiency curve in figure 5. The efficiency and concentration ratio are the same as defined previously for figure 2 and an efficiency curve for a perfect concentrator with a reflectance of 0.91 is included for comparison. At the concentration ratios of interest for thermionic conversion (above 10,000), the concentrator has an efficiency of only about 0.50 instead of a value near 0.85 to 0.90 which might be obtained on a more accurate paraboloid. The decrease in efficiency with increasing concentration ratio is the result of inaccuracies in the concentrator which are attributable to two facts. First, the master used for this concentrator was of rather poor geometry. Second, minute pinholes in the master, which normally are bridged over during electroforming with aqueous solutions, were penetrated by the ether solution so that aluminum was deposited in the microscopically small holes. When the concentrator was separated from the master small holes were torn out of the mirror (where the aluminum was keyed into the master) and the surface was deformed around each hole.

These small holes and their associated deformed areas as well as a slightly nonspecular appearance of the reflecting surface due to poor coatings are considered to be responsible for the low value of specular reflectance (0.77 at a concentration ratio of about 300). Because of the high throwing power or ability to penetrate small holes, the electrodeposition of aluminum from ether solutions should give more exact replications than electrodeposition from aqueous solutions when suitable masters are used.

Large Masters

Much of the development done on relatively accurate one-piece concentrators suitable for thermionic conversion systems utilized 1.52-meter-diameter glass searchlight mirrors as masters. Larger concentrators are now desired and several proposals for fabricating the masters have been advanced. One method being investigated uses the spin casting process to produce a concave paraboloidal surface. Three separate operations required in the process are as follows: (1) spin casting with a concave surface, (2) master with a convex surface, and (3) solar concentrator with a concave surface. Under NASA contracts, two spin castings have been fabricated and used to produce two solar concentrators 2.90 meters in diameter.[6] For the spin castings, epoxy resins were filled with an inert material to reduce shrinkage and then rotated at constant speed until the resins hardened. The two convex masters were formed by electroforming nickel on the spin castings and the concentrators were then formed by electroforming nickel on the masters.

Both concentrators have been solar tested and the results are shown in figure 6 which has calorimetric efficiency plotted as a function of concentration ratio. The theoretical maximum efficiency circumferential wrinkles has been accomplished. For the original model, the dispersion of energy in the circumferential direction, figure 10(b), was apparently caused by deviations in the circular shape of the membrane similar to those in a parachute.[1] A slight increase in the image width is noted for the modified model which is not considered to be significant in terms of concentrating ability of the concentrator. A definite improvement in the concentrating ability of the whirling membrane has been achieved by the cable modifications, although, the desired parabolic cross section has not been attained.

Inflatable-Rigidized Concentrators

A review of inflatable-rigidized technology has recently been made[9] which included information on concentrators rigidized in a simulated space environment as well as concentrators rigidized in an earth atmosphere environment. In the present paper, the discussion will be restricted to concentrators that have been rigidized in a vacuum chamber to simulate space environment and for which quantitative data on their concentrating ability exist. A sketch of one type is shown in figure 11. A plastic paraboloidal membrane, aluminized on the concave side, forms one section of a lenticular body. A disposable plastic membrane forms the front of the body, and an inflatable torus, used to maintain the correct diameter, is attached at the disposable membrane-paraboloid juncture. Once in space, the body would be inflated, the paraboloidal portion would be rigidized by such methods as indicated in figure 11, and the plastic membrane discarded. Three rigidizing methods have been proposed and development of these methods into reliable rigidizing processes suitable for space application has been studied. All three processes have one thing in common; i.e., the rigidizing material while still in a plastic state is applied to the membrane before packaging. Two methods utilize the foam approach shown in figure 11. One is an epoxy syntactic foam which is formed by adding small hollow phenolic spheres to an epoxy resin.[10] Rigidization occurs upon heating the foam to about 365° K for 24 hours. The second is an azide base polyurethane foam formulation,[11] and foaming occurs upon heating the formulation to a temperature between 350° to 365° K. This process takes only about 30 minutes. The third process also shown in figure 11 utilizes a reinforced laminate of fiber-glass and polyester resin[10] attached to the reflective membrane with a flexible layer of polysulphide to prevent show-through of the fiber-glass fabric weave. Ultraviolet radiation acts as a catalyst to the resin and complete rigidization occurs after an exposure of approximately 16 hours.

Demonstration models, each 1.52 meters in diameter, have been fabricated in vacuum chambers utilizing the three rigidizing processes[10,12] and the results of solar tests of the models are shown in figure 12. The calorimetric efficiency and concentration ratio have been defined previously for figure 2. A solar concentrator design point for a Rankine cycle power system is indicated on the figure to show a typical requirement for this type of concentrator. The polyurethane foam model has the highest efficiency which is about 0.20 below the Rankine cycle design point but is about 50 percent higher than the efficiency measured on the epoxy syntactic foam and polyester fiber-glass models. The difference in concentrating ability that exists between the polyurethane foam model and the other two models cannot be wholly attributed to the rigidizing process as varying degrees of surface irregularities or "orange peel" were noted on all models. Another possible source contributing to the difference in concentrating ability may be the construction methods used in forming the paraboloids. The polyurethane foam model had a reflective parabol… constructed of gores built up on a convex master while the two other models consisted of flat reflective membranes shaped into paraboloids by the stretch-relaxation process.[10] Briefly this process consists of inflating the flat membranes to the shape of an oblate ellipsoid followed by the relaxation of the inflation pressure until the desired paraboloid is obtained. A direct comparison of the effect of the two construction methods on the membrane contour has not as yet been evaluated. However, both the epoxy syntactic foam and polyester fiber-glass models used the same construction methods and the performance of these two models essentially equal; it is probable therefore that construction methods rather than the rigidizing processes are the major source contributing to the difference in efficiencies. The encouraging fact should be noted that an inflatable concentrator … been rigidized in a simulated space environment is within 0.20 of the Rankine cycle design point. Prior to obtaining these data, only concentrators that had been rigidized at atmospheric pressure … efficiencies approaching the design requirements … the Rankine conversion devices.

Concluding Remarks

In summary, a description of the various sol… energy concentrator technology projects under NA… sponsorship has been given. Investigations have been made on several of the concentrators and so… results are indicated.

In the area of one-piece concentrators, the stretch-formed aluminum process has been develop… to the point where concentrator accuracy approac… closely the high quality formerly obtained only … electroforming nickel. The aluminum electrofor… process has been scaled up to the point where 0.76-meter-diameter concentrators have been fabr… cated. The process appears promising for very … replication when suitable masters are used. Two accurate 2.90-meter-diameter spin castings have … fabricated, however, the solar concentrators sub… quently electroformed of nickel were not of comp… ble quality. The loss in accuracy has been attr… uted to problems associated with replication of … convex master that forms the intermediate step between the spin casting and the concentrator.

In the area of expandable concentrators, a modified model of the whirling membrane concept … improved concentrating ability because of a redu… tion in circumferential wrinkles. However, the desired parabolic cross section has not been attained. A 1.52-meter-diameter inflatable concentrator has been rigidized with a polyurethane foam in a simulated space environment. The concentrator gave an efficiency within 0.20 of a Rankine cycle design efficiency of 0.85.

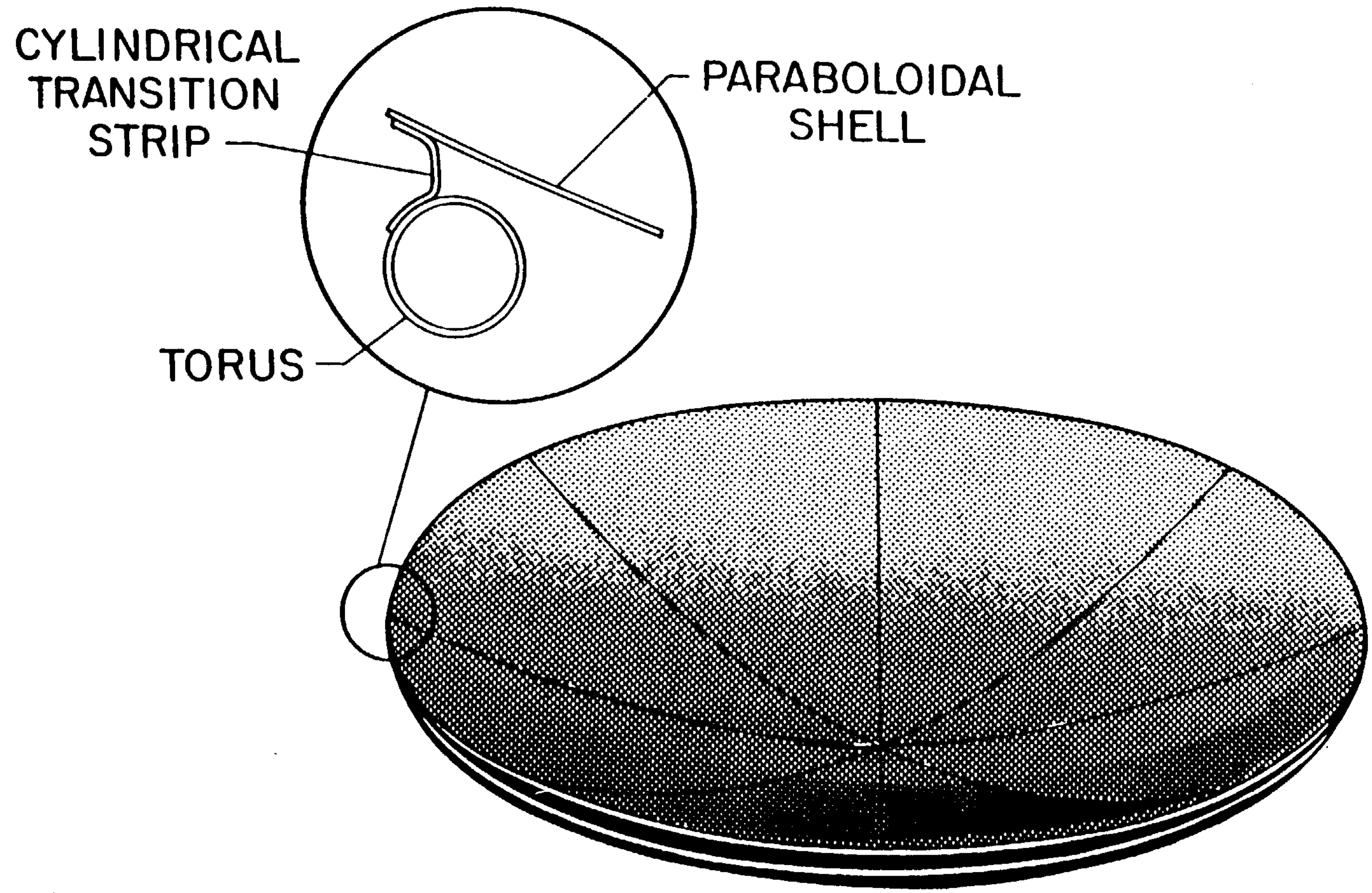

Stretch-formed aluminum solar concentrator 1.52-meter diameter.

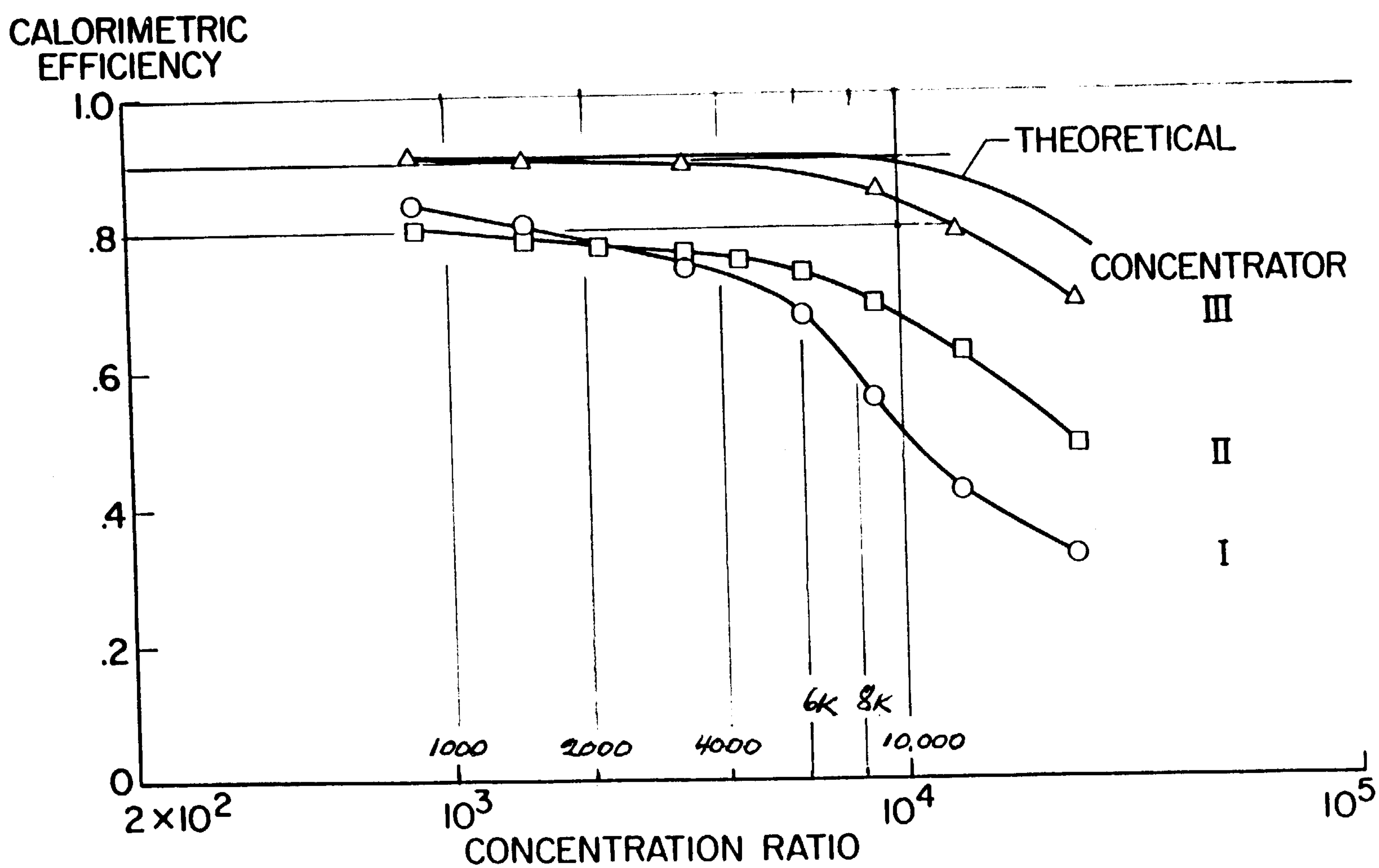

Calorimetric efficiency of 1.52-meter-diameter stretch-formed aluminum concentrators.

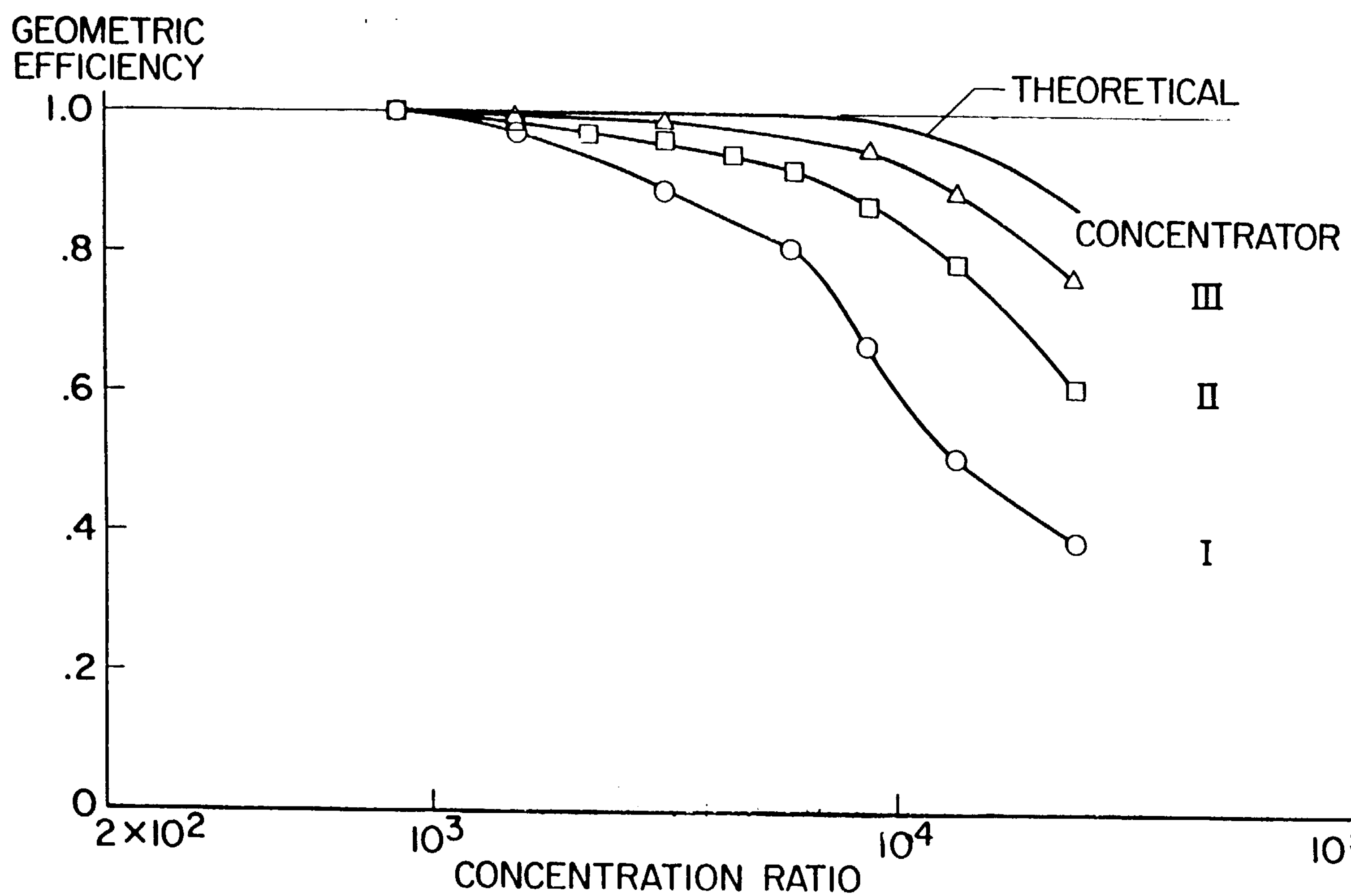

Geometric efficiency of 1.52-meter-diameter stretch-formed aluminum concentrators.

A-16

NASA TECHNICAL NOTE **NASA TN D-4889**

NASA TN D-4889

CALORIMETRIC, OPTICAL, AND VIBRATION INVESTIGATIONS OF STRETCH-FORMED ALUMINUM SOLAR CONCENTRATORS

by Marvin D. Rhodes and Conrad M. Willis

Langley Research Center
Langley Station, Hampton, Va.

NATIONAL AERONAUTICS AND SPACE ADMINISTRATION • WASHINGTON, D. C. • NOVEMBER 1968

CALORIMETRIC, OPTICAL, AND VIBRATION INVESTIGATIONS OF STRETCH-FORMED ALUMINUM SOLAR CONCENTRATORS

By Marvin D. Rhodes and Conrad M. Willis
Langley Research Center

SUMMARY

Three stretch-formed aluminum solar concentrators were evaluated in this investigation. The models represent three phases of a research and development program and all were 1.52-m-diameter paraboloids with a nominal rim angle of $\pi/3$ rad. Calorimetric tests were made on each model to determine the improvement in model performance caused by changes in model design and fabrication. Model 3 was superior to the other models in both geometrical accuracy and specular reflectance and is considered suitable for thermionic applications.

Optical-ray-trace tests were performed on models 1 and 2 to determine the magnitude and location of surface slope errors. The largest slope errors occurred near the gore seams but the region of high error was only about 8 percent of the total area. Ray-trace data were also used to calculate geometric efficiency by three methods. Only the random error method gave reasonable results for both models.

Vibration tests on model 1 caused failure in the welds of the rim support ring structure but subsequent calorimetric tests revealed little or no reduction in concentrator efficiency.

INTRODUCTION

Studies of space power systems have indicated that solar thermionic systems are resistant to radiation damage and are capable of operating in a high-temperature environment (ref. 1). Since the thermionic convertor requires temperatures of about 2000° K (ref. 2) for efficient operation, the solar concentrator must have good geometrical accuracy and high specular reflectance. Concentrators which are capable of achieving this goal have been fabricated of electroformed nickel (ref. 3) and investigations of one of these concentrators are reported in references 4 and 5. Nickel concentrators, however, may interfere with magnetically sensitive instruments, such as the magnetometers, used on some spacecraft.

In an effort to circumvent the problem of magnetic interference, other materials have been investigated for the fabrication of solar concentrators. Aluminum is one such material, and in addition to its nonmagnetic property it also makes possible the use of a considerably thinner shell (ref. 6) than is required with nickel. Since aluminum is less dense than nickel the concentrator will also have a lower mass. One of the fabrication techniques that appeared practical for obtaining aluminum concentrators was to form them by stretching flat sheets over a paraboloidal die. Therefore, a three-phase stretch-forming development program (refs. 6, 7, and 8) was conducted to determine the feasibility of fabricating efficient stretch-formed solar concentrators. At least one model was constructed during each phase and a preliminary evaluation made to indicate the areas of possible improvement before starting the next phase. The object of the present study was to investigate three 1.52-m-diameter paraboloidal stretch-formed solar concentrators and to evaluate their possible use with thermionic convertors. Each model represents one phase of the development program and the third phase model is considered representative of the state of the art for this type concentrator.

The investigation reported herein consists of calorimetric tests of all models, optical tests on two models, and vibration tests on one model. The calorimetric tests were performed in sunlight using a water-cooled-cavity calorimeter with aperture diameters ranging from 1.56 to 8.34 solar-image diameters. The optical tests consisted of directing a collimated beam of light parallel to the optical axis and intercepting the reflected beam with a focal-plane image plate. The image displacements from the optical axis were used to calculate the deviation of concentrator slope from that of a perfect paraboloid. The optical data were also used to calculate approximate concentrator efficiency. Vibration tests were made on one of the models to determine its resonant frequencies and its ability to withstand loads simulating a launch vibration environment. Calorimetric tests were repeated after vibration tests to determine any change in concentrator efficiency.

SYMBOLS

The units used for the physical quantities defined in this paper are given in the International System of Units (SI). Factors relating this system to U.S. Customary Units are presented in reference 9.

f nominal design focal length, centimeters

f_a distance from concentrator vertex plane to calorimeter aperture or from vertex plane to ray-trace image plate, centimeters (see fig. 9)

g	acceleration of gravity, 9.82 meters per second^2
h	distance from point on concentrator surface to plane of image plate, $f_a - \frac{r^2}{4f_a}$, centimeters (see fig. 9)
i,j,k	axes for rectangular Cartesian coordinates; origin is on surface of design paraboloid, k-axis lies along paraboloid normal, and j-axis intersects optical axis (see fig. 9)
R_a	radius of calorimeter aperture, centimeters
R_i	calculated radius of solar image formed at focus by cone of rays reflected from paraboloid vertex, $f \tan \alpha$, centimeters
R_s	radius of solar concentrator, centimeters
r	test radius, distance from concentrator axis to collimated light, centimeters
S_p	projected area of solar concentrator, πR_s^2, centimeters^2
S_t	partial area assigned to a set of test data, centimeters^2
S_u	unobscured concentrator area, S_p minus Projected area that is shaded by calorimeter and its supports, centimeters^2
ΔT	temperature increase of water flowing through calorimeter, K^o
w	mass-flow rate of calorimeter water, kilograms per second
x,y,z	rectangular Cartesian coordinates with system origin at focal point, z is measured along concentrator axis, centimeters (see fig. 9)
α	half-angle subtended by sun, 4.6 milliradians
β	misorientation angle, angle between concentrator axis and solar rays, milliradians
γ	measured solar irradiance on unit area normal to rays, watts per meter^2

δ_c — circumferential error in slope of reflective surface, angle between paraboloid normal and projection of concentrator normal on ik plane (fig. 9(b)), milliradians

δ_r — radial error in slope of reflective surface, angle between paraboloid normal and projection of concentrator normal on jk plane (fig. 9(b)), milliradians

$\bar{\delta}_c, \bar{\delta}_r$ — mean value of slope error, milliradians

η — calorimetric efficiency, ratio of energy absorbed by calorimeter water to energy incident on concentrator, $\frac{4.183 \times 10^7 \, w \, \Delta T}{\gamma S_u}$

η_g — geometric efficiency calculated from ray-trace data, ratio of energy entering a given size focal-plane aperture to energy specularly reflected from concentrator

$\eta_{g,m}$ — geometric efficiency measured by calorimetric tests, η/ρ

ρ — specular reflectance of concentrator surface

σ — standard deviation of circumferential or radial component of slope error from mean error, $\left[\frac{\sum \delta^2 - \frac{1}{N}\left(\sum \delta\right)^2}{N - 1}\right]^{1/2}$ where δ represents either δ_c or δ_r and N is number of data points

ϕ — azimuth angle, measured in plane normal to concentrator axis and used to locate points on concentrator, radians (see fig. 9)

MODELS

Three stretch-formed aluminum paraboloidal solar concentrators were investigated. The models were about 1.52 m in diameter with a nominal rim angle of $\pi/3$ rad. Sketches of each model are presented as figure 1 and photographs of model 2 are shown as figure 2. The concentrator shells were formed by stretching sheets of aluminum alloy over a paraboloidal male die. After stretch-forming, the aluminum sheets received a surface improvement coating of thinned epoxy, a buffer coating of silicon oxide, and a reflective coating of vacuum-deposited aluminum. Two $\pi/4$-rad sectors were then cut from each stretched sheet and eight sectors were assembled on the die now used as a jig. The sectors were joined by overlap strips cut from stretched stock and bonded to the back surface. The concentrator was vacuum bagged to hold it against the die until the epoxy bonds had cured. A rim support ring containing three mounting brackets was bonded to the back surface of the concentrator before removing it from the die. The master die, which was an accurate glass searchlight mirror, was used directly in fabricating models 2 and 3 and an epoxy replica of the master die was used for model 1.

Model 1

The shell material for model 1 was 0.041-cm-thick sheets of 5052-O aluminum alloy. This material was chosen because it is a work hardening alloy and is therefore less susceptible to age hardening which may result in contour changes. In addition, it can be supplied in large widths with a surface finish less than 30 nm rms. One disadvantage in this material which became apparent during stretch-forming was that it developed strain lines which could not be completely covered by the surface improvement coating. The sheets were stretched over a reinforced epoxy replica of the glass master die. The replica was made in a two-step process and the surface had defects not present in the master. The thinned-epoxy surface improvement coating was applied by a dip coating process. This technique left small runs and bubbles in the surface which reduced the reflectivity of the subsequent vacuum-deposited aluminum (ref. 6). The aluminum reflective surface received a protective overcoating of silicon oxide. The sectors were bonded together with 2.5-cm-wide overlap strips. A rim support ring was fabricated from sheets of aluminum alloy and was rectangular in cross section (fig. 1(a)). Total concentrator mass (rim support plus shell) was 5.1 kg. The shell mass was estimated to be 2.2 kg in reference 6. (Model 1 is called S/N 2 in ref. 6.) Reference 6 also contains additional model details.

Model 2

The shell material for model 2 was 0.043-cm-thick sheets of 3003-O aluminum alloy. This material was selected because it did not develop the undesirable strain lines associated with stretching the model 1 material. The 3003-O alloy also had a surface finish which was less than 30 nm rms. The difference in thickness in the sheets for the two models was incidental and is not believed to have had any effect on concentrator accuracy. The aluminum sheets were stretched over the glass master die instead of a replica of the die as was done for model 1. Surface improvement coatings received a great deal of effort during this phase of the study and a spray process was developed that gave a uniform coating. However, the formulation selected for use failed to completely fill the grainy surface and may have caused an increase in the diffuse reflectance of the surface. The reflective surface had a protective overcoating of silicon oxide. The silicon oxide coating was not uniform and may have further lowered the specular reflectance of the surface. The stretched sectors were bonded together with 2.5-cm-wide overlap strips. A preliminary investigation of this model reported in reference 7 indicated that the sector edges have surface errors larger than the general level of error in the concentrator. The rim support ring for this model was formed of two sections bonded together (fig. 1(b)). Shell mass was estimated to be 2.5 kg (ref. 7) and total concentrator mass was 5.3 kg. Additional details can be found in reference 7.

Model 3

The shell of model 3 was made from 0.041-cm-thick sheets of 3003-O aluminum alloy similar to that used for model 2. The glass master was used as the stretch-forming die and new positioning techniques were incorporated so that the stretched sheets could be accurately positioned during trimming and assembly. The surface improvement coating used during this phase was superior to that used on model 2 and was sufficient to cover the grainy surface of the stretched sheets. No protective overcoating was used on this concentrator as had been used on the two previous models. A new trimming guide was developed and used to reduce trimming distortion of the joints. In addition, a new sector joint design was incorporated. The sectors were joined by two overlap strips 3.8 and 1.9 cm wide (fig. 1(c)). The rim support ring for this model was an aluminum torus which was attached to the shell with an aluminum skirt. The aluminum skirt was used because tests on several rim support ring configurations indicated this design introduced less surface distortion than other techniques. The mass of the concentrator shell was estimated to be 2.5 kg (ref. 8) and the total mass was 4.9 kg. Fabrication procedure and additional details can be found in reference 8.

APPARATUS AND TESTS

Calorimetric

The calorimetric investigations were performed in sunlight utilizing the solar tracker shown in figure 3. The tracker automatically maintained any preset alinement of the concentrator axis with the solar rays. A water-cooled-cavity calorimeter located in the focal region was equipped with various sized aperture plates.

Tests were performed to determine the effect of aperture size, the effect of mislocation of the calorimeter along and transverse to the optical axis, and the effect of misorientation of the optical axis with the sun. The ranges of test variables were calorimeter aperture sizes from $1.56R_i$ to $8.34R_i$, axial calorimeter movement of 0.06f, transverse calorimeter movement of $\pm 4R_i$, misalinement of the optical axis with the solar rays of ±30 mrad. A more complete description of the apparatus and test techniques can be found in reference 4.

error $\bar{\delta}$ and standard deviation σ of models 1 and 2 as determined in the present investigation is shown in the following table:

Source	Model 1				Model 2				Model 3			
	δ_r		δ_c		δ_r		δ_c		δ_r		δ_c	
	$\bar{\delta}_r$	σ	$\bar{\delta}_c$	σ	$\bar{\delta}_r$	σ	$\bar{\delta}_c$	σ	$\bar{\delta}_r$	σ	$\bar{\delta}_c$	σ
Present investigation	0.73	3.03	0.01	3.08	0.24	0.86	0	1.71				
Reference 8					.24	.83	.12	1.10	0.13	0.46	0.15	0.61

Also shown in the table are the same statistical parameters for models 2 and 3 as reported in reference 8. The investigation reported in reference 8 used a different ray-tracing technique (the projected grid method) from the one employed in this study. However, a comparison of the results of both methods for model 2 shows good agreement. The circumferential components do not agree quite as closely as the radial components. This is probably due to a difference in the reduction of data rather than a difference in test techniques. The data for the investigation reported herein were reduced in such a manner that the average circumferential error was made zero because the concentrator surface at any test radius forms a closed curve. The improvement in geometry in successive models as first observed from calorimetric tests is substantiated by the optical tests. The standard deviation of both error components decreased by a factor of approximately 2 from model 1 to 2, and an equivalent decrease was noted from model 2 to 3.

Figure 11 presents the fraction of concentrator area having slope errors less than a specified value. The data for model 3 were obtained from reference 8 and do not include 6.5 percent of the concentrator projected area because it had errors too large to measure by the projected grid method. Each model shows a significant improvement over the previously fabricated model in both radial and circumferential error components. The improved geometrical accuracy of model 2 over model 1 has been attributed to stretch-forming over a more accurate die and the use of a material having superior plastic strain properties (ref. 7). Reference 8 attributes part of the improvement in geometry between models 2 and 3 to improvements in seam design and trimming methods. Other differences (ref. 8) between models 2 and 3 which may have improved the geometry were a reduction in the airborne dust deposited on the aluminum stock during stretch-forming operations, the use of pilot holes for accurate location of the stretched panels, and a different rim support ring design.

During the present investigation data were taken in the vicinity of the seams on model 2 to determine the amount of seam distortion and the area affected. Figure 12 presents slope error as a function of distance from the sector seam for two test radii, and after vibration tests is presented in figure 18(b). At aperture radius ratios of 2 to 3 suitable for thermionic converters the decrease in geometric efficiency after vibration is only about 0.04. Since the accuracy of data is ±0.02, the loss in concentrator efficiency due to vibration appears to be small.

CONCLUDING REMARKS

Three stretch-formed aluminum solar concentrators representing three phases of a stretch-forming development program have been evaluated for possible use with thermionic convertors. Model 3, which represented the third phase, had the highest geometrical accuracy and specular reflectance of any model tested. The calorimetric efficiency of this model was 0.85 at an aperture radius of 2.5 solar images (considered suitable for thermionic applications), which is only about 0.05 lower than the efficiency the model would have had with perfect geometry. It is therefore considered suitable for use with thermionic convertors. The increase in efficiency of this model over models 1 and 2 may be attributed to improvements in design and fabrication developed during the program. Models 1 and 2 were optically tested and compared with published data for model 3. These tests permitted the location and magnitude of surface slope errors to be determined and improvements in the fabrication techniques to be evaluated. Comparison of the slope errors on the three models confirmed the results of the calorimetric tests which indicated an improvement in geometry with each phase of development. The surface slope errors were largest near the sector seams but this region of large error extended only to the edge of the overlap strip. The surface slope errors were used to calculate geometric efficiencies. The calculated geometric efficiency can provide useful information and reduce the calorimetric testing required to evaluate concentrator performance. Vibration tests were performed on model 1. Failure of the support structure to withstand flight qualification tests did not impair the geometrical accuracy of the shell.

Langley Research Center,
National Aeronautics and Space Administration,
Langley Station, Hampton, Va., June 24, 1968,
120-33-06-08-23.

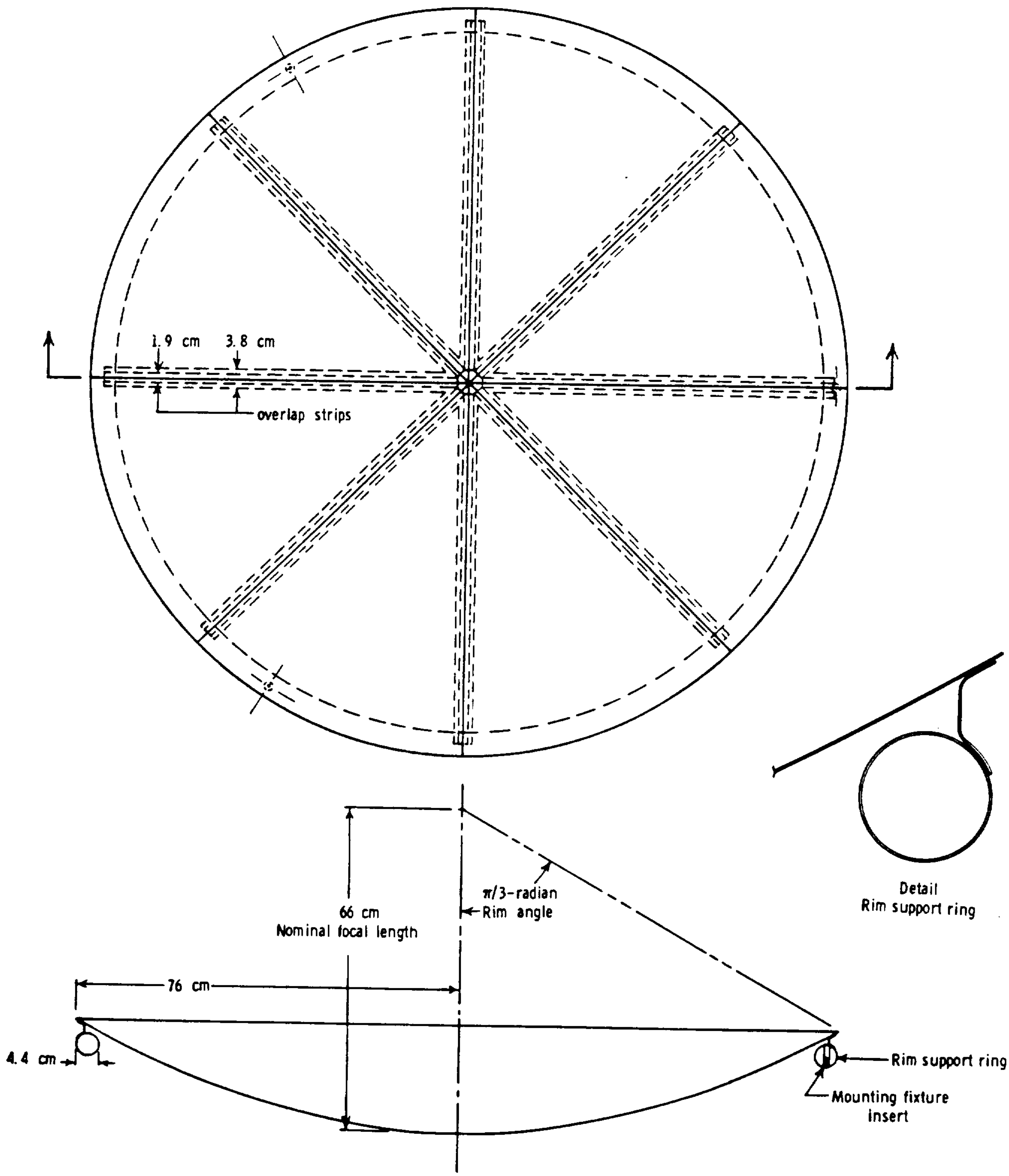
1.9 cm
3.8 cm
overlap strips
π/3-radian
Rim angle
66 cm
Nominal focal length
76 cm
4.4 cm
Rim support ring
Mounting fixture insert
Detail
Rim support ring

(c) Model 3.

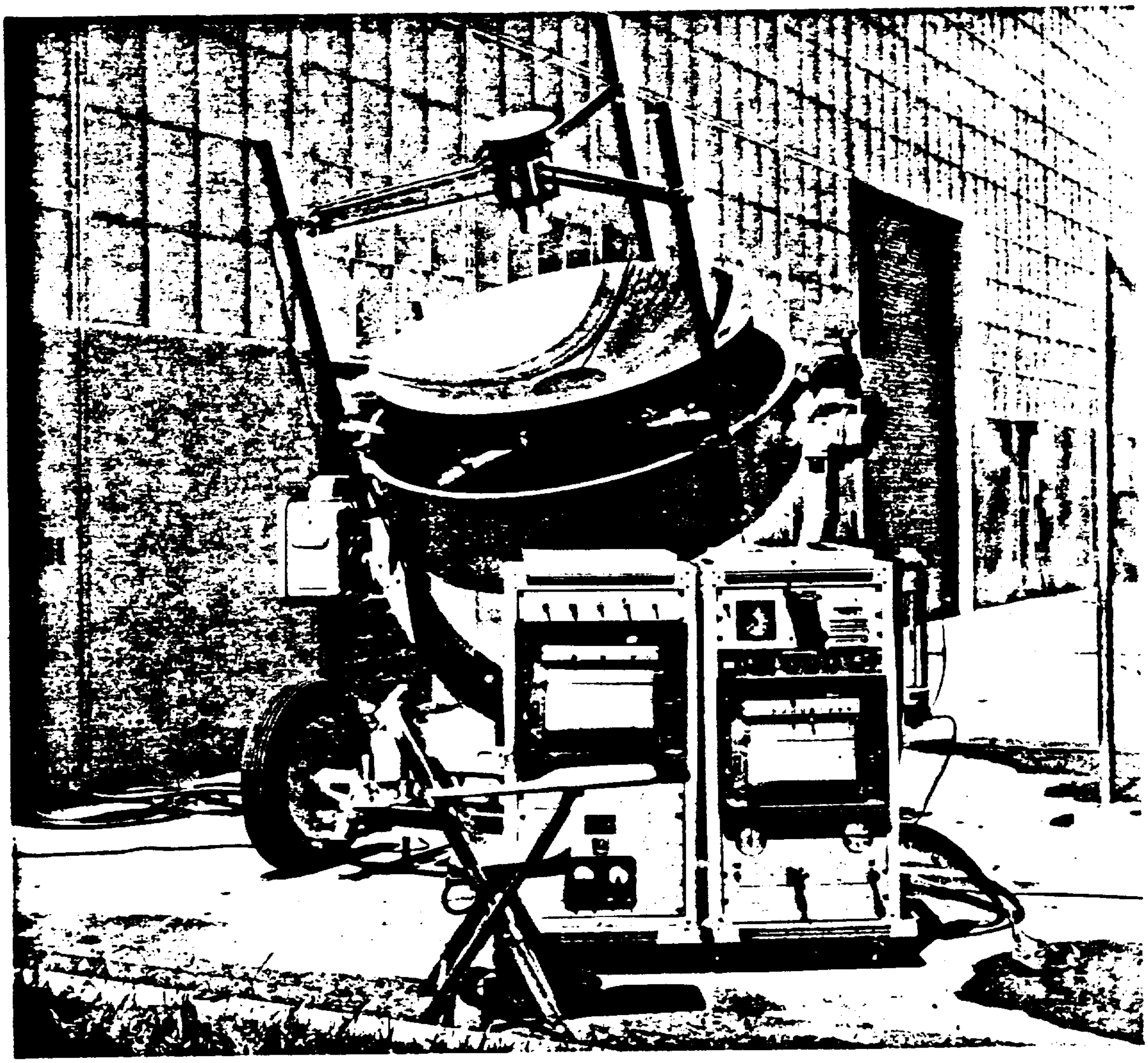

Concentrator mounted on solar tracker for calorimetric efficiency tests.

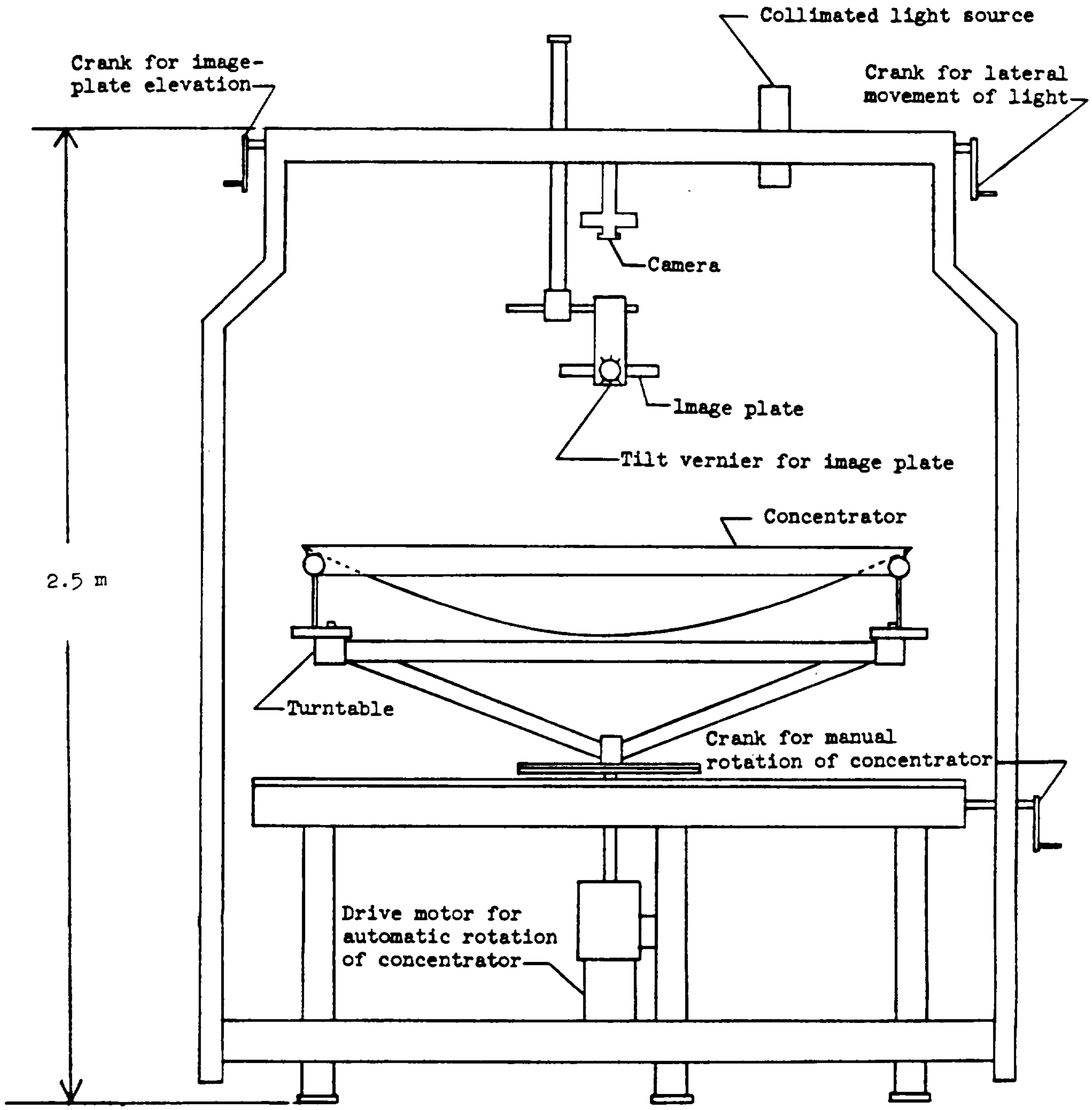

Sketch of optical test fixture.

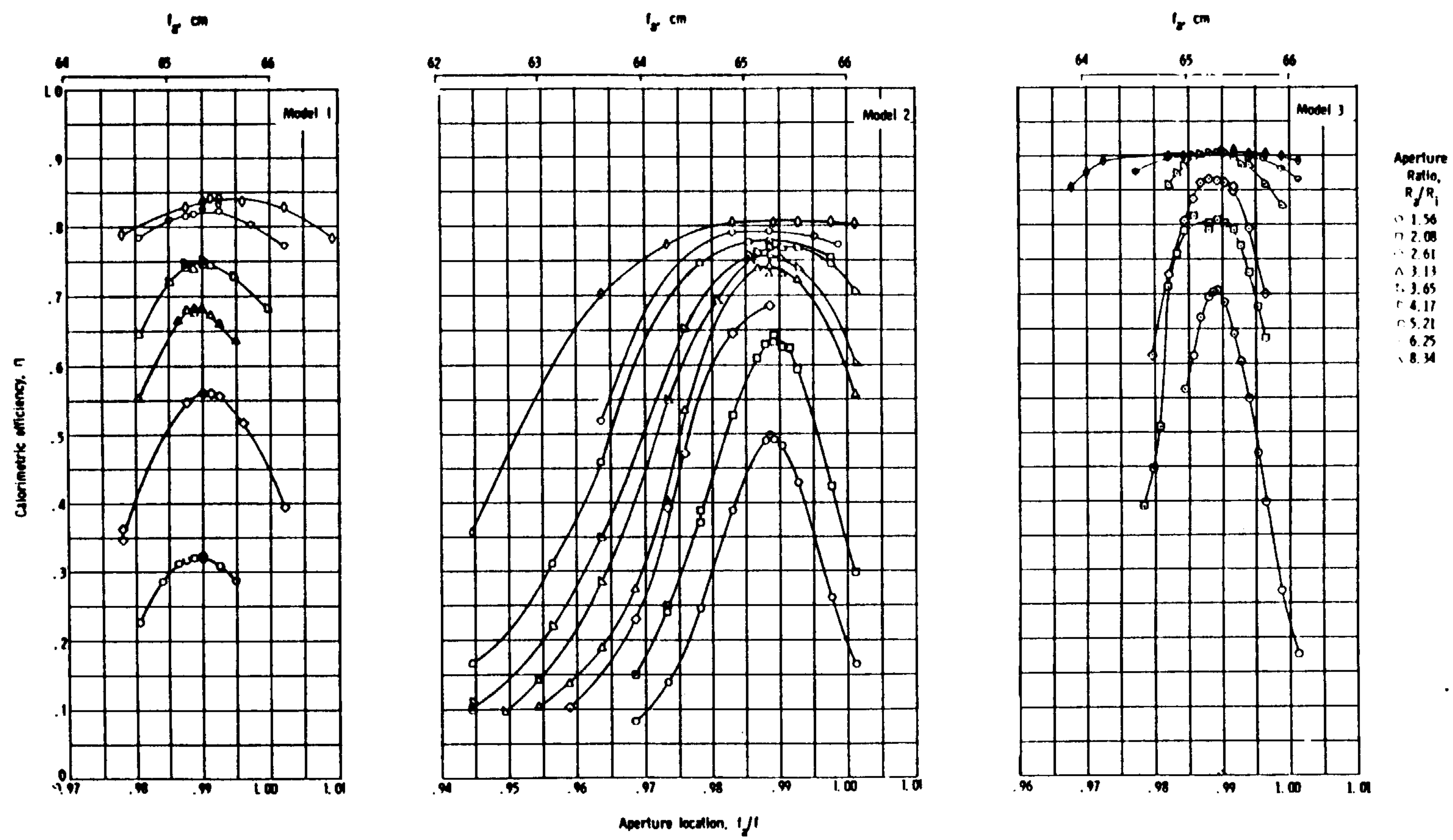

(a) Variation in efficiency with axial location of calorimeter.

Calorimetric efficiency of all models.

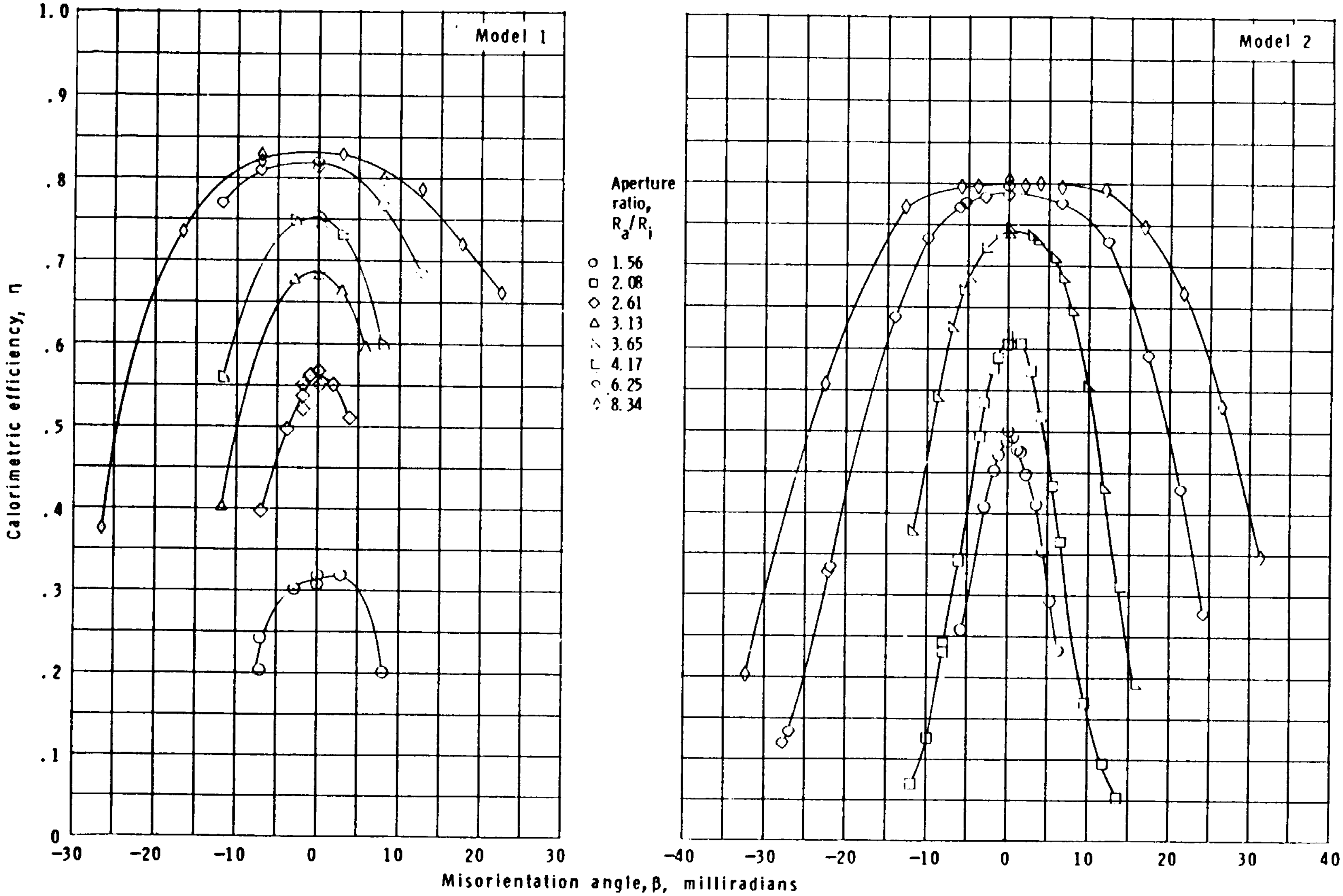

(c) Variation in efficiency with misorientation of the concentrator axis with the solar rays.

Continued.

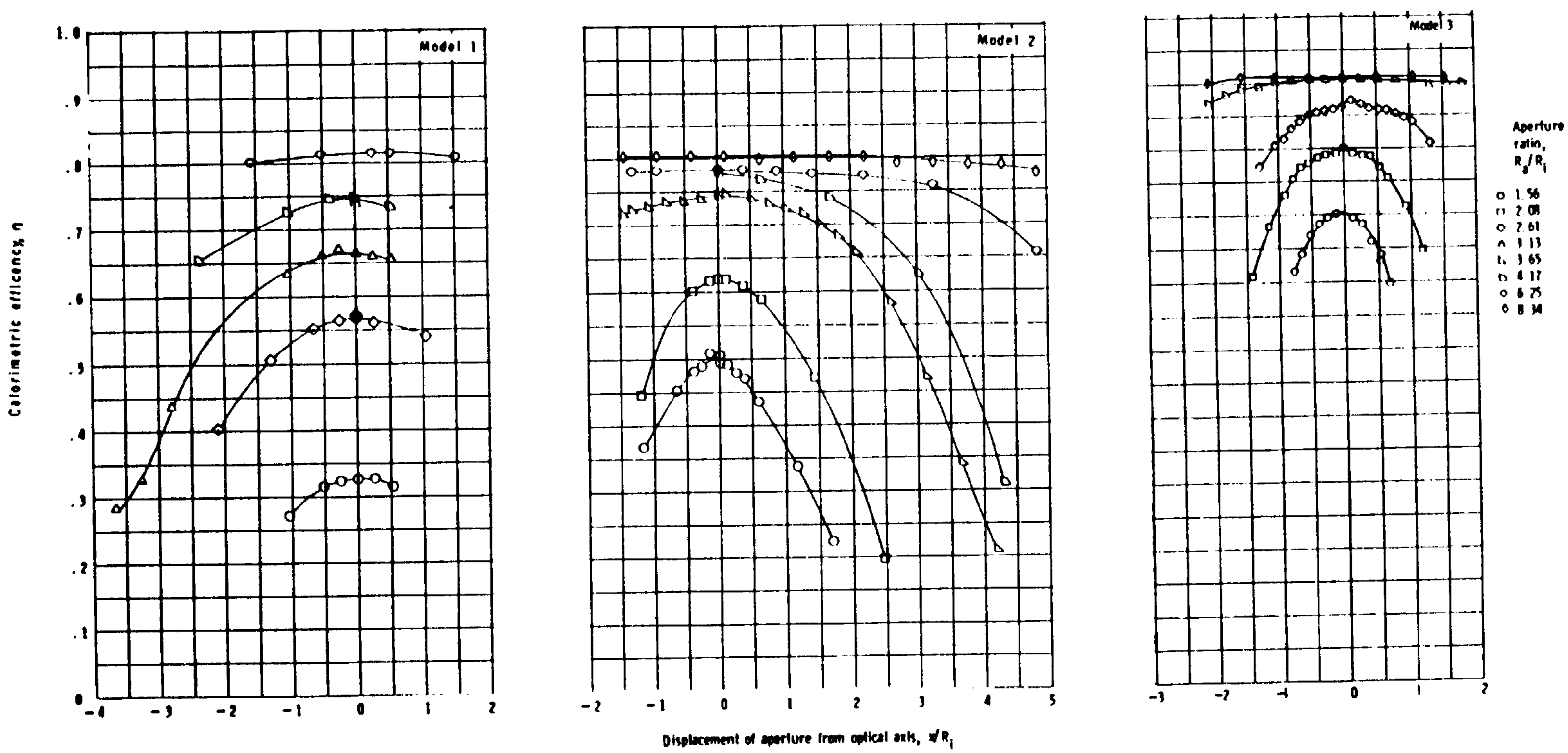

(b) Variation in efficiency with lateral location of calorimeter.

Continued.

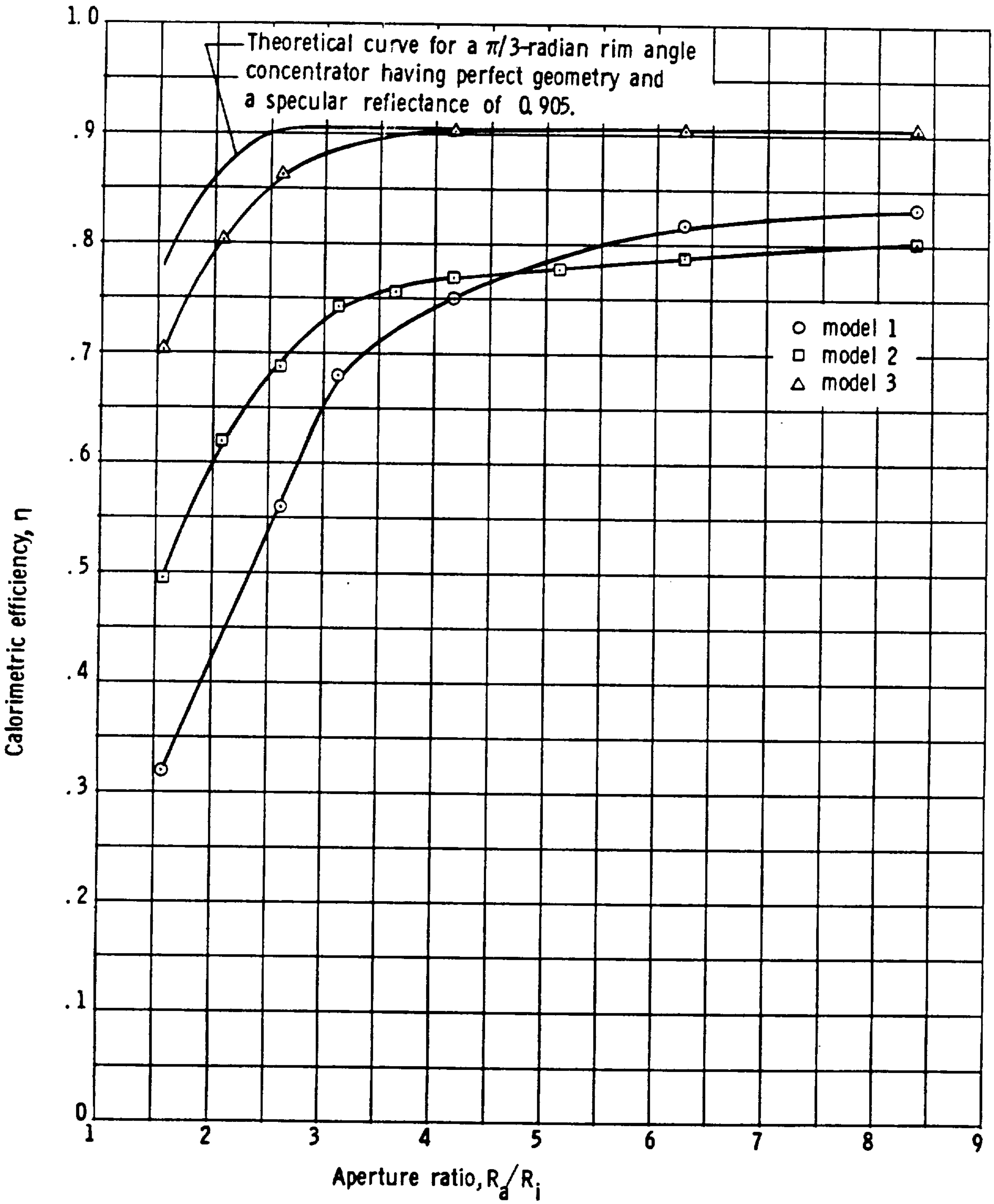

(d) Variation in efficiency with aperture size.

Concluded.

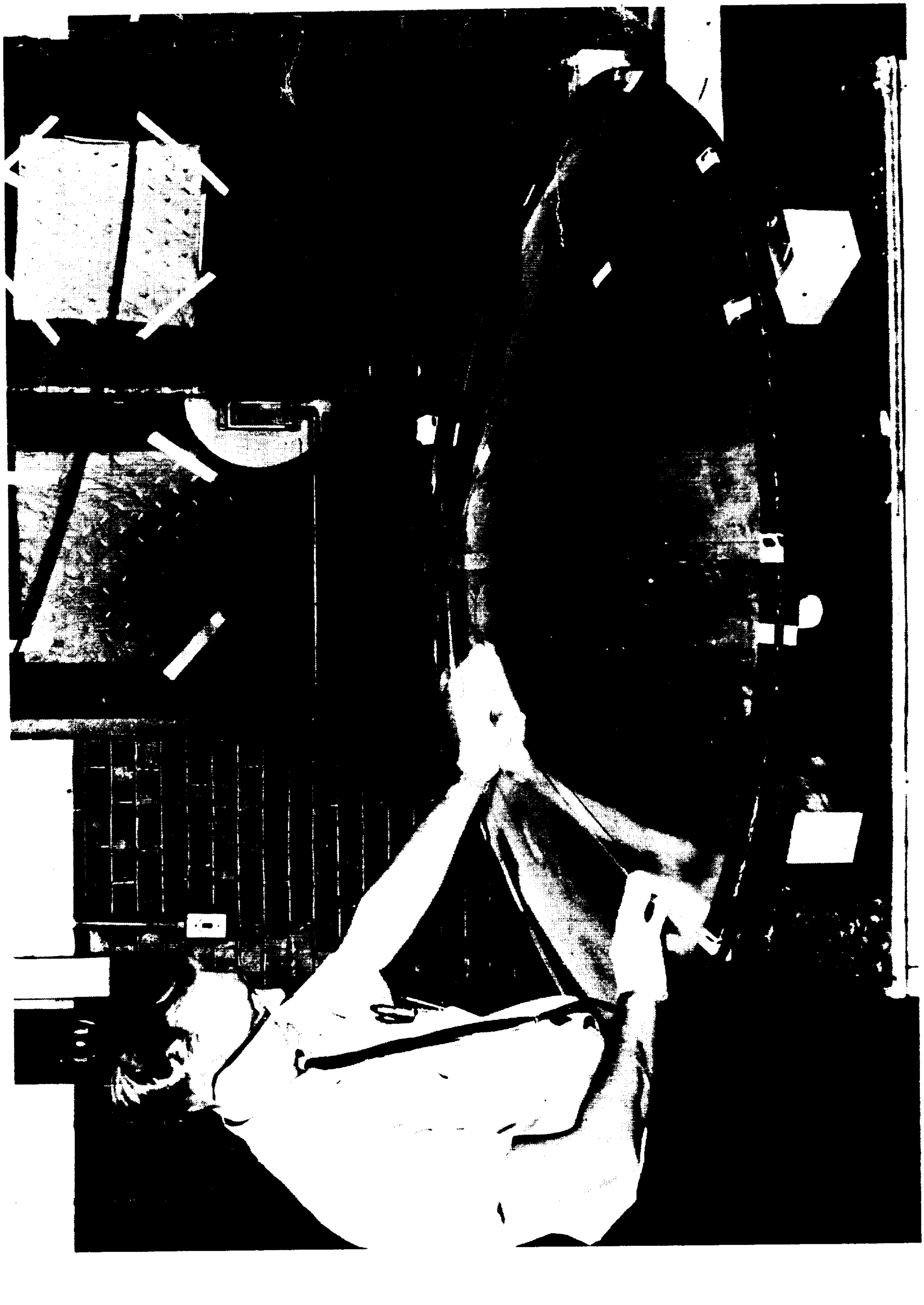

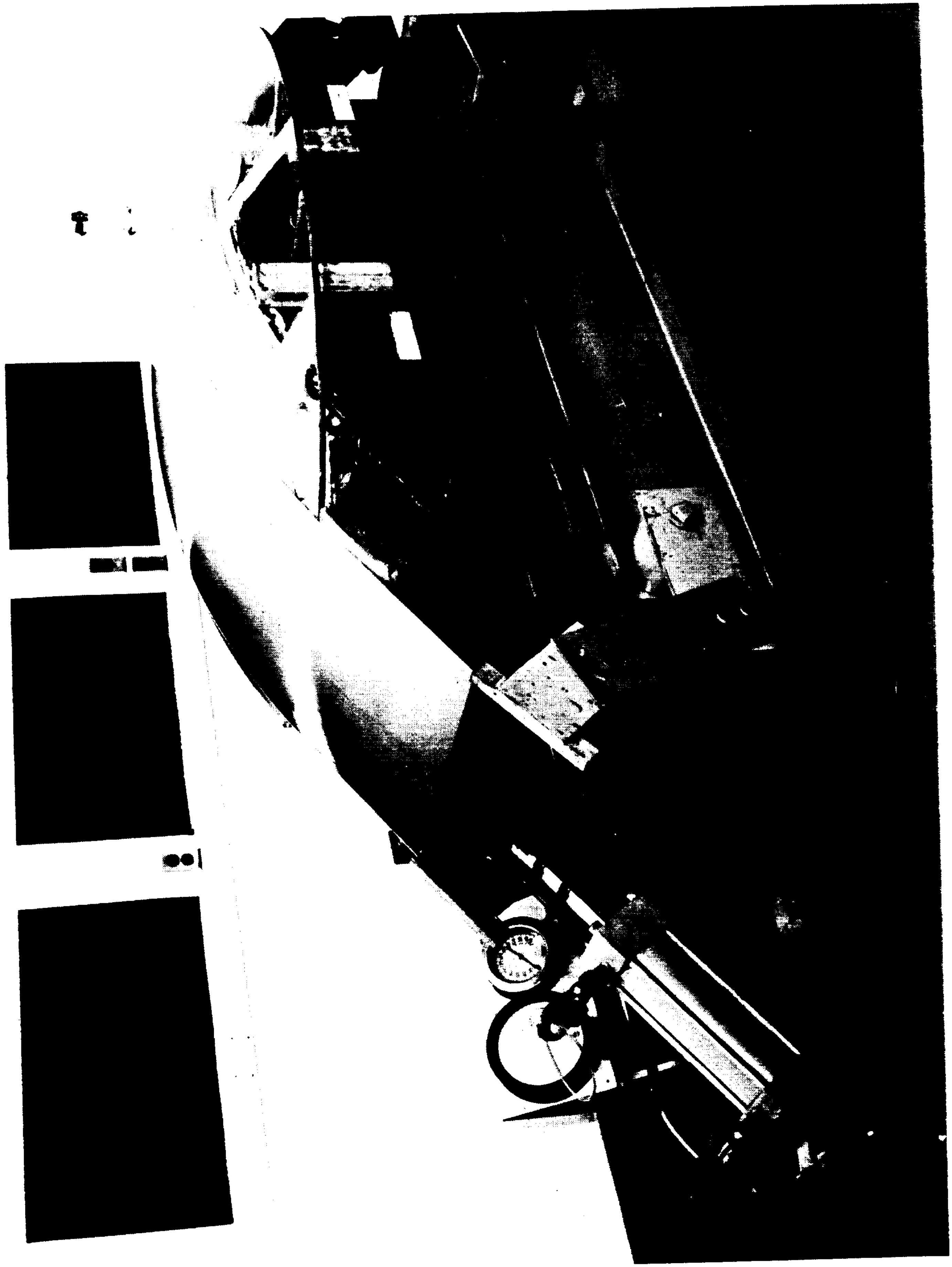

Appendix B

NASA CONTRACTOR REPORT

NASA CR-46

NASA CR-46

SUNFLOWER SOLAR COLLECTOR

Prepared under Contract No. NAS 5-462 *by*
THOMPSON RAMO WOOLDRIDGE, INC.
Cleveland, Ohio
for

NATIONAL AERONAUTICS AND SPACE ADMINISTRATION • WASHINGTON, D. C. • MAY 1964

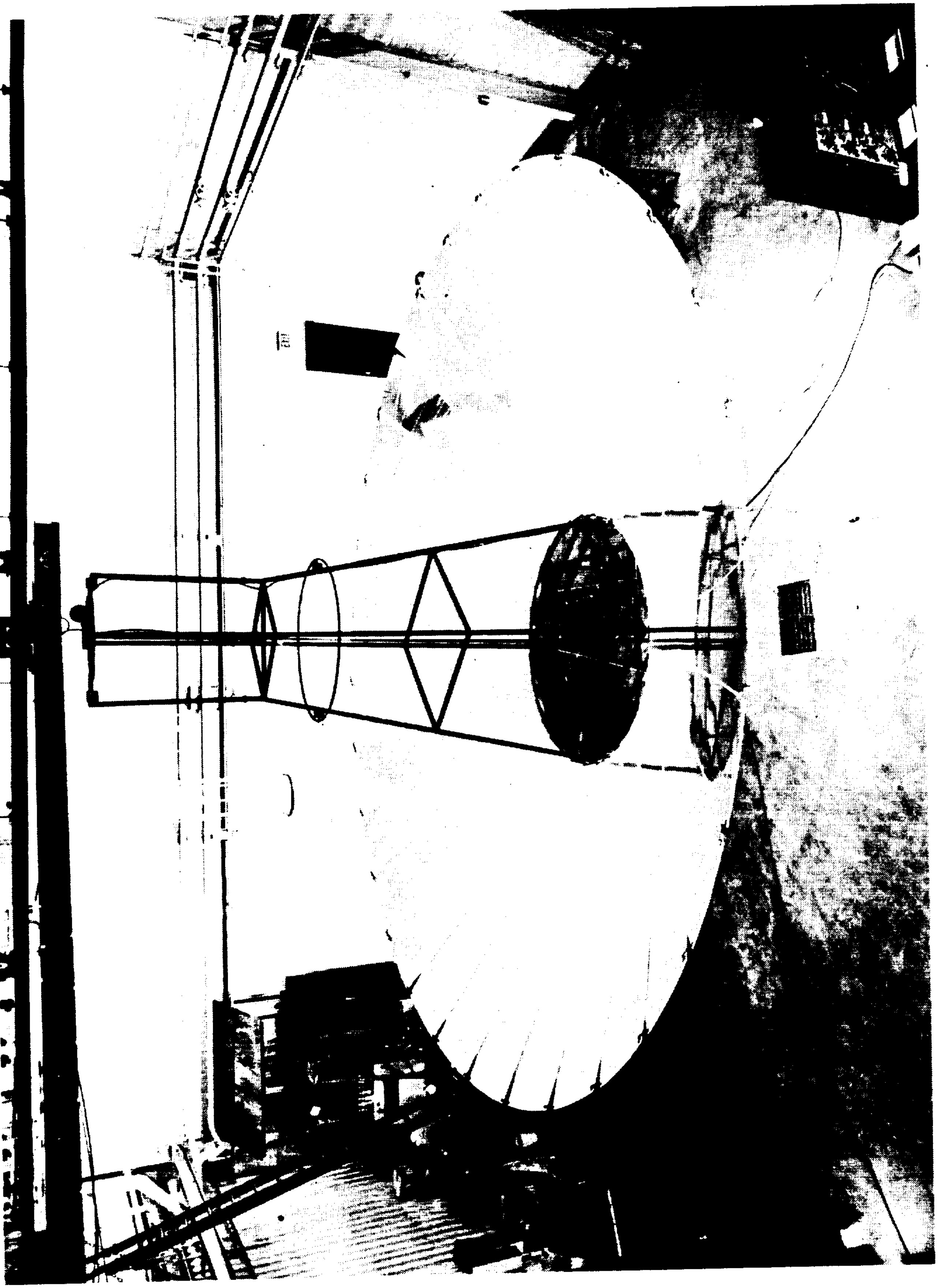

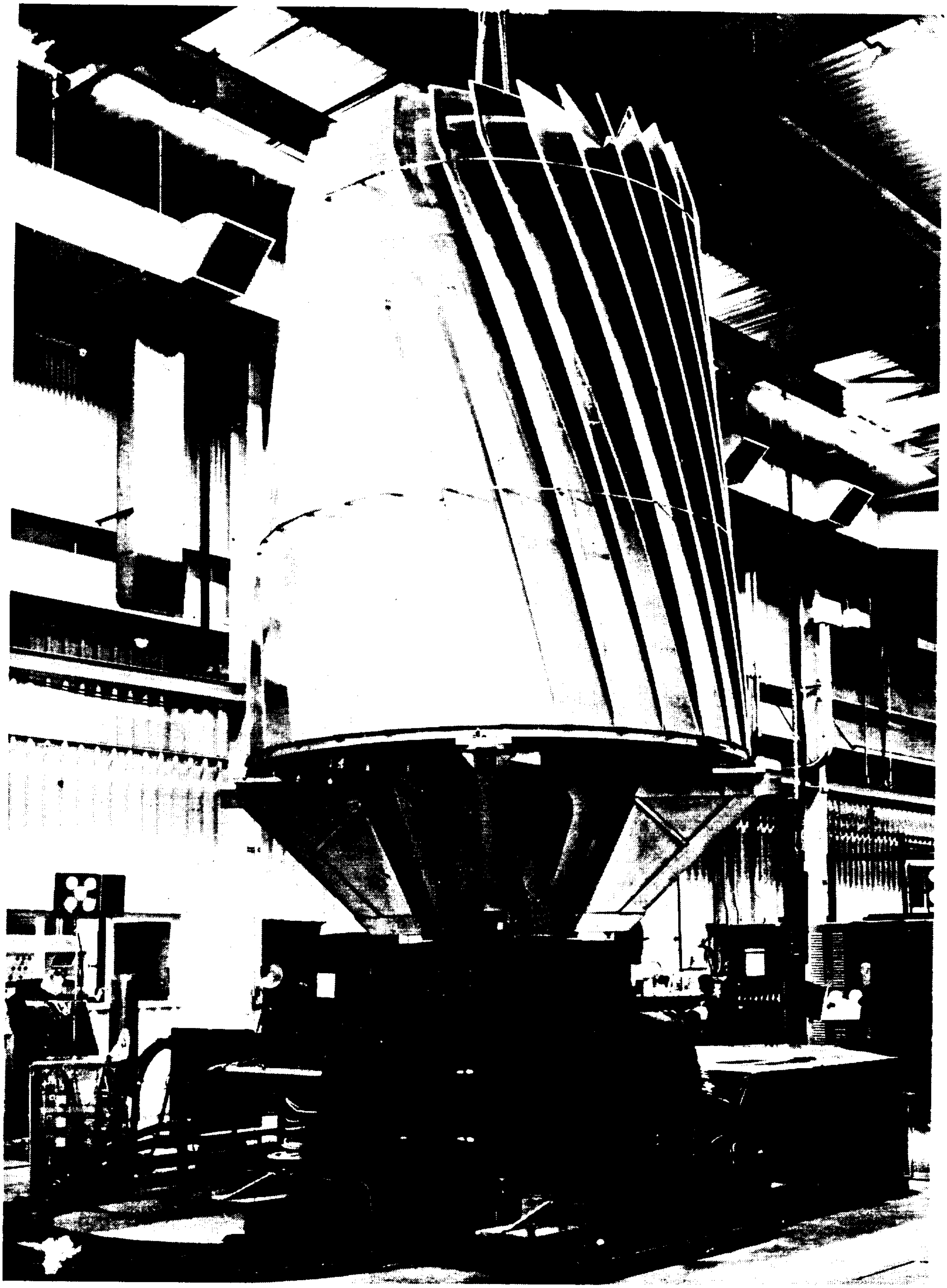

3.2.3 Concentration Ratio

3.2.3.1 Nominal area concentration ratio, $\left(\frac{32.2}{1.2}\right)^2$: 720

3.2.3.2 Actual intercepted area concentration ratio, $\frac{D_o^2 - D_1^2}{D_a^2}$: 660

3.2.4 Collector Performance

3.2.4.1 Concentrator efficiency: 73.6% at.

Reflectivity: 0.92

Solar misorientation: 3/4° max

Surface slope deviation: ± 1/2° max

Surface translation deviation: ± 1 inch max

Solar constant: 130 watts/ft^2

3.2.4.2 Receiver efficiency: 90.3%

3.2.4.3 Overall collection efficiency: 66.5%

3.2.5 Stowage and Development

The concentrator shall be stowed in the envelope defined in a petaline manner. Deployment upon achieving orbit shall be as follows:

3.2.5.1 A restraining hoop shall be severed upon command.

3.2.5.2 Preloaded torsion bar springs in each petal hinge shall accelerate the petals toward the open position.

3.2.5.2 The petals shall be decelerated to and locked in the open position by a locking device at the petal tips.

3.2.6 Concentrator Structure

The materials and construction of the petals shall be of adhesive bonded aluminum honeycomb sandwich. The dimensions and fabrication of face, core, and sandwich cross section shall provide the concentration efficiency defined in Section 3.2.4.1.

TYPICAL CONCENTRATOR-RECEIVER GEOMETRY

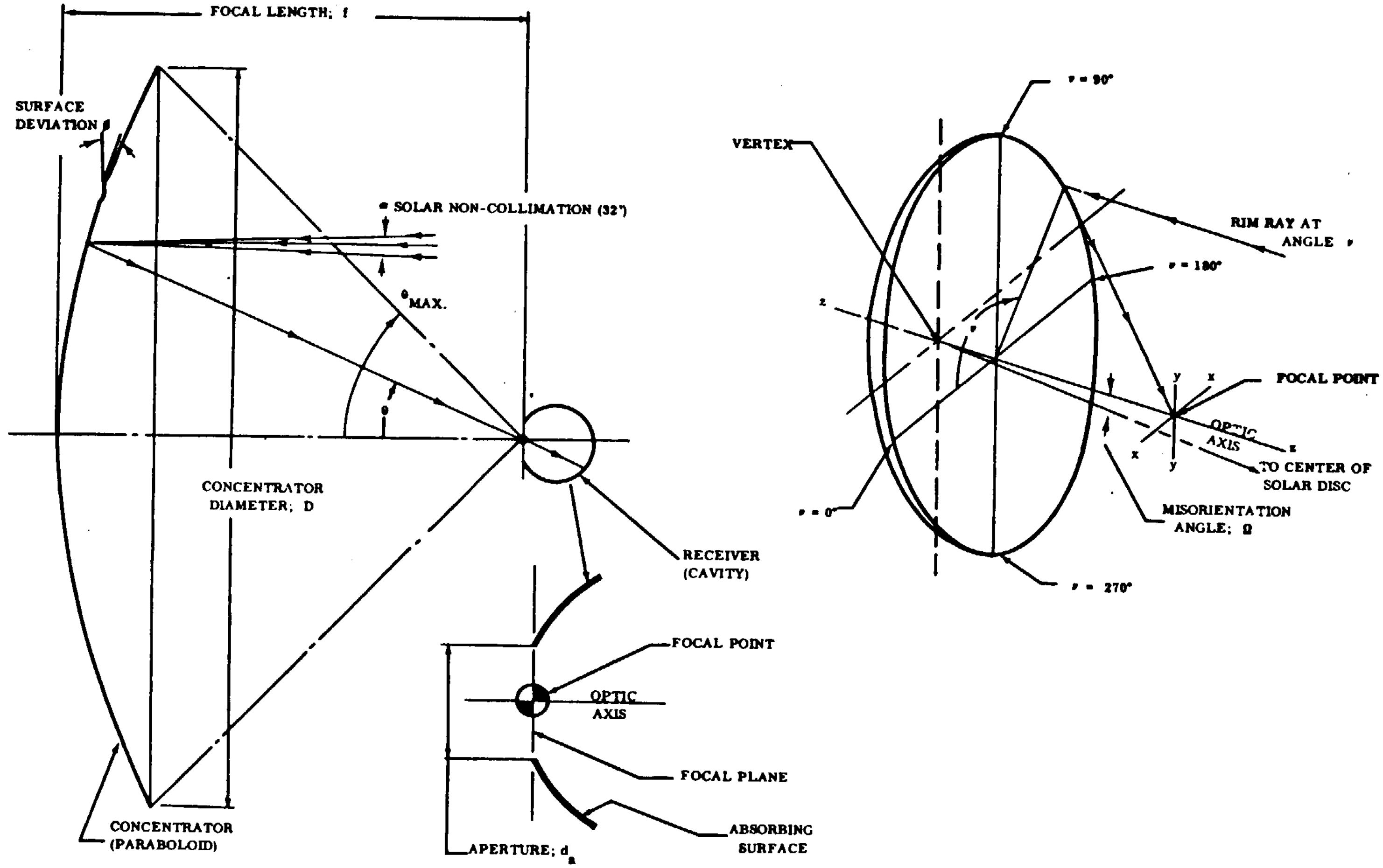

A COMPARISON OF
SURFACE ERROR DISTRIBUTION CURVES

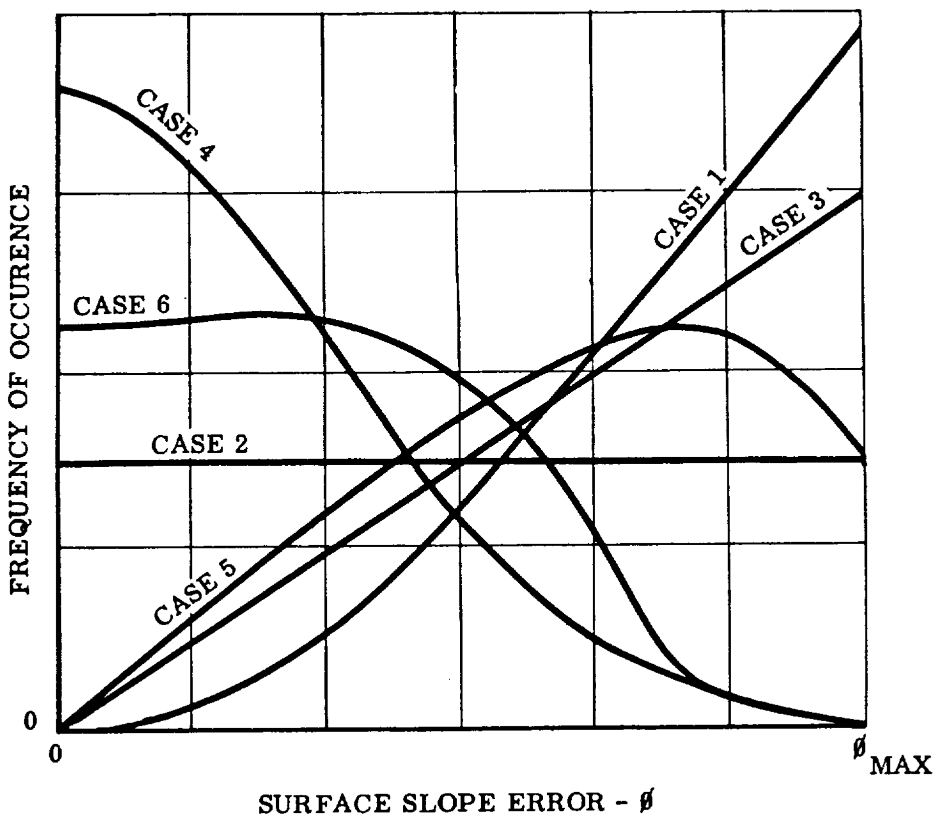

CASE 1; π COSINE (HANSON, REF. 15)
CASE 2; 2 π COSINE (TYPICAL OF HONEYCOMB MARKOFF)
CASE 3; PROPORTIONAL (HUKUO-MII, REF. 17)*
CASE 4; NORMAL OR GAUSSIAN (SILVERN, REF. 23)
CASE 5; SOLAR LIMB DARKENING (CONSIDERED AS AN EQUIVALENT SURFACE DEVIATION)
CASE 6; SUNFLOWER (FIG. 7.4-3)

*ALTHOUGH THE REFERENCE IS NOT EXPLICIT AS TO THE SURFACE CHARACTERISTICS, THE DISTRIBUTION SHOWN WOULD BE REQUIRED TO SATISFY THE "UNIFORM ILLUMINATION" IN THE FOCAL PLANE SCATTERING CIRCLE AS STATED BY THE AUTHORS.

PARAXIAL FLUX PROFILE GEOMETRY

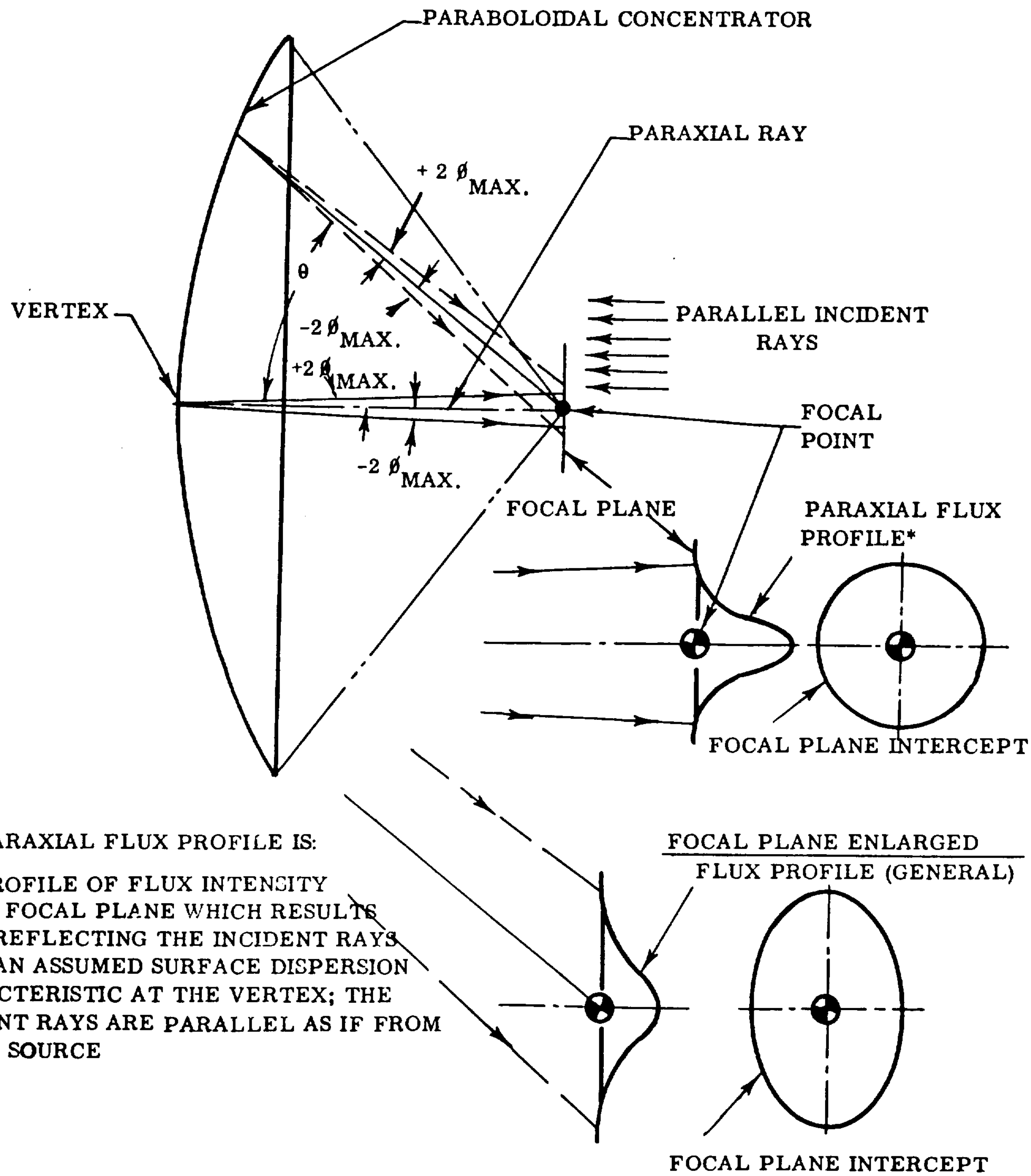

*THE PARAXIAL FLUX PROFILE IS:

THE PROFILE OF FLUX INTENSITY IN THE FOCAL PLANE WHICH RESULTS FROM REFLECTING THE INCIDENT RAYS FROM AN ASSUMED SURFACE DISPERSION CHARACTERISTIC AT THE VERTEX; THE INCIDENT RAYS ARE PARALLEL AS IF FROM A STAR SOURCE

PARAXIAL FLUX PROFILES
DUE TO SPECIFIC ERROR DISTRIBUTION CURVES

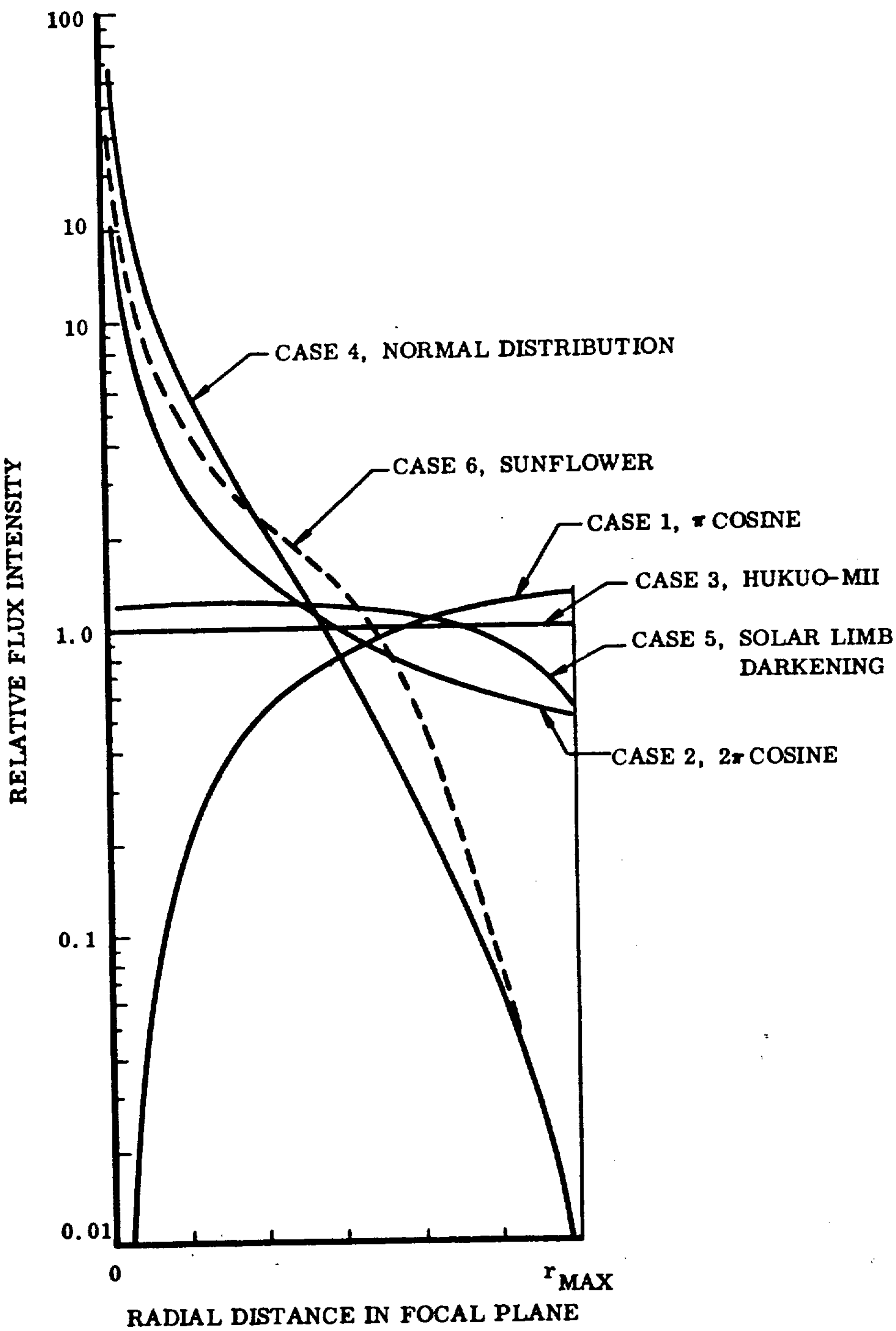

EFFECTS OF VARIOUS SURFACE ERROR MODELS
ON SURFACE GEOMETRIC EFFICIENCY

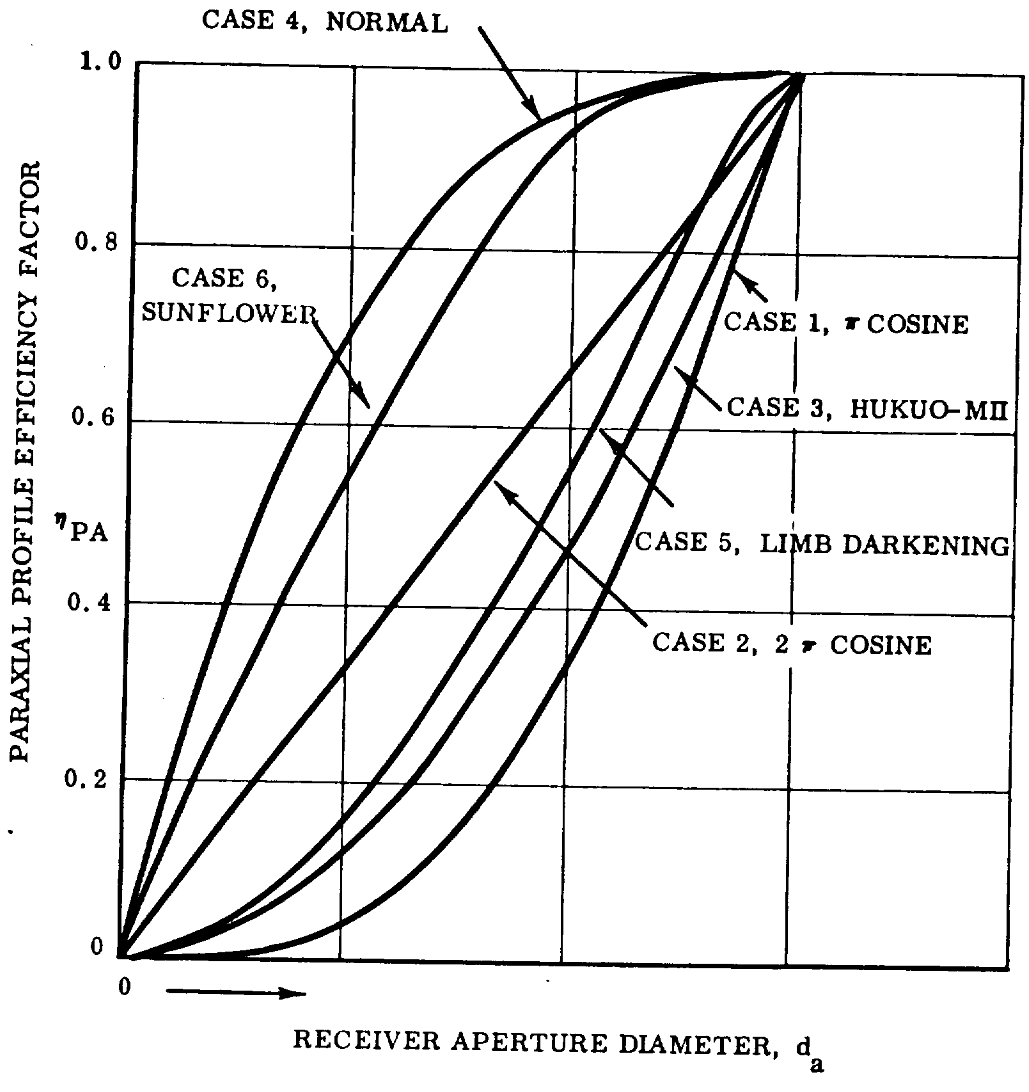

HONEYCOMB MARKOFF GEOMETRIC CHARACTERISTICS

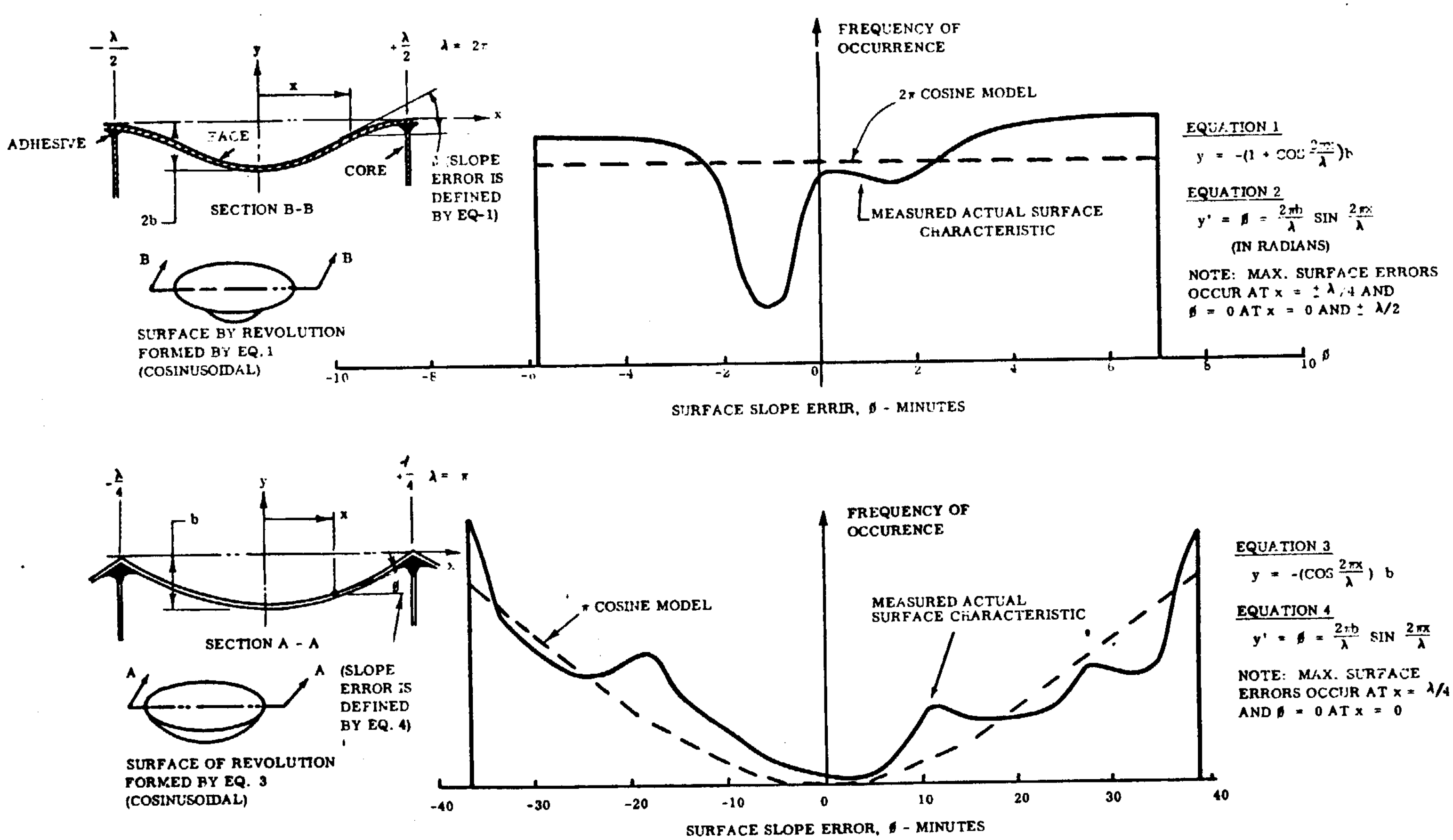

COMPARISON OF MEASURED DISTRIBUTION
WITH NORMAL DISTRIBUTION MODELS

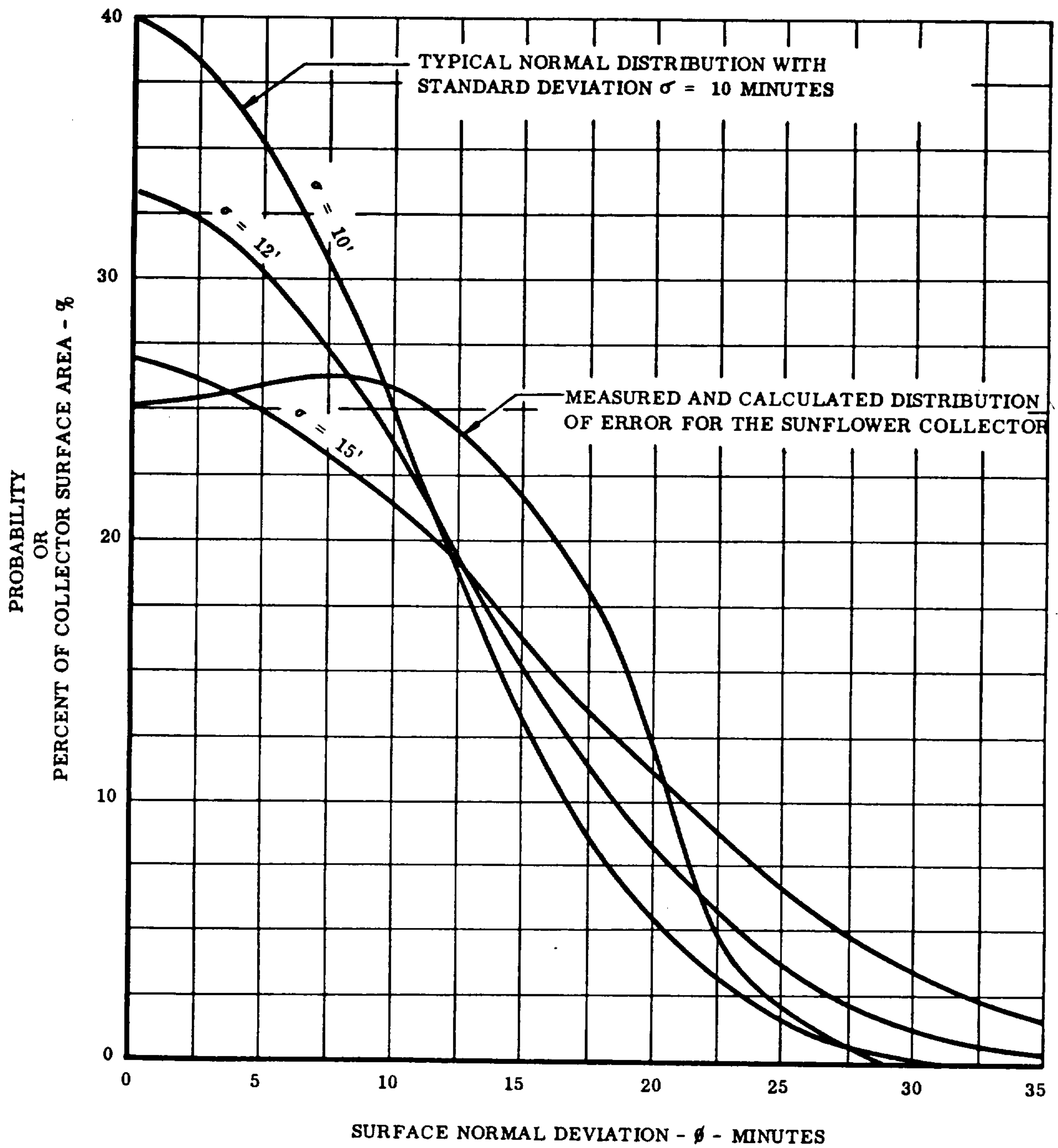

The second idealization is made to allow solution of the problem by digital computation using established general structural analysis computer programs.[5] Essentially, the continuous material of the elastic body is replaced by a three-dimensional gridwork of equivalent straight elastic beams and diagonal members interconnected at joints called nodal points.

A further description of the idealized structural model is presented in TRW ER 5028[19].

Since the collector is composed of 30 sectors, both a single sector and a quadrant of the collector were programmed for solution. The quadrant was selected since Δ T's are approximately symmetrical on a quadrant basis. The equations representing the mathematical model were formulated by a stiffness matrix approach based upon small deflection theory. These equations were automatically formed and solved in terms of deflections at nodal points and constraint forces using General Dynamics/Electric Boat Division's IBM 704 general structural analysis computer program.

Thermoelastic Analysis Results

Computed results for thermal distortion modes are shown in Figure 4.2-13 for the various cases which were investigated. Before presenting the effects of these distortions on optical performance, the structural analysis will be discussed further.

As a check on the accuracy of the analysis model, solutions for the dead weight deflection of the collector were computed for comparison with measured data obtained from developmental testing of the full scale preprototype collector (see Section 8.3.1). Results of these comparisons are shown in Table 4.2-2 and Figure 4.2-14. Reactions and stresses were obtained from strain gage measurements during dead weight testing. It can be seen that reasonable correlation is obtained except for the compressive stress in the upper skin.

TABLE 4.2-2

COMPUTED VS MEASURED REACTIONS AND STRESSES

	Computed IBM 704	Measured Preprototype COL II-2
Rim Lock Constraints		
Force	49.3 lb	50 lb
Moments	15.8 in-lb	13.7 in-lb
Stresses		
Upper Skin	4500 psi (compressive)	1285 psi (compressive)
Lower Skin	3600 psi (tensile)	3210 psi (tensile)

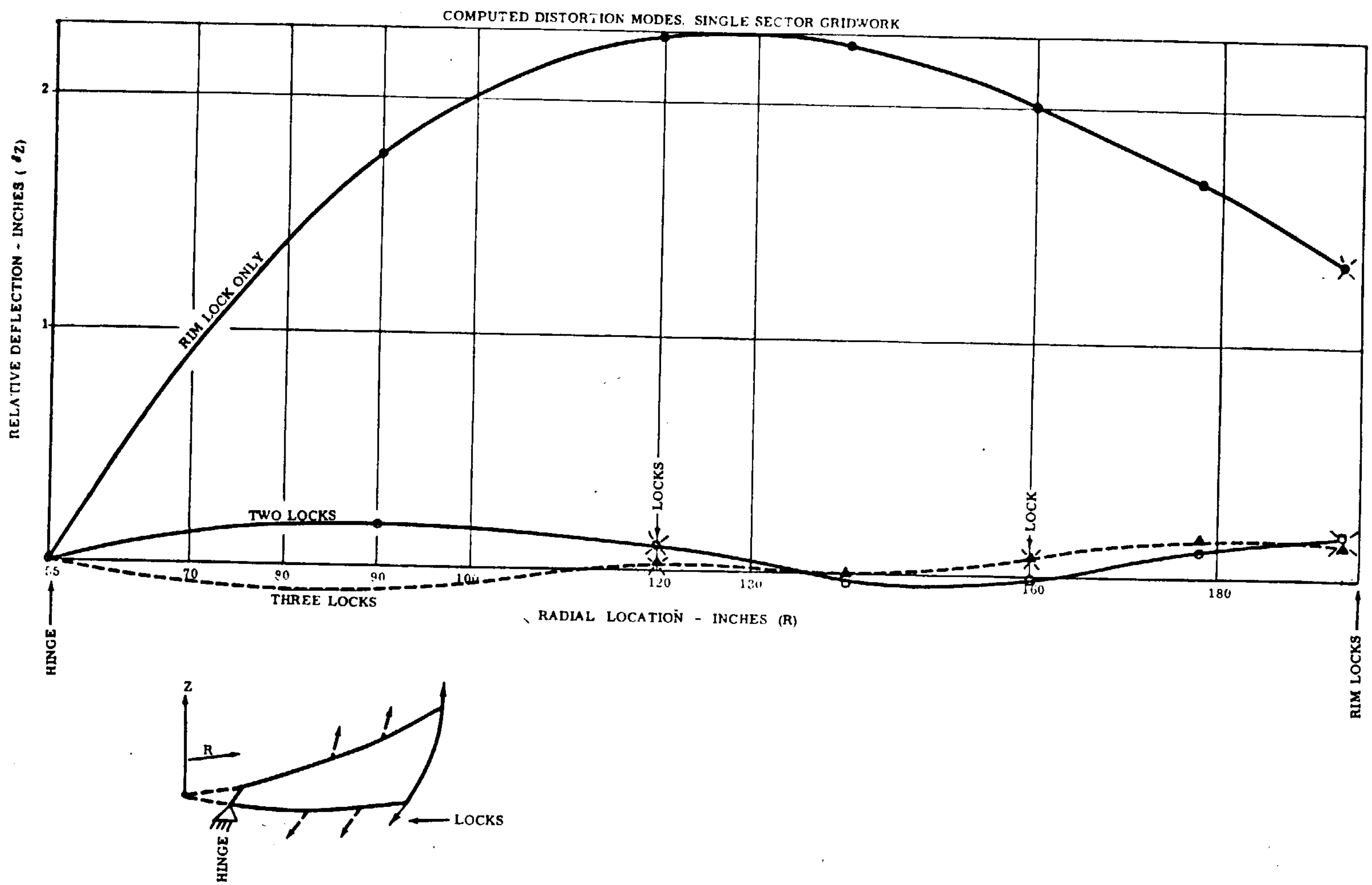
COMPUTED DISTORTION MODES, SINGLE SECTOR GRIDWORK
RELATIVE DEFLECTION - INCHES (δZ)
RADIAL LOCATION - INCHES (R)
RIM LOCK ONLY
TWO LOCKS
THREE LOCKS
LOCKS
LOCK
HINGE
RIM LOCKS
1
2
70
80
90
100
120
130
160
180
Z
R
HINGE
LOCKS

OPTICAL QUALITY OF THERMALLY DISTORTED COLLECTOR

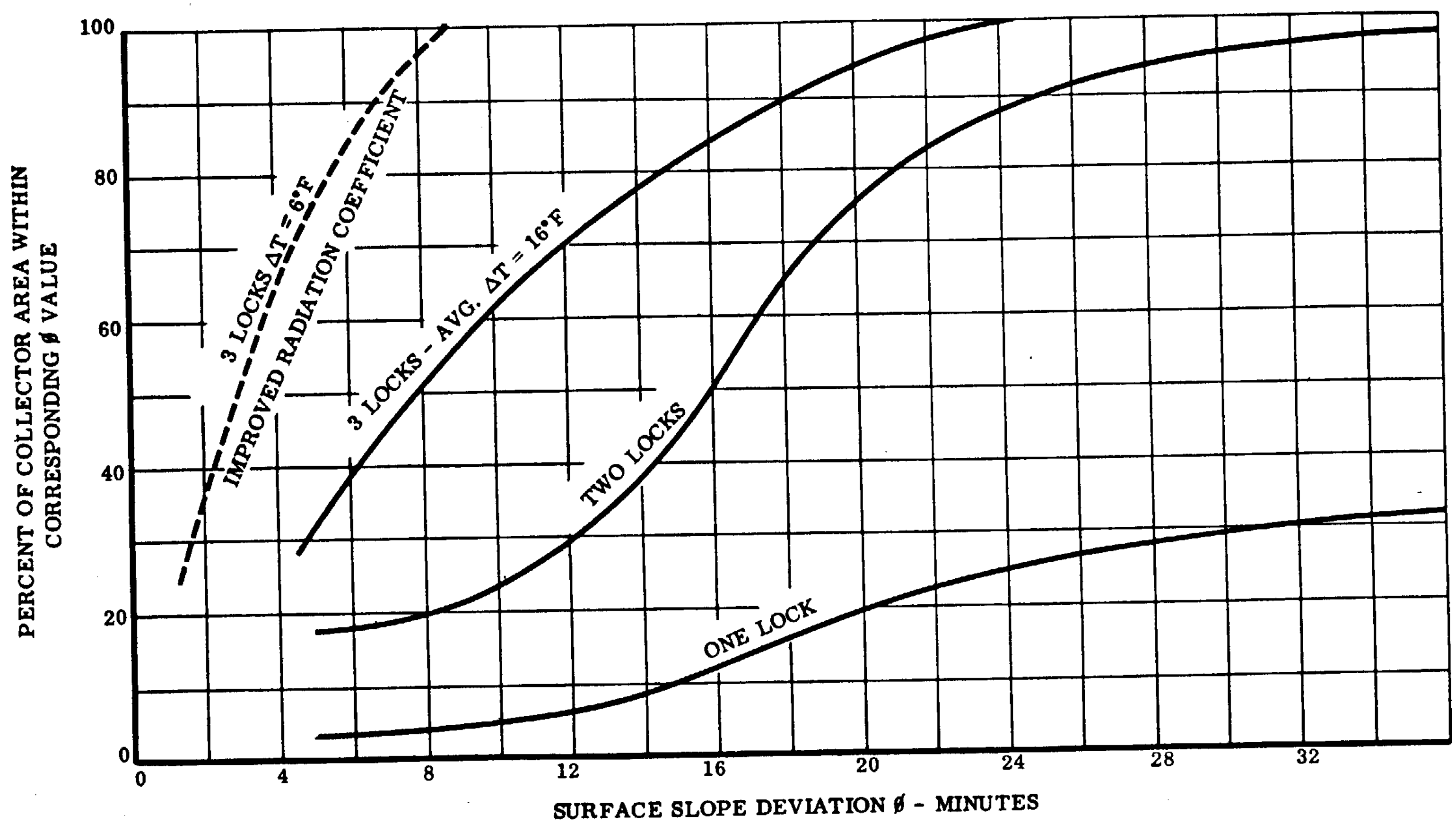

COMPOSITE MATERIALS HEAT TRANSFER RESULTS

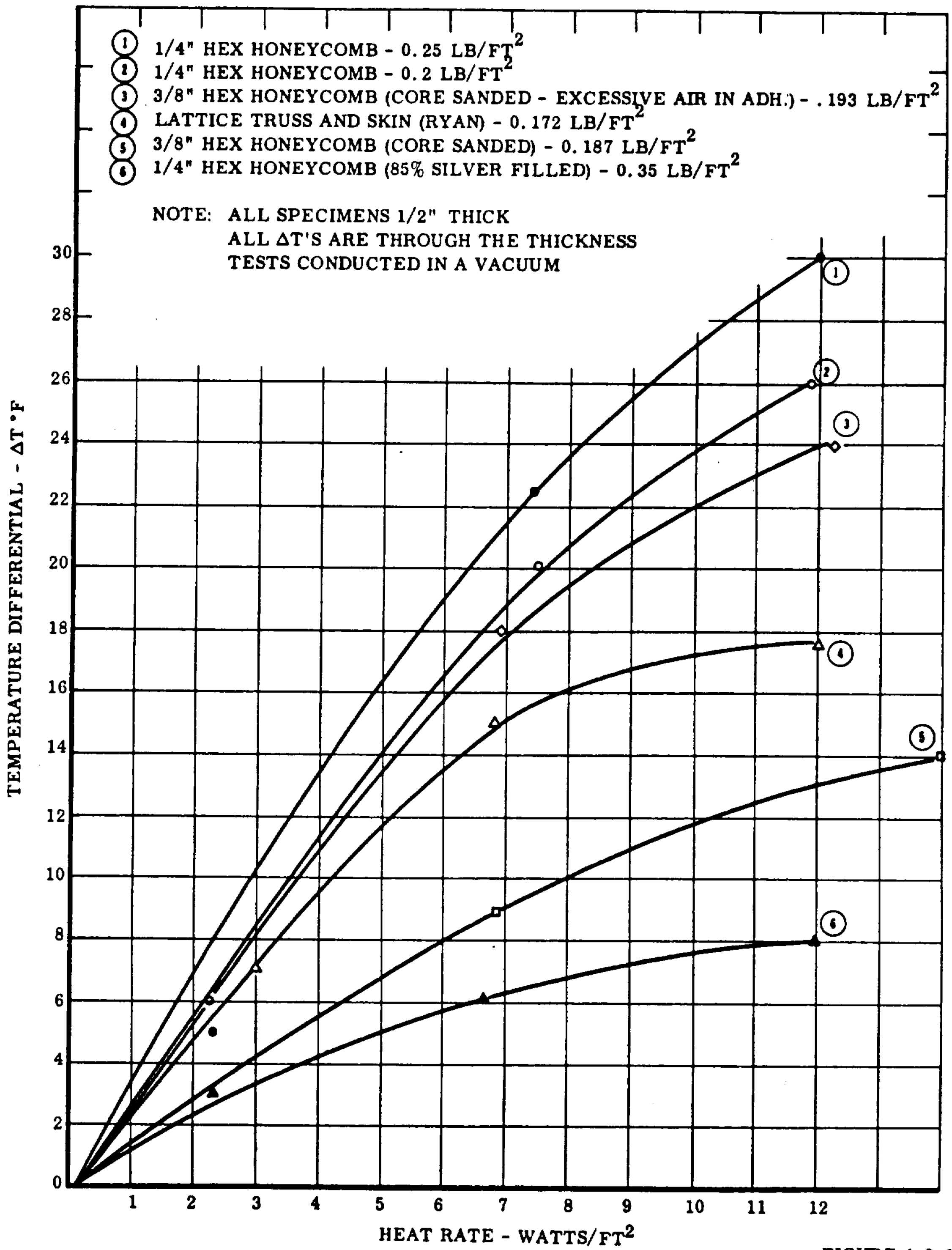

FIGURE 4.2-18

TABLE 4.2-3

ADHESIVE THERMAL CONDUCTIVITY TEST RESULTS

Adhesive System	K	Specimen Bond Thickness Inches
Plain epoxy (Bondmaster 688)	0.14	0.018
Epoxy with 70% by weight Ag	0.34	0.028
Epoxy with 80% by weight Ag	0.45	0.011
Epoxy with 85% by weight Ag	0.51	0.009
Epoxy with Al filler (Raymond R-86002)	0.29	0.006
Epoxide based adhesive (Eccobond 57C)	1.10	0.120

Note: "K" is the thermal conductivity in Btu/hr-ft^2-°F-ft

Composite Material Thermal Distortion Tests

Honeycomb sandwich composite material thermoelastic distortion testing was accomplished on the rig shown in Figures 4.2-20, 4.2-21, and 4.2-22. This test set-up consists of a mount for holding the test sample in a vertical position attached only at the bottom end. An electrical heater is used to heat one face of the specimen with a water cooled copper plate as the heat sink for the back face. This arrangement provides a controlled temperature differential across the specimen thickness. To observe deflections, optical targets are attached to the specimen and their movement is observed and measured with a micrometer microscope. The specimen, heaters, and cold plate are enclosed in a specially built vacuum chamber and tests are conducted in a high vacuum.

Typical results are shown in Figure 4.2-23 for the prototypical sandwich material. These test results were used to calculate an apparent coefficient of thermal expansion of the sandwich material for the thermoelastic structural analysis of the collector as mentioned previously in Section 4.2.5.3.

Composite Material Mechanical Testing

Mechanical testing of the composite sandwich material was performed per MIL-STD 401 A for short beam specimens. Also, long plate beam tests were performed. Values for flexural rigidity and shear modulus were obtained and correlated well with formulas given in MIL-STD 401 A. These values were used in the structural analysis to define the elastic characteristics of the sandwich material.

SANDWICH MATERIAL THERMAL DISTORTION TEST SCHEMATIC

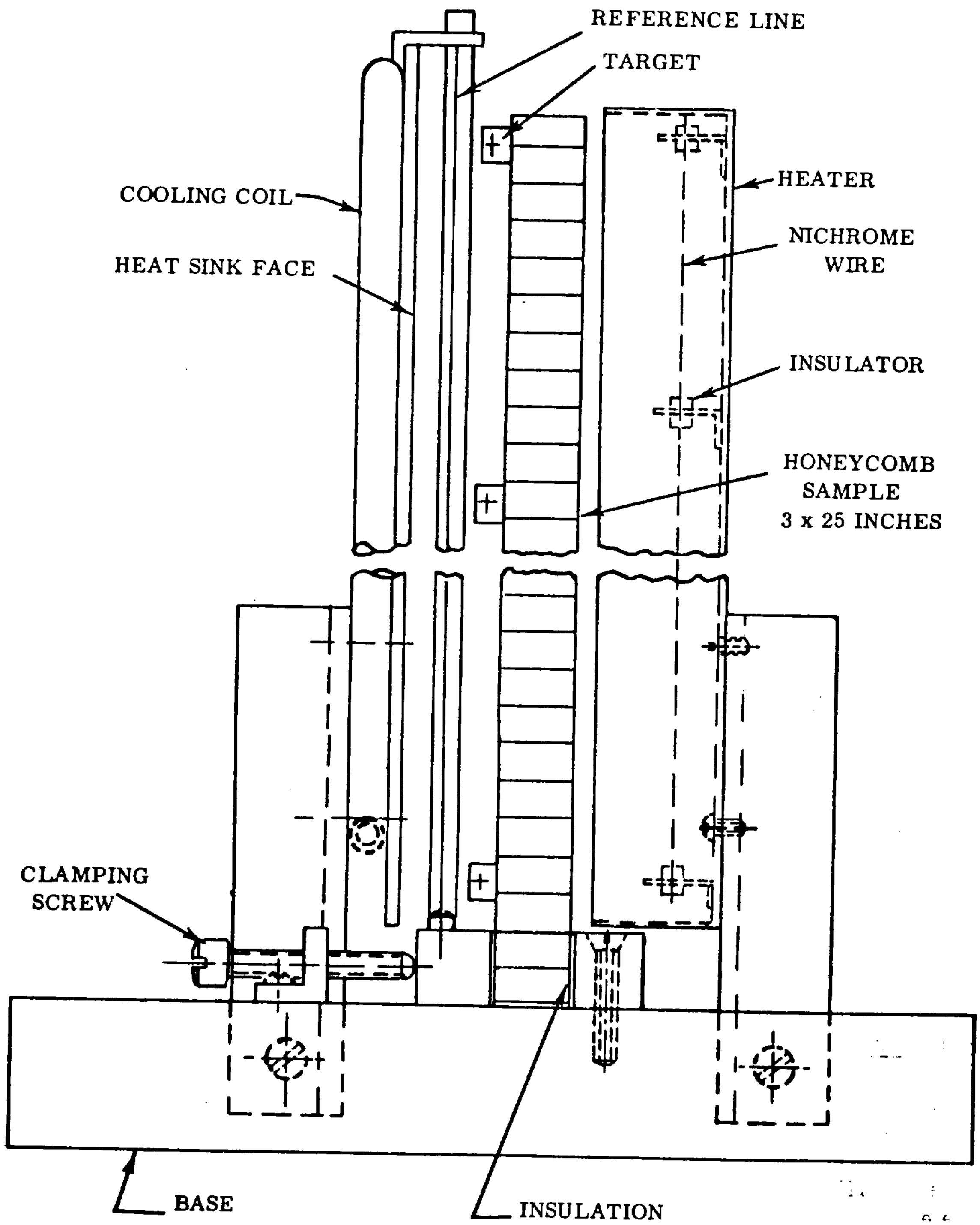

TEST I
RIBBON PERPENDICULAR TO LENGTH
DEFLECTION VS LENGTH AND
DEFLECTION VS ΔT

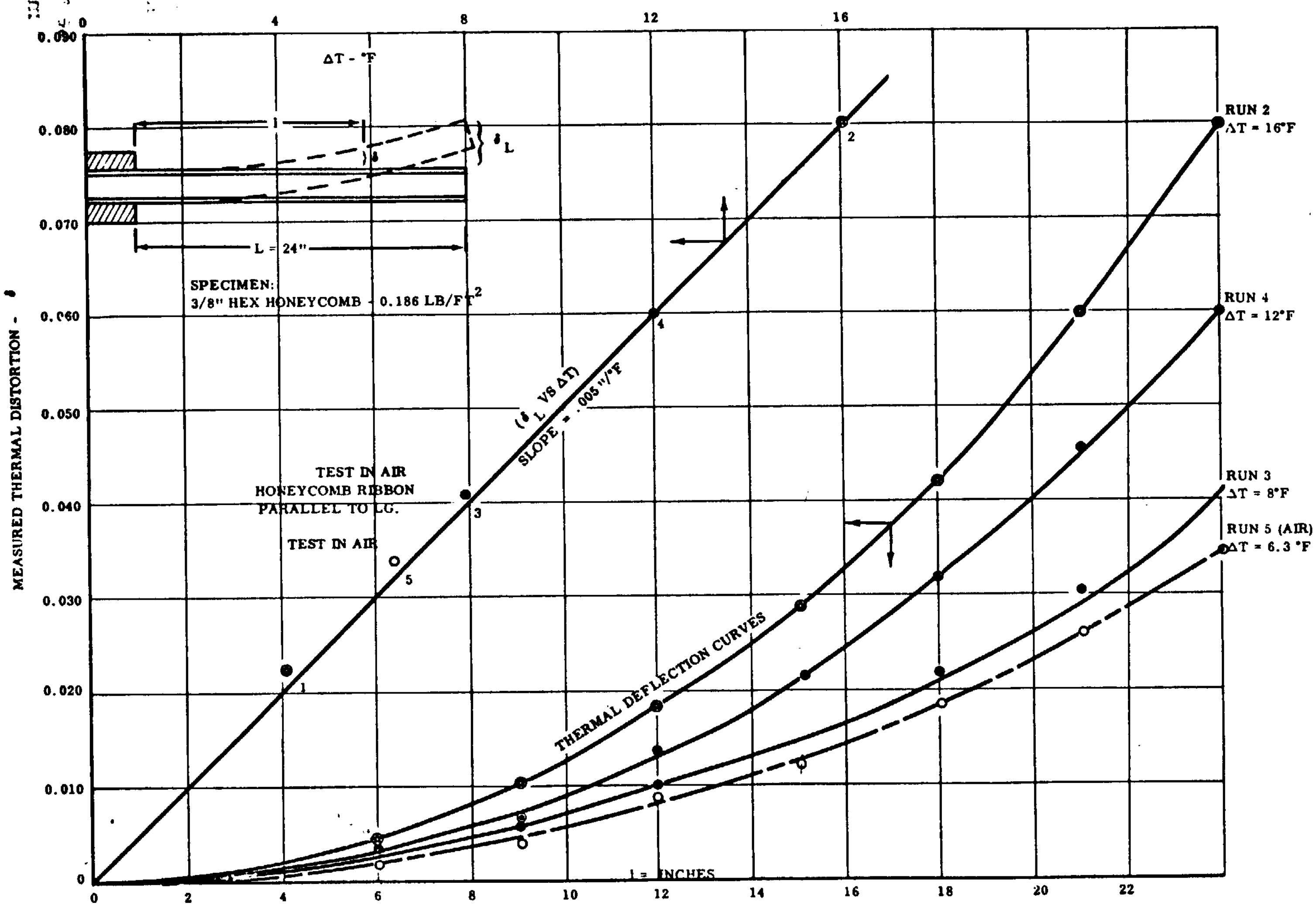

B-18

ment of the grid shadow on the screen. The shadow box traverses the entire length of the part and photographs are made of the screen to record the deviations. Dimensional measurements are also made and recorded using the template coordinate system.

7.3.3 Sector Optical Inspection Results

A typical grid screen inspection photograph is shown in Figure 7.3-3. It is seen that error deviations in both the radial and circumferential directions can be measured. A composite photograph of sector SPTR-1 is shown in Figure 7.3-4.

Error indications for each increment can be measured. By using a geometric relationship, the gross angular deviation of the surface at each location was plotted as shown in Figures 7.3-5 and 7.3-6 for the radial and circumferential deviations, respectively. Spring back effects can also be seen.

An indication of optical quality can be obtained from this data by relating surface area to the surface deviations. Figure 7.3-7 shows the percentage of collector intercepted area which is within various degrees of quality. The shaded area shows the range of differences between a row of data points along the centerline and those at the edges. The spring back is also shown plotted, and in the worst case would be additive with the gross waviness.

Figure 7.3-6 shows that the measured circumferential errors are large and are an overcurvature of the sector in the short direction. This characteristic was traced to be a permanent set which had occurred in the fabrication tool after several curve heating cycles.

7.3.4 Honeycomb Markoff Inspection Results

The honeycomb markoff, which is typical of the Sunflower collector material, was investigated using the proficorder shown in Figure 5.5-1. This instrument not only plots micro-finish but also can be adjusted to plot waviness profiles. Typical honeycomb - markoff profiles are shown in Figure 7.3-8 for specimens which were actually cut from sector SPTR-1 after solar testing (see section 8.1.1). These show the best and the worst cases of honeycomb markoff which were observed. For SPTR-1, an estimated 40% of the surface had the lower value of markoff, while the remainder was between the 6 minute minimum and the 26.4 minute maximum. With improved process control, it is believed that 95% of the surface would have cell markoff within the lower slope deviation.

Since the surface deviation in a cell varies over the hex (Figure 7.3-8), these typical slopes can be area-weighted. The results are shown in Figure 7.4-1 for the measured data from SPTR-1. Other sectors which were inspected showed similar characteristics.

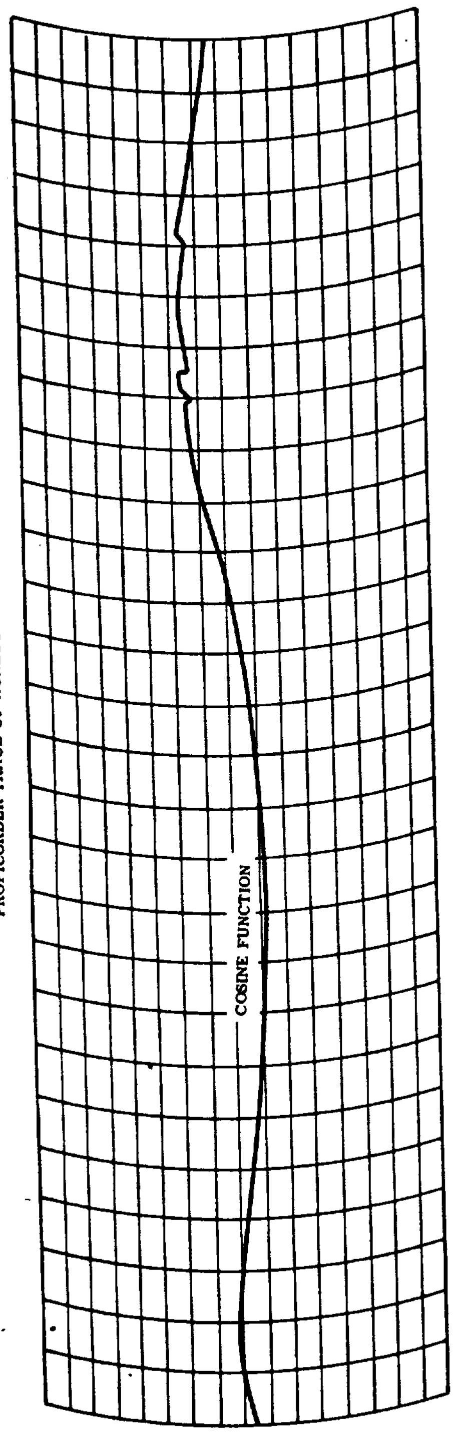

PROFICORDER TRACE OF HONEYCOMB MARKOFF

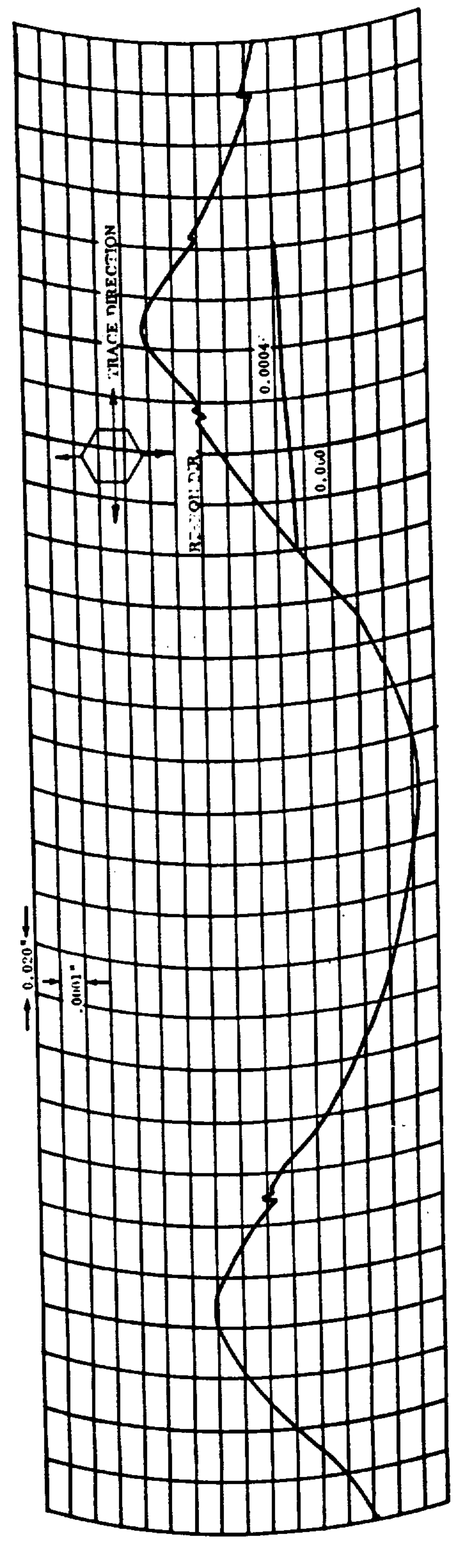

TYPICAL OF SPTR 1 STATION 171

DISTRIBUTION OF RADIAL ANGULAR ERRORS FOR THE SUNFLOWER COLLECTOR

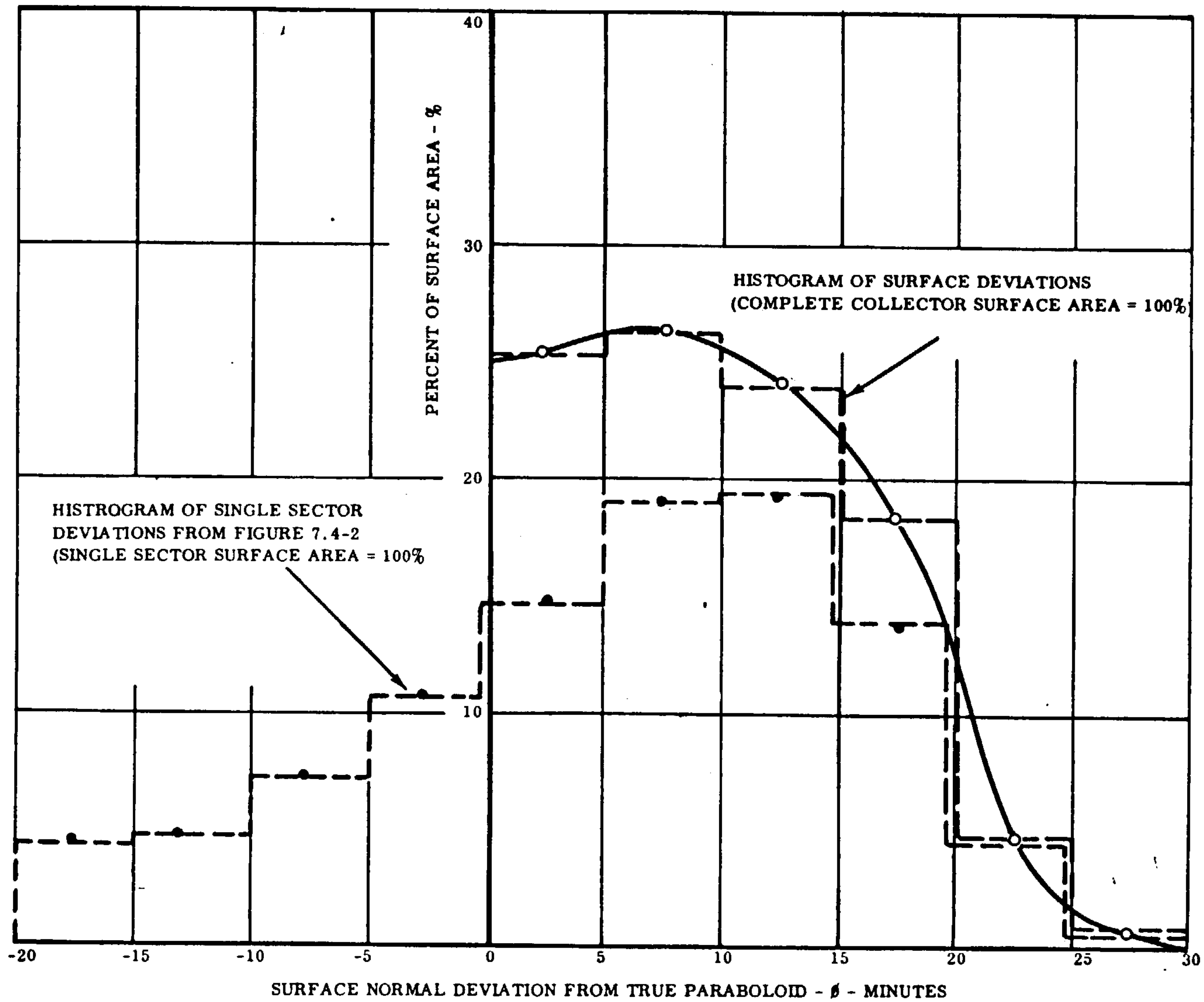

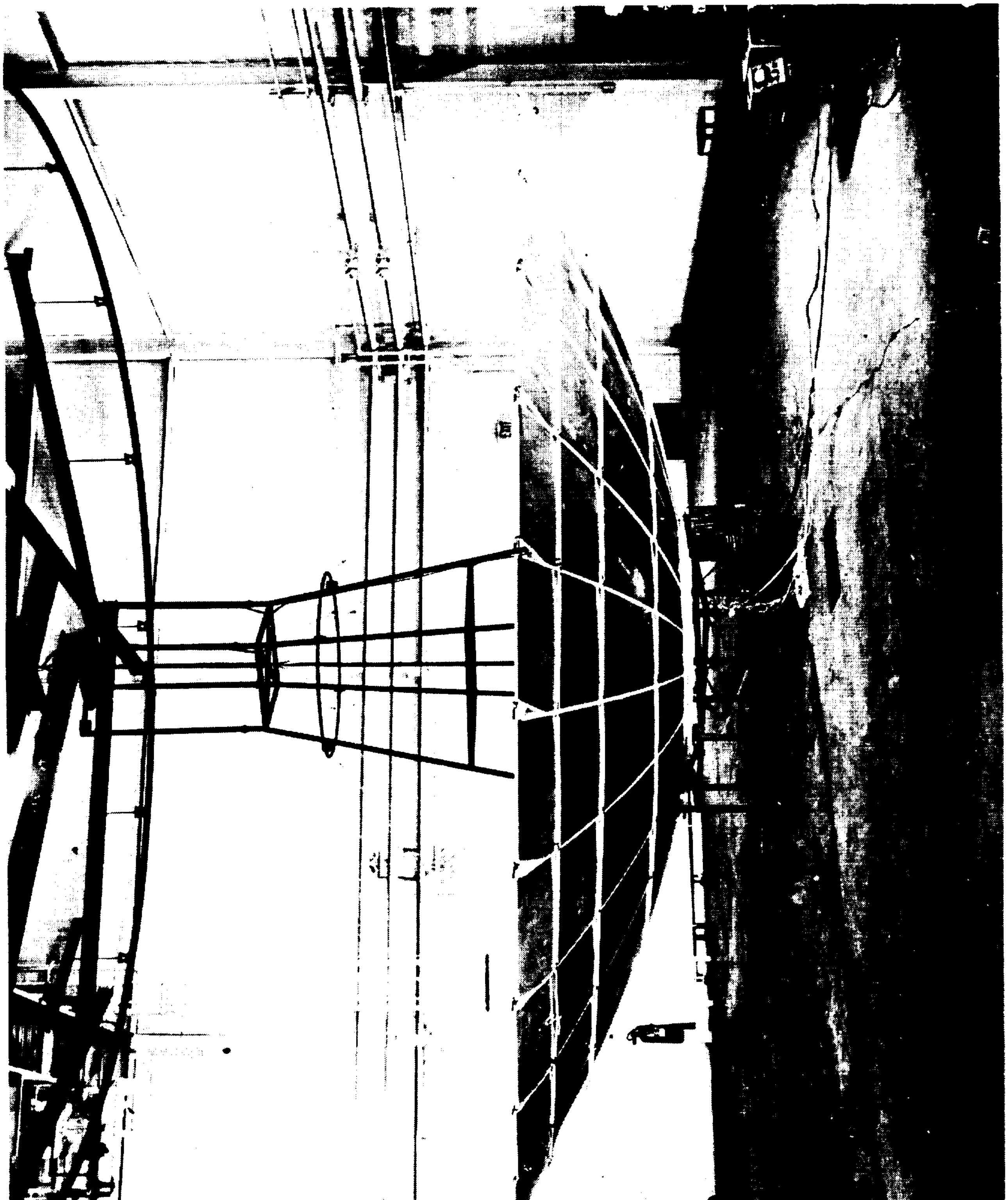

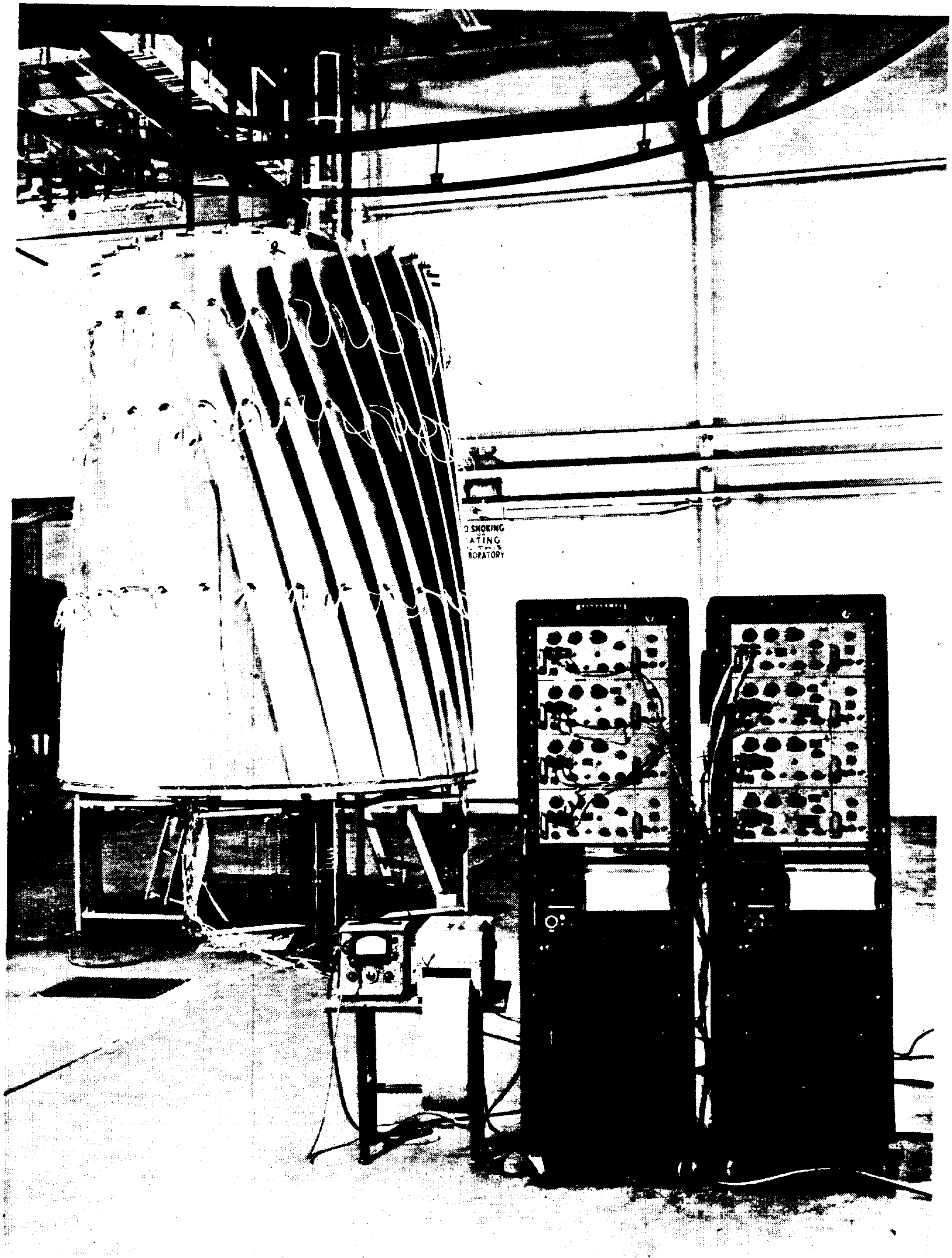

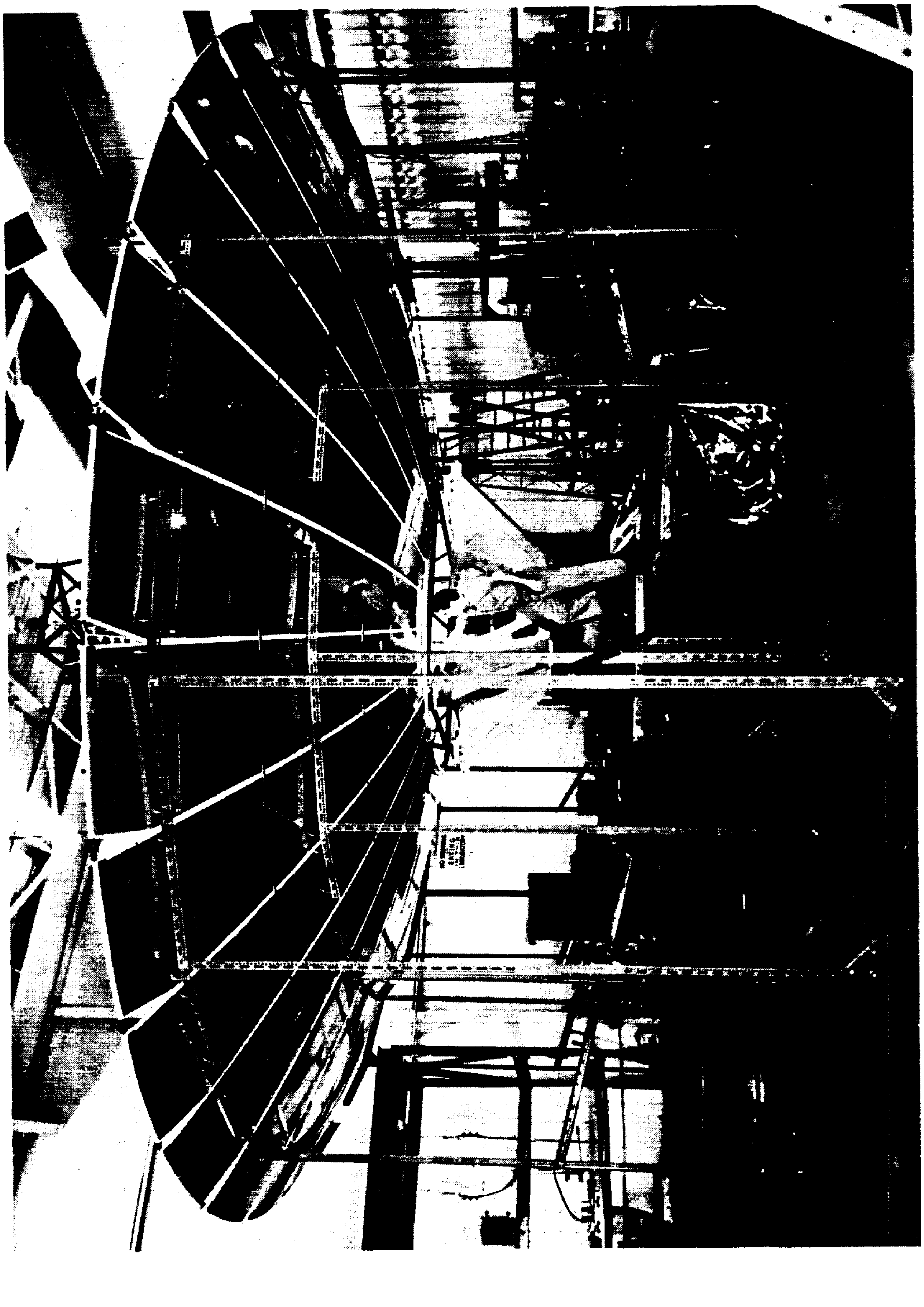

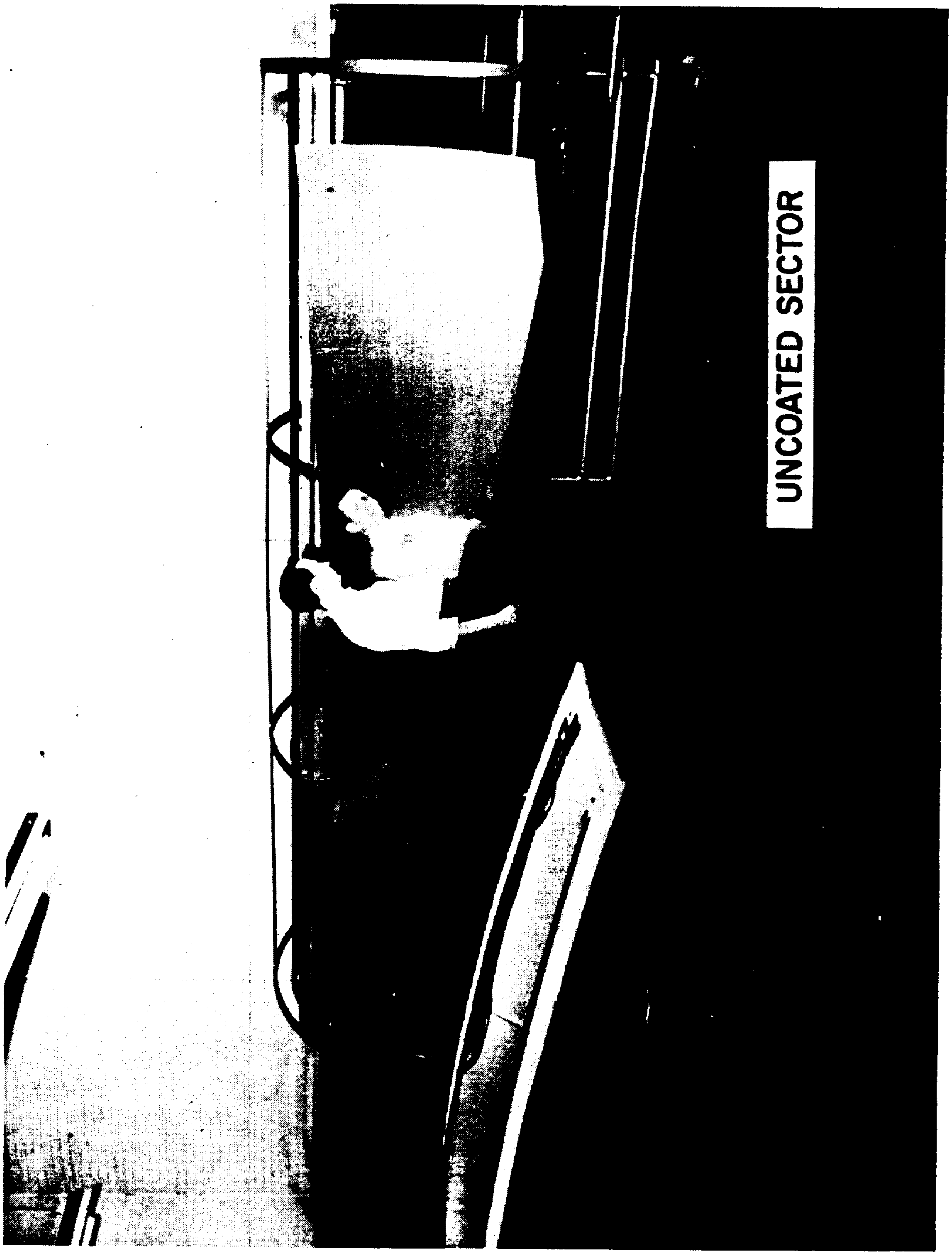
UNCOATED SECTOR

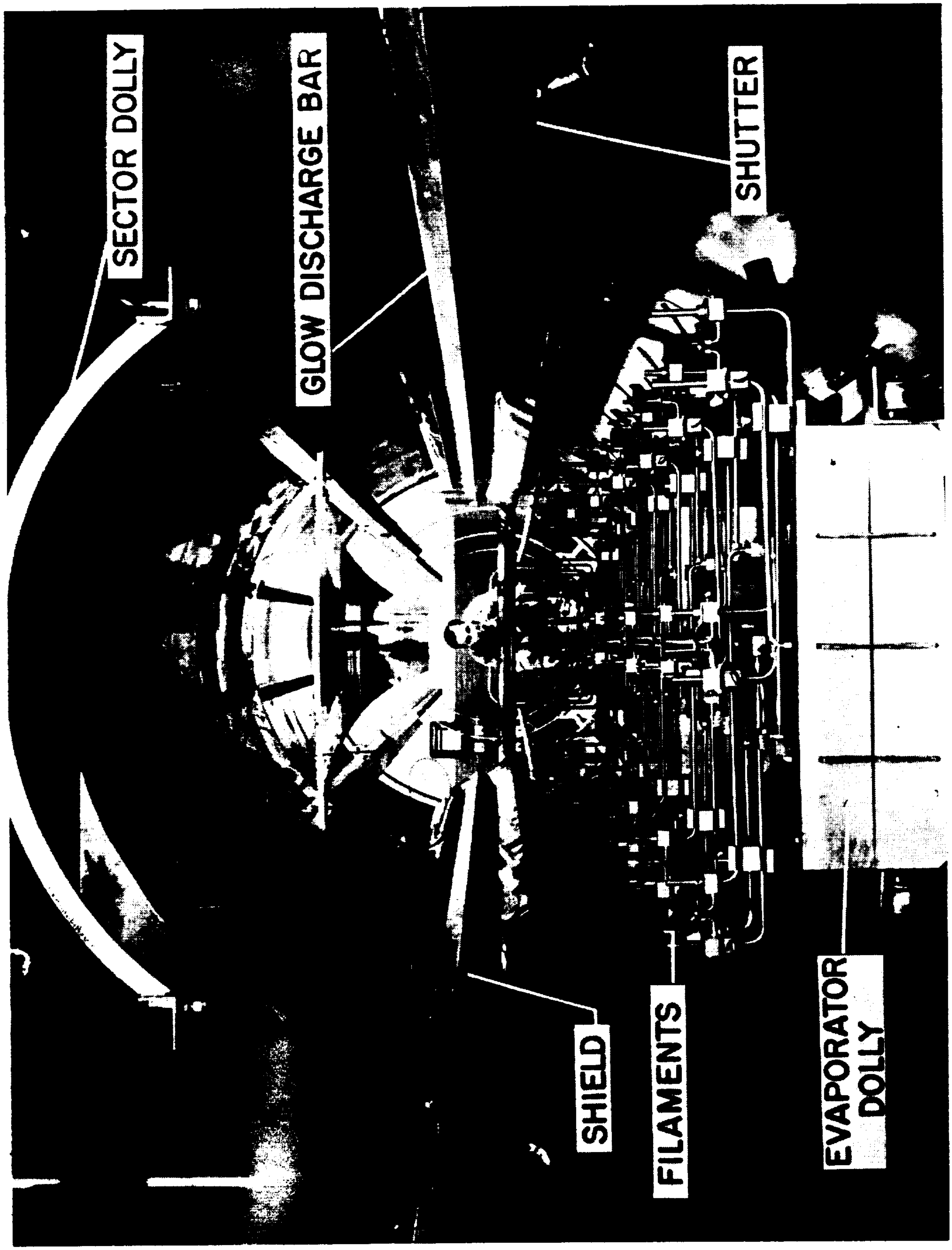
SECTOR DOLLY
GLOW DISCHARGE BAR
SHUTTER
SHIELD
FILAMENTS
EVAPORATOR DOLLY

Appendix C

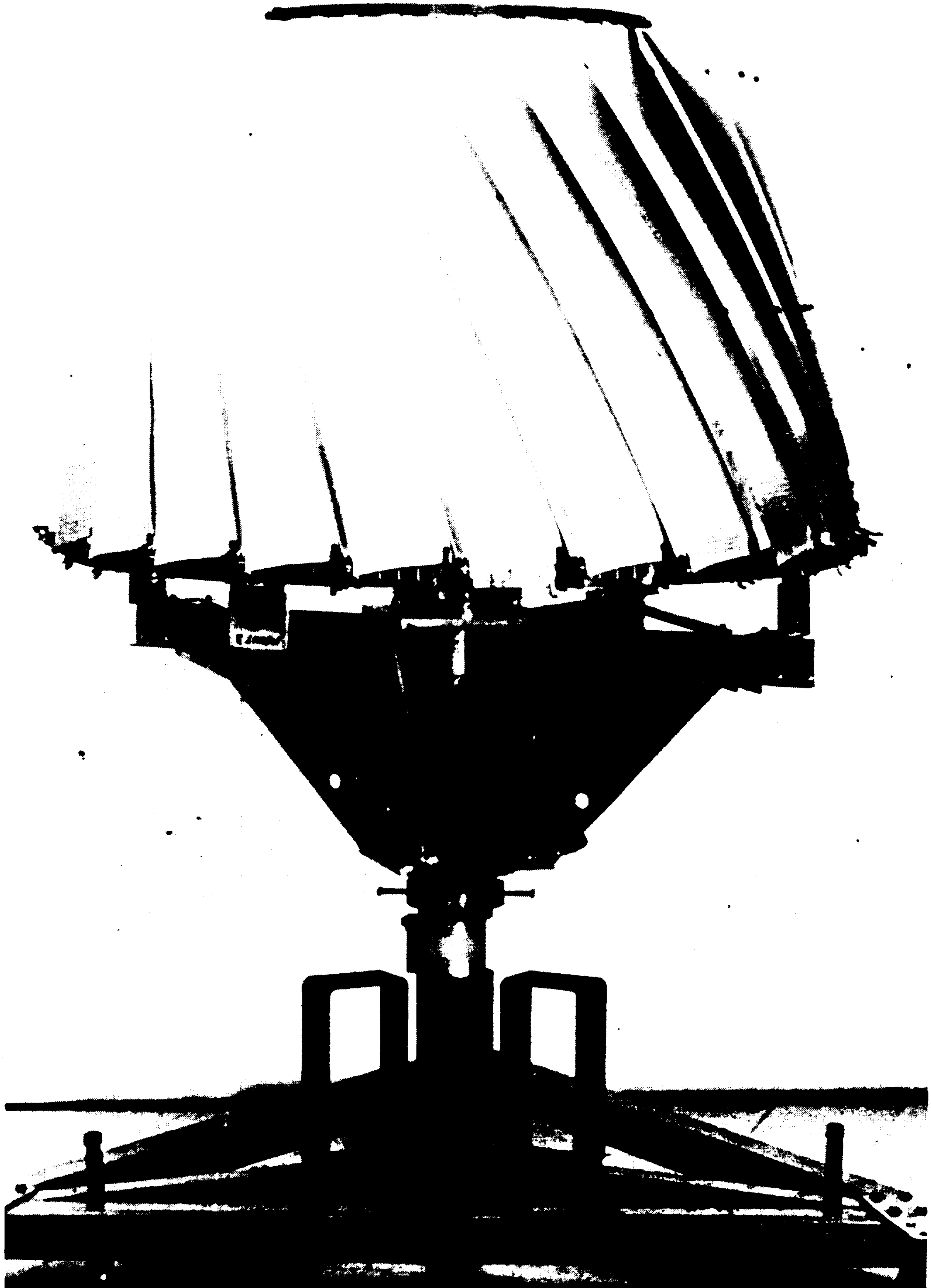

STOWED 9.5 FT. ANTENNA

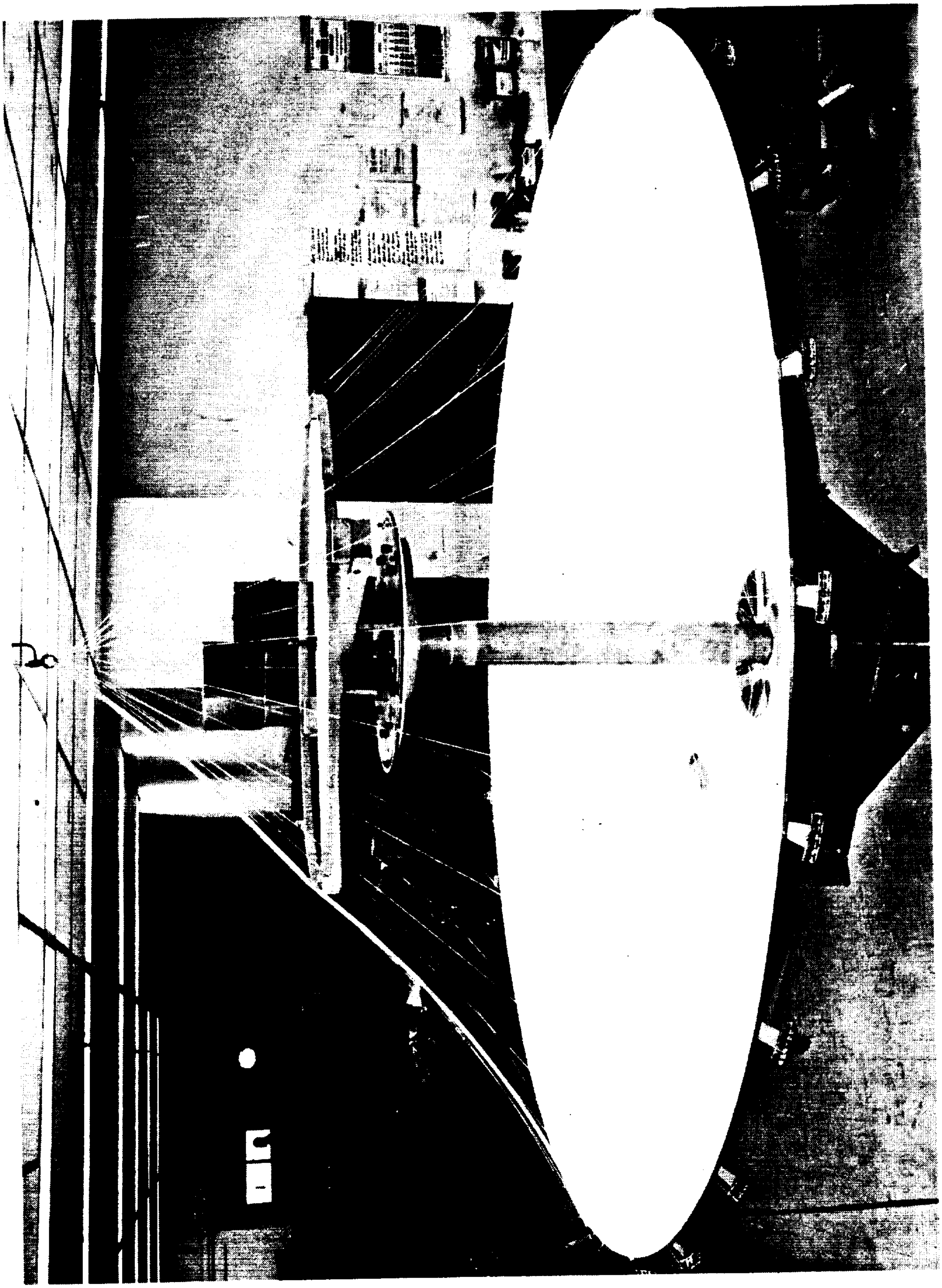

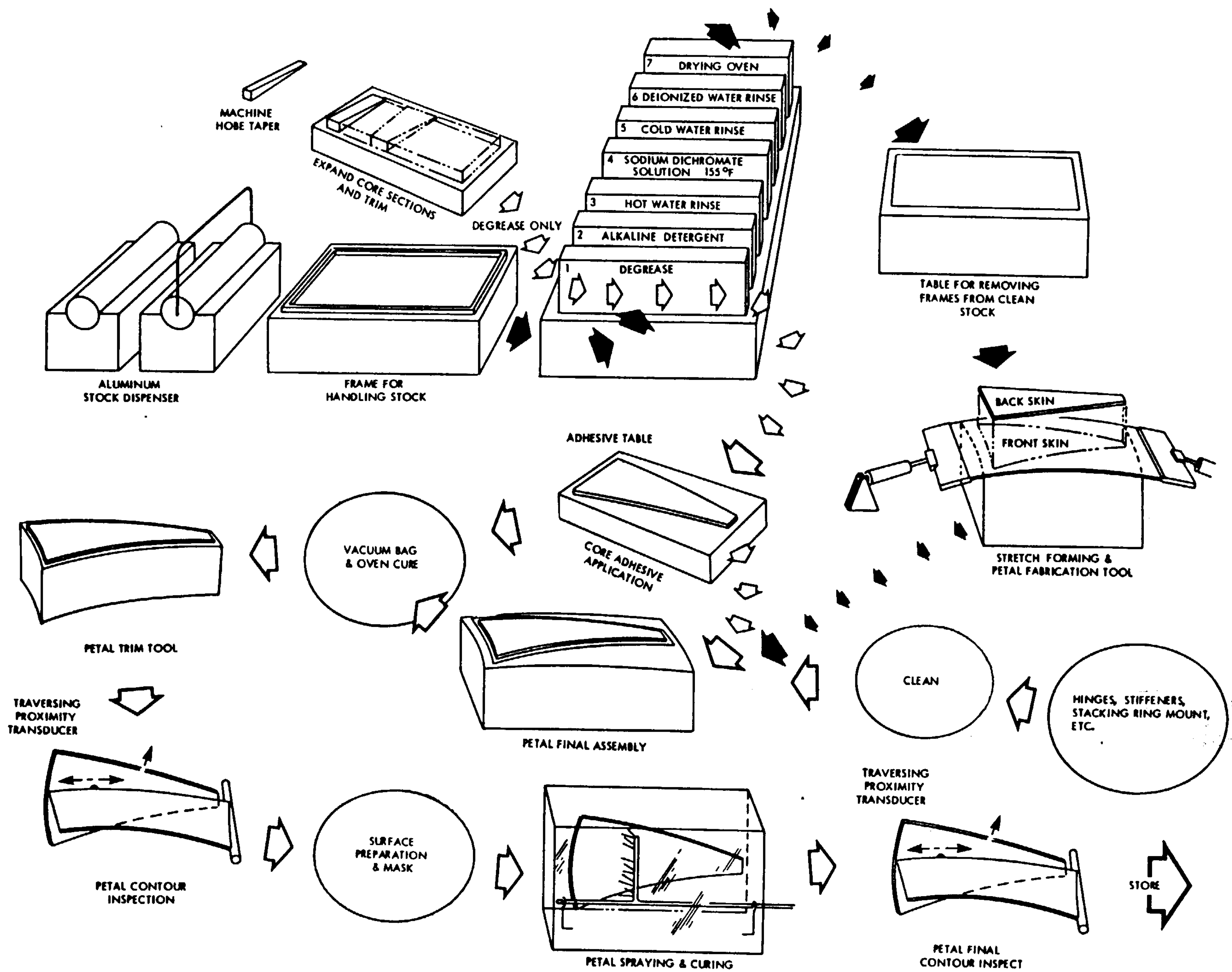
MACHINE HOBE TAPER
EXPAND CORE SECTIONS AND TRIM
DEGREASE ONLY
7 DRYING OVEN
6 DEIONIZED WATER RINSE
5 COLD WATER RINSE
4 SODIUM DICHROMATE SOLUTION 155°F
3 HOT WATER RINSE
2 ALKALINE DETERGENT
1 DEGREASE
TABLE FOR REMOVING FRAMES FROM CLEAN STOCK
ALUMINUM STOCK DISPENSER
FRAME FOR HANDLING STOCK
BACK SKIN
FRONT SKIN
STRETCH FORMING & PETAL FABRICATION TOOL
ADHESIVE TABLE
CORE ADHESIVE APPLICATION
VACUUM BAG & OVEN CURE
PETAL TRIM TOOL
PETAL FINAL ASSEMBLY
CLEAN
HINGES, STIFFENERS, STACKING RING MOUNT, ETC.
TRAVERSING PROXIMITY TRANSDUCER
PETAL CONTOUR INSPECTION
SURFACE PREPARATION & MASK
PETAL SPRAYING & CURING
TRAVERSING PROXIMITY TRANSDUCER
PETAL FINAL CONTOUR INSPECT
STORE

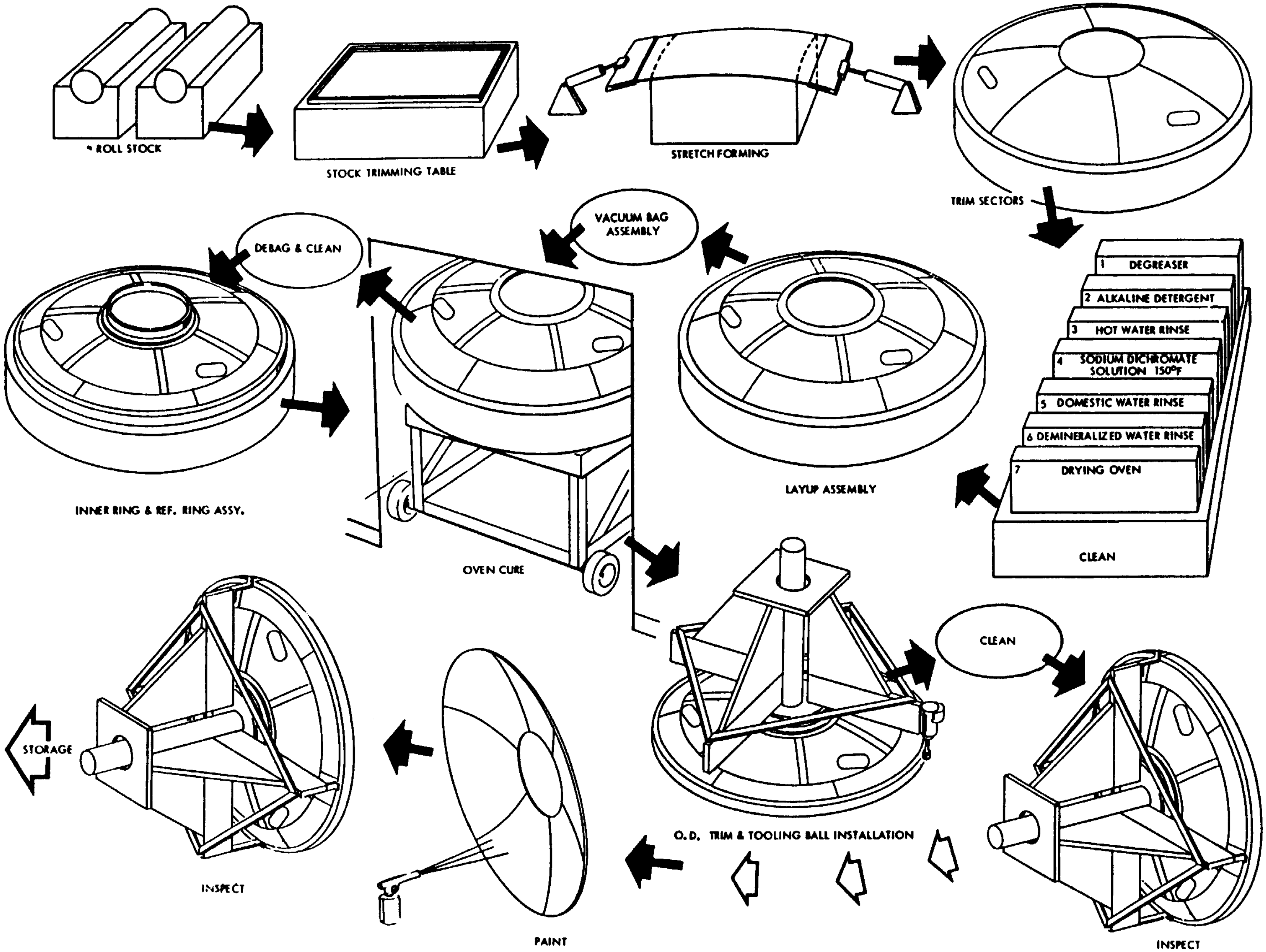
ROLL STOCK
STOCK TRIMMING TABLE
STRETCH FORMING
TRIM SECTORS
1 DEGREASER
2 ALKALINE DETERGENT
3 HOT WATER RINSE
4 SODIUM DICHROMATE SOLUTION 150°F
5 DOMESTIC WATER RINSE
6 DEMINERALIZED WATER RINSE
7 DRYING OVEN
CLEAN
LAYUP ASSEMBLY
VACUUM BAG ASSEMBLY
OVEN CURE
DEBAG & CLEAN
INNER RING & REF. RING ASSY.
CLEAN
INSPECT
O.D. TRIM & TOOLING BALL INSTALLATION
PAINT
INSPECT
STORAGE

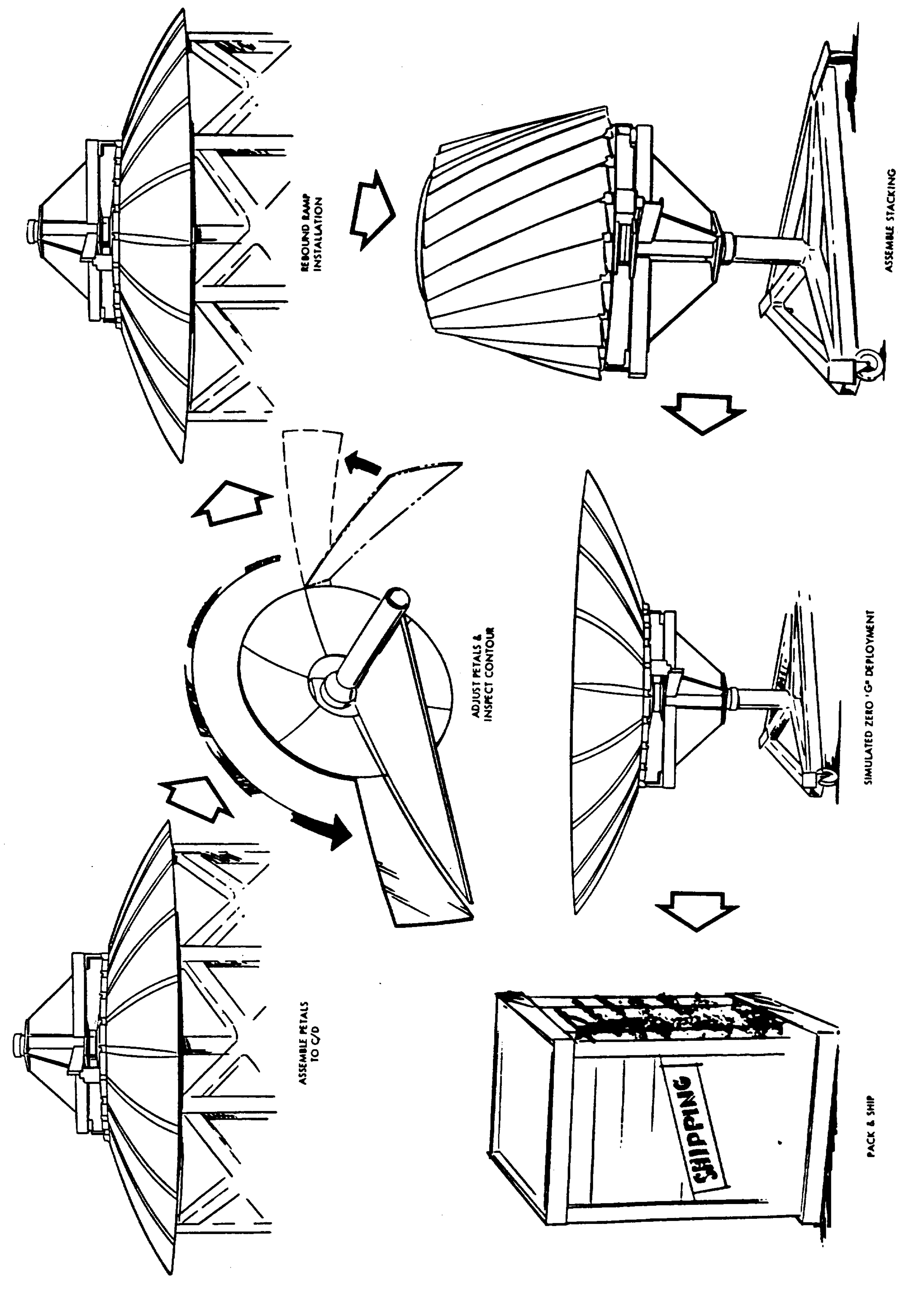
ASSEMBLE PETALS TO C/D
ADJUST PETALS & INSPECT CONTOUR
REBOUND RAMP INSTALLATION
ASSEMBLE STACKING RING
SIMULATED ZERO 'G' DEPLOYMENT
PACK & SHIP
SHIPPING

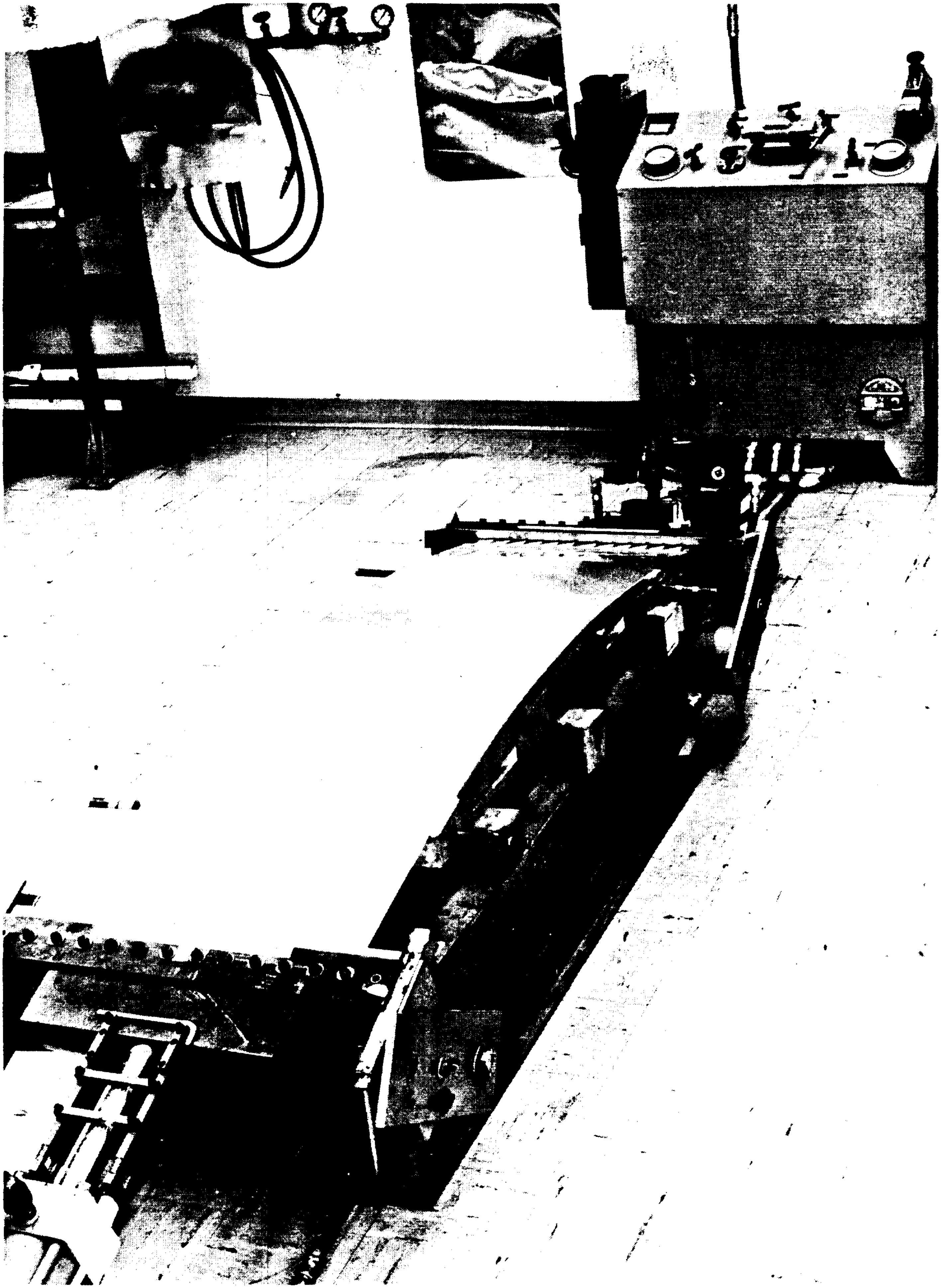

FIGURE 16C

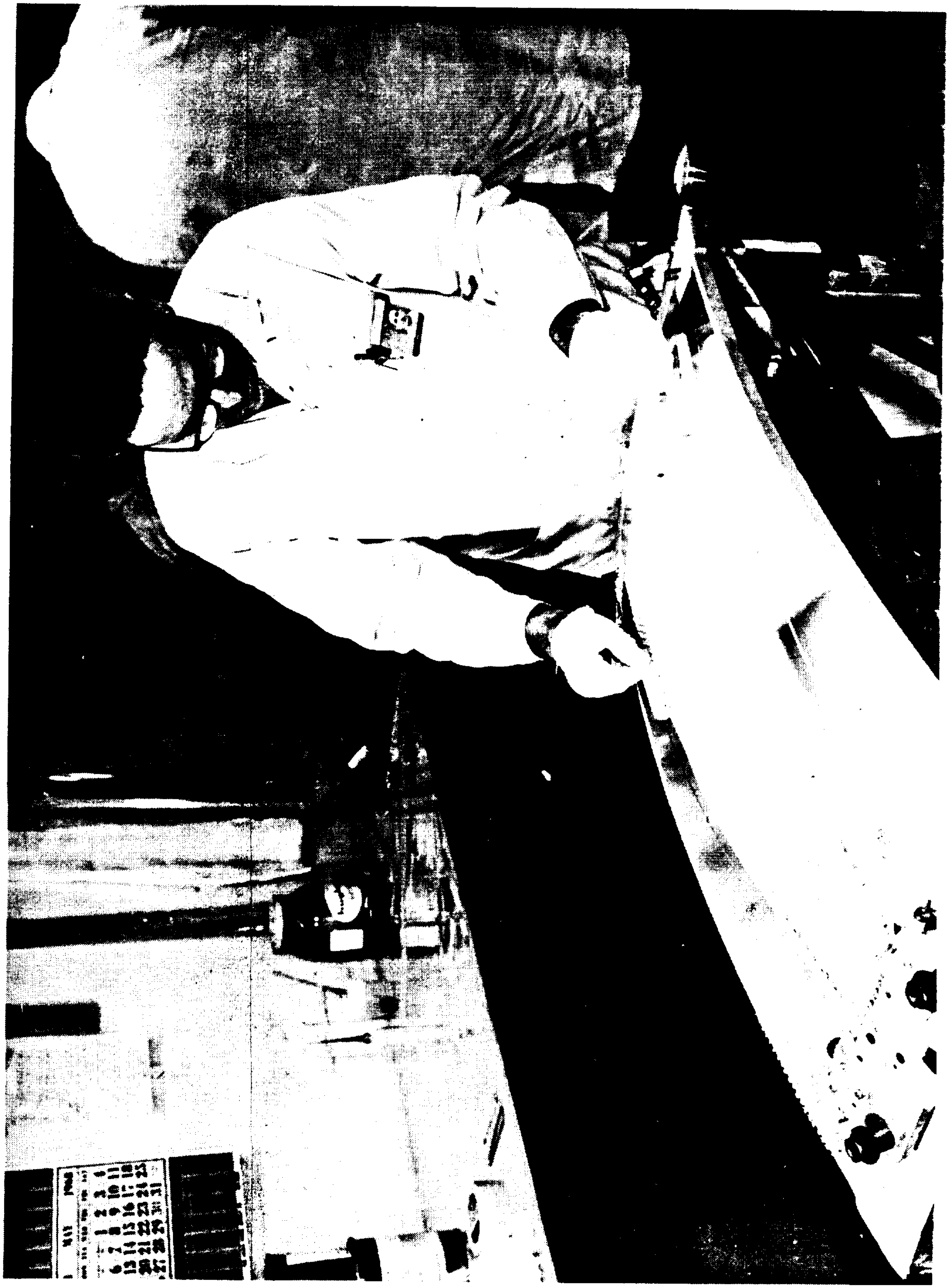

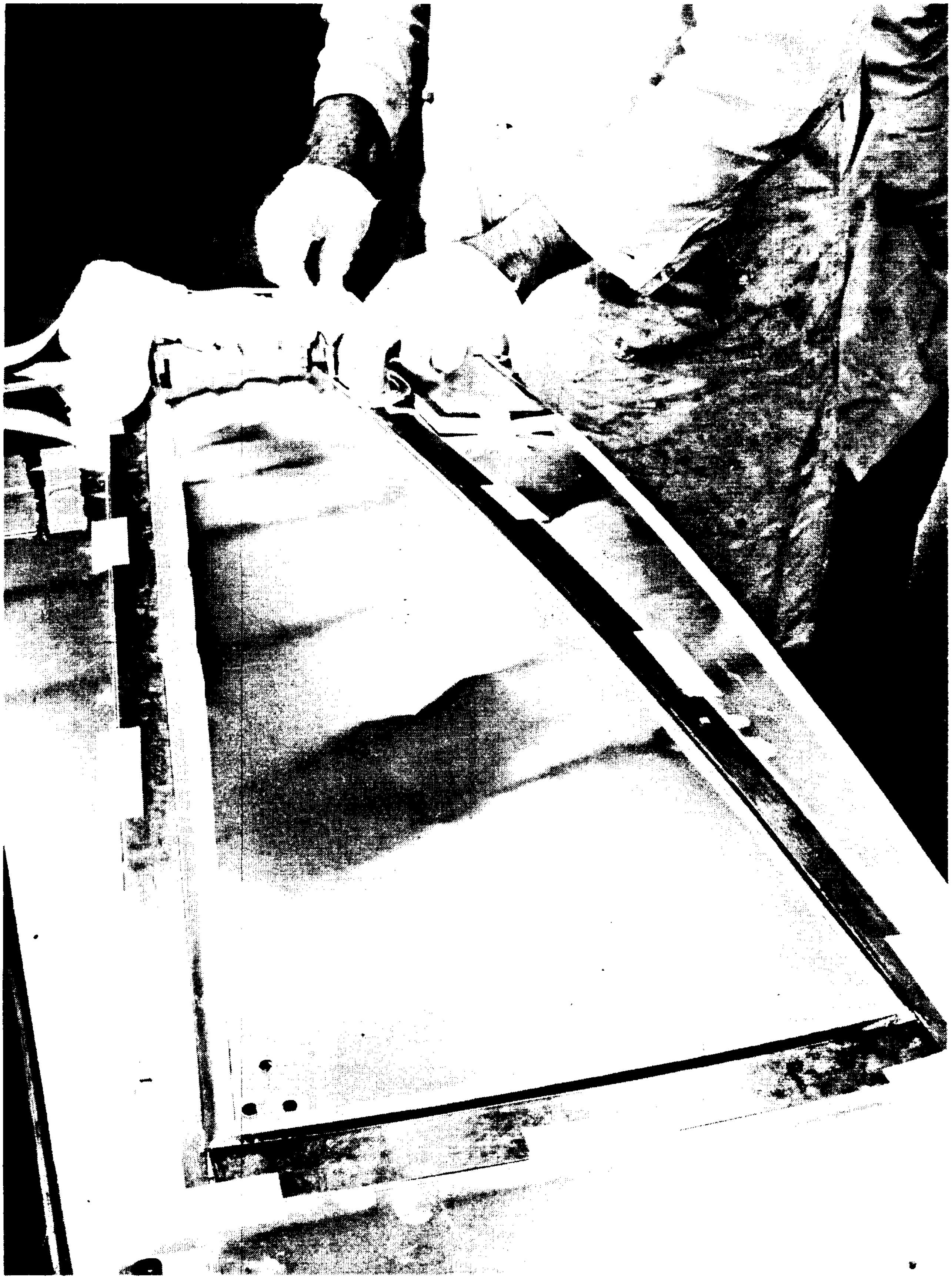

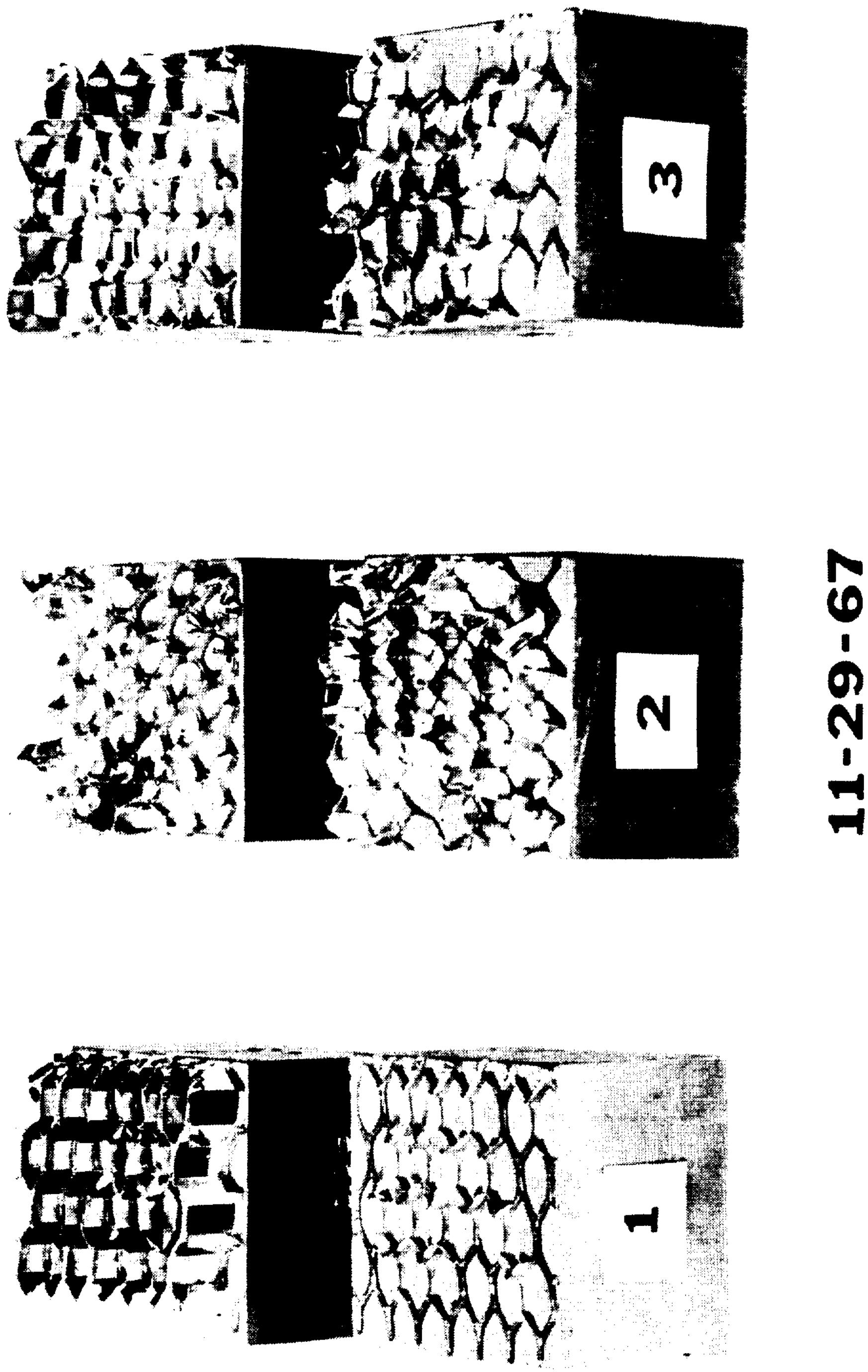

3
2
1
11-29-67

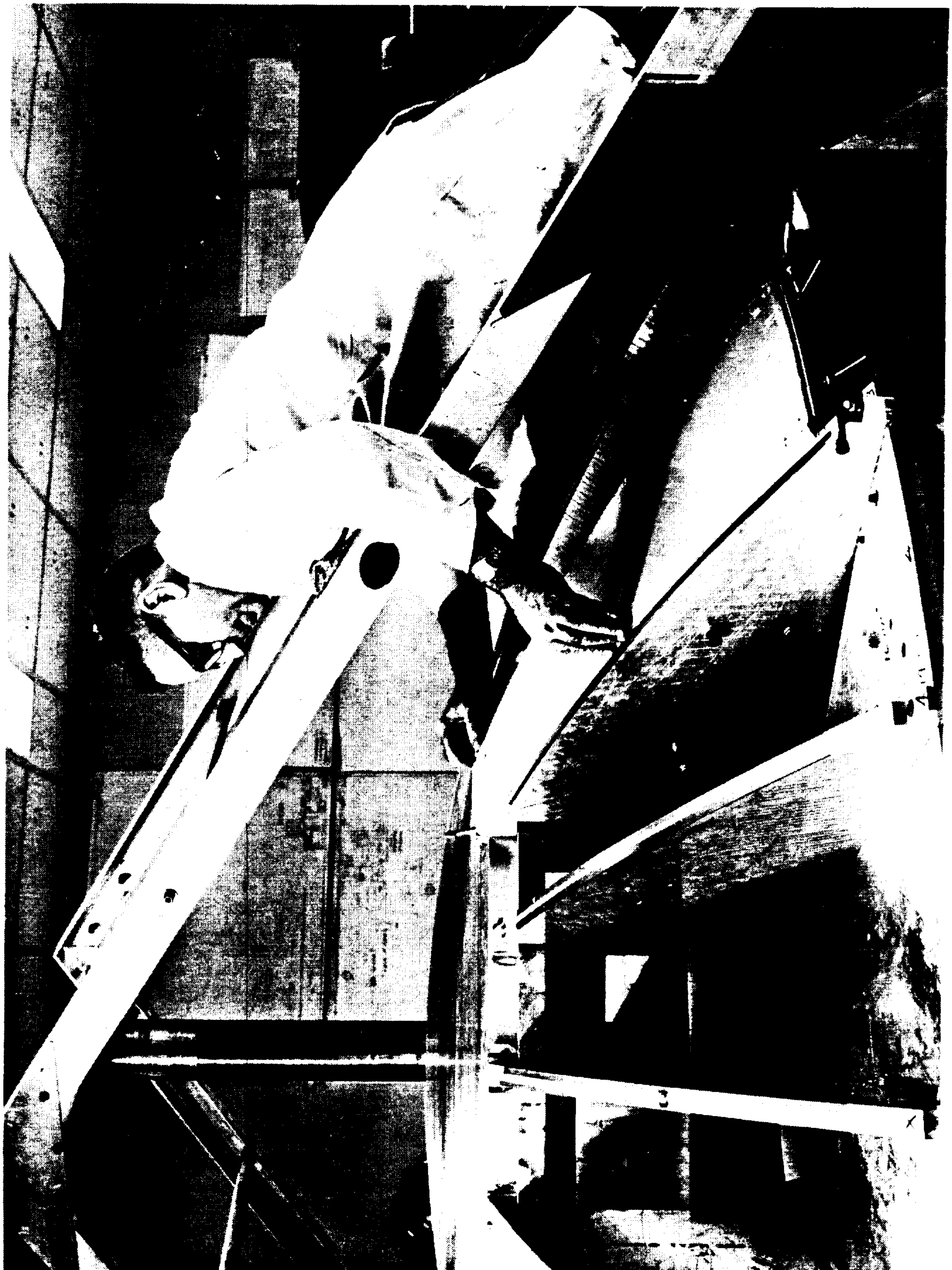

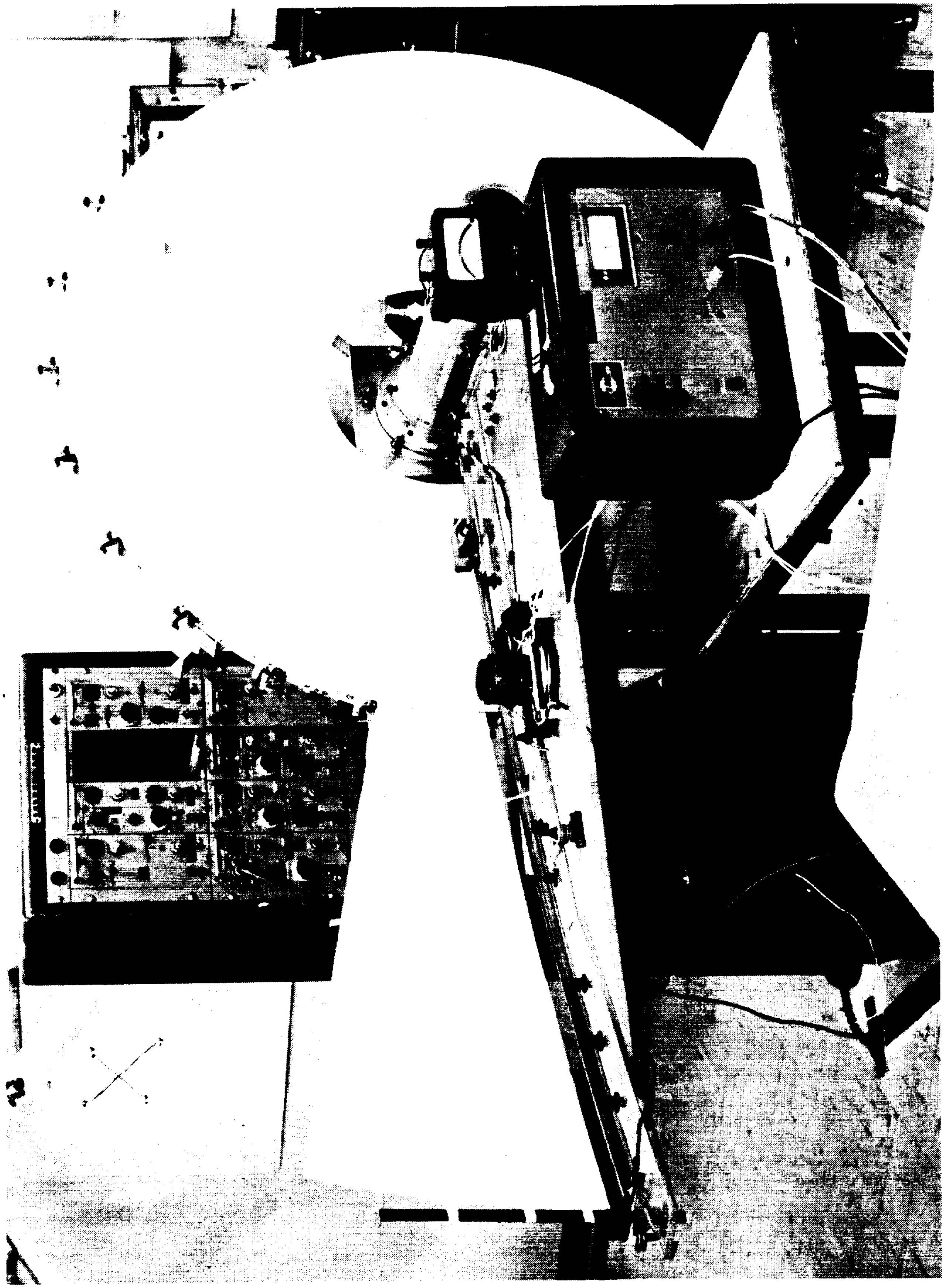

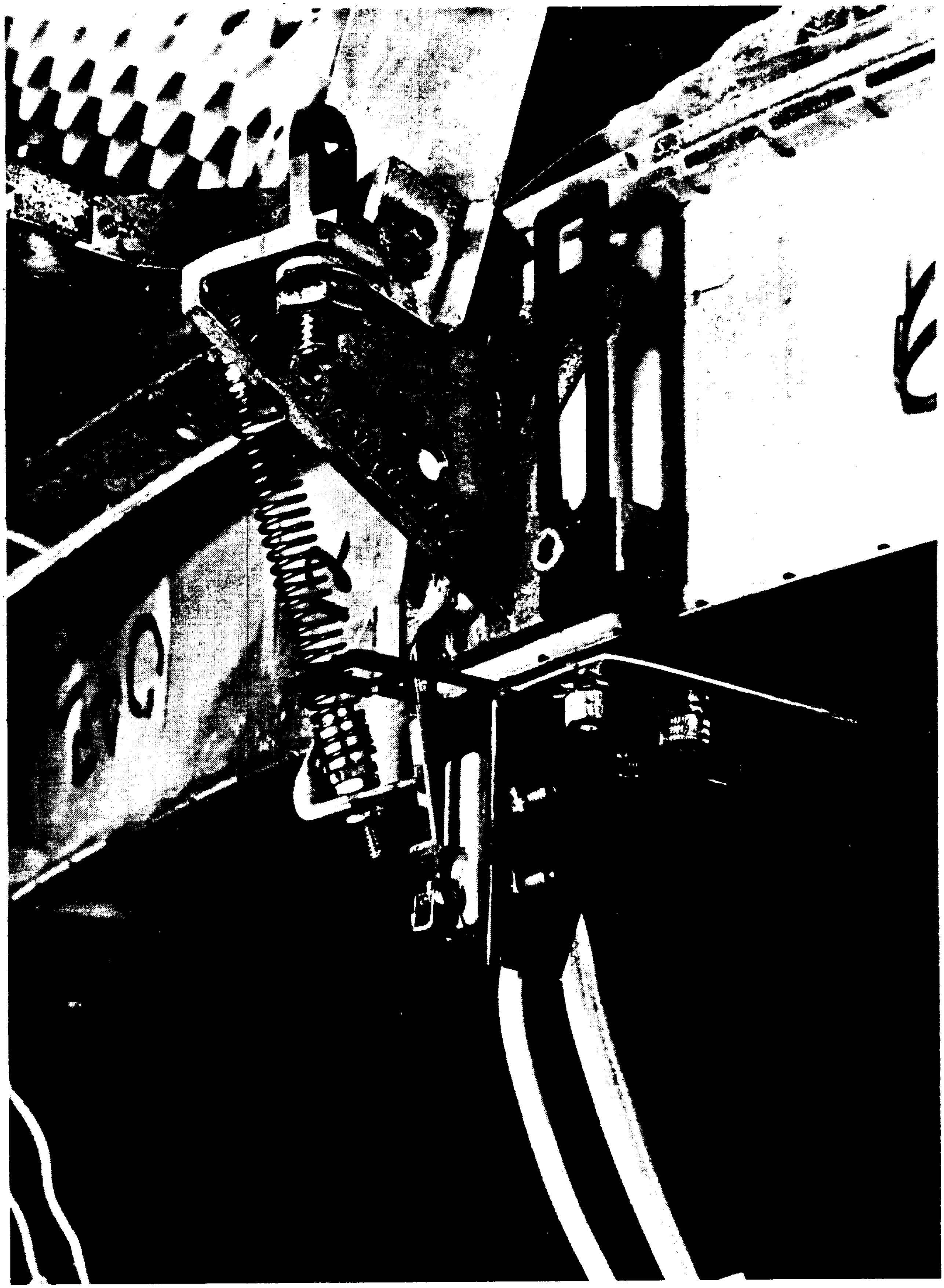

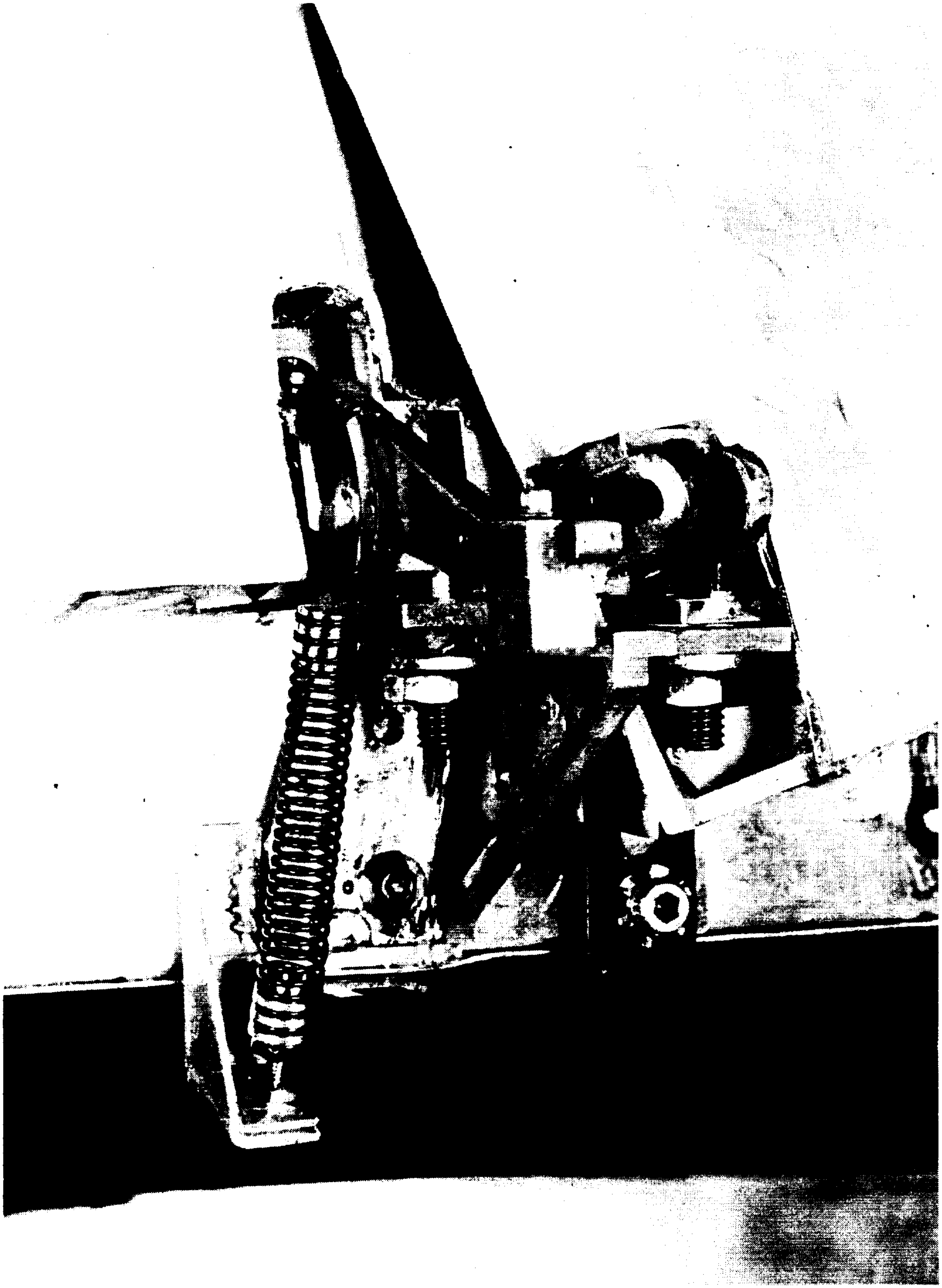

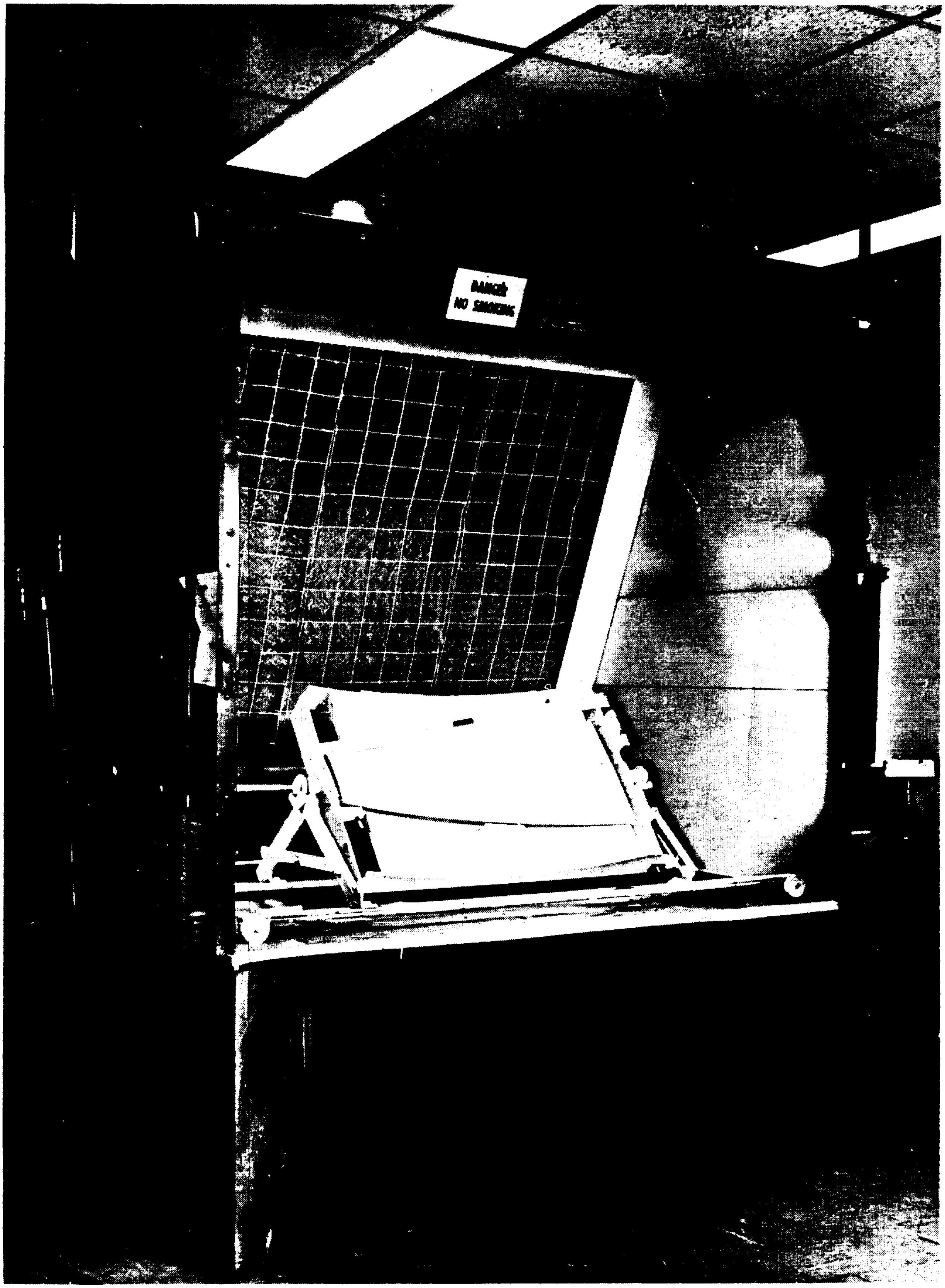
DANGER
NO SMOKING

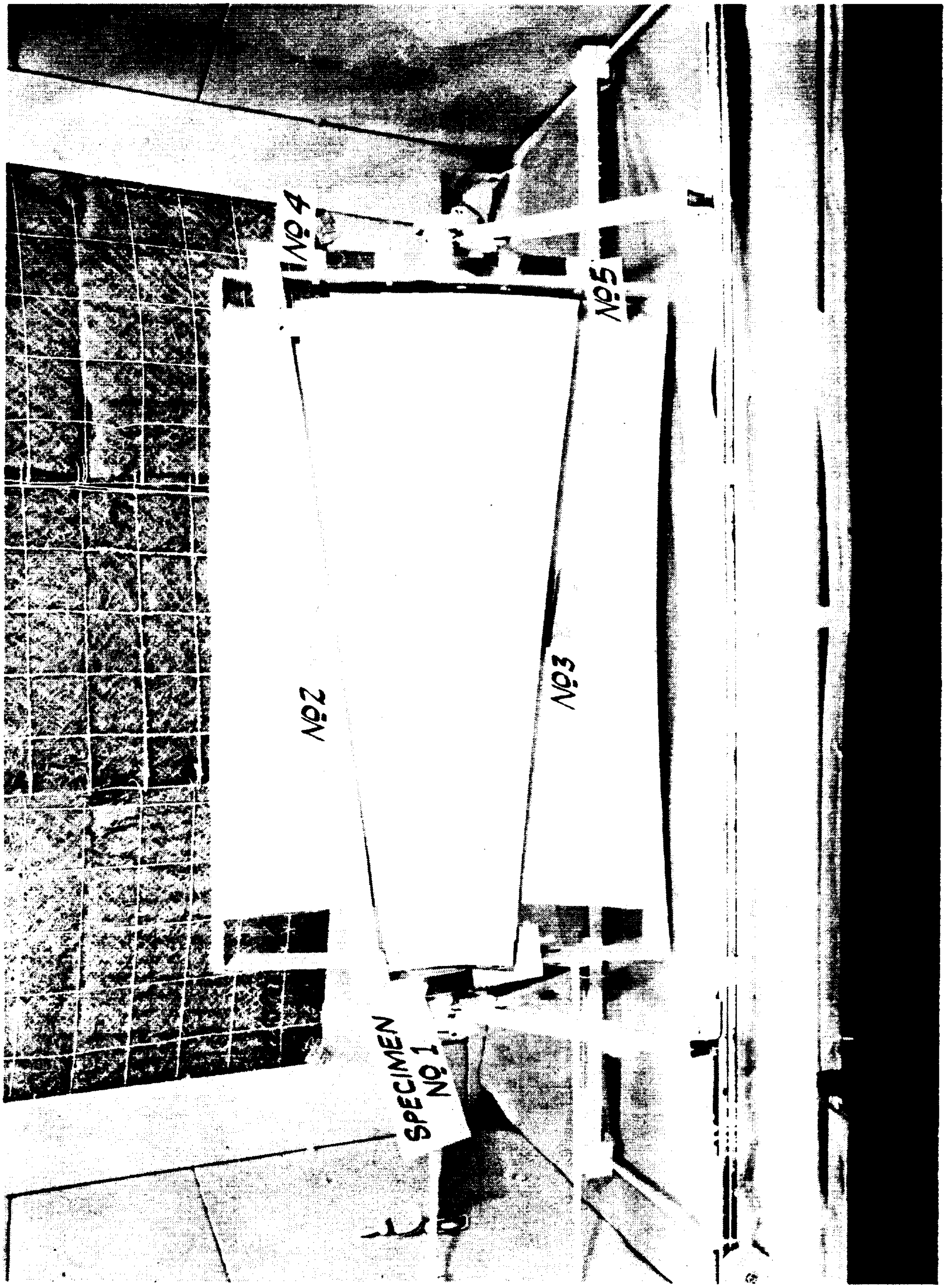
SPECIMEN
NO 1
NO 2
NO 3
NO 4
NO 5

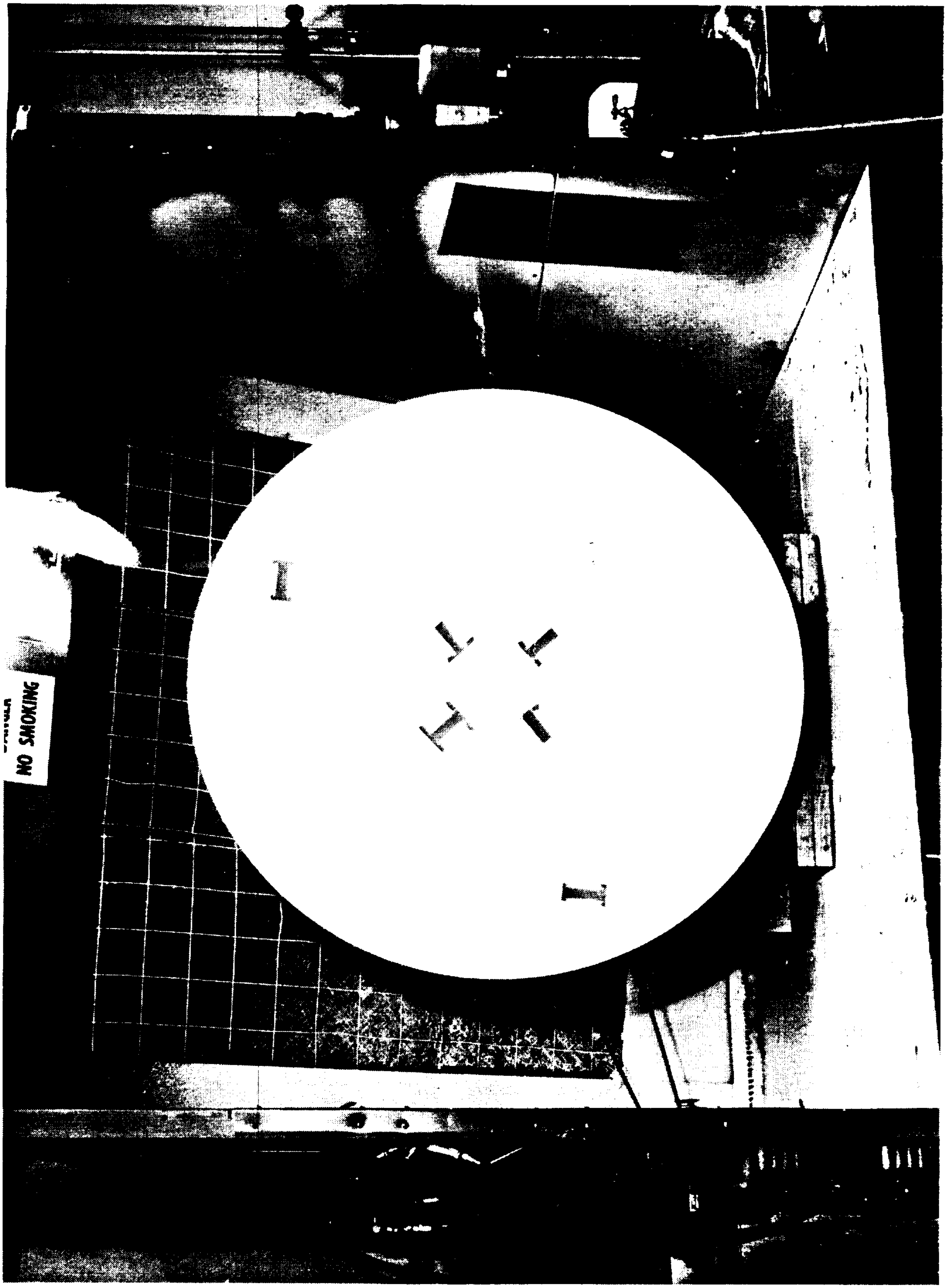
NO SMOKING

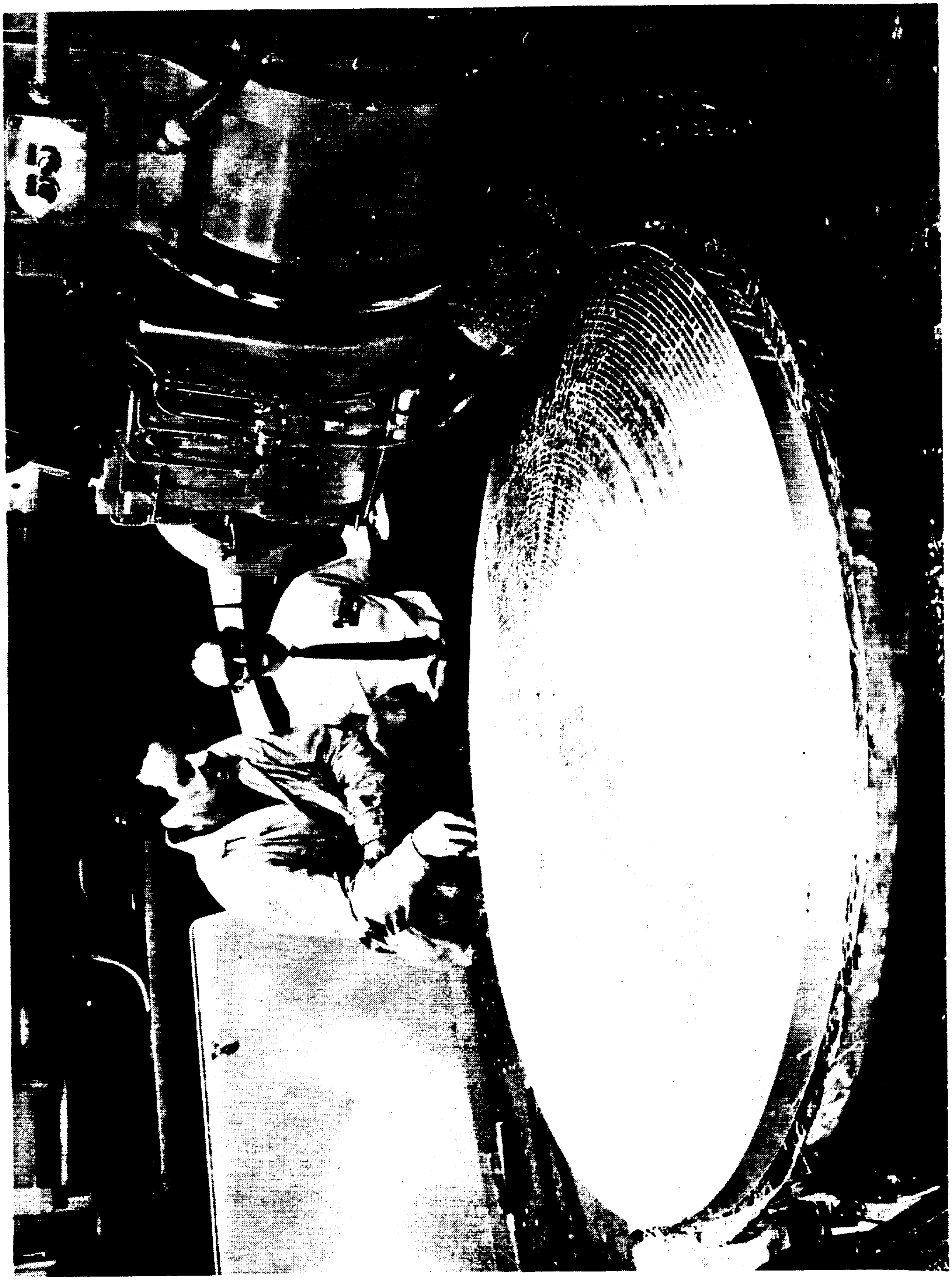

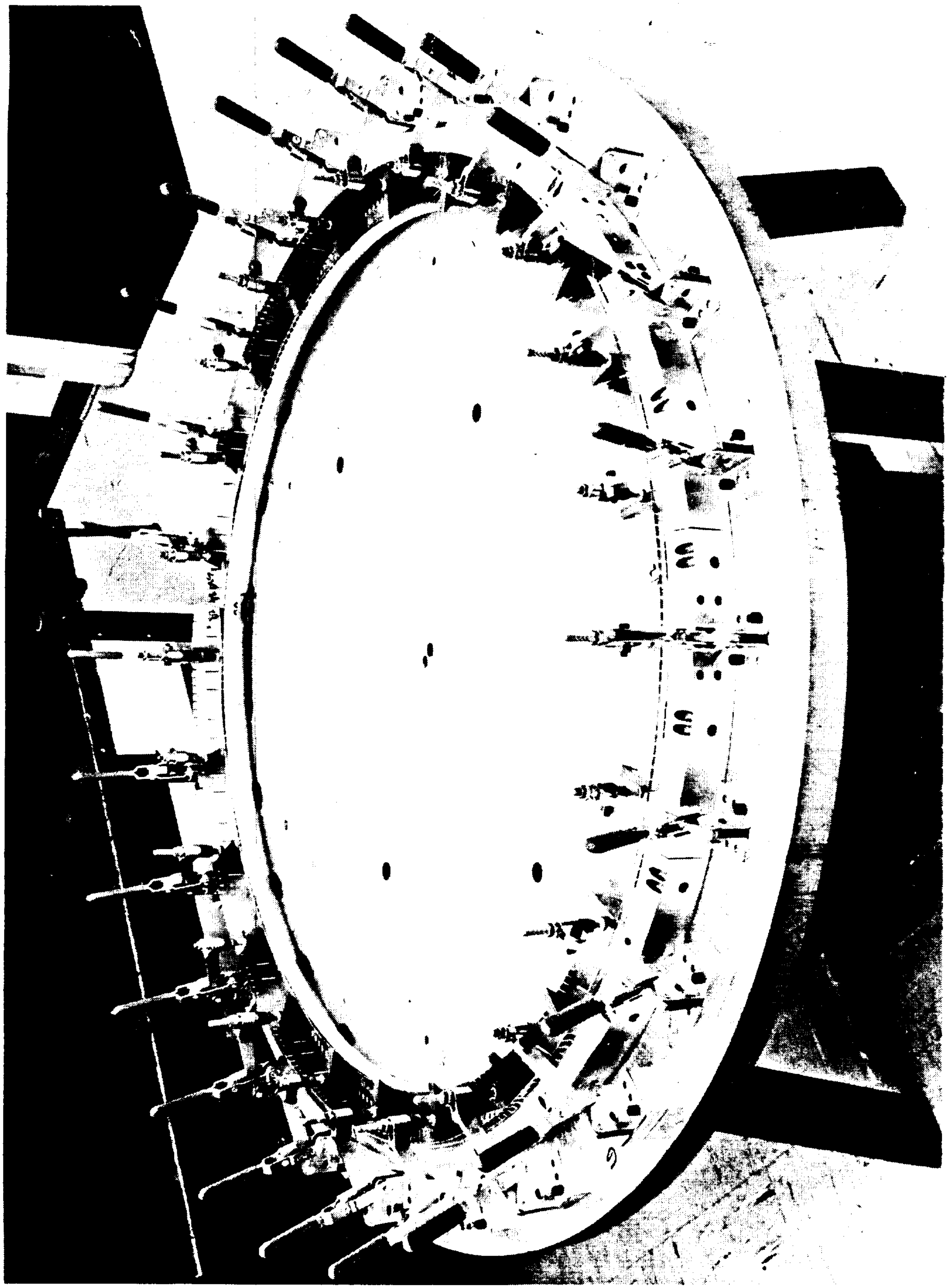

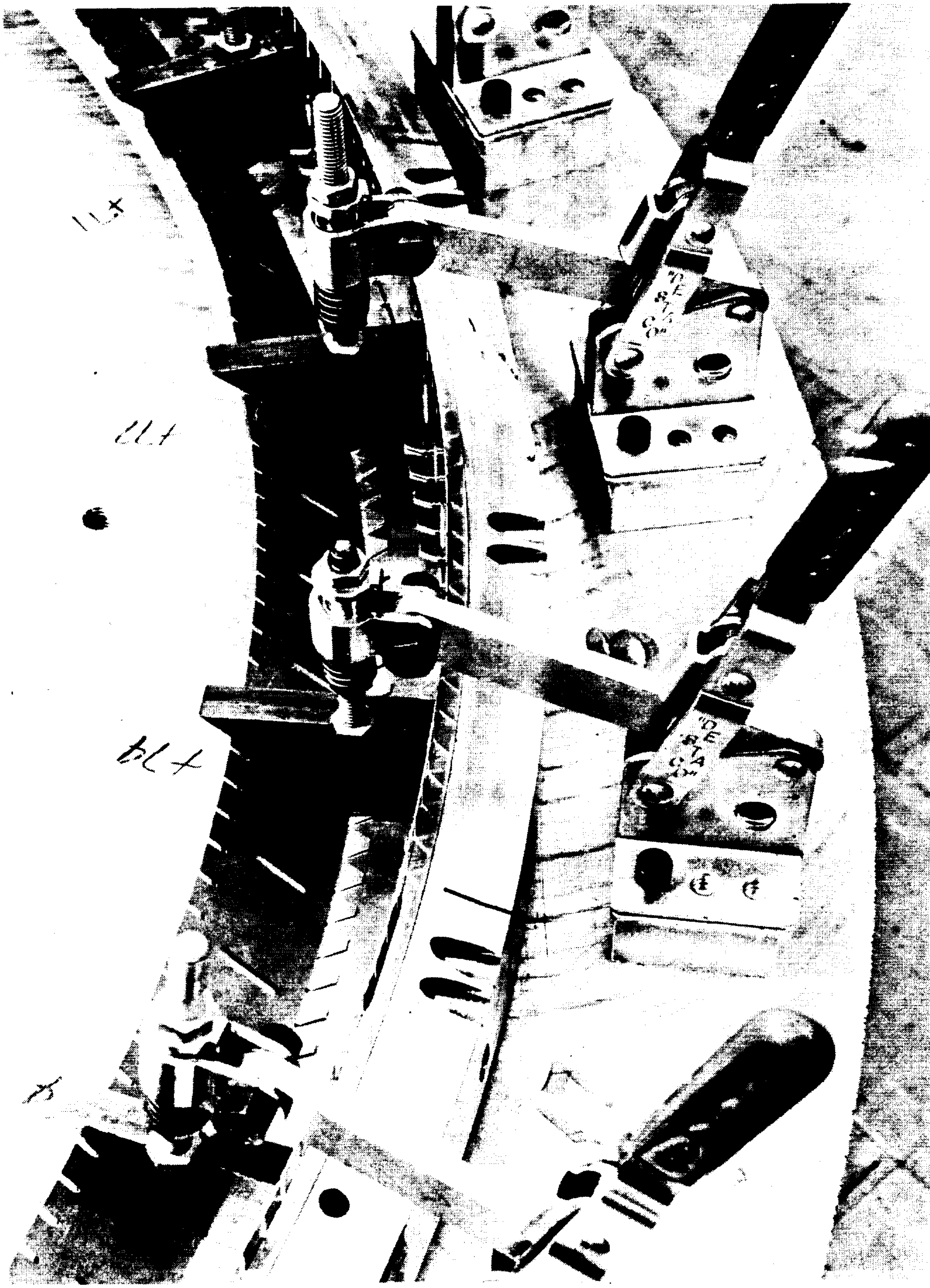

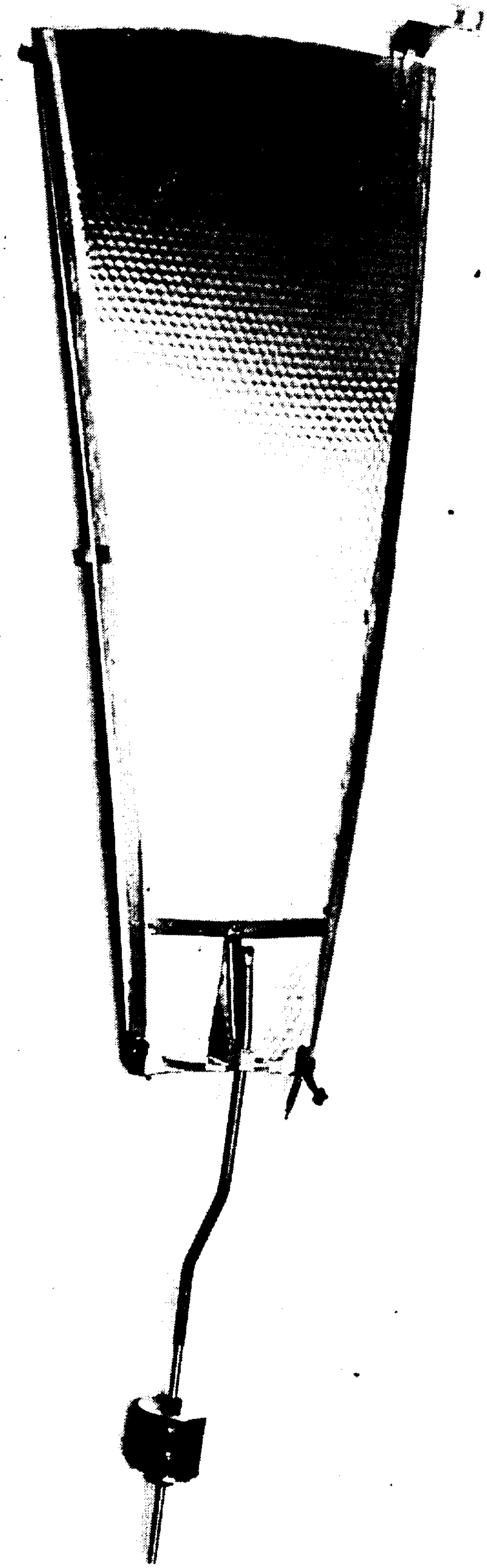

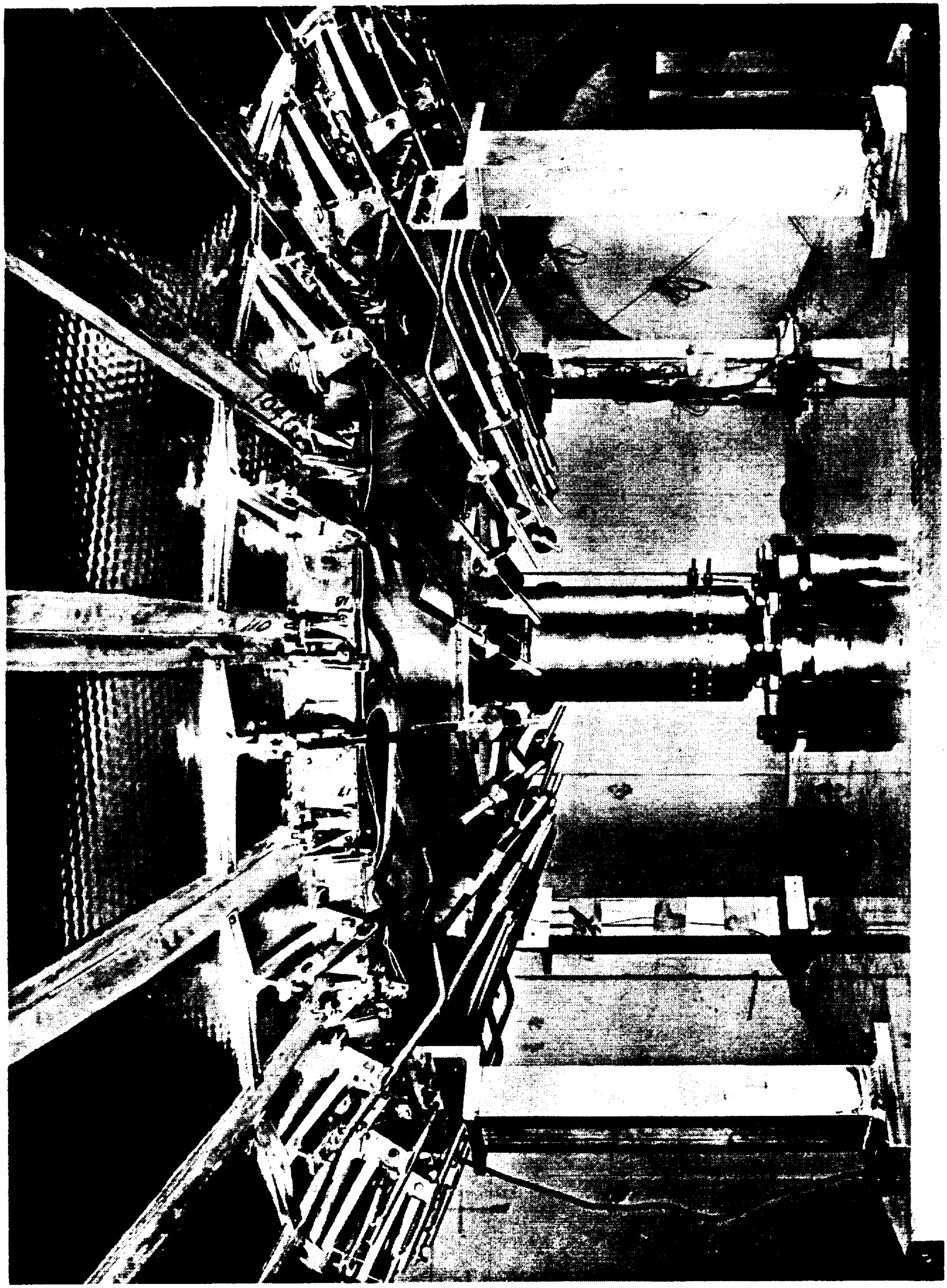

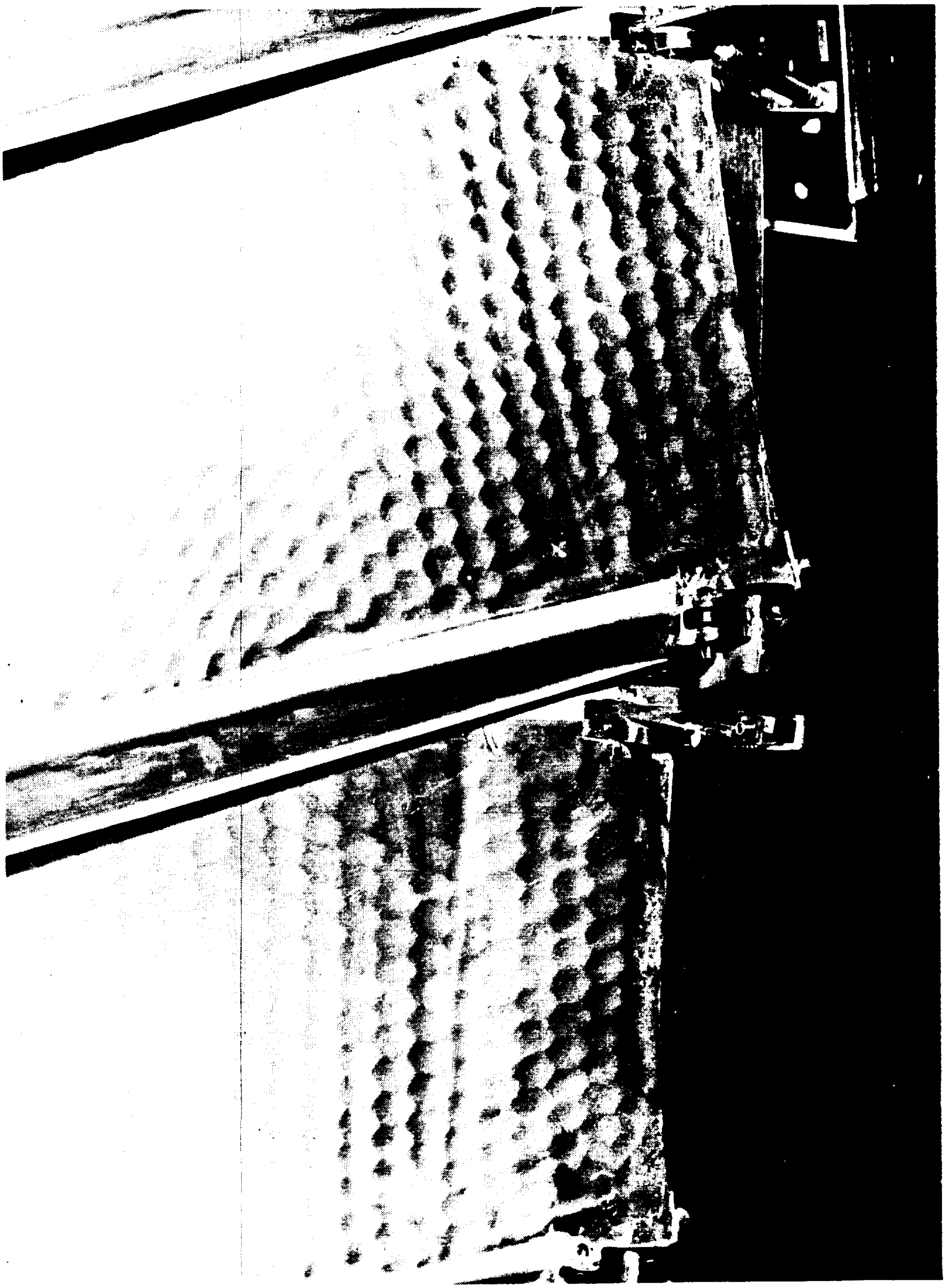

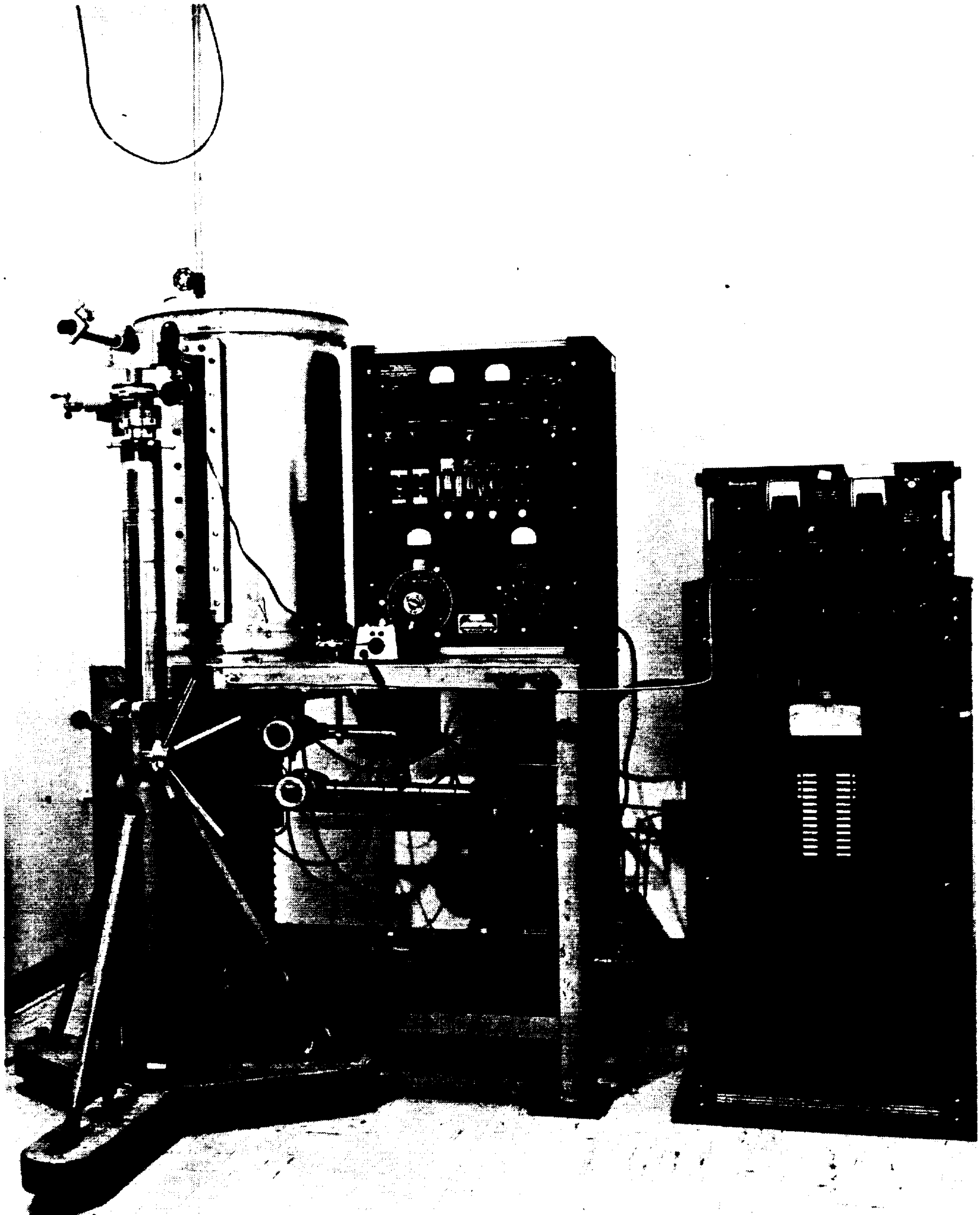

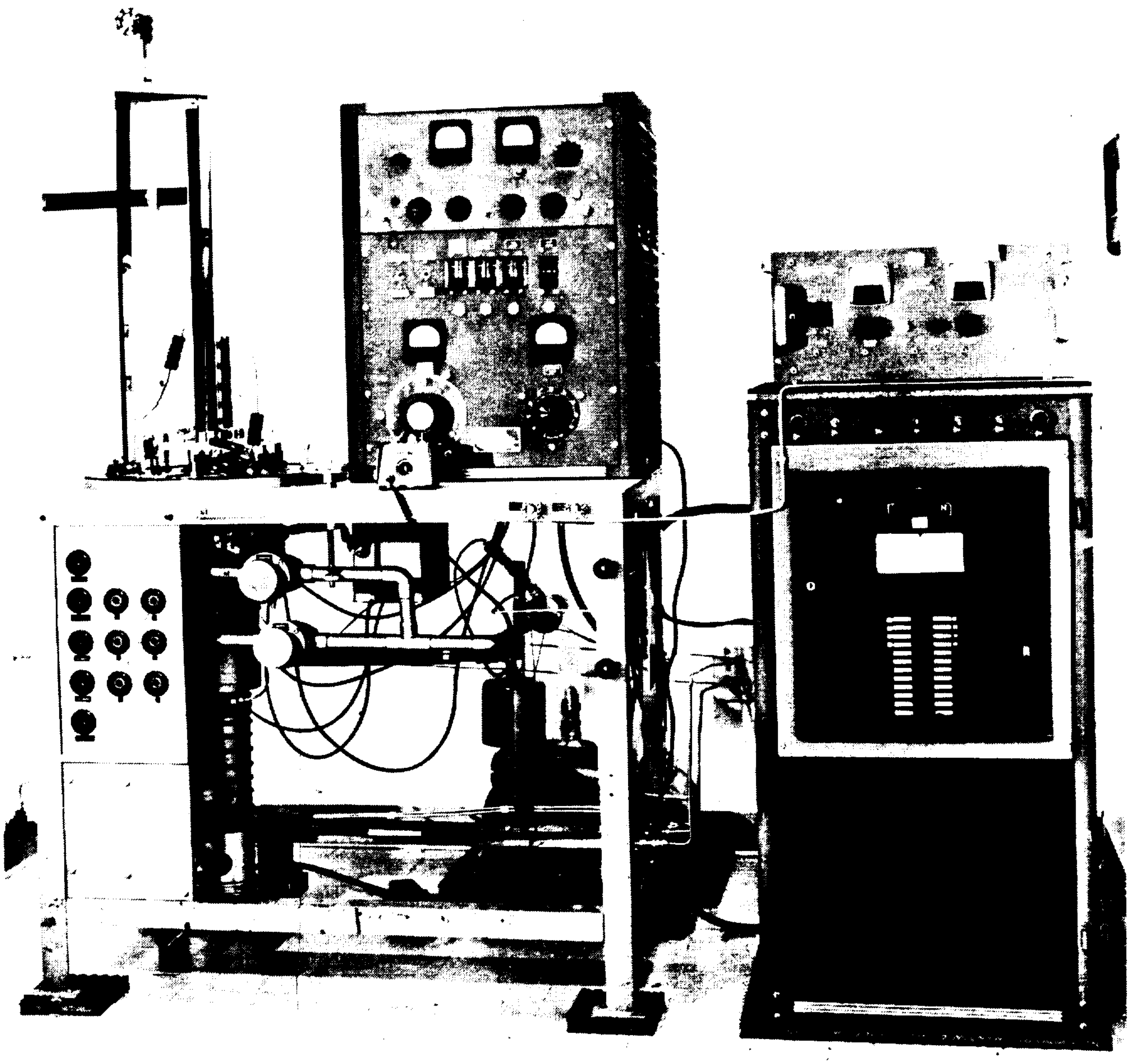

C-2.

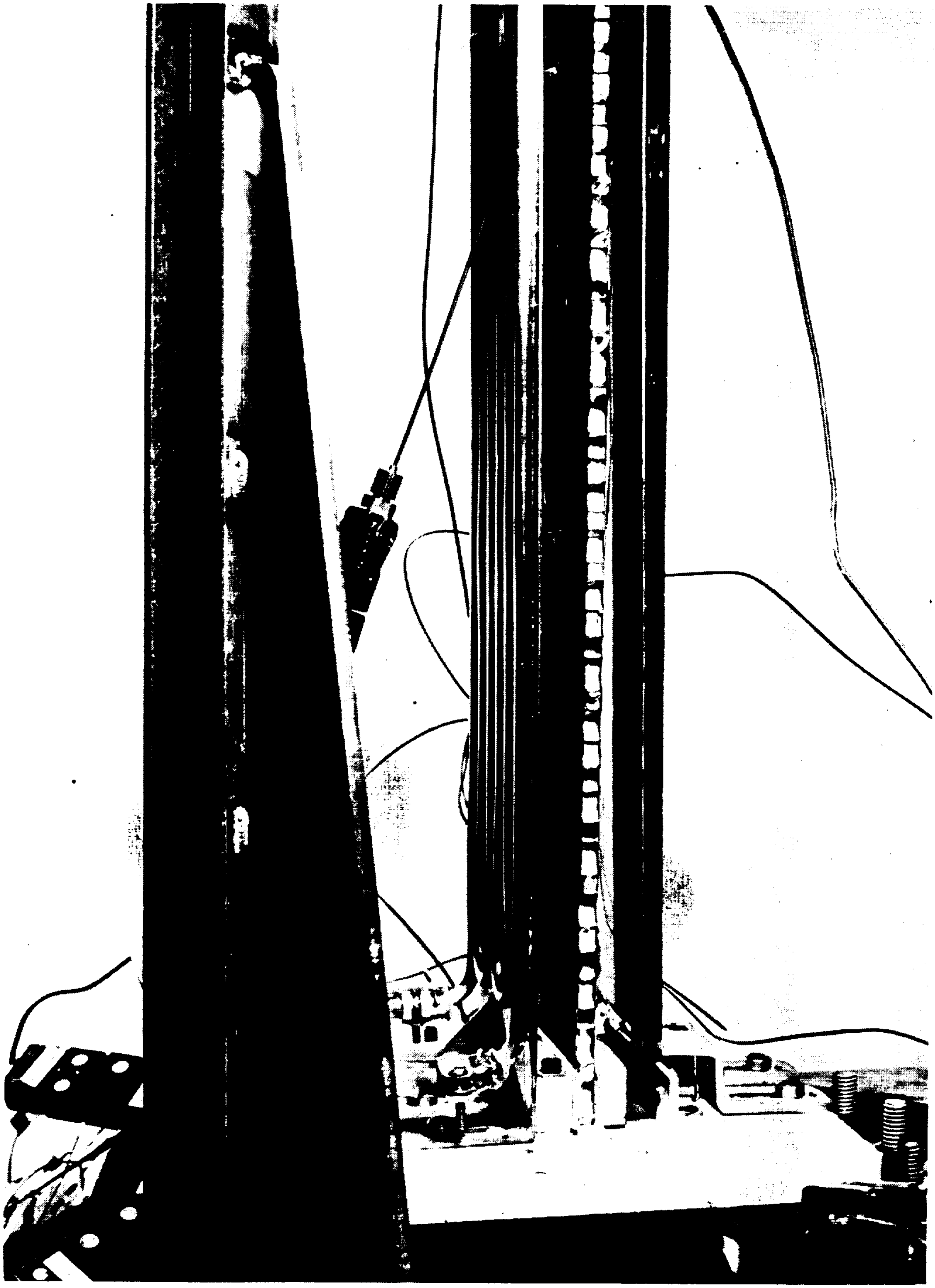

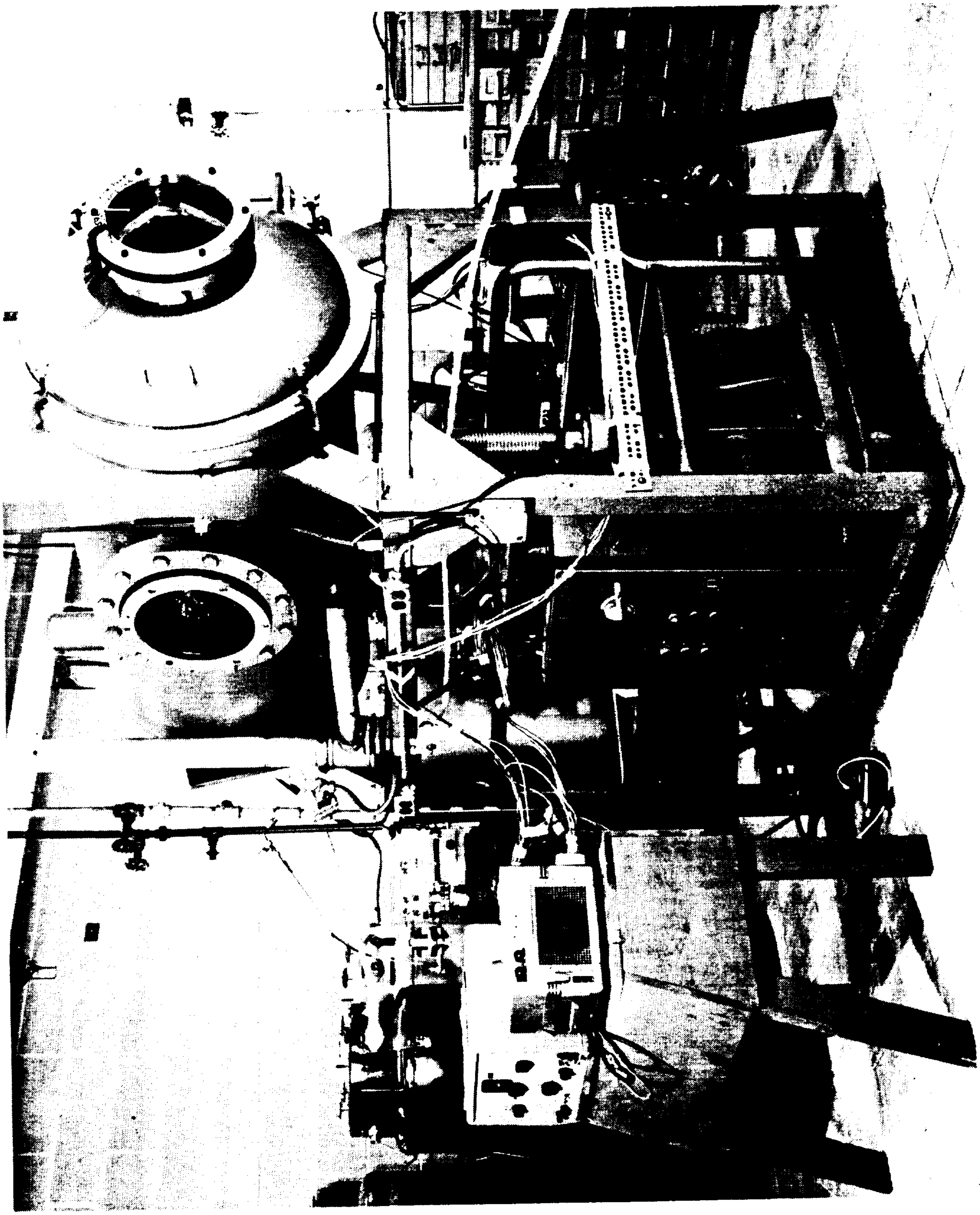

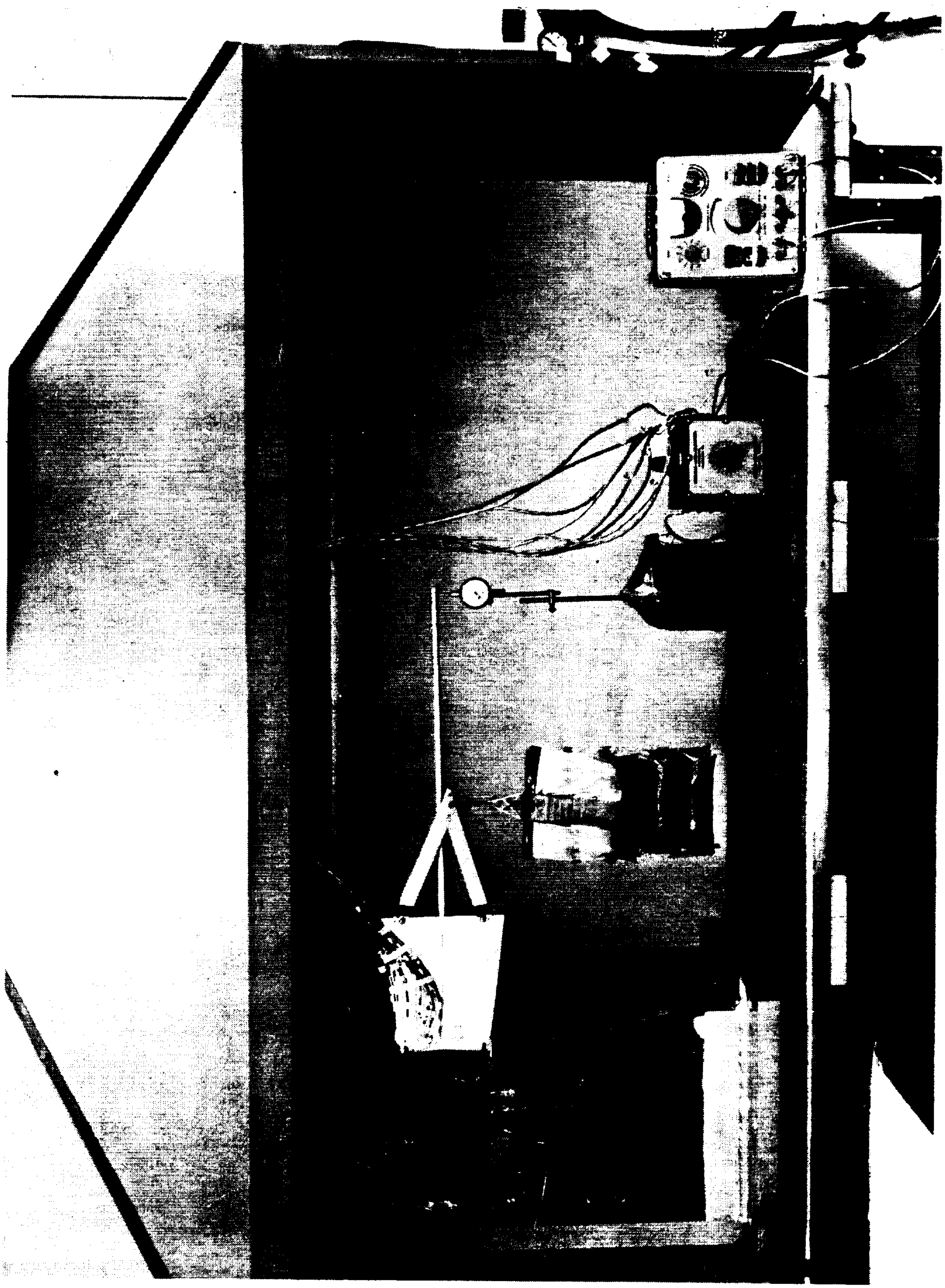

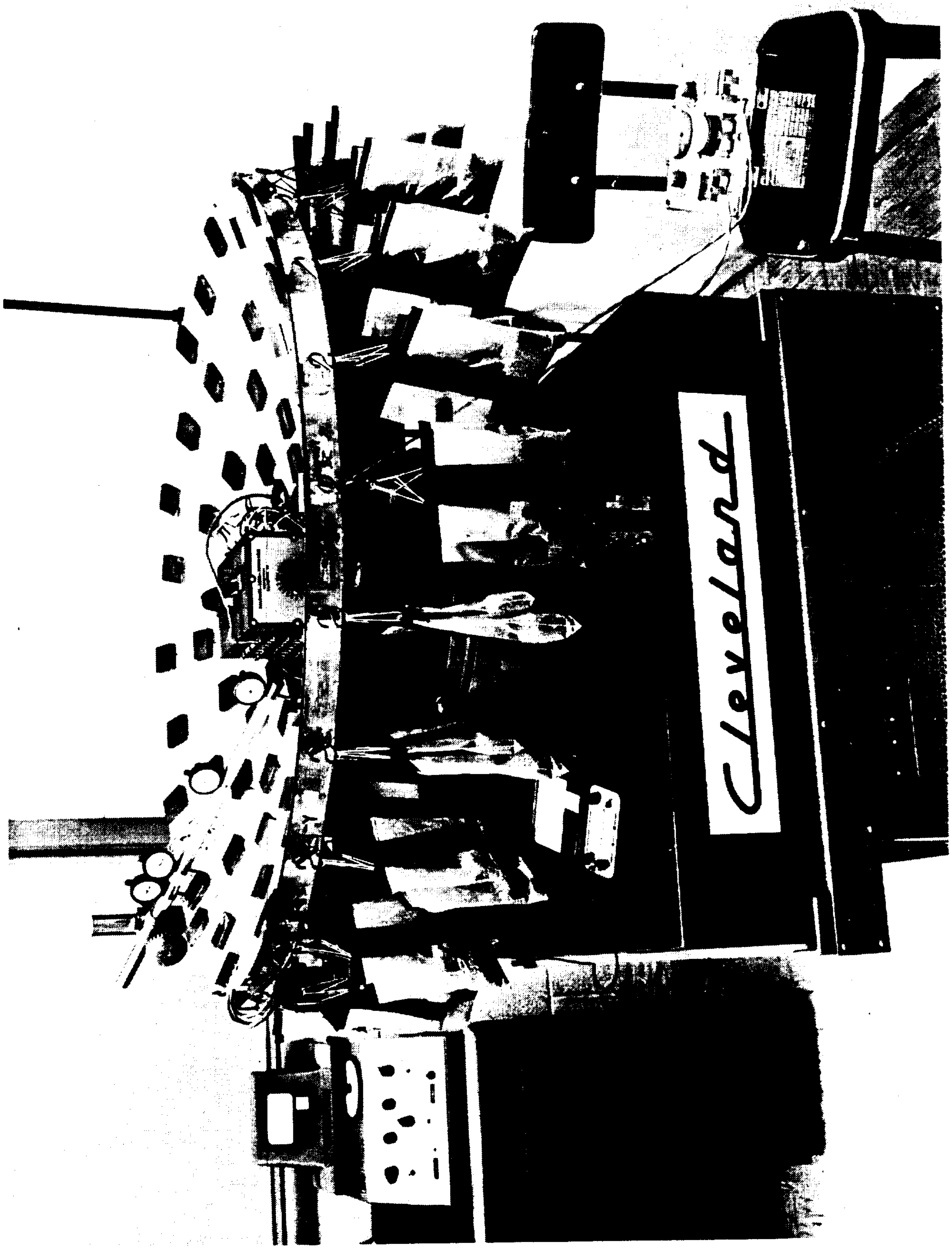
Cleveland

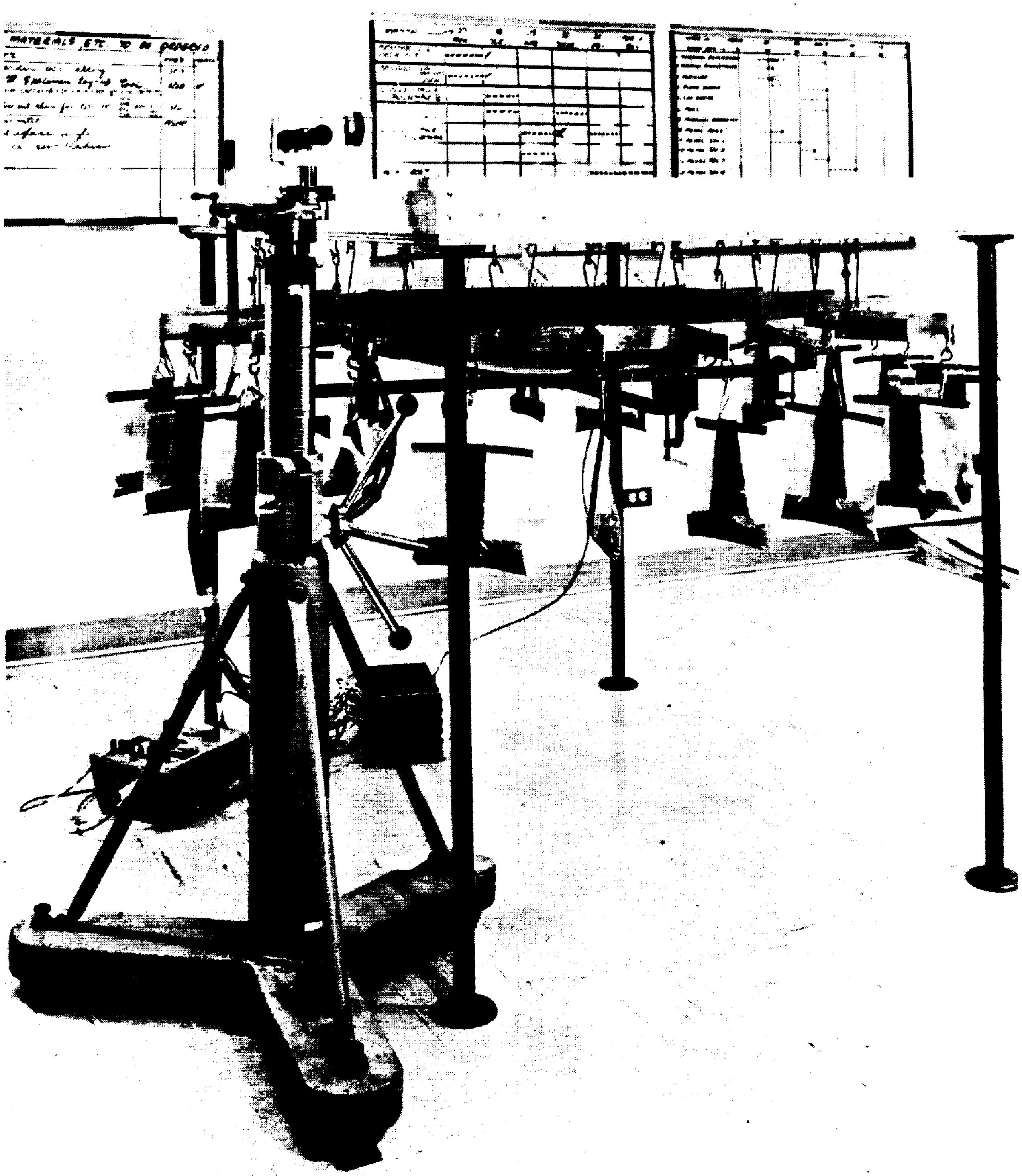
MATERIALS, ETC TO BE ORDERED

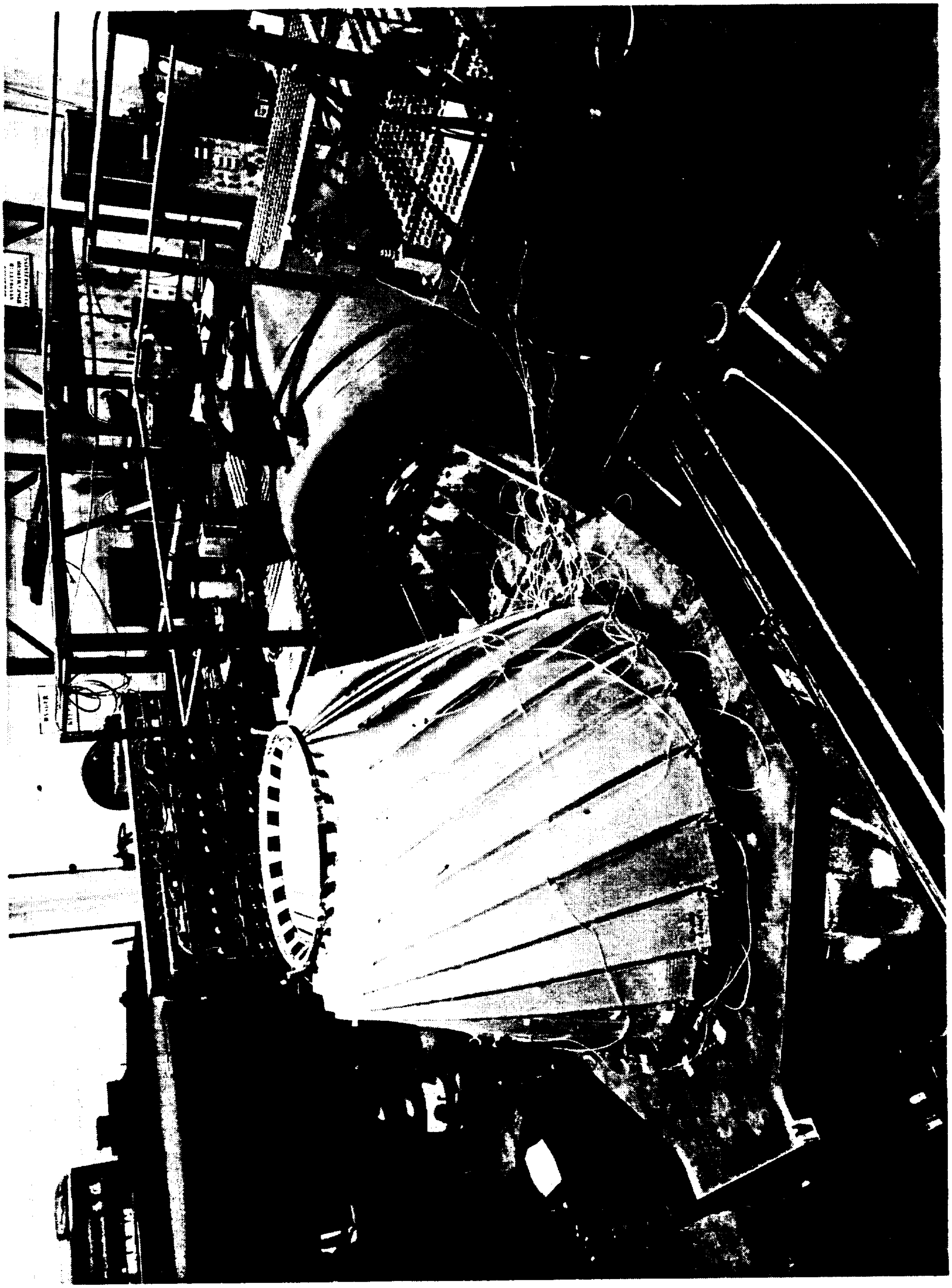

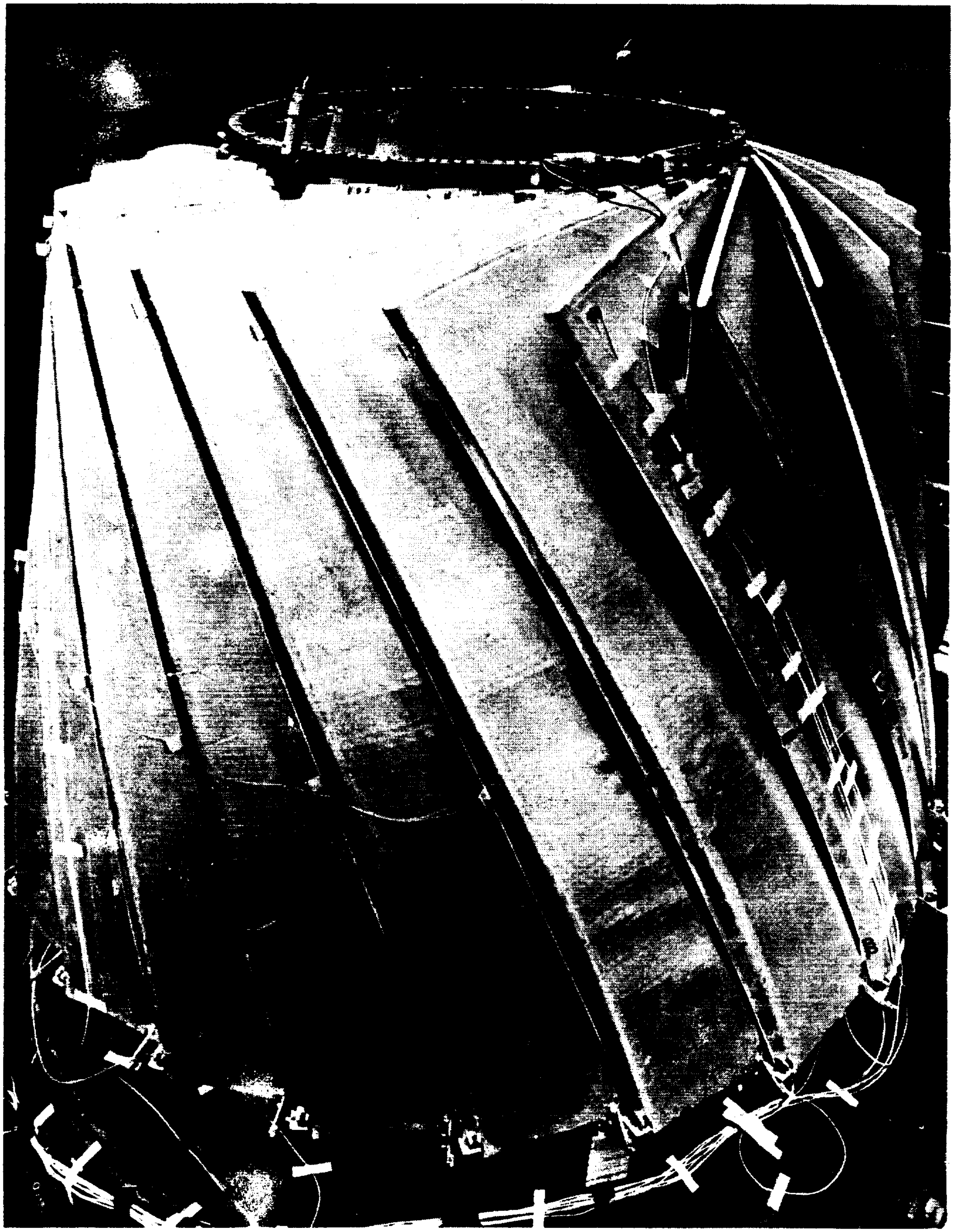

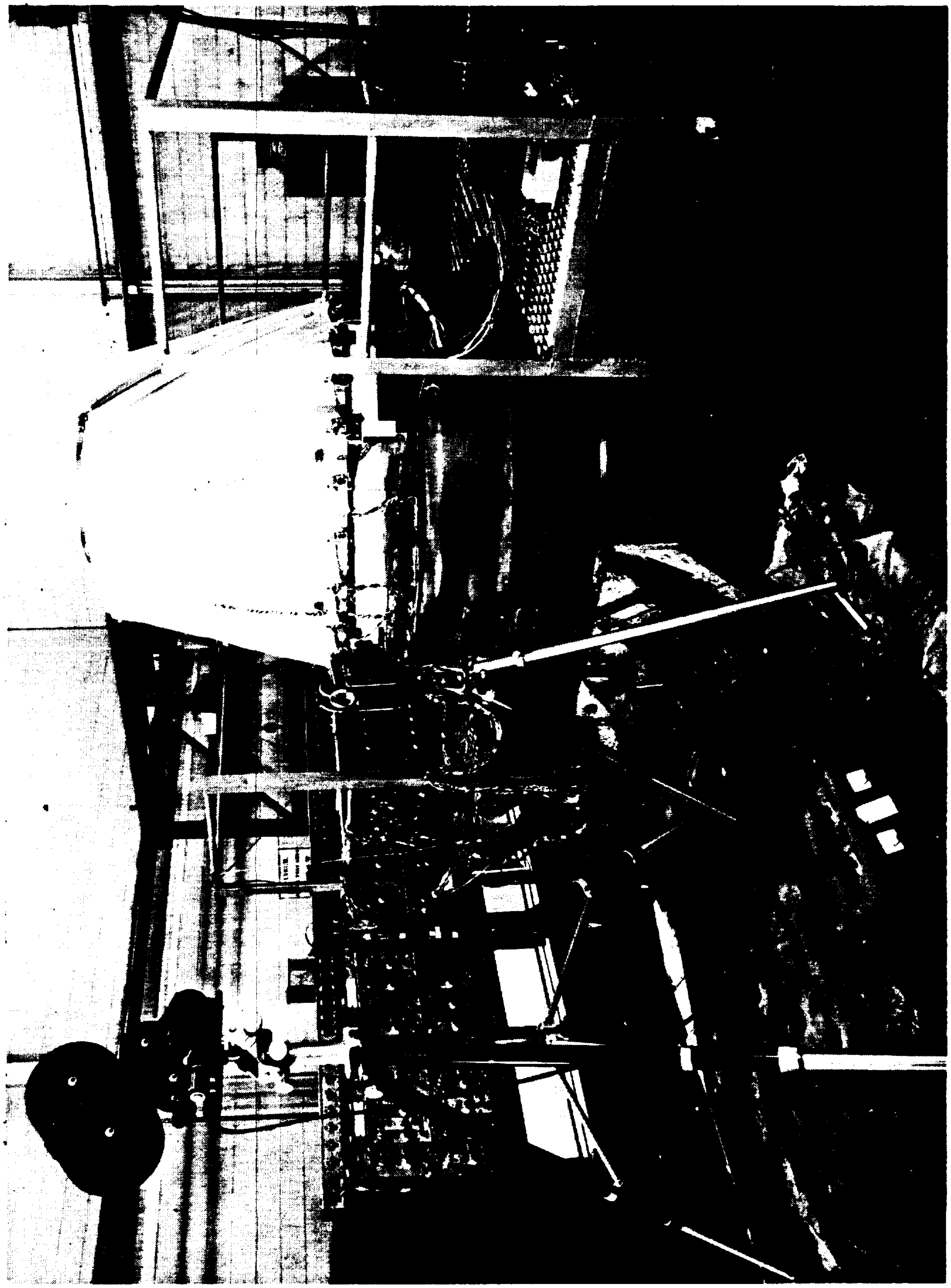

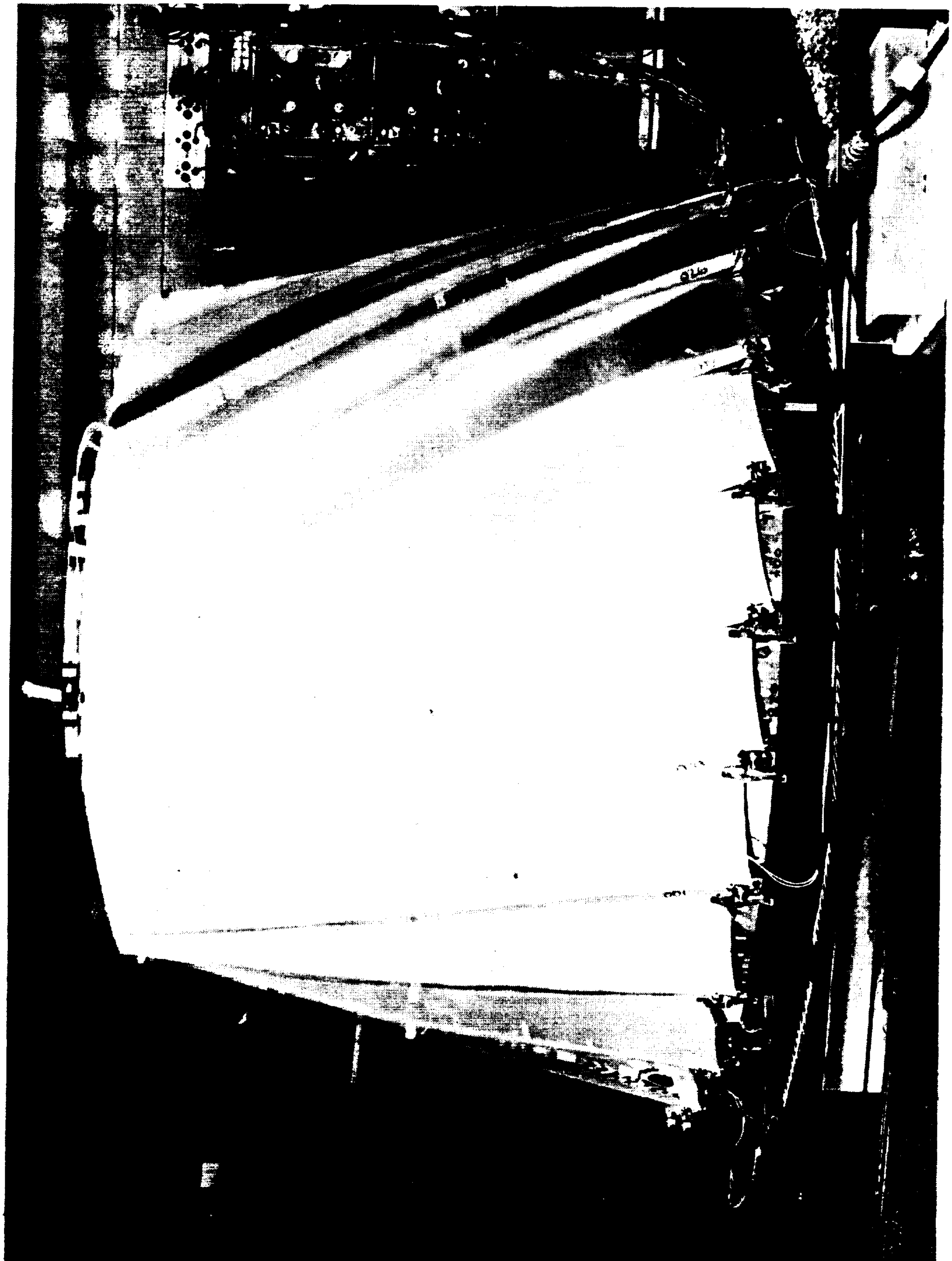

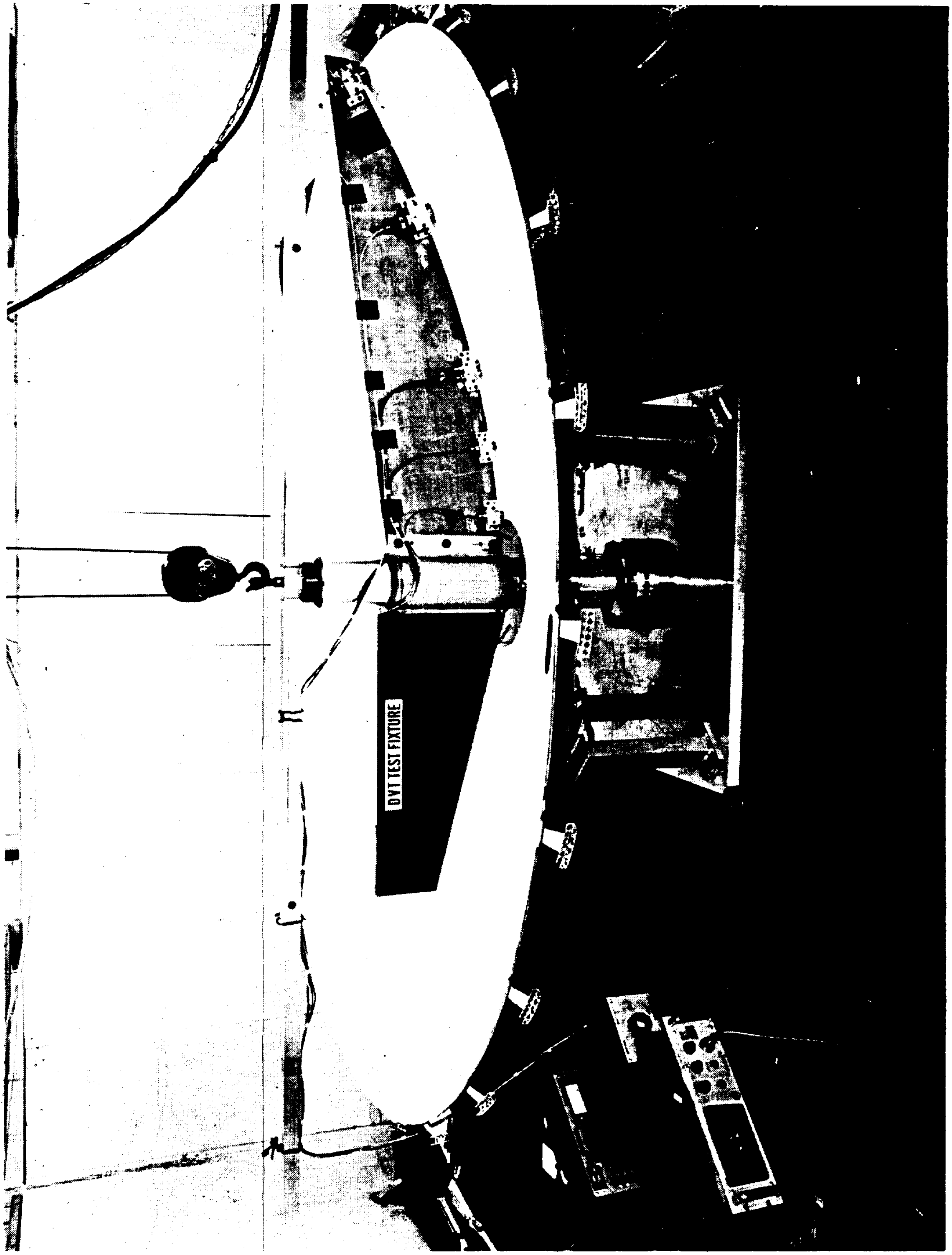
DVT TEST FIXTURE

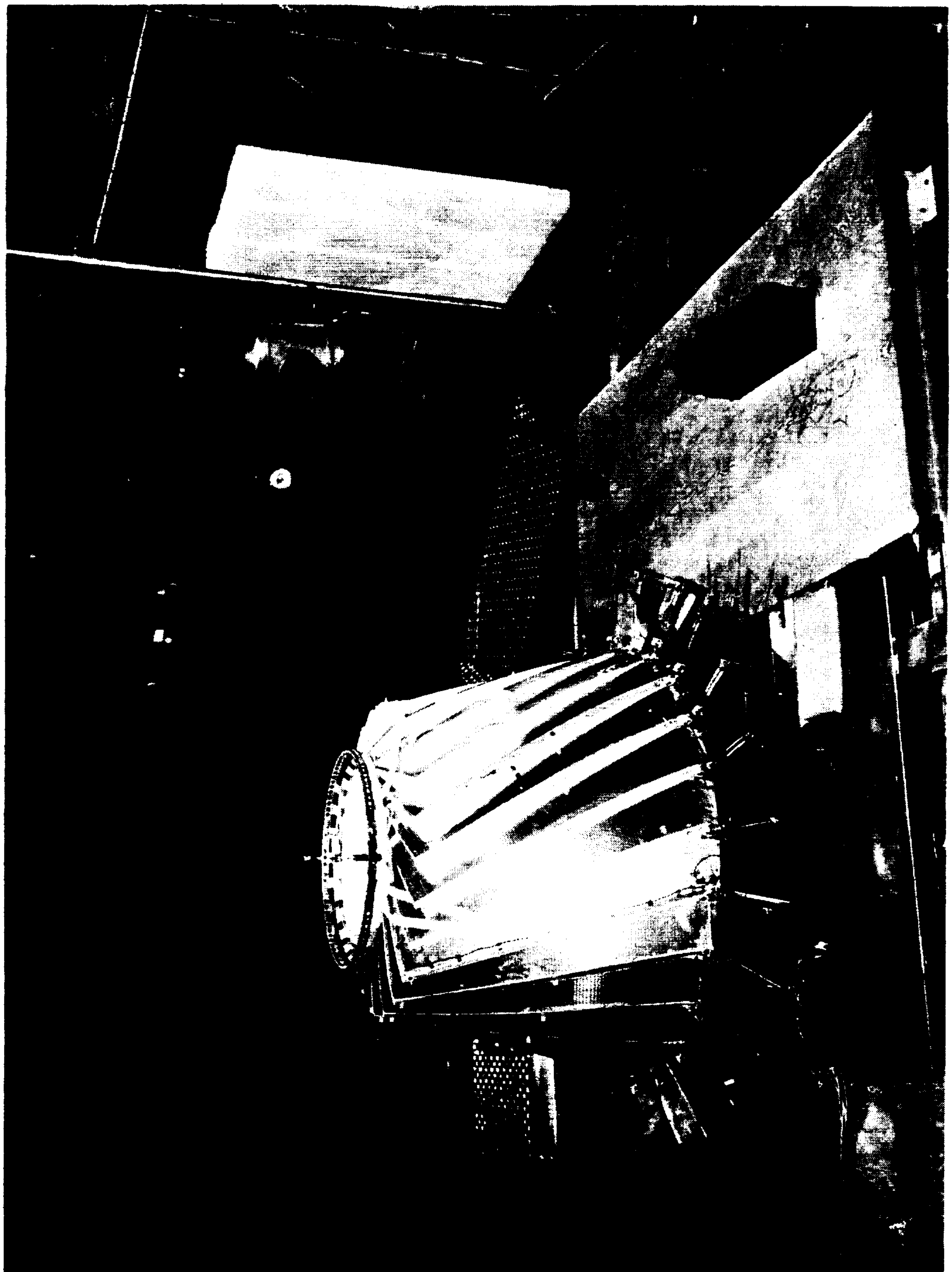

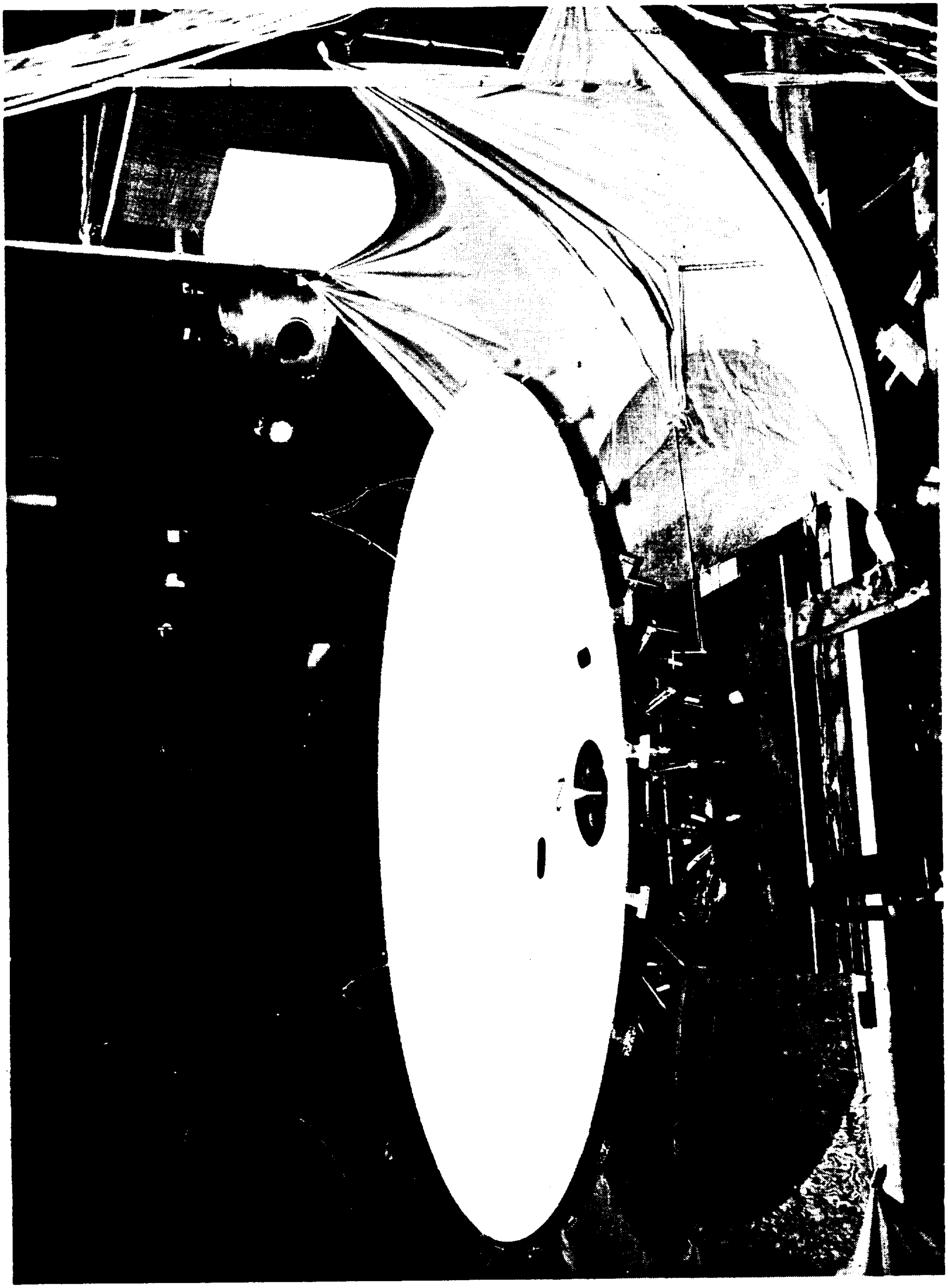

Appendix D

This appendix contains oversized pages that were not filmed because of poor reproducibility.

Appendix E

This appendix contains oversized pages that were not filmed because of poor reproducibility.

Appendix F

This appendix contains oversized pages that were not filmed because of poor reproducibility.

Appendix G

PANEL FABRICATION PROCEDURE & TRAVEL QUALITY LOG (TQL)

Z-CLOSE-OUT (DUAL-V) EDGE with DOUBLER/HIGH TEMPERATURE CURE/4-DAY PROCEDURE

DAY ONE Date:_________

Assemblers ____________________ ____________________ ____________________

Recorder ____________________

The objective of the first day of Panel Fabrication is to determine what stock will be used for front and back faces; edge configuration, material and technique of adhesive application. Any design or fabrication technique changes must be added. All pieces/parts are also to be cut and/or fitted. Then a thorough accounting of all parts, equipment, tools & fixtures, and expendable items must be taken and their availability prepared. A check mark should be placed next to the item as it is readied and a list made of those needing further preparation or procurement and this list must be fulfilled by the end of day one. Spacing left between processes, throughout this EN, is to be used for changes made "on the fly".

1. List of Parts Required for Panel Fabrication

Aluminum Stock	Front Face	Back Face
Alloy, as received		
Temper		
Thickness		
Finish		
Supplier		
Size: Length x Width		
Anneal: Time		
Temp		

1. <u>List of Parts Required for Panel Fabrication</u> (Con't)

<u>Adhesive</u>

Formulation_______________ Batch_______________

Supplier_______________

Mix Ratio: Part A_______________ Part B_______________

Manufactured Date:_______________ Receival Date:_______________

<u>Honeycomb Core</u>

Supplier:_______________ Block Number:_______________

B/L_______________ JOB_______________ P/S_______________

Designation Number:_______________
Coating Cell Mat'l Gage Perforation Density

Thickness After Flycutting:_______________

<u>Edge Stiffeners</u>

Type:_______________ Density:_______________

Material:_______________ Thickness:_______________

Adhesive Application Technique:_______________

Radial Edge 'A'...DWG_______________

Radial Edge 'B'...DWG_______________

O.D. Edge.........DWG_______________

I.D. Edge.........DWG_______________

1. <u>List of Parts Required for Panel Fabrication</u> (Con't)

<u>Corner Hardware</u>

Material:______________________________

Adhesive Application Technique:__________________________________

I.D./Radial Edge 'A'...DWG________________

I.D./Radial Edge 'B'...DWG________________

O.D./Radial Edge 'A'...DWG________________

O.D./Radial Edge 'B'...DWG________________

<u>Doublers</u>

Material:_________________________________ Thickness:_________

Adhesive Application Technique:__________________________________

Radial Edge 'A'...DWG_______________

Radial Edge 'B'...DWG_______________

O.D. Edge.........DWG_______________

I.D. Edge.........DWG_______________

<u>Index Washers</u>

Material:__________________________________ DWG_____________

Adhesive Application Technique:_________________________________

1. **List of Parts Required for Panel Fabrication** (Con't)

Z-Close-Outs

Material:____________________ Thickness:__________

Adhesive Application Technique:

Upper 'V':____________________

Lower 'V':____________________

Preparation

Radial Edge 'A'...DWG__________

Radial Edge 'B'...DWG__________

O.D. Edge.........DWG__________

I.D. Edge.........DWG__________

Application

Radial Edge 'A'...DWG__________

Radial Edge 'B'...DWG__________

O.D. Edge.........DWG__________

I.D. Edge.........DWG__________

2. **Panel Fabrication Accessories**

Equipment	Qty	Description
Vacuum Pump	1	Welch Duo-Seal®
Vacuum Pump	1	Watsco Oil-Less®
Manometer	1	36" U-Tube H_2O
Vacuum Gage	2	
Flash Light	1	
Impact Wrench	1	
Torque Wrench	1	
Utility Knife	1	
Small Utility Knife	2	
Quick Disconnect	1	
Relative Humidity Meter	1	
Scissor	2	Black Handled
Scissor	1	Stainless Steel

2. **Panel Fabrication Accessories** (Con't)

Equipment	Qty	Description
Acid Paste Brush	2	Nylon
Soap Brush	1	Nylon (shortened bristles)
Squeeze Bottle (Solvent)	3	Polypropylene (MEK, MIBK, Toluene)
Waste Acid Container	2	30 gal Polypropylene
Balance Scale	1	with Weights
Beaker	3	Stainless Steel, 250 ml
Adhesive Reconstitution Equip	1	See EN-1002A
Heat Gun	1	Master®
Heat Gun	3	Makita®
Thermocouple	9	J-Type with Stainless Steel Shims
4-Zone Temp. Control Unit	1	Watlow®
Data Collection System	1	H.P. (See Section 8.30)

Qty	Tools & Fixtures	DWG	Rev
1	Stretch Forming/Layup Tool (SF/L Tool)		
1	Back Face Handling Frame		
2	Clean/Rinse Dam (Front Face)		
2	Clean/Rinse Trough (Front Face)		
1	Clean/Rinse Trough (Back Face)		
1	Stock Cleaning Wand		
2	HEPA Enclosure Doors		
1	Core Template		
1	Back Face Template		
3	Breather Templates		
2	Foam Edge Specifications		
1	Foam Adhesive Dip Plate		
1	Foam Adhesive Screed Bar		
1	Core Adhesive Dip Plate		
1	Core Adhesive Screed Bar		
1	Vacuum Manifold		
6	Drill Bushing Seals		
2	Index Washer Alignment Pins		
1	Vacuum Groove Indention Tool		
1	C & E Stretch Tool Support		
2	Jaw Shim Set		
4	Jaw Wedge		
1	Dummy Corner Etching Fixture		
1	Core Razor Knife Handle		
1	4" Spatula with Curved Blade		
1	1" Spatula		
4	Doubler Over-Rail		
1	Doubler C & E Fixture		
3	Vacuum Bag Hold-Down Strip		
1	Core/Back Face Hold-Down Fixture		
2	12" x 12" V-Close-Out Preparation Plate		
9	Aluminum Layup Weights		

2. Panel Fabrication Accessories (Con't)

Qty	Tools & Fixtures	DWG	Rev
1	Urethane Close-Out Form (60°)		
1	Urethane Close-Out Form (30°)		
1	Sharp-Edged Steel Bar Stock (12" Scale)		
1	Dummy Corner Shaping Tool		
2	Jaw Shim		

Qty	Expendables	Description
1 can	Tool Lubricant	Teflon®, Spray, Osborn®
1 roll	Tape, Masking	1" Width
1 roll	Tape, Teflon®	1" Width x .002" Thickness
1 roll	Tape, Double-Backed	2" Width x .002 - .004" Thickness
1 roll	Tape, Double-Backed	1 1/2" Width x .002 - .004" Thickness
1 roll	Tape, Sealant	Airtech®, GS100, 1/8" x 1/2"
5 gal	Distilled H_2O	2 - 2 1/2 gal containers
5 gal	Hot Tap H_2O	2 - 2 1/2 gal containers
5 gal	Hot Tap H_2O	5 gal Bucket (Glove Rinse)
1 roll	Vacuum Bagging Film	Airtech®
1 roll	Vacuum Breather	Airtech®
1 roll	Vacuum Bleeder	Airtech®
4 box	Wipers	15" x 17" Kimwipes®
1 bag	Clean Room Clothes	12" x 12"
2 box	Anti-Static Wipers	
1 bottle	Window Cleaner	Windex®
3 pad	3-D Abrasive	Scotch-Brite® Ultra-Fine #7448
1 tube	Liquid Glove	
1000 ml	Soap	CSP Cleaner, Hilliard® #125
1 box	Glove, Polyethylene	Throw-away (hand oil prevention)
2 pair	Glove, Silvershield®	(impervious to solvents)
2 pair	Glove, Neoprene	(impervious to acids & soaps)
1 liter	Solvent	Methyl-Ethyl-Ketone (MEK)
1 liter	Solvent	Methyl-Isobutyl-Ketone (MIBK)
1 liter	Solvent	Toluene

2.10 Fill in information of Section 1. List of Parts Req. and place a check-mark next to each item as it is accounted for and/or prepared, and place the item(s) in perspective area or cleanroom.

3.00 Material & Hardware Preparation

3.10 **Dummy Corner Facing**

3.11 Cut 2 pieces of 3" abrasive grid cloth (240 grit). Attach to tool using double-back tape in respective I.D. and O.D. areas, just inside of vacuum groove.

3.12 Screw Dummy Corner Shaping Tool to dummy corner (those with #10-24 thread) ensuring bolt does not protrude.

3.13 Applying even pressure to both ends of shaping tool, such that pressure is applied to dummy corner at center, resting hands on Stretch Forming/Layup Tool (SF/L Tool) to keep alignment, sand each dummy corner in x & y directions, shaping to respective curvature of SF/L Tool. Edges of dummy corners should end up being sanded last with this technique or possibly not sanded at all.

3.14 Repeat for 3 dummy corners with threading.

3.15 Drill hole in orthogonal end of I.D./Radial Edge 'A' dummy corner with a #50 drill, 1/2" deep. Clamp in vice with wood protecting dummy corner from steel jaws, while drilling.

3.16 Double-back tape a 6" x 3/8" x 1/4" aluminum bar stock to I.D./Radial Edge 'A' dummy corner on slant and centered. Repeat above sanding procedure.

3.17 Remove abrasive grid cloth and clean SF/L Tool without scratching.

3.18 Abrasive blast dummy corners at a ∠45° to surface, holding pieces with freshly washed neoprene gloves.

3.20 **Doubler Preparation**

3.21 Cut 40 - 45" length of doubler material from roll stock, with black handled scissors. Trim both ends square to a length of 32.5".

3.22 Cut two (2) Radial Edge Doublers, 0.719" (23/32") wide, from stock of Step 3.21 using small utility knife and MIBK as lubricant. Lightly cut a groove in doublers at one end, 1" from end, approximately 1/3 thickness of doubler material deep (handling tabs).

3.23 Outlining I.D. Edge Doubler Template, placed on doubler material, cut I.D. doubler, leaving an extra 1" at ends for tabs. Groove one (1) end of doubler at end of template as above.

3.24 Place SF/L Tool on bench-in inspection fixture against stops. Attach a cutting back-up strip of naugahyde on lay-up tool with double-back tape at O.D. end, such that the radial grooves are still visible, yet covers

3.00 Material & Hardware Preparation (Con't)

3.24 (Con't) inside edge of the O.D. section of the groove. Attach added naugahyde outside of radial grooves. Place a scribe in adjustable sliding holder of inspection fixture aligning tip with inside edge of O.D. groove. Tighten sliding holder in place. Raise scribe well above naugahyde. Cut a 3" x 18" section of doubler material. Fasten to naugahyde with midpoint of a long edge at midpoint of outer edge of O.D. groove and perpendicular to Edge 'A' of lay-up tool, using masking tape. Lower the scribe until touching doubler material. Lubricate doubler material with MIBK and with light pressure applied to I-beam of inspection fixture, scribe a groove along aluminum strip. Loosen scribe and slider, and re-adjust scribe to doubler material with a .844" (27/32) offset towards the Vertex end. Re-lube and scribe a groove at offset. Remove scribe and swing I-beam away. Re-lube grooves and finish cutting doubler edges with small utility knife. Cut doubler ends inside of inside radial grooves.

3.25 Remove doubler from set-up and place appropriate template on doubler centered. Lightly cut a groove in doubler at one end of template approximately 1/3 thickness of doubler material deep (tab). DWG___________________

3.26 Remove all above cutting apparatus from SF/L Tool and clean.

3.27 Perform a dry layup of doublers and dummy corners, consistent with drawing above and aligning groove of each doubler and end placement. Mark other end of each doubler for tab removal, with scribe. Remove doublers and cut groove in each at scribe as above.

3.28 Drill 1/8" holes in all doubler tabs. Remove burrs from edges of all doublers using file.

3.29 Secure all doublers to C & E support plates with shims on top of tabs of doublers and 1" C-clamps.

3.30 **Honeycomb Core Cutting**

3.31 Place Back Face Handling Frame in C & E area. Remove scratches using abrasive grid cloth. Wash with soap (CSP, Hilliard® #125) and rinse. Clean frame using Toluene, then MEK ==> Prepare two sets of folded wipers (Kimwipes®). Wet one set with solvent. Wipe surface with consistent linear motion with wetted wiper while in opposite hand the dry wiper follows directly (R^3 Method). Several overlapping swipes are necessary to clean complete surface area.

3.32 Place Handling Frame on table. Clean an adjacent table. [Polyethylene gloves should be worn for this procedure] Remove honeycomb core from storage and place on clean table with 'best' side down. Place core template on honeycomb with longitudinal center line of template aligned with ribbon direction of honeycomb. Using core cutting razor tool and

3.00 <u>Material & Hardware Preparation</u> (Con't)

3.32 (Con't) direct, swift perpendicular downward force (DSPDF) trim honeycomb within 1/2" of edges of template.

3.33 Place honeycomb in back face handling frame, 'best' side up, in relative layup position. Invert (flip) core template and place on honeycomb, centered. Weight (ceramic mugs) template and honeycomb against frame in two equidistant places. Using 4" wide spatula (with sharpened curved blade), cut Radial Edge 'B' using DSPDF method above, perpendicular to frame surface and rocking spatula to complete the cut. Next, cut O.D. Edge using spatula, <u>however</u>, rock the spatula blade from the frame surface through uncut honeycomb, as opposed to a downward force.

3.34 Lift edges of template (with weights in place) carefully allowing residual stresses to relax. Re-align template (if necessary) and proceed with two final edges, incorporating DSPDF method on Radial Edge 'A', and rocking cut method on Vertex Edge.

3.35 Trim four corners with core cutting razor tool and/or stainless steel scissors to match template.

3.36 Place all honeycomb, including core in storage.

3.37 Remove any scratches from frame surface with abrasive grid cloth and re-clean (soap & R^3 method). Place 1 1/2" x 2" strip of .012 -.014" thick double-back tape on back face handling frame, as shown, 6 places. Do not remove backing. Place frame in cleanroom.

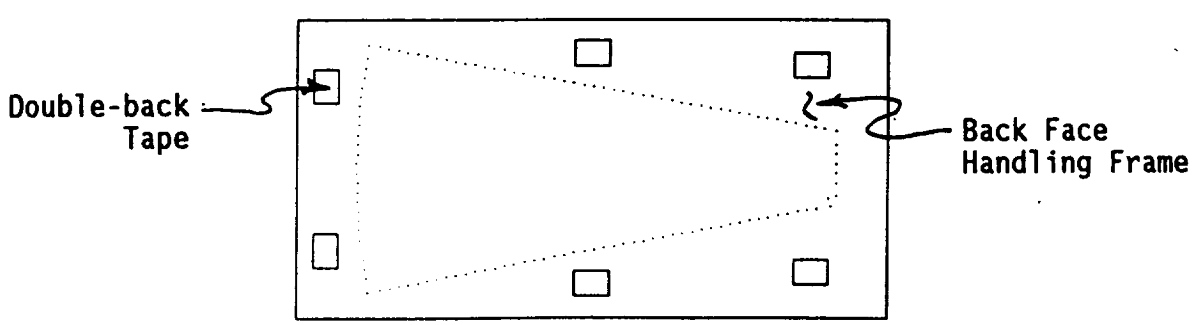

3.40 **Bagging Material**

3.41 Cut vacuum bag material to 22"W x 38"L and attach it to core hold tool with small binder clips.

3.42 Cut breather material according to table below:
- 2 each -- 1 1/2" x 31"
- 1 each -- 1 1/2" x 17"
- 1 each -- 1 1/2" x 6"

3.00 <u>Material & Hardware Preparation</u> (Con't)

3.50 Z-Close-Out (V-Close-Out) Material Layout

3.51 Remove scratches from preparation plates, using abrasive grid cloth on aluminum and emery cloth on stainless steel and clean with Windex® and wipers.

3.52 Plot two sets of V-Close-Out cutting templates. Cut two pieces of V-Close-Out material 10.5" x 11.0". Place material on preparation plates and attach using 1" wide teflon tape, overlapping material 1/4 - 3/8". Protect corners from leakage by adding Teflon® tape over intersection of preceding taping at ∠45° to each leg and 3/8 - 1/2" from intersection. Place one set of templates over material for protection.

3.60 Jaw Shim Stock Preparation

3.61 Cut aluminum alloy to match that of front face and back face materials, with dimensions:
2 each -- 18" x 7/8"
Clean each piece with Toluene dampened wiper, and label as jaw shims.

3.70 Hardware Preparation

3.71 Clean remnant sealant tape from vacuum manifold with razor knife, MEK and wipers. Spray manifold with Teflon® dry lube.

3.72 Spray 'HIGH' vacuum extension threads with dry lube above.

3.73 Clean Over-Rails with Toluene and spray with Teflon® as well.

3.74 Check surfaces of all dip plates for cleanliness, loose and/or non-uniformity of dip thickness taping. Clean using R^3 Method and replace tape as necessary. Cover for protection and post notification of clean and prepared surface.

3.75 Clean lay-up weights with Toluene and/or MEK.

3.76 Clean Back Face Sheet Template with Toluene and MEK using R^3 Method. Place in a clean, secure place.

3.77 Cut two (2) Trim Guards from 1100-H14 x .013" aluminum stock, with dimensions: 1"W x 22"L. Clean with Toluene.

4.00 Stretch Forming Tool Preparation

4.04 Turn on HEPA air filter on at high speed setting and turn ionization bar on. Turn pressurized air on to cleanroom. Set regulator for cleaning wand to 50 psi.

4.06 Observing cleanroom restrictions, remove unnecessary items from cleanroom and remove remnants from jaws. Remove any jaw shims. Place drying equipment on floor. Replace C-clamps on bases of enclosure walls. Wipe all surfaces of enclosure and airfoil with anti-static wipes. Leave enclosure lid up. Wipe table in cleanroom with anti-static wipes. Exit cleanroom.

4.08 Assemble seals in 6 drill bushing holes of stretch forming/lay-up tool.

4.10 Clean SF/L Tool ==> Check Teflon tape at O.D. and Vertex ends of tool for cuts, missing sections or loose edges. Remove all tape if any of the preceding is true. Flood wash tool with Toluene and then wipe to remove majority of Teflon® spray. Fold wiper (Kimwipe®) to fit groove using squeeze bottle of Toluene, clean groove again. Changing wiper surface often, clean until surface of groove is shiny. Using Toluene then MEK, clean surface of tool using R^3 method. Replace Teflon® tape if removed. Clean sides of tool with wiper dampened with Toluene.

4.14 Return tool to cleanroom and place tool in position against stops of stretch former supports. Place airfoil in enclosure around tool. Lower enclosure lid. From this point on, move about confines of cleanroom very slowly as to minimize disruption of laminar air flow. Place doors on sides of enclosure and secure with masking tape. Blow off surfaces of enclosure, airfoil and tool; top to bottom, rear to front of enclosure, with cleaning wand.

4.16 Exit cleanroom opening and closing door very slowly. Roll up shirt sleeves (if wearing long sleeved shirt) and wash hands and arms. Using clean, dry air (Spray Booth air nozzle), blow loose particles from person, especially arms. Close eyes while nozzle is pointed anywhere near face. Remove particles from Teflon® spray lube can in same manner.

4.18 Return to cleanroom; opening, closing and moving slowly. Perform an intense Dark Room/Flash Light (DRFL) inspection of tool surface, removing particles with a gloved hand. If particles are difficult to remove or 'jump' back to tool surface, allow 1/2 hour period for the ionization bar to take effect, then re-inspect tool.

4.00 <u>Stretch Forming Tool Preparation</u> (Con't)

4.20 Into nozzle of Teflon® spray lube can, insert accompanying tube. Curve and tape tube parallel to can (Sketch_______). Shake can vigorously for 1 - 2 minutes. Using cleaning wand, remove any remnant particles from can and arm, while positioned directly in front of cleanroom exhaust filter. With top of spray can as close as possible to enclosure lid (without touching), apply 2 coats of Teflon dry lube to surface of tool using patterns Sketch_______, and overlapping passes.

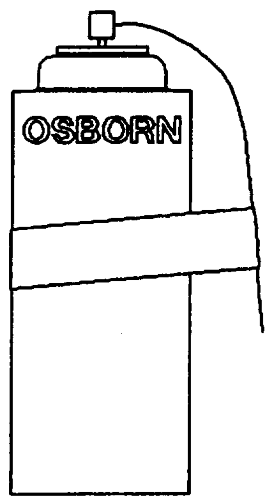

Teflon® Spray Nozzle Configuration

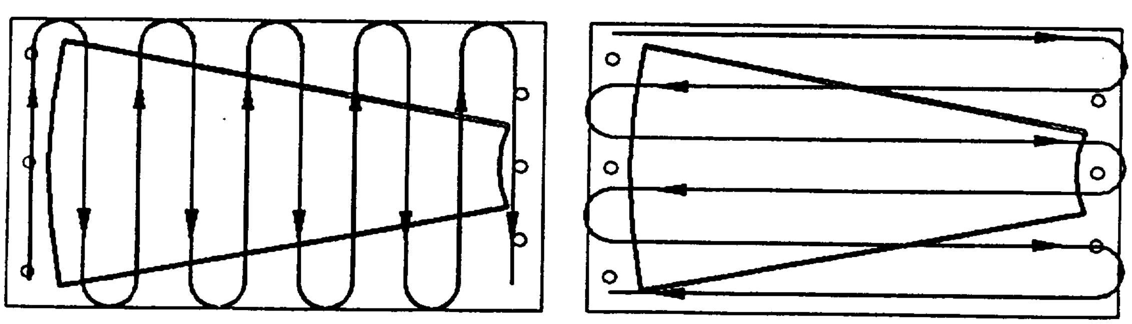

Teflon® Dry Lube Coating Patterns

DAY TWO Date:________

Assemblers ________________ ________________ ________________

Recorder ________________

4.00 Stretch Forming (Con't)

4.30 **Face Sheet Material Preparation**

4.32 Sand steel cutting plate on stock cutting table to remove scratches. Clean with Windex® and Kimwipes®. Clean stock cutting table with anti-static wipes and Windex®. Perform a DRFL inspection of table (as best as possible).

4.34 Cut an 80" length of stock from front face material roll using black handled scissors, being careful of surfaces. Place sheet on stock cutting table, O.D. of coil side down. Without sliding sheet, align sheet parallel to longitudinal table marking and overlapping length marker. Check surface of side up for scratches and material defects, as this will be the reflective surface. If defects are present, re-position to avoid defects or cut a new sheet.

4.36 Trim end of sheet on cutting plate at indicated marking, using small utility knife lubricated with MIBK. Turn sheet 180° on table and re-align with markings with trimmed end at length marking. Trim untrimmed end as above.

4.38 Clean both surfaces of sheet at ends inward approximately 8" with Toluene, using R^3 method. Either turn sheet over, placing paper under sheet to avoid damaging surface of interest or roll ends up carefully so as not to distort sheet when cleaning. Punch three (3) holes in one end with paper punch and hang sheet in cleanroom.

4.40 Place back face sheet material roll and dispenser on stock cutting table. Dispense stock to length marker allowing enough slack in stock to avoid distortion while cutting. Check material for defects and dispense stock as necessary. Align sheet.

4.42 Trim end(s) of sheet on cutting plate at indicated marking and clean ends of sheet as performed on front sheet. Punch three (3) holes in one end with paper punch.

4.44 Gather the following items:

Back face sheet	Jaw shims	Toluene (squeeze bottle)
1" masking tape	Kimwipes®	Trim guard
1" Teflon® tape	9/6" six point socket	Cutting guide
Ratchet or speed wrench	Torque wrench	6" socket extension

4.00 <u>Stretch Forming</u> (Con't)

4.46 Face Sheet Material Preparation (Con't)

4.48 With items of 4.44, enter cleanroom, remembering to open, close and move slowly. Hang back face sheet and place other items off to the side.

4.50 Turn on hydraulic pump. Move jaws in & out 10 - 12 repetitions to ensure fluid motion and equal travel/time relationship. Place pistons in farthest out position possible. Turn off hydraulic pump. Record piston free motion elapsed time:__________sec

4.52 Move cleanroom table directly in front of enclosure. Clean table with antistatic wipes and perform DRFL inspection of table, sweeping dirt towards exhaust.

4.54 Place front face sheet centered, tool side down, onto table. With 2" length of masking tape, secure enclosure edge of face sheet to table at ends. Using Toluene and R^3 method, in a direction perpendicular to sheet length and away from enclosure, degrease sheet. Perform DRFL on sheet, sweeping crumbs towards exhaust.

4.56 Remove tape, flip sheet (tool side up), re-secure to table and wash this side of sheet as above. Perform an intense DRFL inspection.

4.58 Very slowly and carefully, remove doors from enclosure.

4.60 Pick up sheet and flip over carefully so as not to deform, place sheet at a 45° angle to laminar air flow directly in front of enclosure. Carefully shake sheet and perform a final DRFL inspection. Alert to motion of other person holding sheet, yet watching only the side one is holding, and keeping tension in sheet, place sheet in enclosure and onto tool. Place ends of sheet into jaws, one side at a time.

4.64 Repeat above sequence, on tool side only, with back face sheet.

4.66 Place jaw shims between jaws behind tightening bolts.

4.68 Place dirt shield between jaws and enclosure. Place wood bar between jaw and machine frame to brace jaw during torque operation. Tighten clamping nuts of jaws using manual torque wrench to <u>60</u> ft-lbs (three (3) stages: 25, 50, and 60 ft-lbs; The last 10 ft-lbs need be done with continuous motion), using tightening pattern:

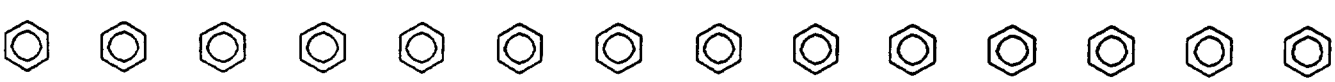

25 ft-lbs Sequence													
13	11	9	7	5	3	1	2	4	6	8	10	12	14
50 ft-lbs Sequence													
14	12	10	8	6	4	2	1	3	5	7	9	11	13
60 ft-lbs Sequence													
14	1	2	3	4	5	6	7	8	9	10	11	12	13

4.00 Stretch Forming (Con't)

4.70 Stretch Forming Procedure

4.71 Turn on hydraulic pump. Pull control lever such that jaws separate at a creep rate, until tension in back face sheet is noted at crown of tool.

Record pressure on inlet of control valve: ___________psi.

Adjust piston travel scales on jaws to 0.0

Record intended piston travel: _______in.

Pull control valve lever, again such that jaws separate at a creep rate, to start stretch. Release lever to neutral position upon appearance of the complete tool contour displayed through the face sheets or above intended piston travel, which ever is largest. Record actual piston travel:

Piston travel: Left _________in.

Right _________in.

4.72 Immediately and carefully, ==> temporarily tape entire length of long edges of both sheets to tool using 1" wide masking tape, leaving room at ends to place trim guards under sheets. Turn off hydraulic pump.

4.73 Rough cut sheets about 3 - 4" from jaws using black handled scissors. Vertex end is cut from filter side to front. Opposite end is cut from front towards filter.

4.74 Place trim guards between tool and front face sheet, aligned with end of tool. Tape trim guards to tool. Place a layer of masking tape over intended cut. Tape trimming guide on top of previously laid tape, 1/2" from edge of tool. Lubricate intended cut line with MIBK and using small utility knife, cut sheets along guide. Remove guide and all tape at end while tape is still saturated with solvent. If dried, apply more solvent.

4.75 Repeat above procedure at other end.

4.76 Allow enough time to for MIBK to evaporate, then apply 1" wide Teflon® tape on vertex end, holding face sheets to tool. Remove masking tape from radial edges (one at a time), while applying Teflon® tape along entire length of radial edges. Tape O.D. edge.

4.80 **Back Face Sheet Stress Relief Abrasion**

4.81 Remove tool from enclosure and place on table in C & E area. Make sure edge taping is complete and secure. Tape corners ∠45° to preceding taping.

4.82 With polyethylene gloves on cut 3-D abrasive (Scotch-Brite® #7448) into 6 equal sections and place into clean box.

4.83 Clear vented hood of all tools and materials. Ensure hood vent is on. Place C & E stretch tool support in hood.

4.84 Place tool on support in hood, vertex end to the right, being mindful of electrical gangliation of underside. Feet on radial sides of tool are to be against outer edge of support. Using Toluene, flood wash face sheet x 2 with fresh wiper each time. Dry with clean wiper. Use R^3 method as final solvent cleaning with Toluene, and repeat process with MEK.

4.85 Remove tool from hood and replace on table. Re-check edge taping. With hands in polyethylene gloves, abrade surface of face sheet with 3-D abrasive pads cut above, in 4 directions, 45° apart, abrading 6" x 6" patches and overlapping generously. Change pads often. When abrading close to taped edges, abrade carefully, keeping abrasive pad off tape.

4.86 Using a dry wiper, sweep abrasion crumbs from sheet surface. Wipe tape and face sheet/tape/tool interfaces with distilled water and R^3 Method. Once again, check all taping to insure leak proof.

4.87 Attach rinse troughs on ends of tool. Teflon® tape seams of troughs and face sheet ends.

4.88 Place fresh distilled H_2O 2 1/2 gal container in suspension on left side. Likewise, suspend hot H_2O container on right side. Fill 5 gal container 2/3 full of hot H_2O for glove rinsing. A full box of wipers (Kimwipes®) should be double-backed taped to top of hood.

4.89 Mix a solution of 50% each of soap (CSP, Hilliard® #125) and water for a total of 250 ml. Using nylon brush (1 1/2" wide with shortened bristles) and soap solution, scrub surface of face sheet. With bristles shortened it is easy to contact metal parts of brush with surface being cleaned, which would destroy face sheet, therefore, ample care is necessary to avoid such a situation, and is dealt with by keeping brush perpendicular to face sheet surface. Avoid lifting tape with scrubbing action. Rinse sheet with hot water, directing flow towards troughs. Repeat soap scrub and rinsing. Final rinse with distilled water. Face sheet may be either air dried or by using Makita® heat gun set on low heat and high air flow. Remove troughs. Re-dry especially at ends. Remove tool from hood and place on table.

4.80 **Back Face Sheet Stress Relief Abrasion** (Con't)

4.90 Bring back face handling frame from cleanroom to C & E area. Inspect back face sheet surface for particles and remove with indirect air flow of compressed air hose. Peal Teflon® tape off of one (1) radial edge and one (1) end, leaving approximately 3" of tape at center of end, allowing pealed tape to hang. Using small utility knife to separate sheets on radial edge, insert three (3) equidistant pieces of Tygon® tape between sheets, securing front face sheet to tool. Repeat tape removal and Tygon® insertion on other radial edge. Remove double-back tape backing on handling frame, align frame with tool and then place firmly onto face sheet. Press on frame in estimated double-back tape placements. Astutely, remove remainder of Teflon® tape securing back face sheet to tool. Remove frame with face sheet attached from tool surface. Invert and tape edges of sheet to frame edges and tape corners as before, with Teflon tape. Re-tape front face sheet to tool, including corners with Teflon® tape. Retain both front and back face sheets in C & E area.

5.00 **Lower V-Close-Out First Side Surface Preparation**

5.10 Designate one (1) of the V-Close-Out material sheets as "Lower" and label preparation plate as such.

5.12 Prepare surface of Close-Out material as described in EN-1002A, "Aluminum Surface Preparation for Adhesive Bonding". Use the following quantities:
Soap & H_2O -- 150ml
Etching Paste -- 75ml

5.13 Time Chart:
Etch Start:_____
End:_____

Dry Start:_____
End:_____

5.15 Upon completion of drying sequence (performed in cleanroom with small part drying set-up), carefully remove Teflon® tape, turn stock over and re-tape.

5.20 Clean hood and C & E area.

DAY THREE

Date:________

Assemblers ________________ ________________ ________________

Recorder ________________

6.00 Surface Preparation of Bonding Areas

6.10 Place protective sheet of polyethylene in Spray Booth and use this arena for surface preparation of Dummy Corners, V-Close-Outs and Doublers. If spray booth unavailable, prepare above pieces in hood before face sheets.

6.12 Place tool on support in hood, again being mindful of electrical gangliation of underside. Feet on radial sides of tool are to be against outer edge of support.

6.15 Place back face sheet with frame in hood.

6.20 Follow procedure set forth in EN-1002A, except for final step of "Forced Air Drying", for all of above surfaces.

6.22 Observe the following when preparing Doublers, as both sides are to be prepared:

- Perform one step of surface preparation on one side of each doubler, then turn over and repeat step on other side.

- Use indirect compressed air to remove as much abrasion residue from first surface and inspect both the doubler and support plate before turning doubler over and re-clamping.

- Remove clamping for soap washing, etching and rinsing, turning doubler over several times during these operations, and holding doubler against support at one end at a time during rinsing.

6.25 After final rinsing, hang doublers using hooks inserted into tab holes inside of spray booth (close booth) or cleanroom, until Day Four.

6.27 While preparing front and back face faying surfaces: be conscious of wiring beneath SF/L Tool; place tool into hood before applying troughs and dams (troughs before dams); prior to first soap washing, place splash guard between front and back faces; and dams are not to be used on back face sheet.

6.30 Allow face sheets to air dry, remove dams and check for residual etching paste and/or soap ==> use distilled water and R^3 Method to clean up edges.

6.32 Remove troughs and allow set-up to remain overnight.

G/8 A.

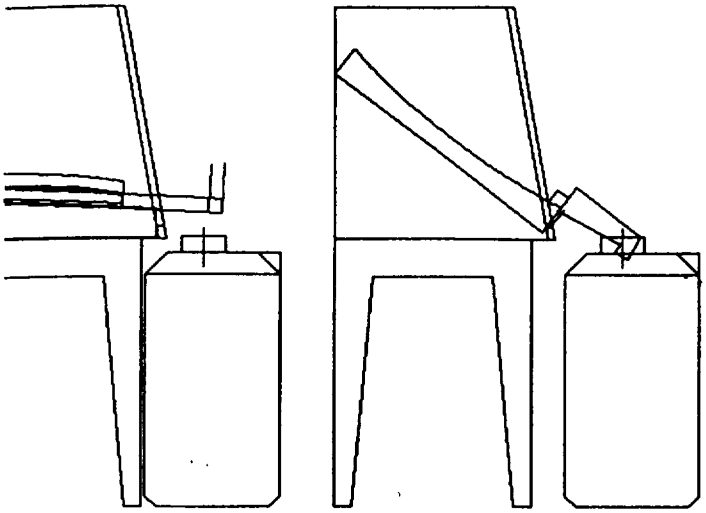

C-E.DWG

6.00 <u>Surface Preparation of Bonding Areas</u> (Con't)

5.13 Time Charts:

Peripheral Parts:

Etch Start:_____
End:_____

Front Face:

Etch Start:_____
End:_____

Back Face:

Etch Start:_____
End:_____

DAY FOUR Date:_________

Assemblers ____________________ ____________________ ____________________

Recorder ____________________

6.00 **Surface Preparation of Bonding Areas** (Con't)

6.10 **Parts Drying**

6.12 Place tool on oven standoffs. Place cardboard oven walls over tool with rectangular slot at O.D. end. Place radial edge doublers on edges of tool. Invert back face sheet frame and suspend over tool. Insert hangers into frame holes and hook onto cardboard walls. Insert thermometer in hole at vertex end of cardboard, assuring horizontal retention of thermometer with black duct tape. Suspend three (3) Makita® air guns from oven framing and tape in place with horizontal directed airflow into oven. Place cardboard lid on enclosure. Sketch______

6.15 Turn heat guns on 'HIGH' air flow and number '2' heat setting. Monitor temperature and adjust heat settings accordingly to keep temperature of air flow between 140 and 160 °F, throughout a period of 30 minutes.

Time Start:_____

Time End:_____

6.20 Dry all other peripheral parts in cleanroom with small part drying apparatus. Duration: 30 minutes.

Time Start:_____

Time End:_____

6.22 Remove heat guns, thermometer and cardboard lid. Careful not to drop hangers on front face sheet, remove back face sheet frame, then remove cardboard enclosure. Also, remove U-plywood oven frame element.

7.00 **Lay-Up Procedure**

7.10 **Part Preparation**

7.12 Tape (masking tape) 1:1 CAD plotting (DWG________) of close-out sections on top of C & E setups, on three (3) sides, leaving bottom un-taped. Clean steel guide with Acetone. Cutting notches out first, cut parts out along plotted lines with small utility knife and steel guide (drafting equipment may also be incorporated to enhance consistency by taping plate to board and placing steel guide against drafting scale), starting from

G 20A

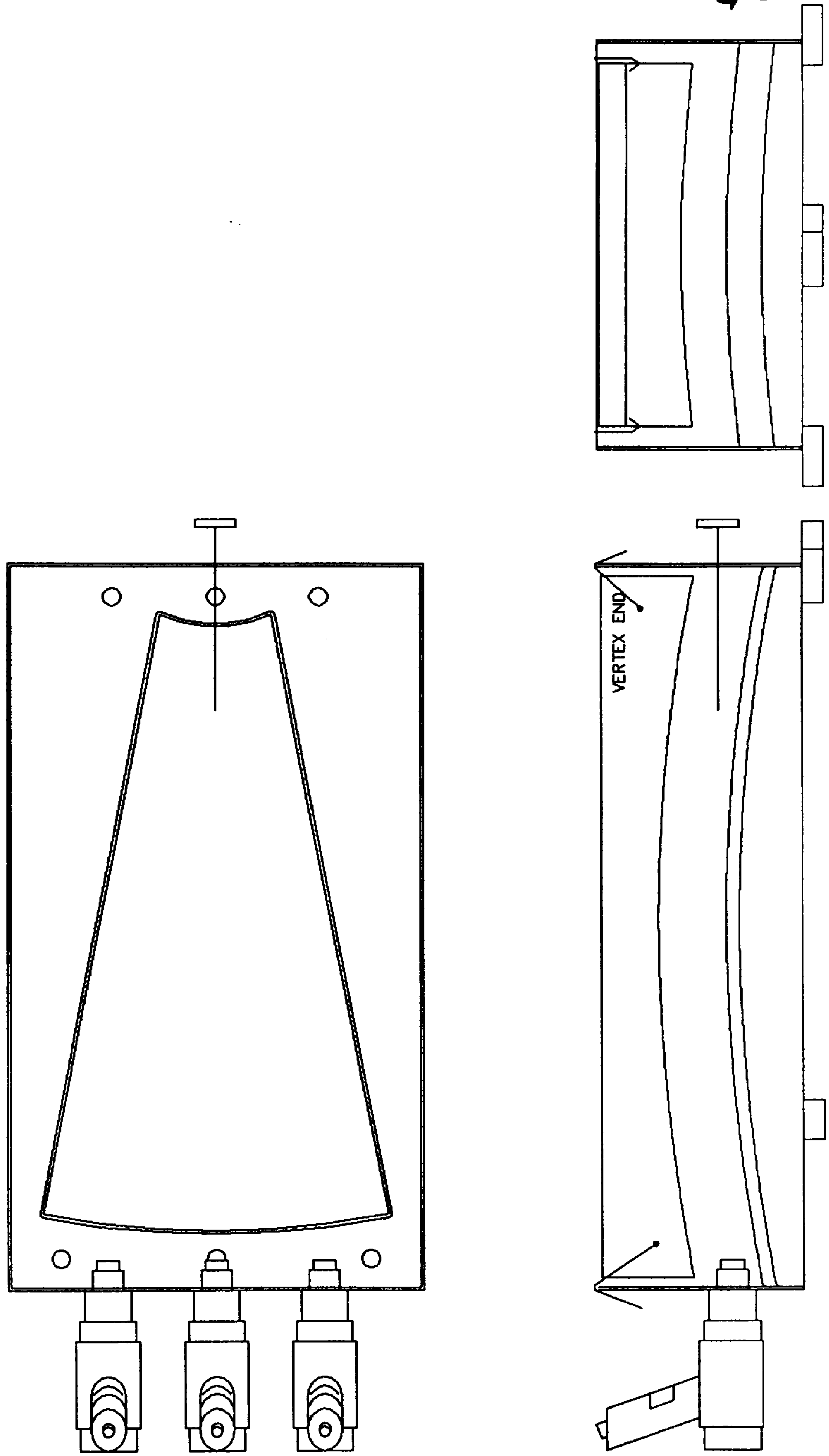

7.00 Lay-Up Procedure (Con't)

7.10 **Part Preparation (Con't)**

7.12 (Con't) bottom up, being as accurate as possible. Scribe bend line on each part ==> Do not use utility knife. Lay each part on Kimwipe® to prevent contamination of etched surfaces.

7.14 Double-back tape wooden handle to 12" steel scale. Bend each piece to proper angle, at scribed line, using urethane close-out forms and steel scale. Parts which were surface prepared on both faces are designed for lower 'V' sections. Single side surface prepared parts are upper 'V' sections and should be bent such that treated side forms the small angle. (Refer to DWG____________________) Replace pieces on Kimwipes®.

7.16 Place cleaned Back Face Sheet Template onto back face sheet respective of orientation and cut sheet with small utility knife with fresh blade. Peel remaining 3 mil sheet away from template while holding template in place securely to insure complete cutting. Place aside.

7.20 **Epoxy Preparation**

7.22 Open APS® Epoxy Resin can and check for separation and/or crystallization. If so, reconstitute epoxy resin, following procedure of EN-1019, "Reconstitution of Advanced Polymer Sciences (APS) Epoxy Resin X115(216)".
Reconstitution necessary? ☐ Yes ☐ No
If yes, record:
Number of reheatings:______

7.24 Use data area below to prepare 200 grams of APS® Epoxy Resin with 4.30 grams of Catalyst:

Polypropylene Beaker (250ml) Tare:__________grams

\+ Resin: 200.0 grams

Subtotal..............__________grams

\+ Catalyst: 4.3 grams

Total.................__________grams

7.26 Mix the above for at least 10 minutes:
Start Time:_____ End Time:_____

7.27 Record Relative Humidity:______%

7.00 <u>Lay-Up Procedure</u> (Con't)

7.30 **Doubler Fitting**

7.32 Thread in high-vacuum copper extension into tool at vertex end. Bend extension to accommodate oven insulation and lid. Attach vacuum line from Welch Duo-Seal® pump via quick disconnect. Turn on pump applying <u>28</u> inHg vacuum (minimum).

7.34 Using back end of magic marker, indent front face sheet along vacuum groove. If groove is not visible from stretching forces, use sketch below to determine starting point.

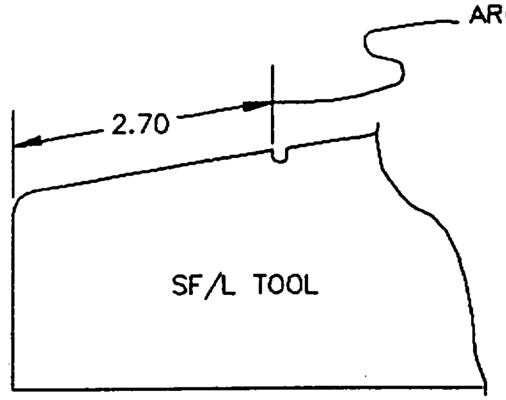

7.36 Indent face sheet at six drill bushing sites. Note location of drill bushings on DWG <u>CSU/AMC-1003: Sheet 1 of 2</u>

7.37 Pour an appropriate amount of mixed epoxy onto dip plates prepared for Doublers and Foam Edges.

7.38 Using steel scale, determine inside edge of vacuum groove (take front face sheet bend thickness into account) at three (3) places on each radial edge, and mark with scribe.

> <u>Note</u>: Although the next step is a fitting and parts must be handled, it is imperative that faying surfaces remain clean. Therefore, heed close attention to drawing specs and handle parts at edges or tabs whenever possible. Also, allow tape only in specified areas.

7.39 With masking tape, temporarily secure radial edge doublers in position on front face sheet, aligning tab removal groove with O.D. vacuum groove inside edge. Using clean steel guide, scribe for tab removal groove with scribe, at inside of I.D. vacuum groove, on both radial doublers. Refer to DWG____________________. Place O.D. and I.D. doublers over radial doublers, aligning tab removal groove with inside edge of radial doubler, temporarily tape in position, as well. Scribe opposite end for tab removal groove. Remove pieces from tool and cut four (4) tab removal grooves at scribe as performed in Step 3.21.

7.00 Lay-Up Procedure (Con't)

7.40 **Panel Fabrication**

7.42 Tape two (2) Kimwipes® side by side, to core dip plate.

7.43 Screed a 36" length by 4" width by .002" depth of epoxy.

7.44 Holding by tabs, dip Radial Edge 'A' doubler into .002" thickness of epoxy, remove and lay epoxy side onto Kimwipes® above, without smearing, to remove excess. Pull doubler slowly, yet directly away from wipers, again being careful not to smear epoxy. While holding doubler by edge, grip end of doubler at tab groove, on doubler side of groove, with needle-nose pliers and gently break off tab. Repeat at other end. Place on front face sheet to the inside of alignment markings as fitted previously. Tape ends of doubler down with small pieces (1" x 1/2") of Teflon® tape. Refer to DWG__________________ and DWG__________________. Secure complete outside edge of double to face sheet using Teflon® tape, overlapping doubler with 1/4" of the tape.

7.45 Repeat above for Radial Edge 'B', O.D. Edge and finally I.D. Edge.

Comment:

7.46 Using scribe, mark doublers for lower V-Close-Out placement. Refer to DWG_____10X_____ and DWG__________________. Begin on Radial Edge 'B', 2 1/4" from O.D. Edge (V8).

7.47 Remove dummy corners from C & E fixture and insert a #10-24 x 1" bolt into each (with threads) without protrusion. Dip dummy corners into epoxy, insure full epoxy coverage, then blot on wipers as performed on doublers. Place corners into respective positions, being careful not to allow dummy corners to slide under doublers. Refer to above drawings. Use C & E holding fixture to perform this procedure on corner without #10-24 threading.

7.48 Re-screed .002" thick epoxy layer.

7.49 Trim foam edges to length by fitting against dummy corners. Dip bottom and both ends of foam into .002" epoxy. Do not blot. Place foam in proper position of layup, against doublers, without sliding, referring to above drawings. Use aluminum layup weights to hold foam against front face sheet.

7.00 <u>Lay-Up Procedure</u> (Con't)

7.40 **Panel Fabrication (Con't)**

7.50 Remove all epoxy from above dip-plate and clean surface using MEK with R^3 Method. Check all areas of dip-plate to insure free of foam 'crumbs'. Screed a fresh .002" thickness of epoxy.

7.51 Dip lower 'V' sections, into epoxy, pushing sections gently into epoxy with tongue depressor. Rotate sections about fold, lifting sections from adhesive with small utility blade and press second half into epoxy with tongue depressor. Lift sections out of epoxy. Examine for thorough epoxy coverage and spread epoxy to dry area(s) with small utility knife.

7.52 Insert lower 'V' sections onto doublers, in order, along each edge, at base of foam, using scribed marks on doubler as alignment guides. Use small pieces of Teflon® tape (1" x 1/2") to secure sections to doubler and to each other. No tape is to be applied to upper half of 'V'.

7.53 Complete one edge at a time, radial edges first. As each edge is completed, further secure sections to layup with 1" wide Teflon® tape applied from fold of sections outward, spanning entire length of panel edge plus an extension of at least 2". Place over-rail on above taping, at crease of 'V', taping ends to front face sheet, while keeping as much tension in over-rail as possible. Further secure over-rail with Teflon® tape as above.

Comment:

7.54 Dry fit core on layup to verify size. Trim as necessary with stainless steel scissors prior to adhesive application.

7.55 Screed .010" thick layer of adhesive onto core dip plate. Dip back face side of core into adhesive layer and ensure even wicking of adhesive on all cells by pressing core down with edge of tongue depressor. Minimize side movement of core to prevent adhesive 'plowing' onto core.

7.00 <u>Lay-Up Procedure</u> (Con't)

7.40 **Panel Fabrication (Con't)**

7.56 While gripping core by 'ears' at edges of vertex end, carefully raise core from dip plate, so as not to scrape up additional epoxy onto core. Screed adhesive to develop a new even layer on dip plate.

7.57 Dip front face side of core into adhesive. Again, press core down using edge of tongue depressor. Remove core from dip plate as above, inspect for thorough coverage of epoxy. Re-dip if necessary.

7.58 Place core onto layup, beginning at vertex end, careful to keep any sliding of core to a minimum. Have trim scissors available for final core fit if necessary.

7.59 Remove template from back face sheet. Loosen edges of back face from frame as some edges may have been pressed into groove on frame caused by cutting action of knife. Carefully remove back face sheet from frame.

7.60 Place back face sheet into proper position on layup and place core weighting fixture with bagging film wrapped about it, on top of back face sheet. Tuck edges of core within limits of foam, using long edge of tongue depressor.

7.61 Spread as small of quantity of epoxy as possible on upper 'V' sections using small spatula (1" wide) or small utility knife, as neatly and uniformly as possible, on surface prepared for bonding. Insert onto layup, in order, along each edge, at top of foam, overlapping back face sheet and lower 'V' sections, staggering ends of lower 'V' sections. Use small pieces of Teflon® tape (1" x 1/2") to hold to back face and each other. See DWG________________________.

7.62 Place vacuum manifold centered around layup and exhaust at vertex end which is also aligned with end of tool by tape marker on manifold. Insert 3" strip of bagging tape under manifold just below 'T' of manifold and press into place. Secure manifold to front face sheet at four (4) places with Teflon® tape. See DWG________________________.

7.63 Place two (2) 1/2" long strips of bagging tape, with backing removed, on top of tape placed below manifold, along each side of web of 'T'.

7.64 With backing intact, place four (4) strips of bagging tape along each outer edge of manifold as close to manifold as possible. Ensure ample overlap at corners. Allow enough length for hump at 'T' and adjacent corner overlap.

7.65 Place bleeder strips along base of V-Close-Out strips (trim if necessary), within limits of manifold. Tape into place with Teflon® tape.

7.00 <u>Lay-Up Procedure</u> (Con't)

7.40 **Panel Fabrication (Con't)**

7.66 Release bagging film from core weighting fixture and spread out over complete layup. At one (1) radial edge, place Vacuum Bag Hold Down Strip in valley between close-outs and manifold. Allow enough slack in bagging film to permit hold down strips to press film to bottom of valley. While strip is held down firmly and bagging film is held away from bagging tape, remove backing on bagging tape, leaving 1 1/2" of backing at corners, for edge being worked on. Bagging film is now evenly smoothed onto bagging tape, starting at midpoint, working towards corners.

7.67 Without allowing bagging film to slide, move radial edge hold down strip to other radial edge and repeat above procedure.

7.68 Using O.D. Edge Bagging Film Hold Down Strip, repeat procedure 7.66 on O.D. edge.

7.69 Repeat once again at vertex edge being careful to take hump at 'T' into consideration when smoothing bagging film towards corners.

7.70 Cut four (4) 2" strips of bagging tape and press into corners of bagging film with thumbs, filling all wrinkles. Remove remainder of bagging tape backing and press film to face sheet in such a fashion that allows but one (1) fold to form at each corner. Press film to set 'T' of manifold firmly.

7.71 If wrinkles or folds in bagging film occur at any other positions besides the corners, use technique of 7.70 above to fill crevice.

7.72 Connect vacuum line attached to Watsco Oil-Less® vacuum pump to manifold and tighten hose clamp. Open needle valve fully and plug pump into outlet. Close needle valve slowly until 2 - 3" H_2O is present on manometer. While watching manometer levels, press onto all contact areas of bagging film and tape. If any change occurs in manometer reading, a leak is present and must be repaired. Usually pressure applied at leak or squeezing of folds will stop leak. Watch for radical changes in manifold readings as a leak may be large enough that if closed, may cause, not only great pressure on layup, but suck H_2O from manometer into pump. If no leaks are evident, or have all been sealed, adjust needle valve to manometer reading of: <u>14.0</u> in differential.

Comment:

8.00 Cure Procedure

8.10 Temperature Control

8.11 Apply a square of 1" wide Teflon® tape to bottom side of each (six (6) J-type thermocouple required) J-type thermocouple shim and trim to within 1/16" of shim. Apply another square to top of each shim and trim as above. Attach five (5) thermocouple to side 'A' of tool, using hold down clamps in positions shown in sketch below. There is an indention in hold down clamps which is to be placed over wire-to-shim connection. Clamps are oriented such that thermocouple are to be clamped to the right of clamping screw for Zones 1 & 2, and to the left for Hi-Limit and Zones 3 & 4. Connect thermocouple leads to corresponding thermocouple jacks of controller. Connect heater electrical leads to corresponding power outlets of controller. The sixth thermocouple (data acquisition) is attached to side 'B' of tool to the right of attachment screw in position shown also in sketch below.

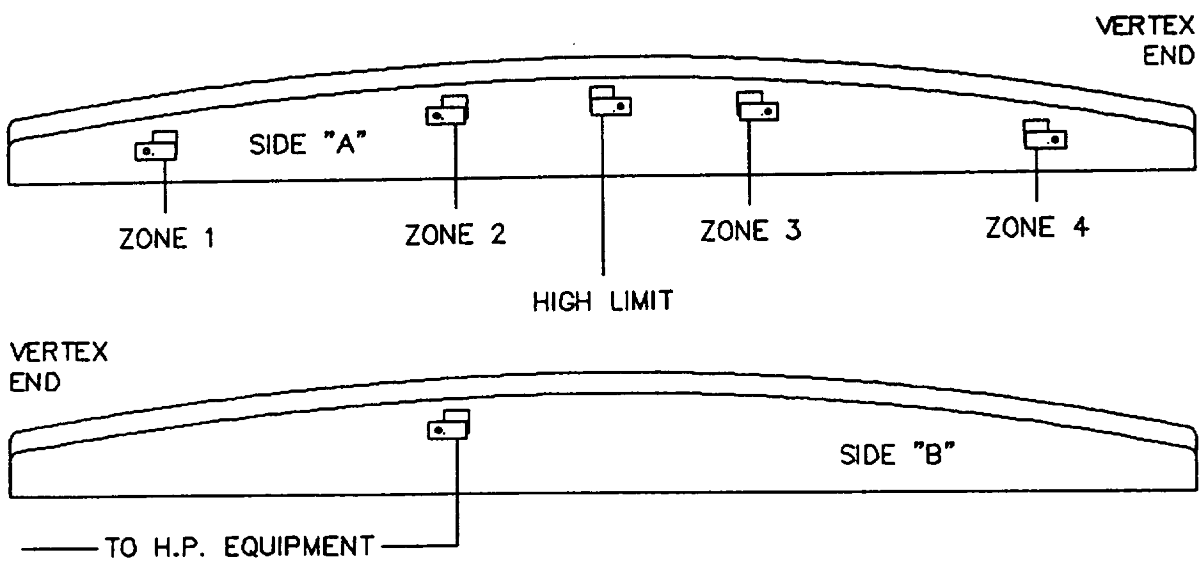

8.12 With all switches of controller in 'OFF' position, turn controller on by lifting lever on main box on side of controller. Press small reset button in center of control panel (unmarked). This resets Hi-Limit circuitry, necessary after any power stoppage or as a result of exceeding Hi-Limit setting.

8.13 Continuity of thermocouples is checked by equal or similar temperature readings (± 2°F) of all four (4) controllers. Greater variance of thermocouple output requires connection check or thermocouple replacement. A dashed line on controller is indicative of an open thermocouple circuit. Check lead connections and refer to procedure 8.15 to return to operative mode.

8.00 <u>Cure Procedure</u> (Con't)

8.10 **Temperature Control** (Con't)

8.14 Perform the following 'PROCESS VALUE' settings check of each control unit:

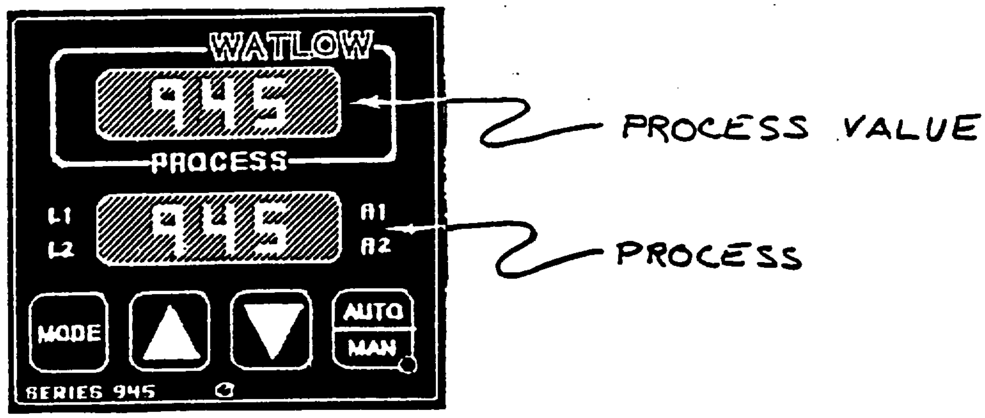

Individual Zone Control Unit (Watlow® controller)
[When turned on and in normal operation, the 'PROCESS' is the temperature set point, and the 'PROCESS VALUE' is the thermocouple output]

Press [MODE] key to change 'PROCESS', and the associative 'PROCESS VALUE' will likewise be displayed. To change any 'PROCESS VALUE', press [▲] or [▼] key to increase or decrease value. Press [MODE] key for each process and associative value in table below:

PROCESS	PROCESS VALUE
Pbl	9
rEl	0.20
rAl	1.35
Ctl	1
AlLO	32
AlHI	350
A2LO	32
A2HI	350
CAL	0
AUt	0

8.00 <u>Cure Procedure</u> (Con't)

8.10 **Temperature Control** (Con't)

8.15 If, at any time, a series of dashes (----) is displayed for a 'PROCESS VALUE', there is an 'OPEN' in thermocouple circuitry. Repair circuit and/or replace thermocouple. Then press [▲] [▼] keys simultaneously until another series of 'PROCESS' AND 'PROCESS VALUE' display (Set-up Menu). These values are not to be changed. Press [MODE] key repeatedly until temperature and temperature set point are again displayed. If dashes are again displayed, thermocouple circuitry is still inoperative and in need of further investigation.

Note: Refer to Watlow Manual for further information.

8.16 High Limit setting is not to change, however, to check, remove front white panel (pull handles) and locate Limit Control Circuit Board (see display below). The High Limit temperature setting is set with the control knob in upper right hand corner of circuit board and setting value is 350°F. If the high limit temperature is reached or Heater Relay switch is turned on without pushing reset button, a red light on control panel and an audible alarm will be energized. In either case, return the Heater Relay switch to OFF position and make appropriate corrections.

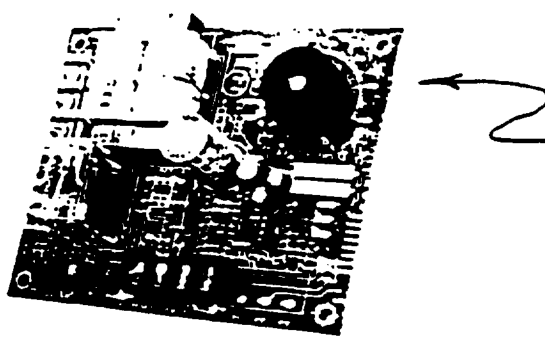

8.00 <u>Cure Procedure</u> (Con't)

8.10 **Temperature Control** (Con't)

8.17 Replace U-shaped plywood oven element on stand-off posts.

8.18 Place 36" x 20" x 3" pillow on top of layup. Place lid on enclosure. Lift one door at a time and insert side insulating pillows, being aware of all leads extending from enclosure. Connect bungy-cords to each other at bottom of doors. Re-tuck bottoms and sides of insulating pillows into enclosure.

8.30 **Data Acquisition**

8.31 Cure cycle includes a 2 hour period (plus 15 minute heat-up) at a temperature setting of 200 °F; a 4 hour period (plus 15 minute heat-up) at a temperature setting of 300 °F; a 12 - 18 hour cool down period to a temperature of 160 °F; two (2) annealing/off-gassing periods of 2 hours each cycling between 160 and 220 °F; an additional annealing/off-gassing period of 2 hours at 300 °F; plus a final cool down period of 40+ hours to room temperature. Add all of the above time periods to determine total time of data acquisition, since these are not exact times due to cool down period changes associated with various ambient temperatures, start up time and work schedules. Consider past data output plus weekend allowances to estimate this total:______________hours and multiply by 60 to acquire:____________minutes.

8.32 Insure all equipment for data acquisition is present (except for plotter as a graphical representation of data can be made at any time) and connected as shown in Sketch__________ of equipment on following page.

8.00 <u>Cure Procedure</u> (Con't)

8.30 **Data Acquisition (Con't)**

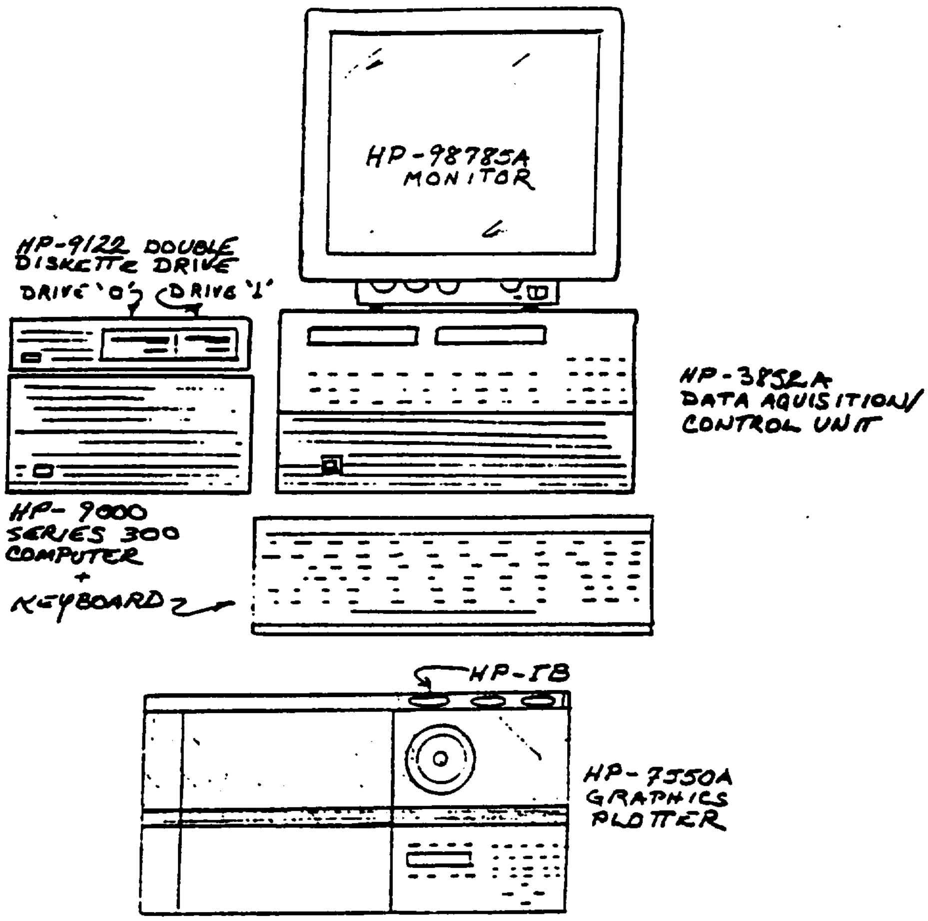

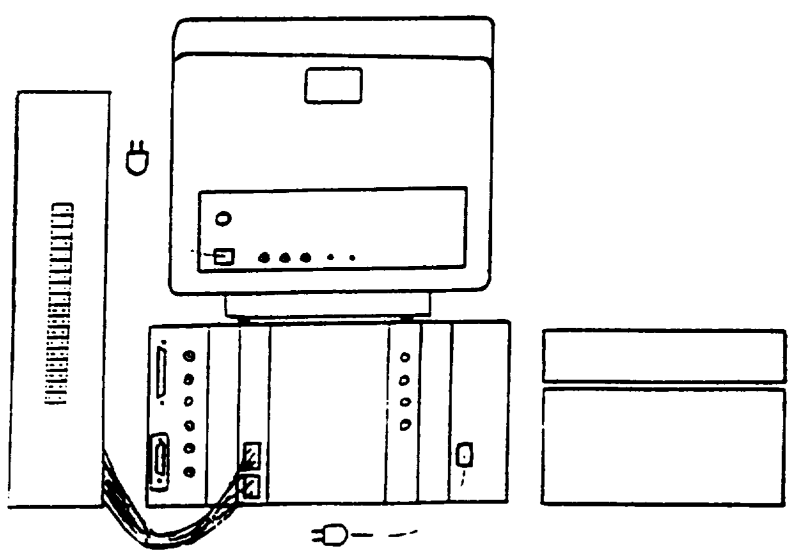

8.00 <u>Cure Procedure</u> (Con't)

8.30 **Data Acquisition** (Con't)

8.33 Connect all power cords of system to a multiple outlet extension and resource this extension from a circuit separate from those supplying power to controller (i.e., C-7).

8.34 In a plastic H/P Diskette case are three diskettes: <u>Disc One</u> BASIC 5.1 System Disc, <u>Disc Two</u> BASIC 5.1 Drivers + Language Ext., and BASIC 5.1 Utilities Disc. Place <u>Disc One</u> into Drive '0' of the HP-9122. Turn on all equipment saving the HP-9000 computer for last. As the system 'boots', green printing will appear (as opposed to off-white which is initially displayed). As this change occurs, there are also two sets of four (4) green rectangles at the bottom of the screen. Each of these rectangles represents a corresponding function of a grey button in the top row of buttons on the keyboard. If printing does not change to green, hold [SHIFT] key down while pressing [RESET/BREAK] key in upper left hand corner of keyboard. Instructions in lower left corner of screen to **Press the softkey 'f2' (Continue) to proceed. will** next be displayed. Do so. Then press button below Drive '0' of the HP-9122 and remove diskette. Insert <u>Disc Two</u> into same drive and push 'f2' key once again. When **Running** changes to **Idle** in lower right hand corner of screen, the system is completely 'booted'.

8.35 Remove <u>Disc Two</u> and return three (3) diskettes to case. From a cardboard diskette case select diskettes labeled "NASA Solar Concentrator/Panel Cure Temp Data Coll Prog/Panel Temp Storage (Data)/Plot Program" and "NASA Solar Concentrator/Panel Temp Storage (Data) X (re: latest version)". Also, insure that a freshly initialized disc is on hand. Place diskette with "Panel Cure Temp Data Coll Prog" into Drive '0'. Press the fifth grey button and **LOAD"█** will appear in lower left corner of screen. Type in, without error (or correct using cursor control keys and [Delete/char] key) **COLL_DATA** then press [RETURN] key.

8.36 When **Idle** re-appears, press the third grey key 'f3' or [RUN] key. A title screen will be observed, plus the prompt: **PRESS Continue KEY** - press the second grey key 'f2' or [Continue] key. A time will be given such as **5400 MINUTES** plus the question, **IS THIS OKAY?**. From derivations of procedure 8.31 decide 'Yes or No". If yes, type **Y** and press [RETURN] key. If no, type **N** and press [RETURN] key and at the prompt type in correct time in minutes, with this format: **XXXX,MIN** and press [RETURN] key.

8.37 The next screen will prompt to press [COLL_DAT] key, which is the second grey key or 'f2' key. Do so and allow at least five readings to be taken (readings are 1 reading per minute). The second reading printed should be an erroneous value of **1.8E+38** (glitch in software, yet to be located). Check the values after this to insure consistency with those of the controller. Press the first grey key or 'f1' key or [END] key and await prompt to store data. While holding [SHIFT] key, press [Reset/Break] key.

8.00 <u>Cure Procedure</u> (Con't)

8.30 **Data Acquisition** (Con't)

8.38 Repeat step 8.36 then await start of cure to press [COLL_DAT] key.

8.50 **Timer Settings**

8.51 Referring back to step 8.31, prepare the following table:

==>Day/Time:________/________Start Heat

Day/Time:________/________Temp Increase

==>Day/Time:________/________Heaters Off

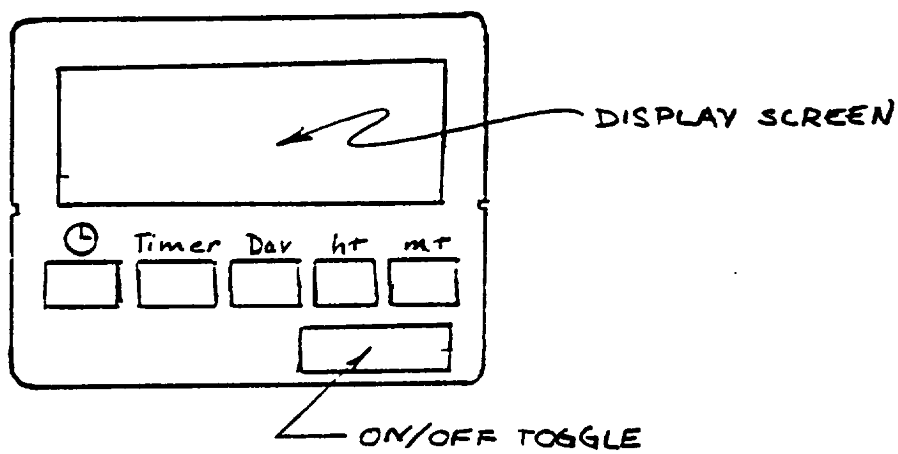

Cole-Parmer Timer

8.52 Press ' ' key on timer. Make sure actual present time/day is correct. To change, hold ' ' key and press appropriate key to change day/hour/minute.

8.53 Press 'Timer' key and "TIMER/1 ON" will be displayed. Change Day/Hour/Minute to correspond to "Start Heat" determination in Step 8.51

8.54 Press 'Timer' key again and "TIMER/1 OFF' will be displayed. Make appropriate changes corresponding to "Heaters Off" of above. Pay close attention to 'Day' setting if timer is to turn off past midnight.

8.55 Press ' ' key to revert back to present Day/Time display. Display should also indicate being in OFF mode. Use ON/OFF toggle to place timer in OFF mode.

8.56 Timer is to be plugged into wall outlet inside control unit (on wall opposite High Limit circuit board) and hanging plug inserted into timer.

8.00 <u>Cure Procedure</u> (Con't)

8.50 **Timer Settings** (Con't)

8.57 Turn 5 switches on front of Control Console to ON position (up) and allow timer to actuate curing cycle. If alarm sounds, turn off 'Heater Relay' switch and press 'Reset' button ==> turn 'Heater Relay' switch back on.

8.58 Stand by to start data collection at same time as heaters are started.

8.59 Monitor data collection, thermocouple readings on controller and manometer to ensure accuracy and consistency as layup begins to rise in temperature.

DAY TEN Date:_________

Assemblers ____________________ ____________________ ____________________

Recorder ____________________

10.00 Panel Removal

10.10 **Shut Down**

10.11 After allowing panel to cool to room temperature, place pre-determined diskette in drive '0' of HP-9122. Type in panel number along with number of data points (data collection time period in minutes) using the format: **PNL9_5400** and press [Return] key. If prompt returns for new name, diskette is full. Place another diskette with known space and retry save.

10.14 Turn off power to control console.

10.16 Remove side insulation 'pillows' from oven enclosure. Remove enclosure lid and sides. Remove pillow covering layup.

10.18 Remove all thermocouples and attaching clamps. Unplug power connections.

10.20 Disconnect plug of Watsco® vacuum pump and disconnect the vacuum line to 'Y' connector at manifold.

10.22 Cut through bagging with utility knife over breather material so as not to deface layup. Carefully peal bagging from layup. Peal remainder of bagging film and bagging tape from layup. Remove tape securing manifold to face sheet and cut bagging tape around 'T' of manifold; remove manifold.

10.24 Carefully peal all tape securing over-rails, V-Close-Outs and doublers.

10.26 Turn power off to Welch® vacuum pump and detach line at quick-disconnect.

10.28 Gently blow into vacuum extension line until panel is apparently lifted form all areas of SF/L Tool.

10.30 **Indexing Panel with Respect to SF/L Tool**

10.31 Cut through face sheet with small utility knife at two (2) drill bushing holes per Sketch____________. Remove vacuum seal plugs from drill bushings. Place double back tape on two index washers. Place .375" dowel pin into drill bushings, slide index washers in place per Sketch_________ and apply pressure to adhere the index washers in place. Remove dowels.

10.00 <u>Panel Removal</u> (Con't)

10.33 Place two (2) nuts on #10-24 x 1" bolts and tighten together such that less than .25" extends past lower nut (5 threads or less). Screw into dummy corners and tighten against dummy corners.

10.35 Peal remaining tape at edges.

10.37 Carefully remove panel from tool holding bolts placed into dummy corners.

10.38 Inspect panel.

Appendix H

H1

Cleveland State University
Advanced Manufacturing Center

EN-1022 Engineering Note

Slope Error Deviations of Panel No. 6

C.H. Castle
10/16/91

NASA GRANT NO. NCC 3-77, SUPP. NO. 2

<u>DISCUSSION</u> Panel #6 was placed in the optical inspection rig and analyzed. It had been levelized with EP-3 and aluminized in the NASA vacuum tank.

The photograph (65% scale) of the projected image is shown in figure 1. No attempt was made to analyze edge distortion errors, only those that are indicated by a matrix pair of numbers as shown. An enlargement is shown in figure 2. With the aid of magnification, the 4 midpoints along a radial shadow projection and 4 along a circumferential projection were drawn in. Midlines were drawn through the two sets of 4 midpoints in "best fit" fashion. The reference crossed pair of lines were drawn through the corners of the reference lines. Radial and circumferential deviations were then measured under 7X magnification with the sign convention shown.

Figures 3 and 6 show the radial and circumferential deviation histograms. Note their approximation to a normal distribution curve. The data was reduced and figures 4 and 7 show the resulting normal distribution curves. Resulting in:

<u>Radial slope deviations</u>
1 Sigma = 0.32 milliradian
3 Sigma = 0.96 milliradian
Median = +.05 milliradian

<u>Circumferential slope deviations</u>
1 Sigma = 0.42 milliradian
3 Sigma = 1.26 milliradian
Median = -0.125 milliradian

The normal curves are superposed on the histograms in figures 5 and 8.

Absolute slope deviations were calculated from the data as in figure 9, and the histogram is in figure 10. This data will not look like a normal curve because it can not, but maximum deviations at each matrix point are obtained. And these maximums are what determine how far the solar rays miss the focal point.

Figure 11 shows the preliminary budget of surface deviations from EN-1014 and reveals the maximum deviations (column 2) that are considered appropriate based on past experience (column 3). Deviation sources 2, 4 and 5 (column 1) are those which would affect the panel shape as analyzed in the optical inspection rig. Their combined maximum error allotment is 0.9 milliradian (0.3 + 0.3 + 0.3).

<u>CONCLUSION</u> Based on this preliminary analysis, panel #6 comes close to meeting requirements:

1.1 milliradian maximum measured
0.9 milliradian maximum allotted

Two additional comments 1.) some of the larger deviations are related to edge effects, and 2.) adjustment of the reference lines (plastic sheet with scribed lines) could result in reduced maximum deviations.

The data does provide near corroboration that the stated error budgets can be met. Refinements would likely allow meeting allotments.

PANEL NO.6
OPTICAL INSPECTION
65% SCALE

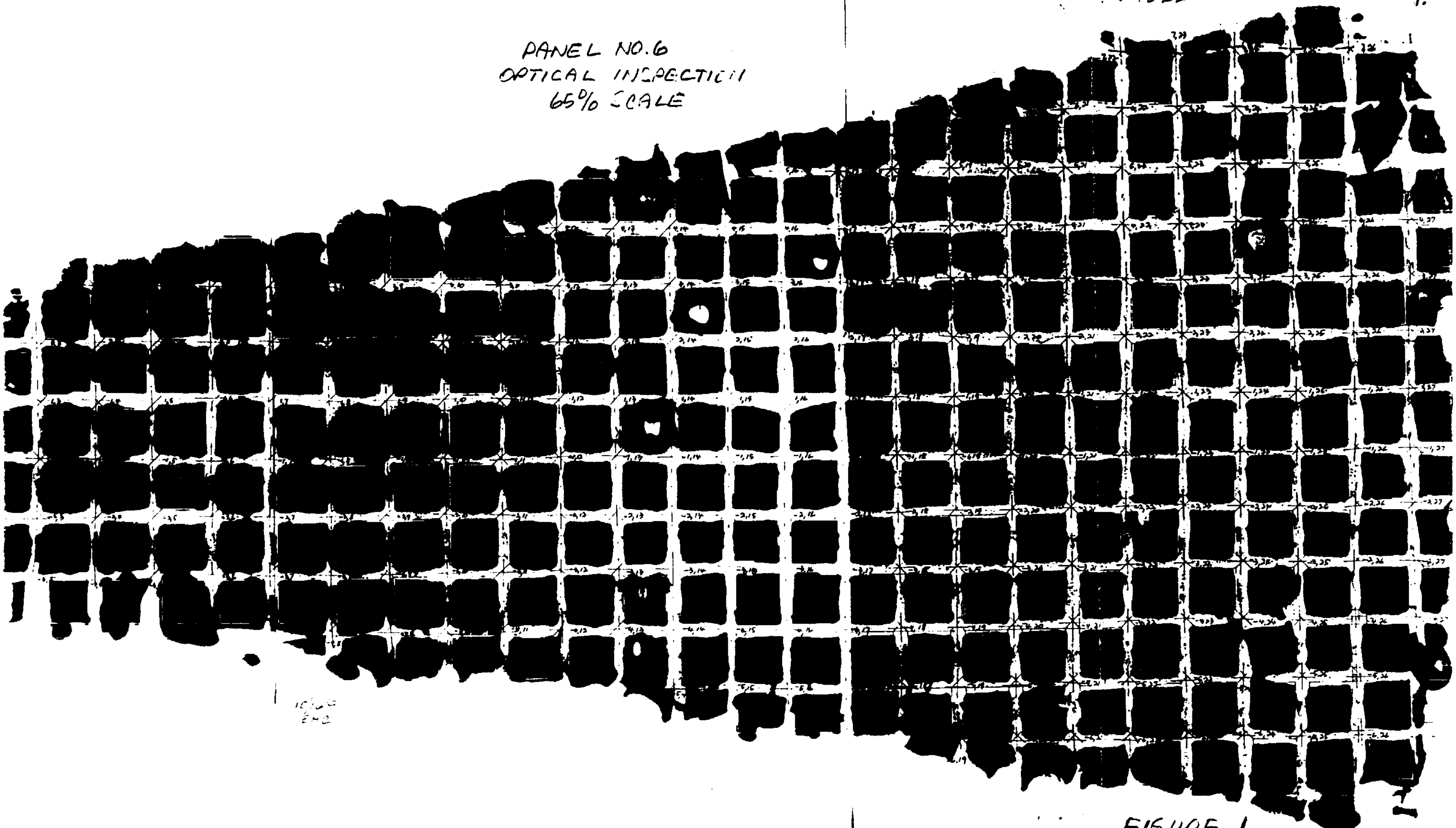

FIGURE 1

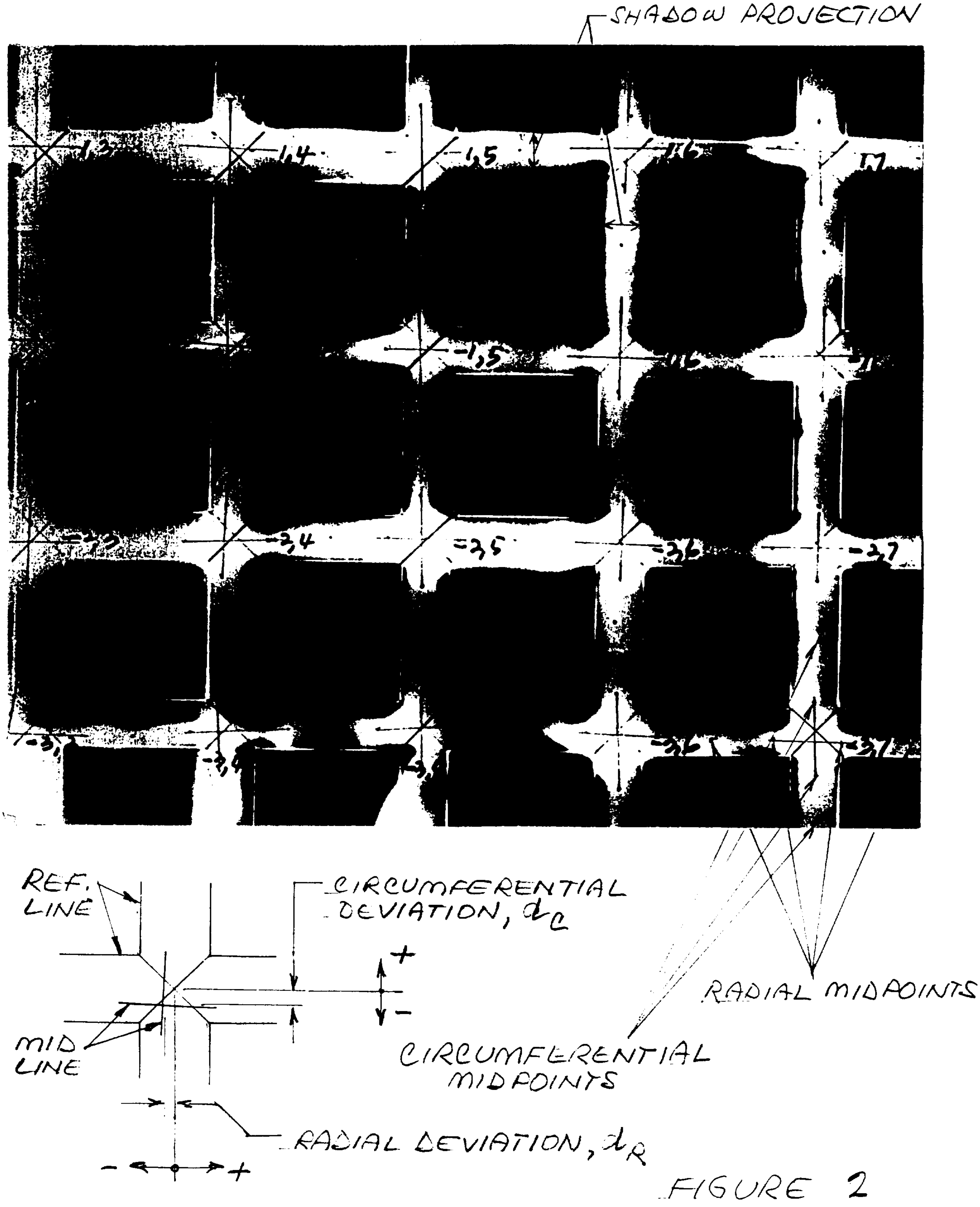

FIGURE 2

1.5 x SIZE

PROBLEM	CLEVELAND STATE UNIVERSITY	NAME	H6
	DEPT.	DATE	

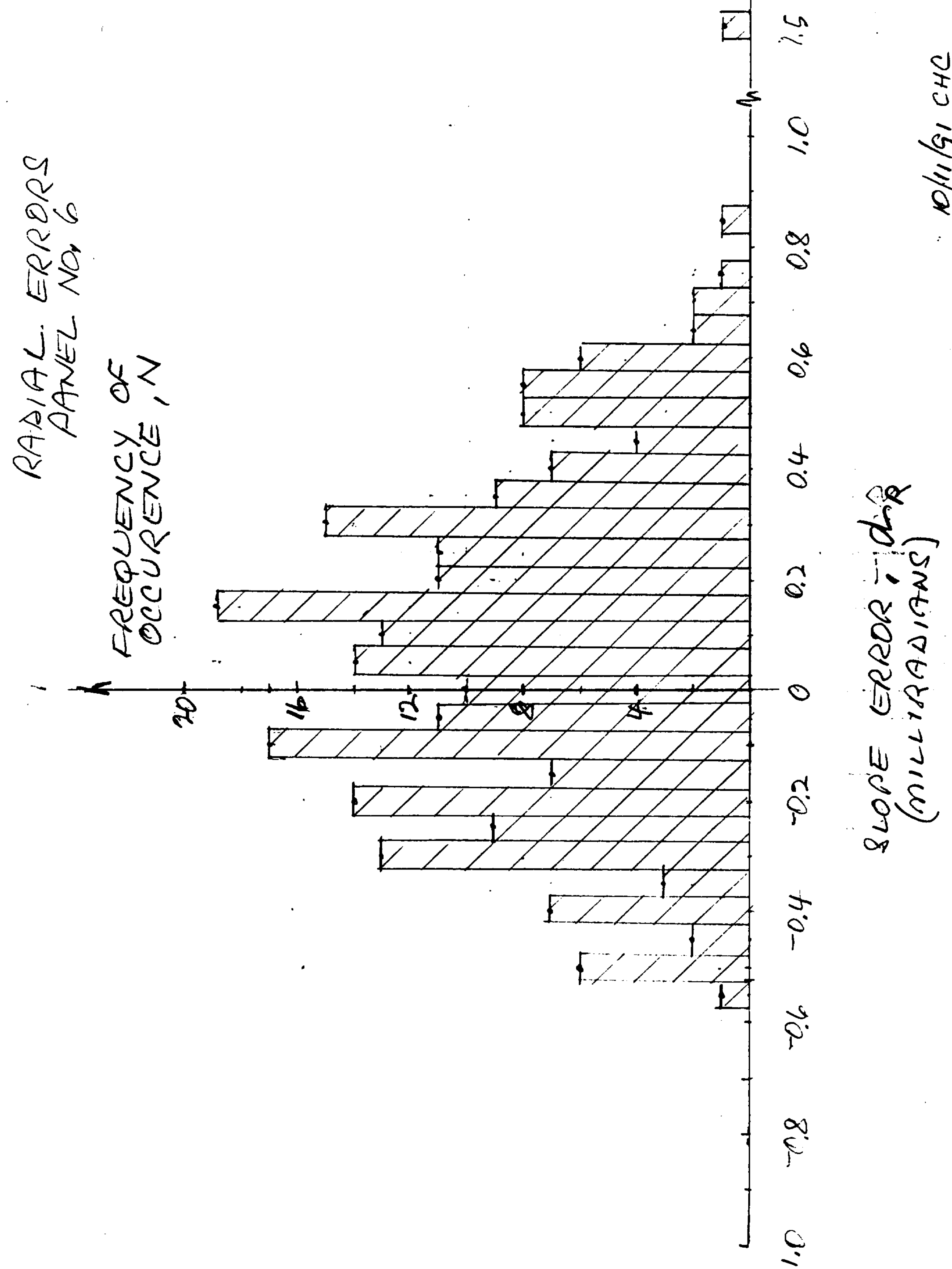

FIGURE 3

PROBLEM	CLEVELAND STATE UNIVERSITY	NAME	H.7.
	DEPT.	DATE	

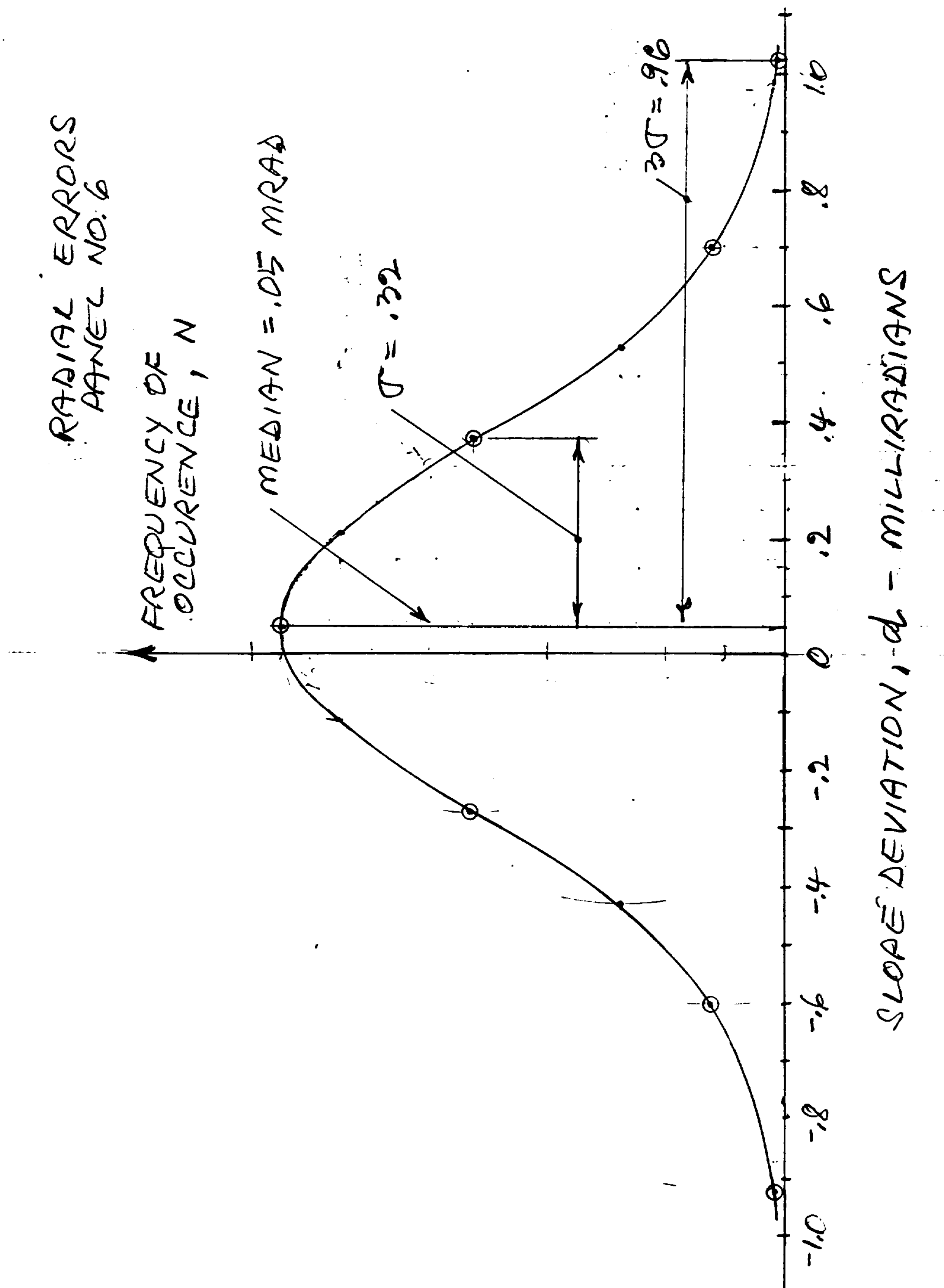

10/11/91 CHC

FIGURE 4

PROBLEM	CLEVELAND STATE UNIVERSITY	NAME	H8.
	DEPT.	DATE	

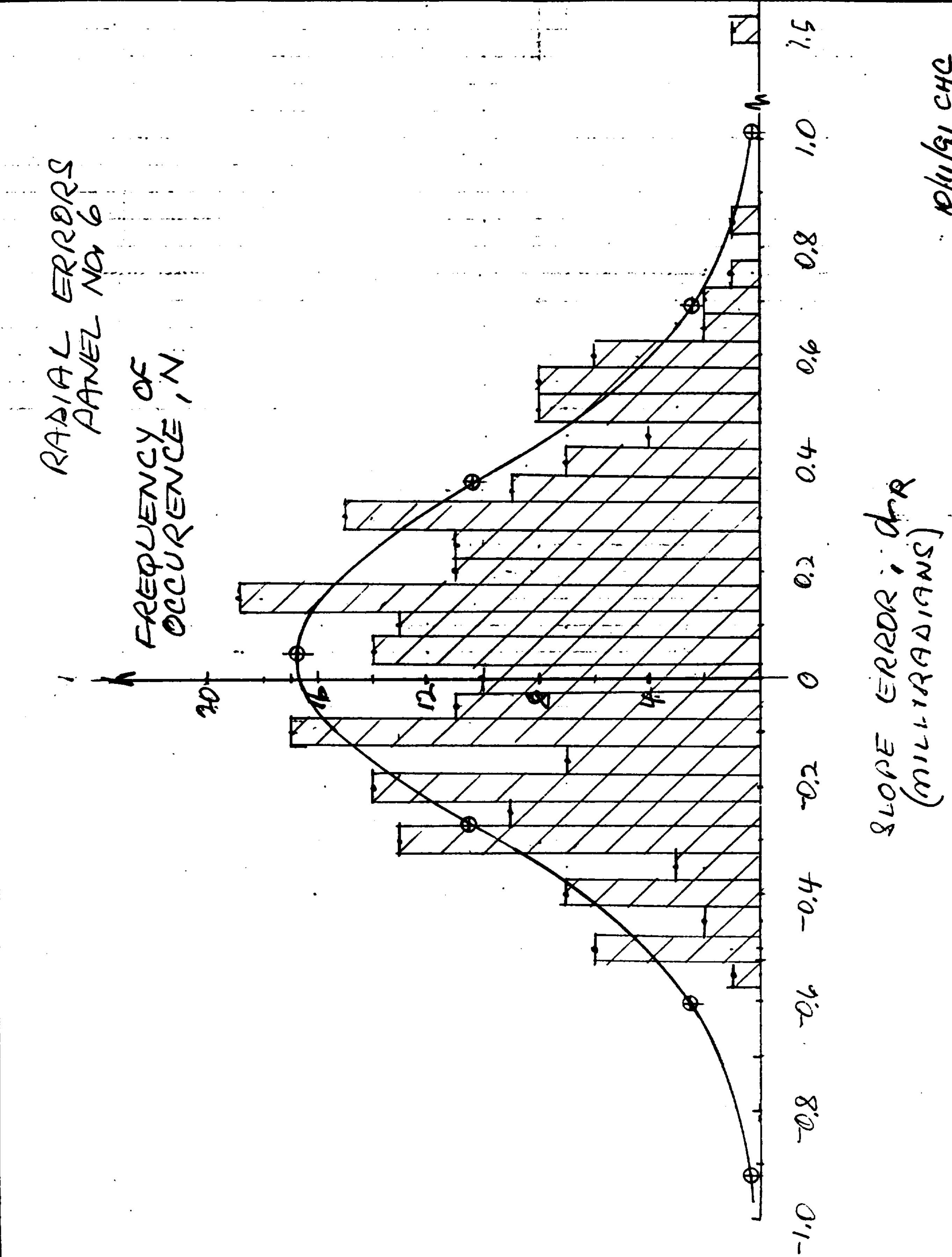

FIGURE 5

PROBLEM	CLEVELAND STATE UNIVERSITY DEPT.	NAME DATE	H9.

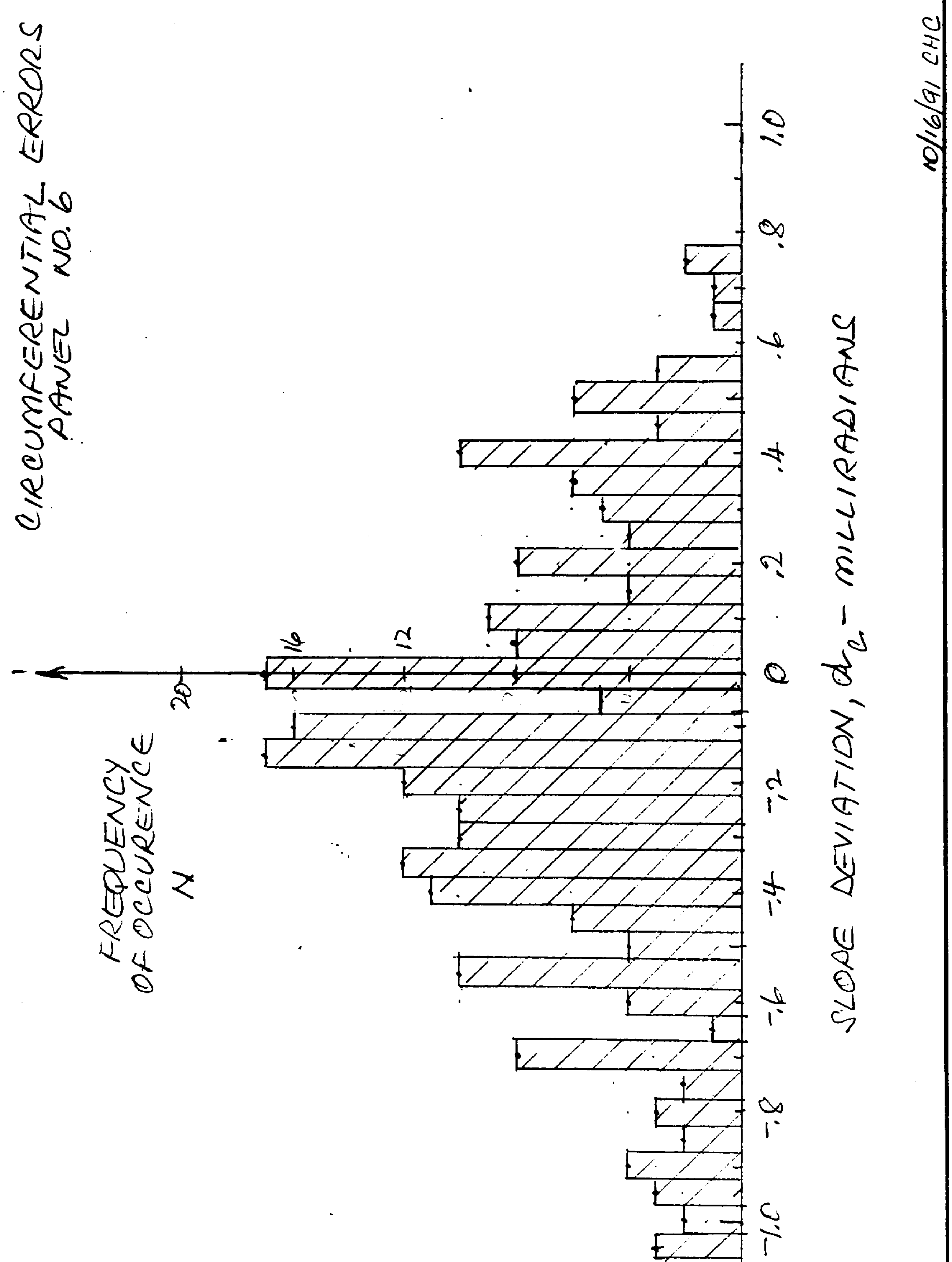

FIGURE 6

PROBLEM	CLEVELAND STATE UNIVERSITY DEPT.	NAME DATE	H 10

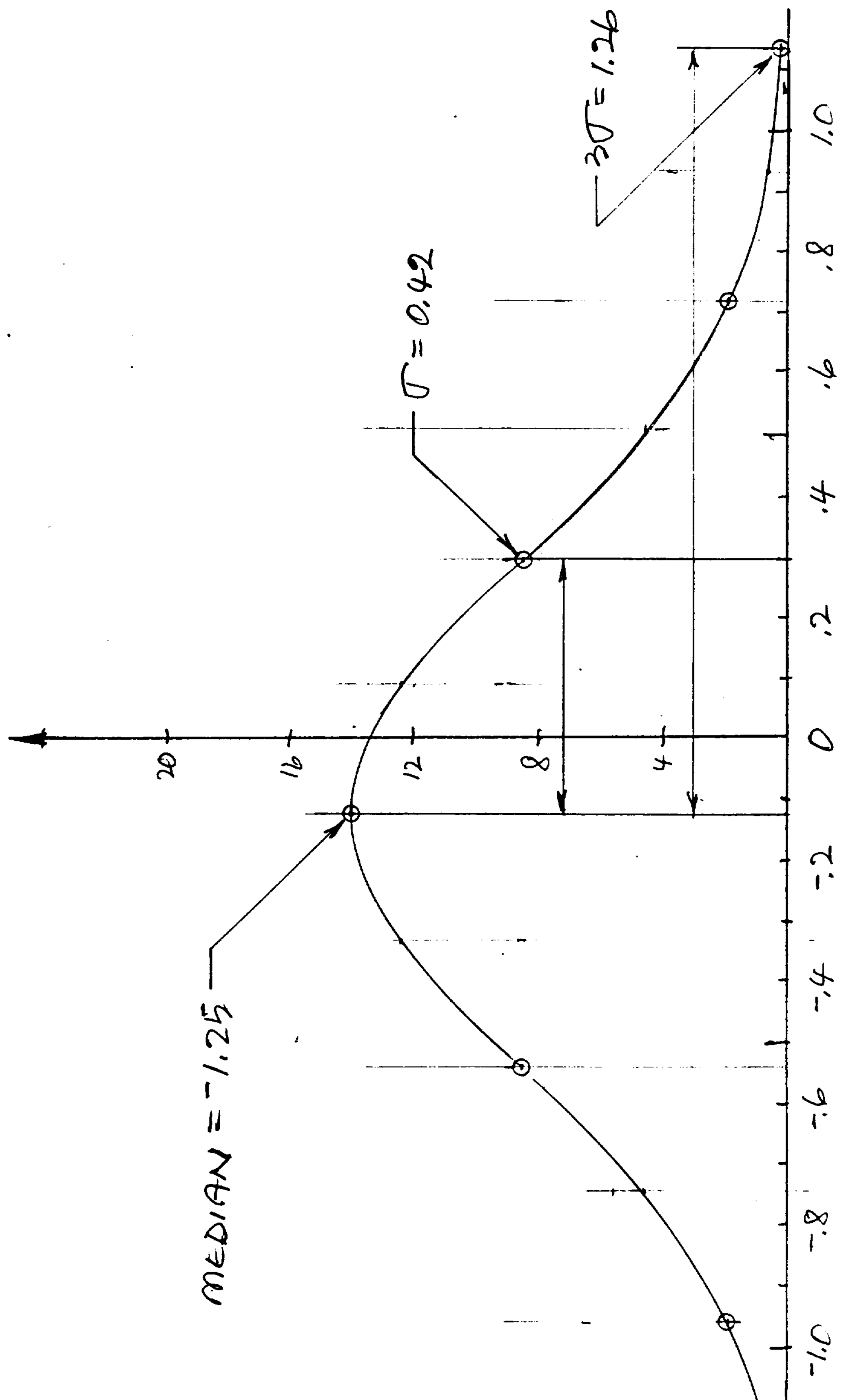

FIGURE 7

PROBLEM	CLEVELAND STATE UNIVERSITY DEPT.	NAME DATE	H 11.

CIRCUMFERENTIAL ERRORS
PANEL NO. 6

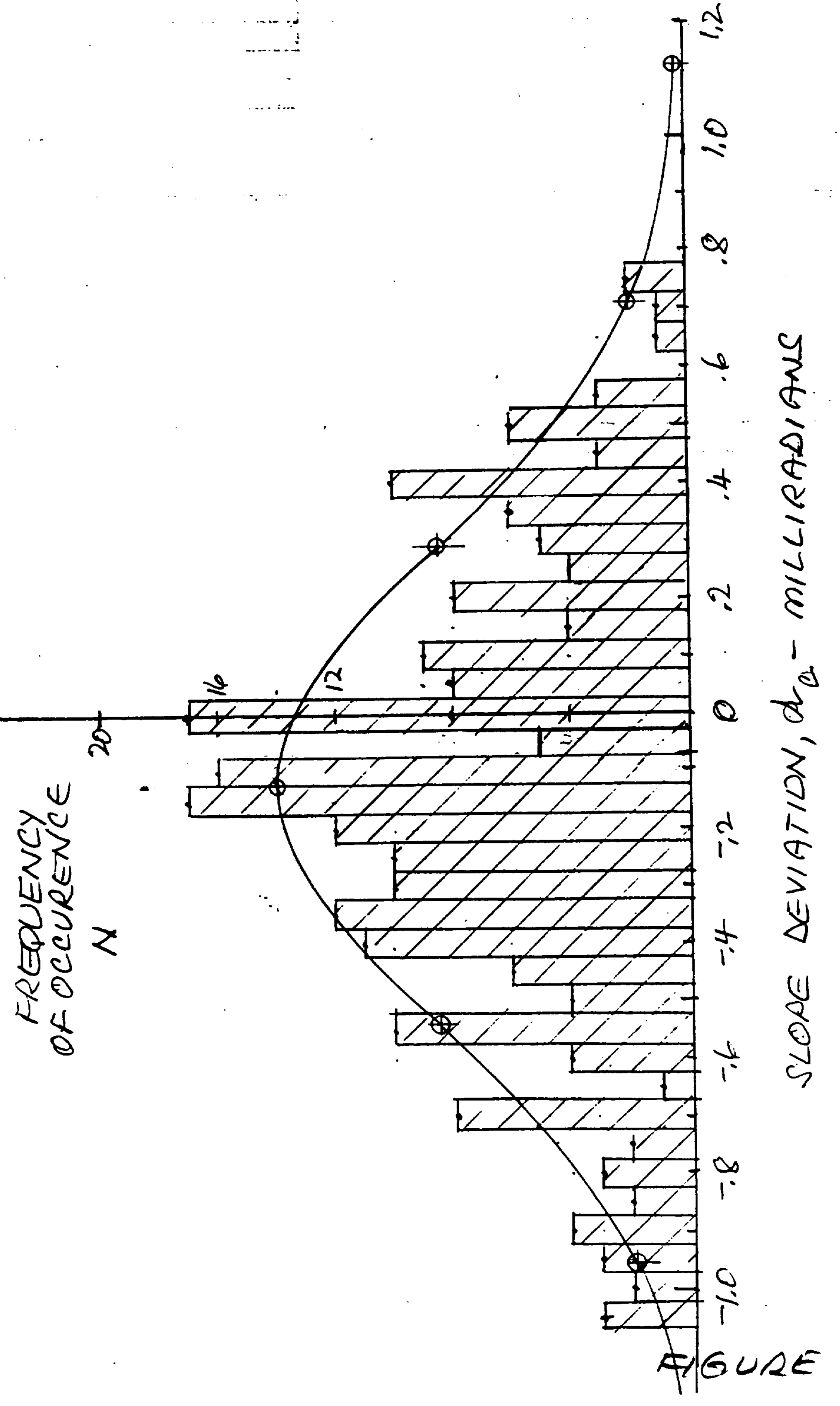

FIGURE 8

10/16/91 CHC

PANEL NO. 6
OPTICAL INSP. DATA

RADIAL POSITION (RADIAL →) / CIRCUMFER. POSITION (↓)

CIRCUMFER. POSITION	1	2	3	4	5	6	7	8	9	10	11	12	13	14	15	16	17	18	19	20	21	22	23	24	25	26	27
7																					[illegible]	+.15 +.50 .52	-.25 -.15 .29	-.05 +.65 .65	-.40 +.40 .56	-.30 +.25 .27	
6																					-.55 +.20 [illegible]	+.20 +.50 .54	-.20 +.70 .73	-.15 +.25 .25	-.20 +.05 .21		
5																0 -.30 .30	-.15 -.15 .21	-.05 -.05 .07	-.25 -.15 .25	+.05 -.10 .11	[illegible]	[illegible] [illegible] .10	-.15 -.15 .21	-.30 0 .30	-.15 0 .15		
4												+.10 +.10 .14	[illegible]	+.20 -.15 .25	+.25 -.10 .27	-.10 -.30 .32	+.10 -.40 .41	-.30 -.50 .58	-.30 -.30 .42	-.30 -.20 .36	[illegible]	+.25 -.25 .35	-.20 -.35 .40	-.35 -.15 .38	-.45 -.15 .47	-.35 -.20 .40	-.60 -.30 .67
3				-.50 +.40 .64	-.45 +.30 .54	-.30 +.05 .30	+.30 -.10 .32	0 0 0	+.10 +.40 .41	-.05 +.40 .40	+.35 0 .35	+.35 -.15 .38	[illegible]	+.10 +.05 .11	+.15 +.30 .33	-.10 +.15 .18	+.20 +.10 .22	-.15 +.15 .21	-.40 +.40 .56	-.40 +.40 .56	[illegible]	+.50 +.10 .51	-.10 -.35 .36	-.20 -.40 .45	-.65 -.15 .67	-.40 -.15 .43	-.40 -.35 .53
2		-.30 +.40 .50	-.55 +.35 .65	-.60 +.40 .72	-.55 +.50 .74	-.15 +.50 .52	+.05 +.55 .55	+.10 +.55 .56	0 +.45 .45	+.20 +.45 .49	+.20 +.45 .54	+.30 +.10 .32	[illegible]	+.05 +.35 .35	0 +.30 .30	+.30 +.40 .50	-.10 +.50 .51	-.25 +.55 .60	-.30 +.20 .36	-.05 -.05 .07	[illegible]	+.20 +.25 .32	-.10 +.35 .36	-.30 +.20 .36	-.60 -.10 .61	-.15 -.10 .18	-.75 +.10 .76
1		-.35 +.35 .49	-.50 +.35 .61	-.50 +.50 .70	-.55 +.30 .65	+.10 +.75 .76	-.05 +.75 .75	+.30 +.20 .36	+.20 +.10 .22	+.30 +.30 .42	+.50 +.35 .61	+.10 +.20 .22	[illegible]	+.30 0 .30	+.30 +.05 .30	+.30 -.10 .32	-.10 0 .10	-.05 -.15 .16	-.05 -.20 .20	-.25 +.10 .27	[illegible]	+.20 -.10 .22	-.10 -.15 .18	-.15 -.25 .29	-.30 -.20 .36	-.10 +.05 .11	-.85 -.05 .85
-1	-.55 +.15 .32	-.30 +.20 .36	-.35 +.10 .36	-.50 -.05 .50	-.50 -.10 .51	-.05 -.35 .35	+.25 -.10 .27	+.45 0 .45	+.25 0 .25	+.40 -.10 .41	+.25 -.45 .67	+.30 0 .30	[illegible]	0 -.20 .20	+.20 -.20 .28	+.10 -.25 .27	+.20 -.35 .40	-.10 -.30 .32	-.15 -.35 .38	-.20 -.55 .59	[illegible]	0 -.95 .95	-.20 -.90 .92	-.20 -.70 .75	-.35 -.60 .69	-.20 -.50 .54	-.75 -.40 .85
-2		-.70 -.55 .89	-.60 -.50 .78	-.55 -.30 .63	-.30 0 .30	+.10 -.20 .22	+.05 -.25 .25	+.50 -.25 .56	+.40 -.20 .45	+.55 0 .55	+.25 -.20 .32	+.25 -.40 .47	[illegible]	0 -.45 .45	+.15 -.60 .62	+.10 -.55 .56	+.35 -.45 .57	+.05 -.40 .40	+.05 -.25 .25	-.15 -.35 .38	[illegible]	-.15 0 .15	-.25 +.05 .25	-.25 -.10 .27	-.45 -.40 .60	-.25 -.60 .65	-.55 -.10 .56
-3			-1.50 -.80 1.70	-.70 -.45 .83	-.15 -.15 .21	-.05 -.25 .25	-.05 -.55 .55	+.30 -.50 .58	+.40 -.55 .68	+.50 -.35 .61	+.25 -.30 .39	+.15 -.10 .18	[illegible]	0 0 0	0 +.15 .15	+.05 0 .05	+.25 -.20 .27	+.10 -.15 .18	-.15 -.15 .21	-.20 -.40 .45	[illegible] [illegible] .45	-.05 -.35 .35	-.25 -.20 .32	-.50 -.10 .51	-.50 -.20 .54	-.60 -.30 .67	-.35 -.35 .49
-4								+.40 -.90 .98	+.50 -.55 .74	+.45 -.80 .92	+.10 -.55 .56	+.20 -.40 .45	[illegible]	-.05 -.60 .60	+.25 -.70 .74	+.10 -.80 .81	+.20 -.85 .90	+.20 -.70 .73	-.10 -.70 .71	-.15 -.75 .76	0 -.30 .30	-.15 -.25 .29	-.40 +.05 .40	-.35 -.35 .49	-.30 -.40 .50	-.55 -.40 .68	-.20 -.25 .32
-5														+.15 -.85 .86	+.15 -.55 .57	+.15 -1.00 1.01	+.25 -1.05 1.08	+.10 -.90 .91	-.25 -1.05 1.08	+.05 -.95 .95	-.05 -.75 .75	-.25 -.70 .79	-.30 -.70 .76	-.30 -.35 .46	-.05 -.35 .35	-.60 -.40 .72	
-6																			+.05 -.35 .35	-.10 -.95 .96	-.15 -.90 .91	-.15 -1.05 1.06	-.40 -1.00 1.08	-.35 -.55 .65	-.35 -.70 .72	-.50 -.70 .99	
-7																											

Key (each cell, top to bottom): RADIAL DEVIATION, d_R; CIRCUMFERENTIAL DEVIATION d_C; ABSOLUTE DEV., d_A*

*CALCULATED

FIGURE 9

PROBLEM	CLEVELAND STATE UNIVERSITY	NAME	
	DEPT.	DATE	H 13.

ABSOLUTE SLOPE DEVIATION α_A

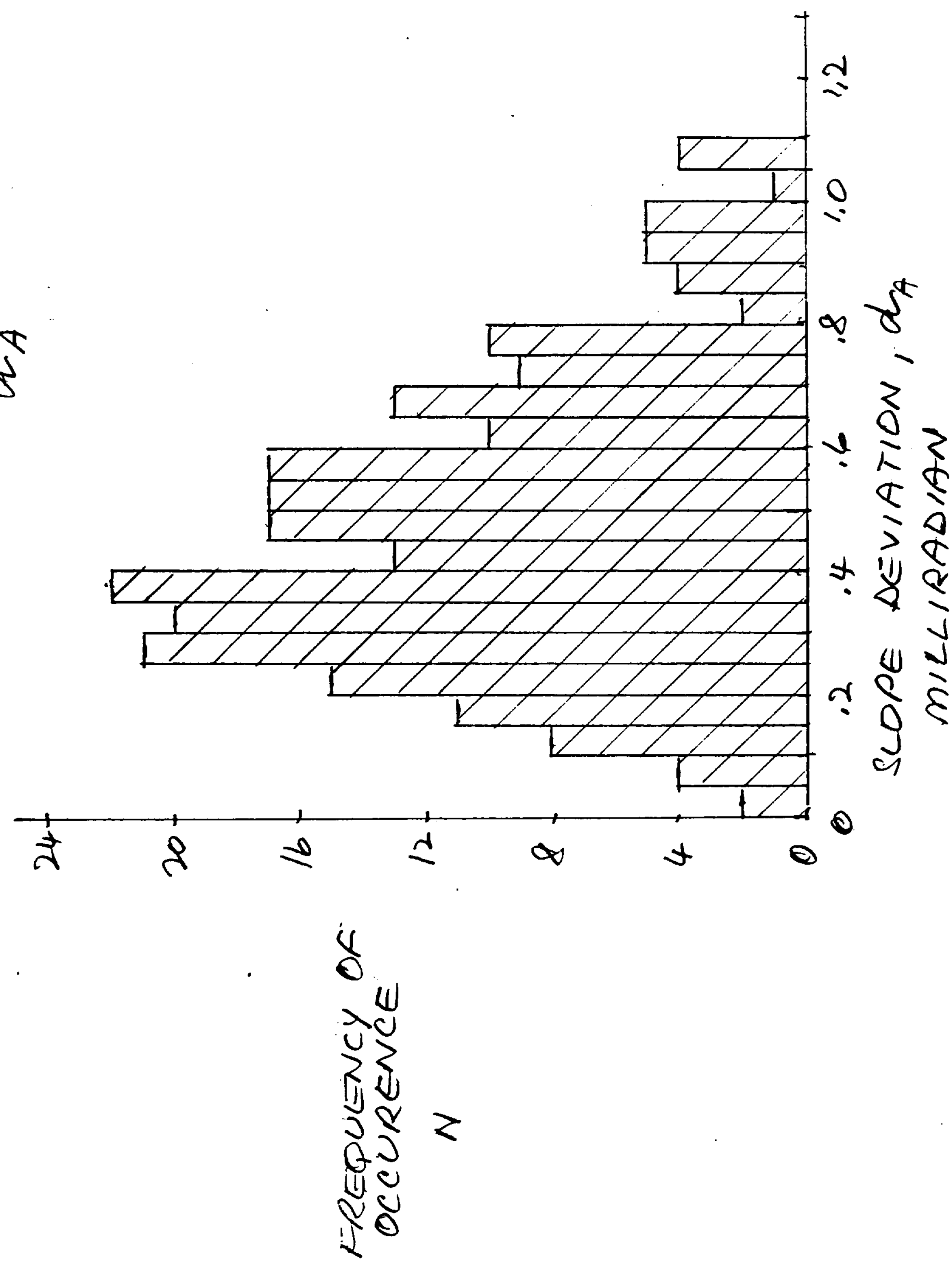

FIGURE 10

EN-1022
H 14.

BUDGET OF SURFACE DEVIATIONS FOR TWO METER SOLAR CONCENTRATOR

EN-1014

	SOURCE OF * DEVIATION	DEVIATION MAXIMUM	DISTRIB. CURVE	REFERENCE SOURCE
1	SPECULARITY	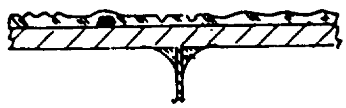	< 2% LOSS TO η_G	REF. 4
2	HONEYCOMB PRINT THRU	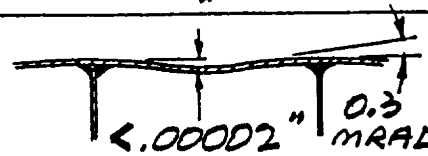	2π COSINE	REF. 3, 2 METER
3	EDGE CONSTRUCTION	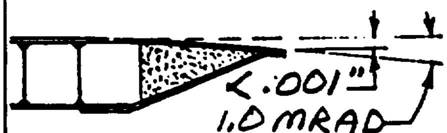		REF. 4
4	CURE TOOL SHAPE	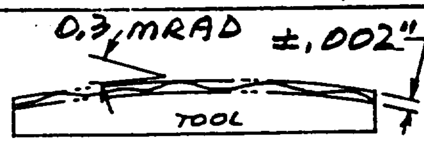	NORMAL	2 METER
5	PANEL REPLICATION OF TOOL	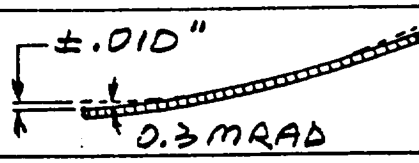		REF. 7, 2 METER
6	ASSEMBLY ACCURACY	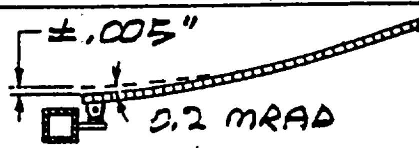		REF. 7
7	POSITION CONTROL	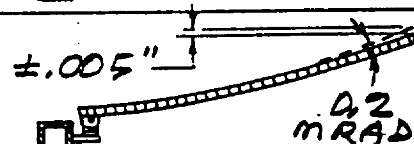		REF. 7
8	THERMOELASTIC DISTORTION	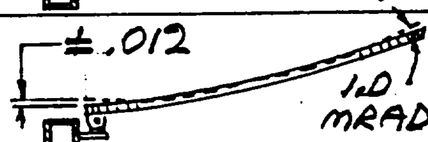		REF. 3, 2 METER
9	ON-ORBIT DEGRADATION	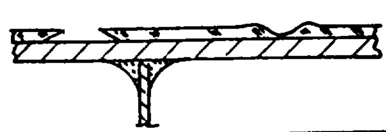	< 5% LOSS TO η_R	
	COMBINED DEVIATIONS	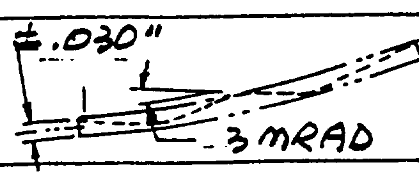	CASE 6	REF. 3 (APPEN. E, PG. 6)

* SEE FIGURE 14

FIGURE 11

~~FIGURE 20~~

EN-1022

Panel No. 6 Radial Errors (10/11/91)

d (milliradians)	N
1.0	
.9	
.8	
.7	
.6	
	1
.5	6
	2
.4	7
	3
.3	13
	11
.2	14
	7
.1	17
	11
0	10
	14
−.1	13
	19
−.2	11
	11
−.3	15
	9
−.4	7
	4
−.5	8
	8
−.6	6
	2
−.7	2
	1
−.8	
	1
−.9	
−1.0	
⋮	
−1.5	1

Circumferential Errors

d (milliradians)	N
1.0	
.9	
.8	
	2
.7	1
	1
.6	
	3
.5	6
	3
.4	10
	6
.3	5
	4
.2	8
	4
.1	9
	8
0	17
	5
−.1	16
	17
−.2	12
	10
−.3	10
	12
−.4	11
	6
−.5	4
	10
−.6	4
	1
−.7	8
	2
−.8	3
	2
−.9	4
	3
−1.0	2
	3
−1.1	

Radial

d	n		d^2n	
1.0				
0.8				
0.6	1		.302	
		6	1.500	
	2		.405	
0.4		7	1.120	
	3		.367	
		13	1.170	
	11		.688	
0.2		14	.560	
	7		.157	
		17	.170	
	11		.028	
0		10	0	
	14		.035	→ 116
		13	.130	
	19		.428	
−0.2		11	.440	159
	11		.688	
		15	1.350	
	9		1.103	
−0.4		7	1.120	
	4		.810	
		8	2.000	
	8		2.420	
−0.6		6	2.160	
	2		.845	
		2	.980	
	1		.563	
−0.8	1		.723	
−1.0				
−1.5	1		2.25	
Σ	234		24.512 (Σd^2)	

$^{234}/_2 = 117$ median

$\sigma = \sqrt{\frac{\Sigma d^2}{N}} = .324$

$3\sigma = .972$

Circumferential

d	n		d^2n	
0.8	2		1.125	
	1		.490	
	1		.423	
0.6	3		.908	
	6		1.500	
	3		.608	
0.4	10		1.600	6.654
	6		.735	
	5		.450	
	4		.250	
0.2	8		.320	
	4		.090	
	9		.090	
	8		.020	8.609
0	17		0	
	5	92	.013	
→	16	108	.160	
	17	125	.383	
−0.2	12		.480	
	10		.625	
	10	157	.900	
	12		1.478	
−0.4	11		1.360	
	6		1.215	15.615
	4		1.000	
	10		3.025	
−0.6	4	204	1.440	
	1		.423	
	8		3.920	
	2		1.125	26.548
−0.8	3		1.920	
	2		1.445	
	4		3.240	
	3		2.707	
−1.0	2		3.000	
	3	232	3.308	
Σ	232		41.168	41.168

$^{232}/_2 = 116$ median

$\sigma = \sqrt{\frac{41.168}{232}} = 0.421$

$3\sigma = 1.263$

Appendix I

Cleveland State University
Advanced Manufacturing Center

Engineering Note EN-1001

Fabrication of a Stretch Forming Tool

C.H. Castle, E.H. Hall
11-29-89

NASA GRANT NO. NCC 3-77, SUPP. NO.2

INTRODUCTION

The tool described in this report was fabricated in preparation for building a two meter solar concentrator demonstrator for NASA Lewis Research Center. The tool will be used for two purposes:

1. To stretch thin aluminum alloy sheets that conform to a paraboloidal shape.

2. To vacuum bag and heat cure adhesive bonded aluminum honeycomb sandwich panels that conform to the same shape.

Figures 1 and 2 show the above sequences used during fabrication of a 9.5 foot diameter spacecraft antenna.

DISCUSSION

Tool Drawing

The tool is defined by CSU/AMC drawing 1003, revision B and CSU/AMC specification No. 1000, revision A. It is made of 2024-T351 wrought aluminum alloy aged after rough machining, at 375°F for 11 hours. The paraboloidal shape is defined by the following equation:

$$Z = \frac{X^2+Y^2}{157.5} \text{ INCHES}$$

The paraboloidal surface must be within ± .005 of the theoretical surface when measured from three datum planes as defined by the tooling balls (DWG 1003). Therefore, the geometrical form tolerance was established as ¦ ¦.010¦A¦B¦C¦. The surface must also meet a maximum waviness of .0003 in./in., per paragraph 3.1.2 of spec 1000, which must also be within the .010 form tolerance zone. Since spherical milling cutters are used in numerical control machining of such tools, a maximum "scallop" depth of .0015" was allowed (Note: the peaks of the scallops were removed as described later). The surface finish, after bench-in, was specified at 63 microinches (AA) maximum.

The .010 form tolerance was established based on the surface deviation requirements specified by NASA. It is but one of eight sources of errors involved in solar concentrator structures used for space applications. Geometric surface errors which contribute to reducing the concentrators efficiency are those caused by:

1. Tiny surface imperfections caused by dirt particles trapped between the aluminum stock and the forming tool during stretching.

2. Tiny particles entrapped in the leveling layers applied on the reflective face of the concentrator panel.

3. Deviations in the stretch forming tool.
(The topic of this report)

4. Print through of the honeycomb core on the thin reflective front face.

5. Replication errors during adhesive heat curing of the honeycomb sandwich panel while vacuum bagged to the tool.

6. Assembly errors during attachment of the panels to the main mounting ring.

7. Deployment errors when the concentrator is opened in orbit.

8. Distortion in orbit due to temperature gradients caused by the thermal environment in space.

The concentrator design specification sets a one milliradian maximum value (one sigma) for all deviations in combination. If the combined errors can be statistically described by a bell shaped (normal Gaussian) curve, then the maximum allowed errors are three sigma, or three milliradians. To relate this to the tool and select an "error budget" for the tool it is necessary to look at Figure 3. The form tolerance is shown in the upper position. An actual measured surface deviation can occur, as an example, within the form tolerance as shown in the lower position. Of course the panels will have a variety of deviations combined to make a more complicated profile, but this simplification allows choice of a tool error budget. The tool errors are very important in achieving the final panel shape. The tool error budget was selected to be 1/3 of the one milliradian specification. This means that the tool budget is 1/9 of the maximum errors allowed. The tool form tolerance is therefore:

$$(1/9 \times .003 \text{ radian}) \times \frac{57.3 \text{ deg.}}{\text{radian}} = .019 \text{ degree}$$

For the profile error shown in Figure 3, this would result in a form tolerance of:

$$\text{Tolerance} = (29\text{" panel length}) \times (\tan .019^\circ)$$

$$= .010 \text{ inch}$$

The tool has a small groove near the periphery of the panel edges which is used to apply a vacuum to the front aluminum sheet during the adhesive curing process. Large pockets were milled out of the base to lighten the tool. This allows the tool to heat up to adhesive cure faster. Foil heaters about 1/16 inch thick and rated at 10 watts / sq.in. will be bonded to all surfaces of the cavities, including the sides, and also on the four outer sides of the tool. The objective is to reach cure temperature within 30 minutes. Holes in the two long outer sides will be used for handling bars and for electrical wire feed-throughs.

Vendor Selection

Five vendors were solicited for quotes. These were reduced to two based on cost, delivery, capability and past experience. They were visited by C. Castle, E. Hall and A. Pintz for more details as to their proposed fabrication and inspection plans. Their shops were also evaluated for engineering, fabrication and inspection capabilities. Tempcraft Corp. of Cleveland, Ohio was selected. A letter of justification was attached to the purchase requisition.

Tool Fabrication

Preliminary meetings with Tempcraft were held to make sure all of the tool requirements were clear and to establish a fabrication process. Specific times were set as to when we would be at Tempcraft to observe machining and inspection events. Tempcraft also graciously accepted our request to allow CSU students to observe the fabrication process and to see the nature of a large tool and die shop in the Cleveland area.

The detailed fabrication sequence was defined after three meetings. Some deviations from the procedure did occur, as usually happens. The sequence and deviations are discussed as follows:

1. Machine all four sides square with each other, within the limits of the machine. This is not a drawing requirement but was done to benefit later operations.

2. Set the aluminum block on a long side and mill out the pockets in the base.

3. Remove excess material from the parabolic side as shown in Figure 4.

4. Age the rough machined block at 375° F for 11 hours minimum.

5. Grind base surface flat within .002 (try for .001) and square with the sides within the limits of the grinding operation.

6. Inspect flatness of base. It was .0015.

7. Before machining the aluminum tool, check the NC program by cutting a 1/3 size model of the tool out of plastic material. This included the vacuum groove and the six tooling ball holes.

8. Place the base on three ground supports as shown in Figure 5. The supports were of equal height so that the base surface can be checked for flatness over time. The three point support also minimized tool shape change after clamp-downs for machining were removed.

9. Machine in the six tooling ball holes and press in drill bushings.

10. Rough cut the paraboloidal shape on a Bostomatic three axis CNC milling machine. Note: It was necessary to machine the paraboloidal surface in two set ups as shown in the top view of figure 5. This was necessary because the Bostomatic table could not reach the full tool surface in one set up. The two cuts overlapped as shown, and the mismatch was controlled to within tenths of thousandths by manual corrections during the second cut. (This was the only concern expressed prior to selecting Tempcraft as a vendor, not due to the accuracy of the Bostomatic, but rather the concern of matching of the two set up cuts to avoid mismatch.) The mismatch is large enough, however, that special bench-in methods will be required as discussed later.

11. Inspect the paraboloid on the three axis coordinate measuring machine. This was done to assure that form tolerances were being met and that a finish cut could proceed. Angular paths were followed during the inspection as shown in Figure 6. Each path is the same parabolic curve:

$$Z=\frac{R^2}{157.5} \quad \text{where } R^2=X^2+Y^2$$

Figures 7 through 11 show photos of the tool on the inspection machine. The inspection showed that the .010 form tolerance was met.

12. Inspect the base for flatness. It was .0035 which indicated some shape relaxation did occur as a result of the rough cut. It was therefore decided to regrind the base, which then measured .0015 flatness. This inspection was done four days after regrind to allow any time dependent relaxation to occur.

13. Finish machine the paraboloid and make initial bench-in.

14. Final inspection of the paraboloid. The form was well within the .010 form tolerance and will be discussed in detail later.

15. Make an additional inspection of the paraboloid by a method independent of the CNC Bostomatic program. This was done primarily to detect any error that may have been inadvertently entered into the CNC Program that could then be repeated in the inspection machine program. The results correlated well with the inspection in NO. 13 above and will be discussed later. This inspection was aided by layouts made on NASA Lewis Research Center's CADAM drafting system. Tooling ball locations were also inspected.

16. Machine in the vacuum groove.

17. Inspect location of groove relative to the theoretical panel periphery. Drawing requirements were met.

18. Inspect base for flatness. Was still .0011 and several recordings are shown in Figure 13.

Tool Inspection Details

In summary, the tool inspection consisted of the following:

* Tooling ball locations relative to the base
* Two different methods of inspecting the paraboloidal surface
* Base flatness
* Vacuum groove relative to theoretical periphery of the panel

They will now be discussed in detail.

The tool was clamped to the granite surface plate of the CMM (Figures 7-11) at the same three points used during machining. These blocks will never be removed, and the tool can be inspected periodically to determine whether a shape change has occurred; either due to time aging at room temperature or to heat cure cycles when panels are adhesive bonded.

The tooling ball locations were inspected with the CMM probe. These balls are numbered in Figure 6 and the inspection results are shown in Figure 12. The upper data shows measurements relative to datums -B- and -J- on drawing 1003. Datum -J- is the theoretical base plane. The nominal tooling ball dimensions are pencilled in below each inspection result. Deviations ranged from .0001 to .0012 and meet print. These inspections relative to datum -J- can be repeated on a simple open inspection set up and would not require a CMM.

The lower data in Figure 12 shows the location of the six tooling balls relative to datums A, B and C on drawing 1003. The data relates the balls to the theoretical X, Y and Z coordinates of the paraboloidal surface. Deviations ranged between .0001 and .0012. Tooling balls 1, 2, 3 and 4 are used to establish the X, Y and Z coordinate axes that establish the inspection references for the paraboloidal surface inspections.

The paraboloidal surface was inspected along 13 paths as shown in Figure 6. Plus and minus sign convention for the angles are shown. Since each angle passes through the vertex, the paths all represent a true section of the paraboloid:

$$Z = \frac{R^2}{157.5} \text{ where } R^2 = X^2 + Y^2$$

Thus each section is theoretically the same.

The inspection results are shown graphically in Appendix A. The .010 form tolerance band is plotted with the nominal (theoretical) form in the center of it. The inspected surface is then shown relative to the band. The small lines that connect the inspected profile with the nominal curve represent data points taken (Between 17 and 60 depending on path length). The inspection point printouts are also included in Appendix A.

Within the boundaries of the theoretical panel (± 11.25°) the deviations range from +.0007 (see +3° sheet) on one side of nominal to -.0026 (see -9° sheet) on the other side. Therefore the maximum deviation is .0026 and the total spread is .0033. This is well within the .010 form tolerance specified.

Two points are worth noting at this time. First, the deviations are predominantly to the minus side of nominal, and the deviations are always larger at the OD end of the theoretical panel shape. It is obvious that the "best fit" paraboloid would have a smaller deviation spread if a least squares analysis were made. The total spread might be more like .0020 instead of .0033.

Second, the deviations along the plus angles all show smaller deviations than those along the zero and minus paths. This gives an indication of the mismatch due to the "two set-up" machining procedure. Comparing the zero° and minus 3° data indicates a step of about .0008. If this is the case, then some significant final benching in will be required along the crown of the tool. This will be discussed later.

A second method was used to inspect the paraboloidal surface. This was done to provide an inspection that was independent of one that relates to the theoretical X, Y and Z axes. Using the CADAM drafting system as a tool, the geometry of inspecting relative to datum -J- (base plane) was established. Appendix B shows the geometry involved when a spherical inspection ball probe contacts the compound curvature of the paraboloid. This results in two parameters, T and K, related to tooling ball number 1 and datum B as shown in Figure 13. The U parameter is then the distance from the tooling ball to the inspection probe, and can be used as an approximate, but close check, on the deviations made along the angular paths discussed earlier. The U deviations varied between +.0006 and -.0021. This compares well with the +.0007 to -.0026 range of the other inspection. This data is shown in Figure 14. The step difference from one side of the paraboloid to the other was also repeated.

Bench-In of Paraboloidal Surface

Because of the scalloped surface produced by the spherical milling cutter, it is necessary to bench-in tools made by this method. Benching-in is a manual operation which is done simply by filing the peaks away. However, it is easier said than done and requires an experienced tool maker's touch. It is <u>very</u> important to not remove too much metal as to go "below the valleys." To avoid doing this, the tool is first coated with a very thin colored dye. The peaks are slowly removed until just a trace of the valleys remain.

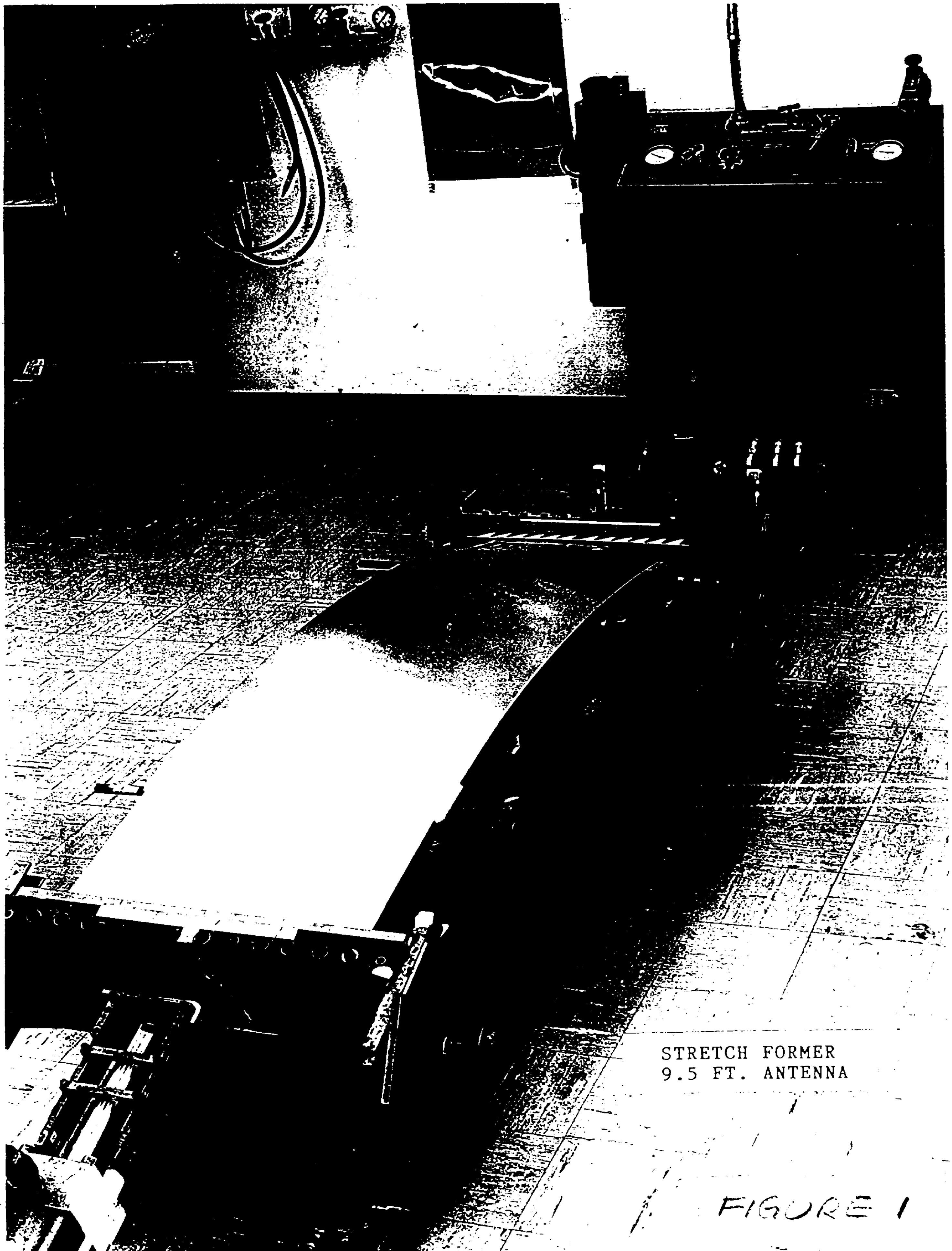

STRETCH FORMER
9.5 FT. ANTENNA

FIGURE 1

FIGURE 2

ORIGINAL PAGE IS
OF POOR QUALITY

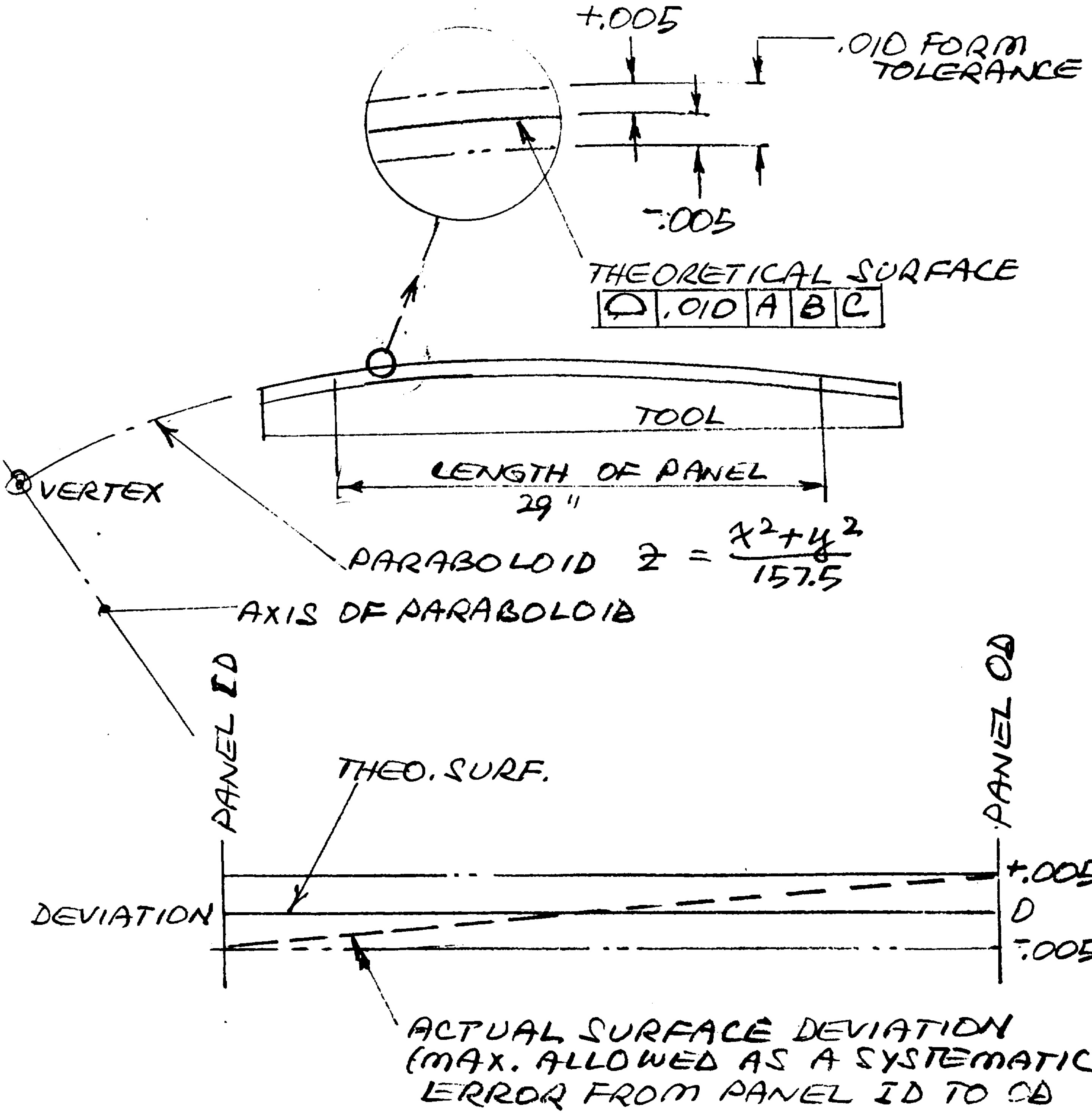
+.005
.010 FORM TOLERANCE
-.005
THEORETICAL SURFACE
.010 A B C
TOOL
LENGTH OF PANEL
29"
VERTEX
PARABOLOID $z = \frac{x^2+y^2}{157.5}$
AXIS OF PARABOLOID
PANEL ID
PANEL OD
THEO. SURF.
DEVIATION
+.005
0
-.005
ACTUAL SURFACE DEVIATION
(MAX. ALLOWED AS A SYSTEMATIC
ERROR FROM PANEL ID TO OD

FIGURE 3

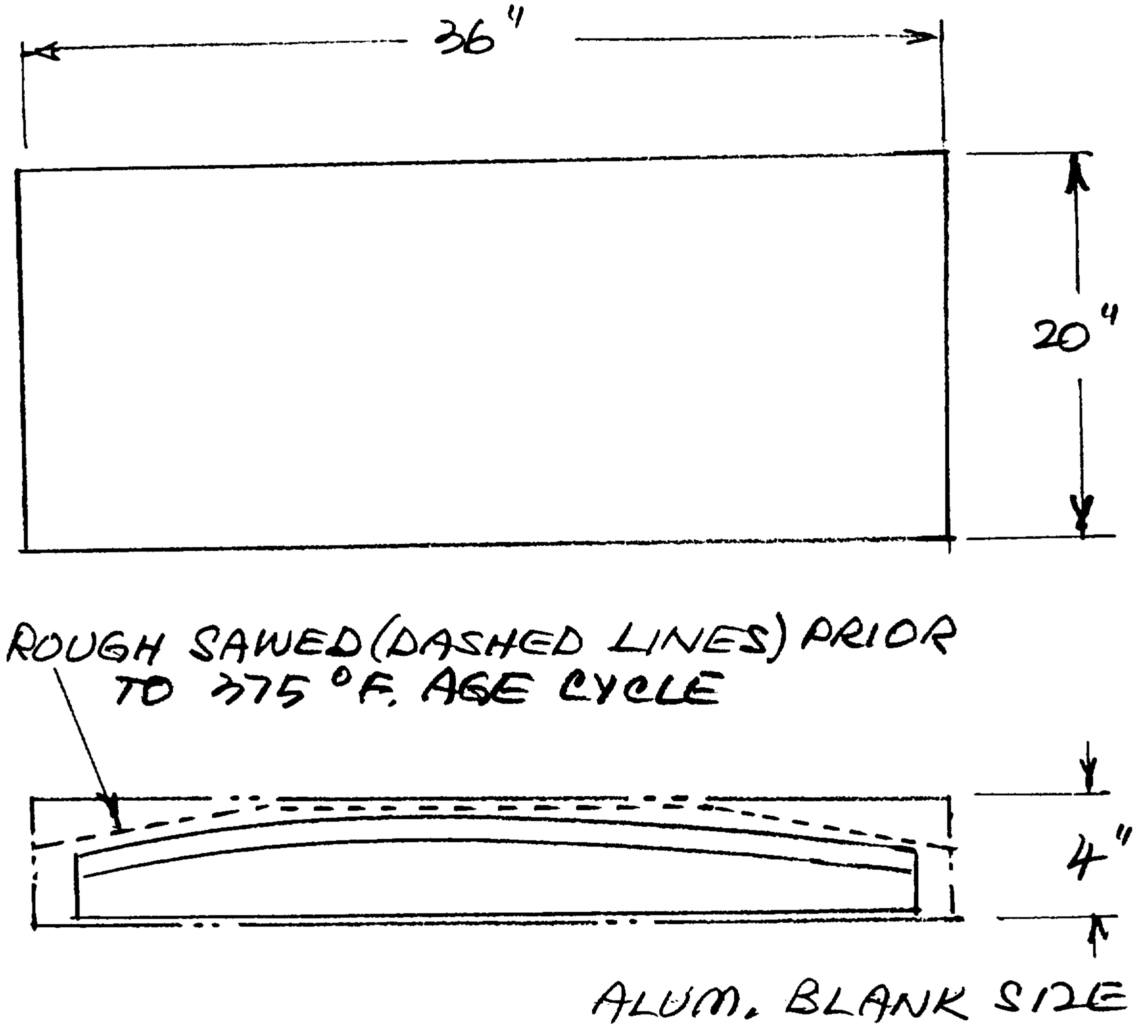
36"
20"
ROUGH SAWED (DASHED LINES) PRIOR
TO 375 °F. AGE CYCLE
4"
ALUM. BLANK SIZE

FIGURE 4

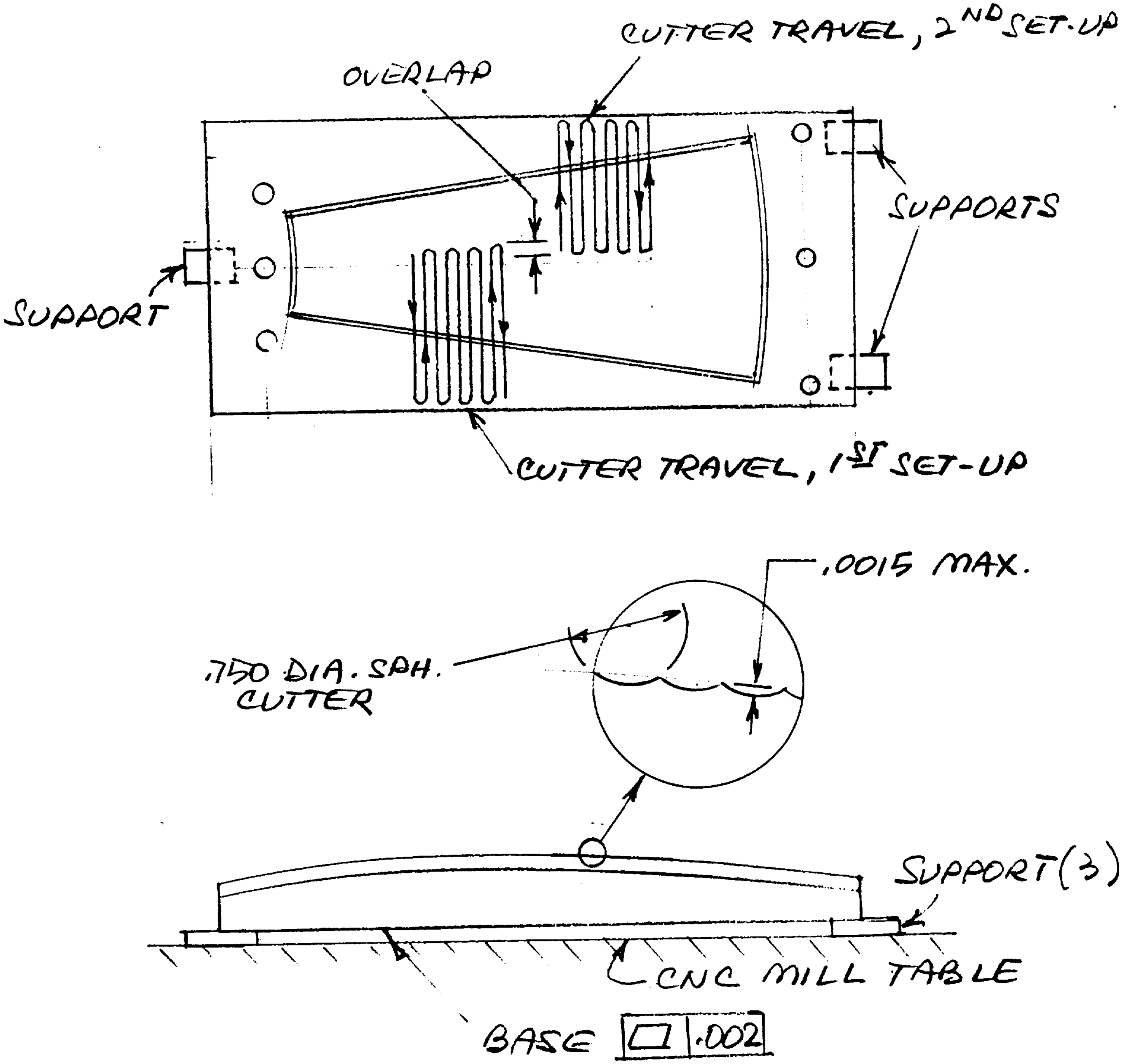
CUTTER TRAVEL, 2ND SET-UP
OVERLAP
SUPPORTS
SUPPORT
CUTTER TRAVEL, 1ST SET-UP
.0015 MAX.
.750 DIA. SPH. CUTTER
SUPPORT(3)
CNC MILL TABLE
BASE ⏥ .002

FIGURE 5

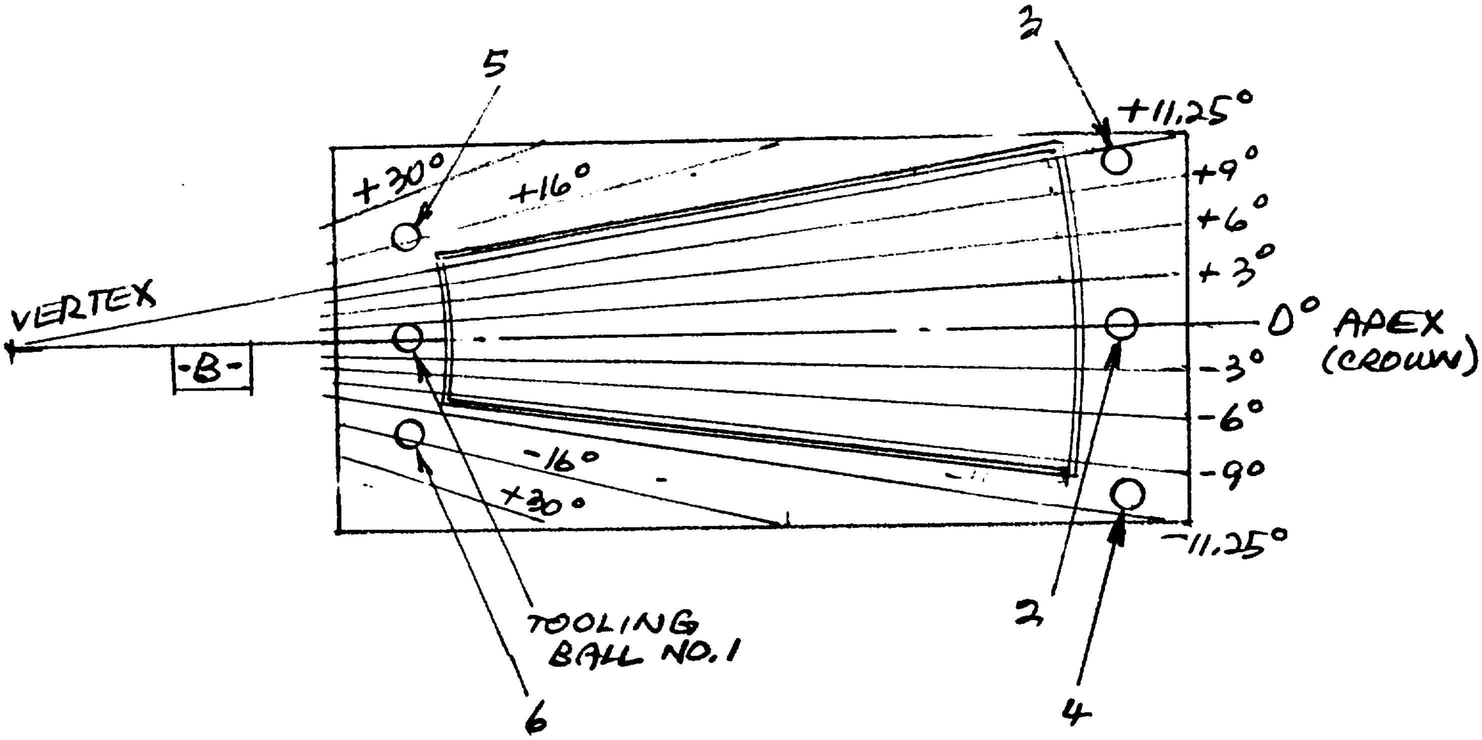
5
3
+11.25°
+30°
+16°
+9°
+6°
+3°
VERTEX
0° APEX (CROWN)
-B-
-3°
-6°
-16°
-9°
+30°
-11.25°
TOOLING BALL NO. 1
2
6
4

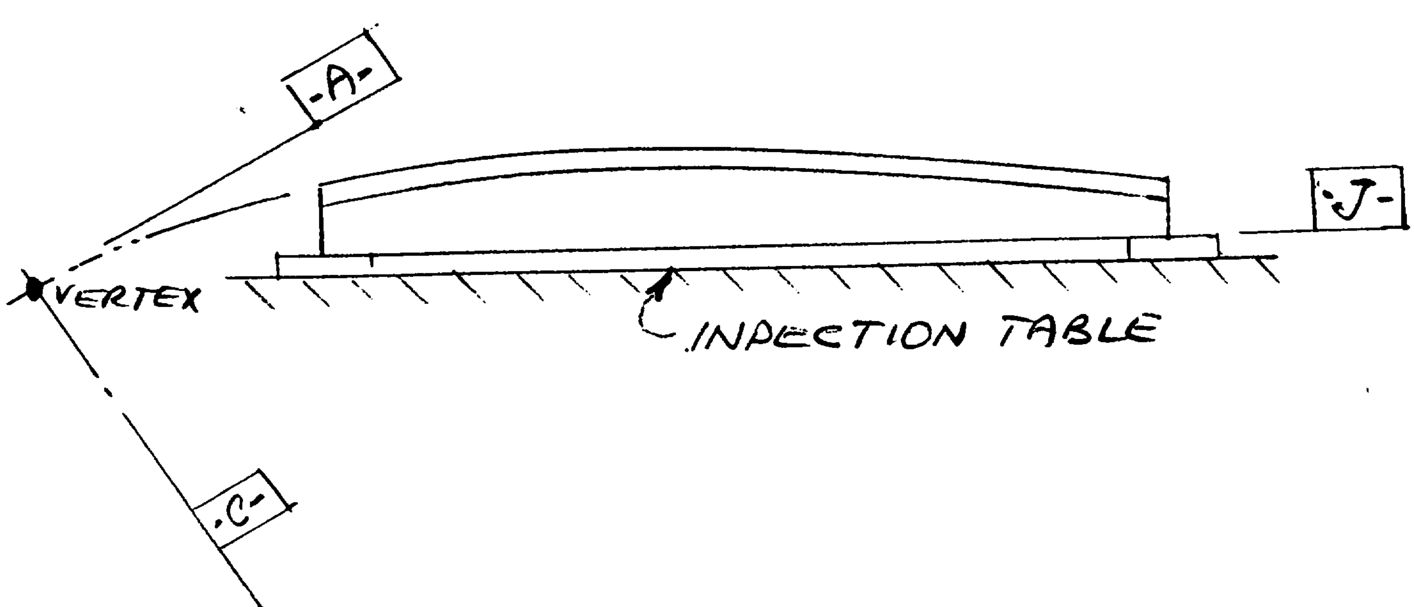
-A-
-J-
VERTEX
INPECTION TABLE
-C-

FIGURE 6

FIGURE 7

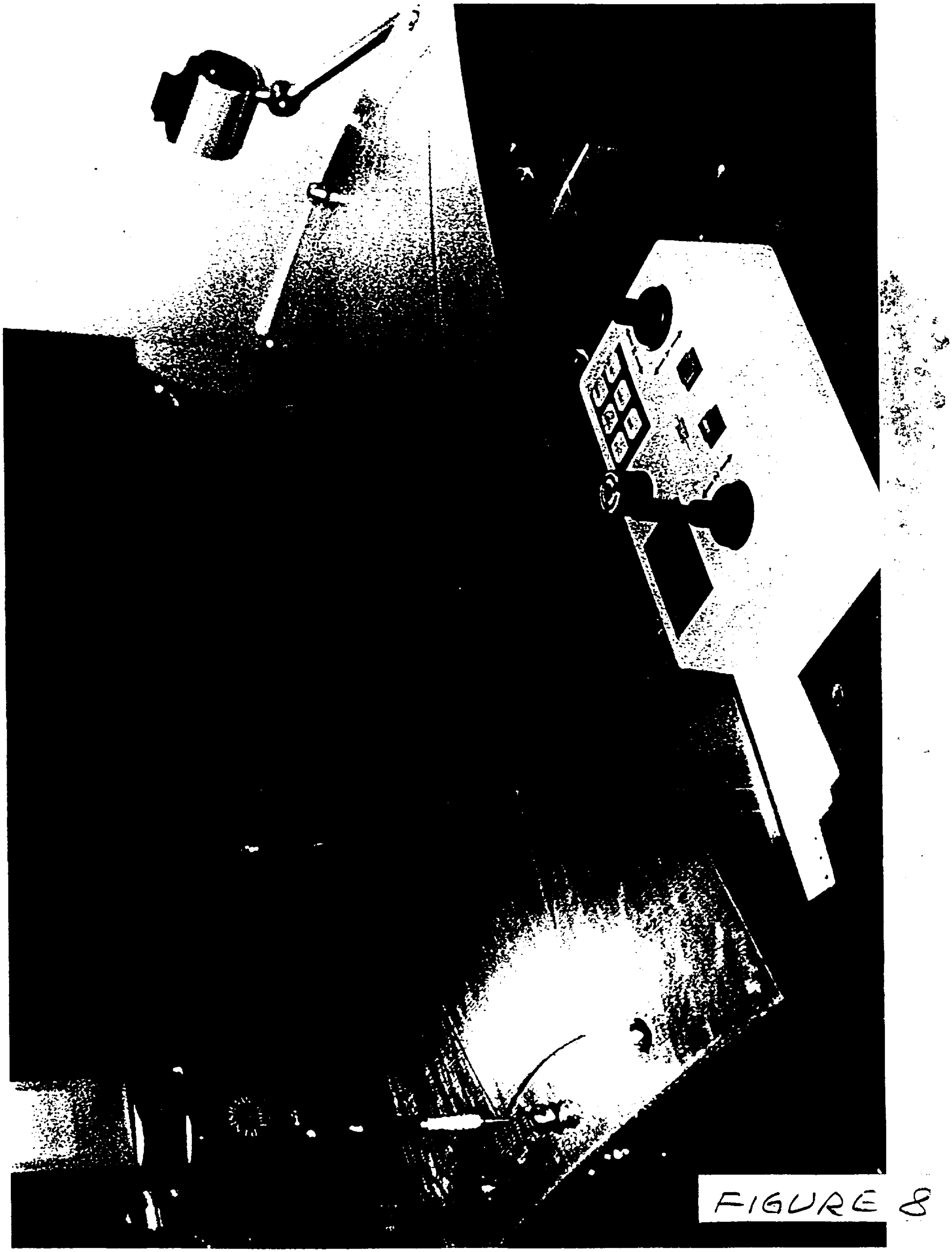

FIGURE 8

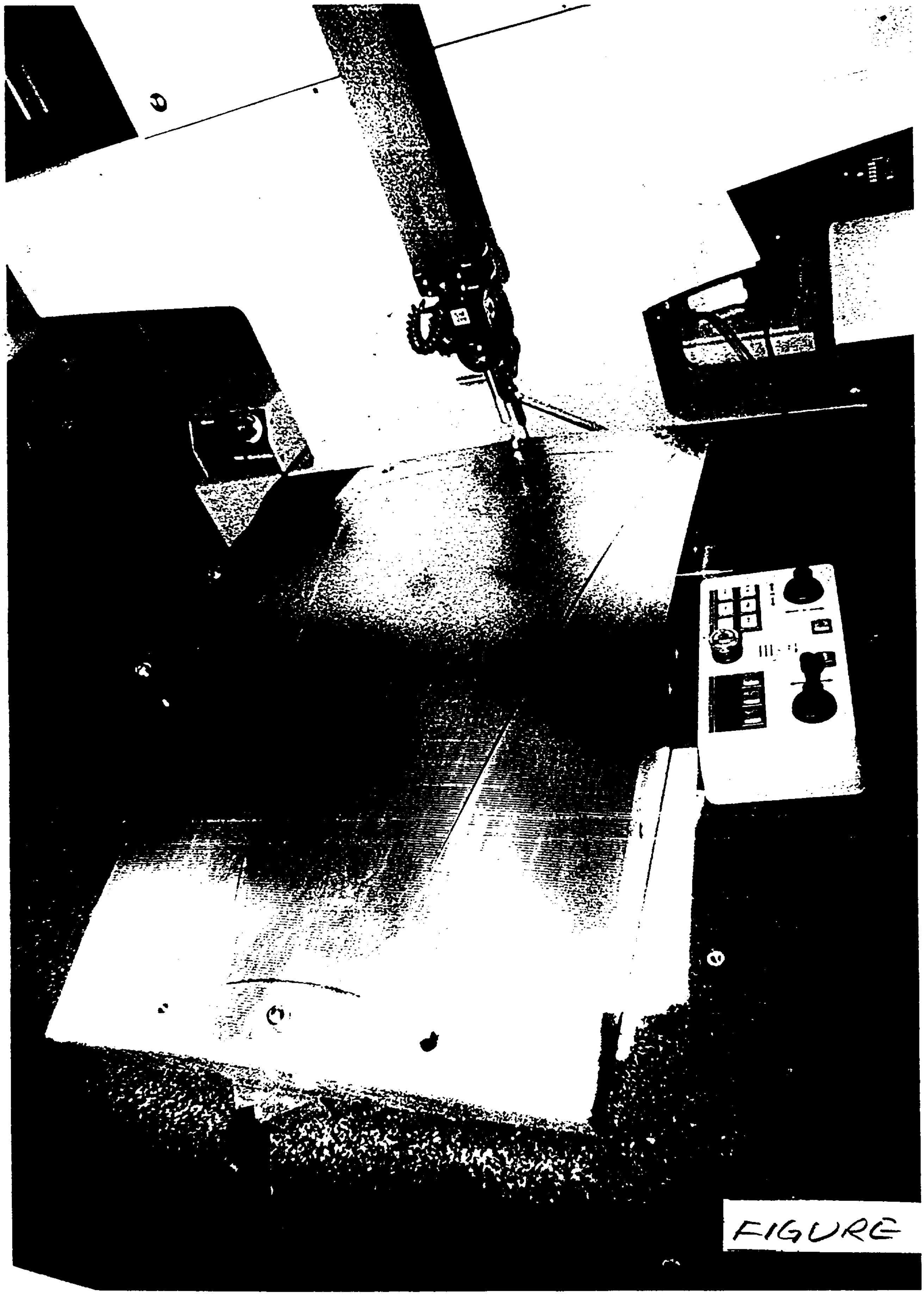

FIGURE 9

FIGURE 10

FIGURE 11

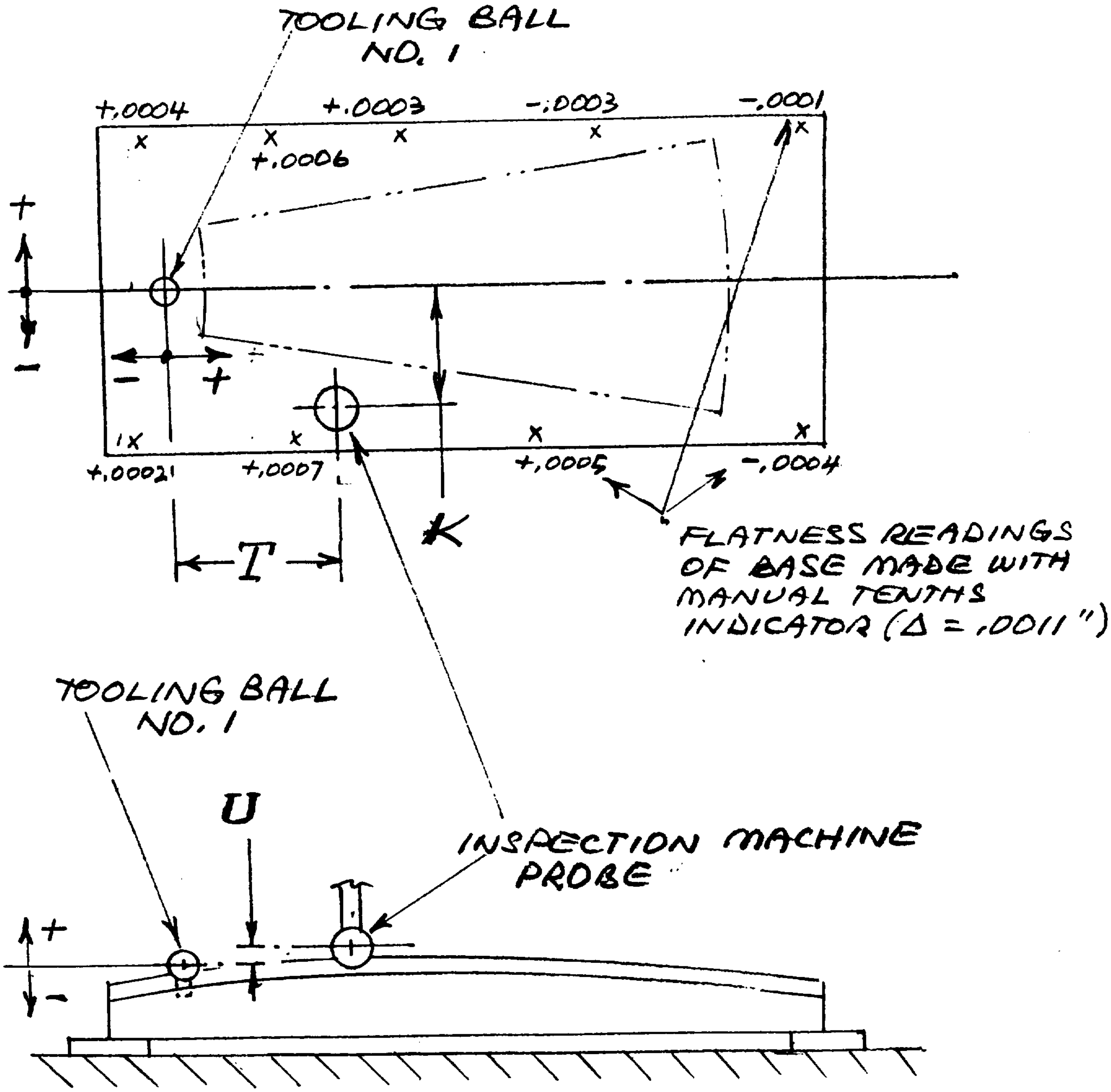

PRECEDING PAGE BLANK NOT FILMED

FIGURE 13

El. No.	Line No.	Element Dg.mi.sc Tolerance	Pts Tl.	X-Coord. X-Angle. Nominal+-	Y-Coord. Y-Angle. Up/Lo Tol	MEAS. U Z-Coord. Z-Angle. Actual	THEO. U ~~Diameter Dist/Ang Error~~	ΔU ~~Max.Diff Dev~~/inch
** Probe Dia.=.1176* ***				T	K	U		
1	N0015	POINT	1	2.2414	0.0001	0.0906	[illegible]	-.0002
2	N0018	POINT	1	2.2527	2.5025	0.0536	.0530	+.0006
3	N0021	POINT	1	2.2527	-2.5023	0.0526	.0530	-.0004
4	N0026	POINT	1	16.6089	-0.0000	1.2035	1.2054	-.0019
5	N0029	POINT	1	16.6579	5.0037	1.0535	1.0543	-.0008
6	N0032	POINT	1	16.6579	-5.0037	1.0522	1.0543	-.0021
7	N0036	POINT	1	29.5360	-0.0000	0.2737	.2755	-.0018
8	N0040	POINT	1	29.6463	7.5049	-0.0648	-.0644	-.0004
9	N0044	POINT	1	29.6464	-7.5075	-0.0665	-.0644	-.0021

(MEAS.) - (THEO.) → ΔU

ORIGINAL PAGE IS OF POOR QUALITY

FIGURE 14

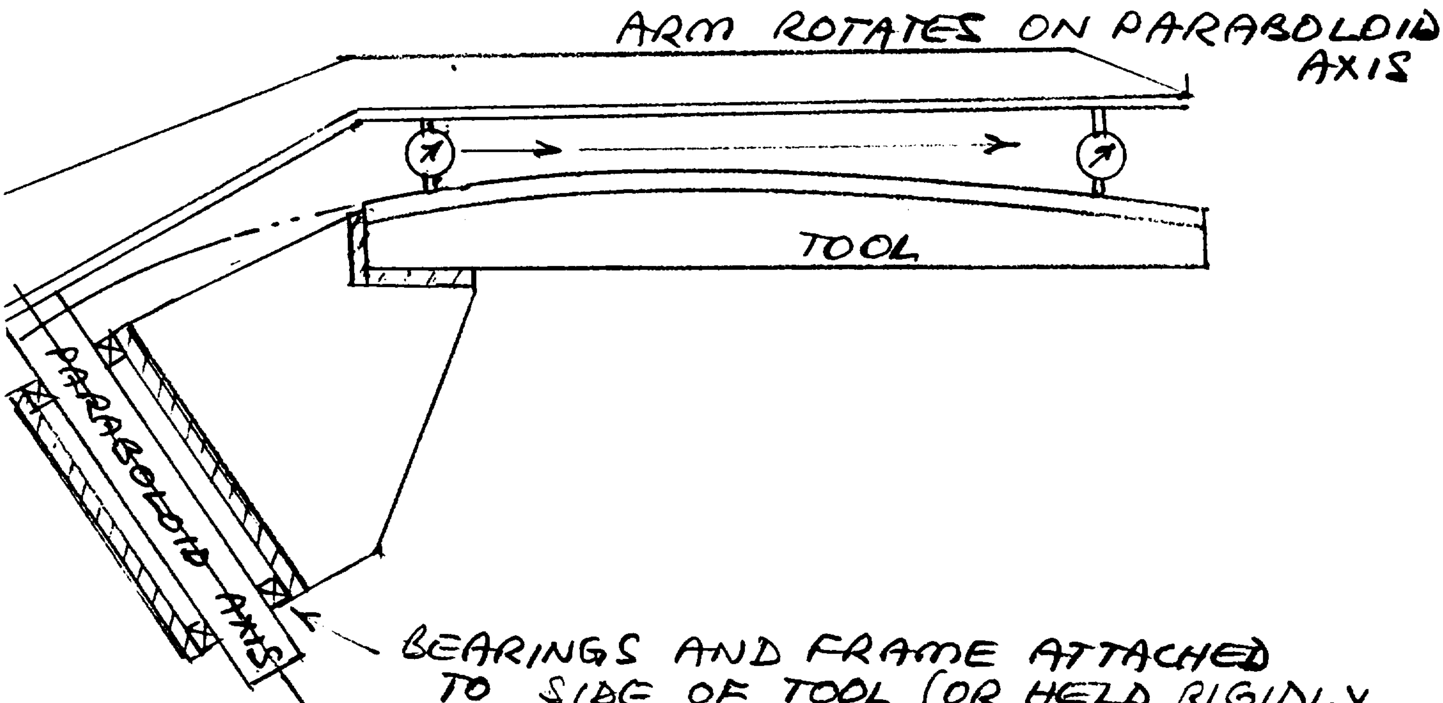

THIS COULD ALSO BE DONE ON A LARGE MILLING MACHINE, THE SPINDLE WOULD PROVIDE THE ROTATING AXIS, AND THE TOOL WOULD HAVE TO BE AT AN ANGLE RELATIVE TO HORIZONTAL VIA A SINE PLATE

FIGURE 15

INSPECTION OF PARABOLOIDAL SURFACE BY METHOD IN FIGURE 6

APPENDIX A

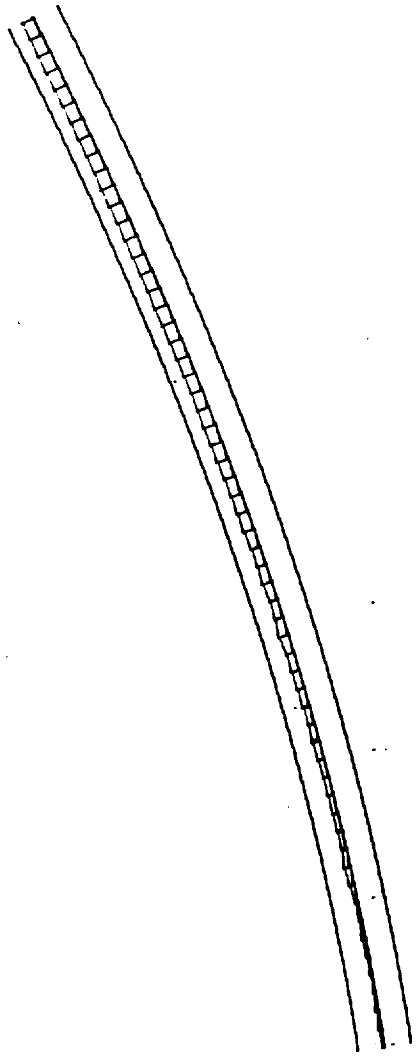

0.01000 0.50000 APPEX PARABOLA D°	Z, X 4.9 : 1 07/25/1989 16.35 h (inch)

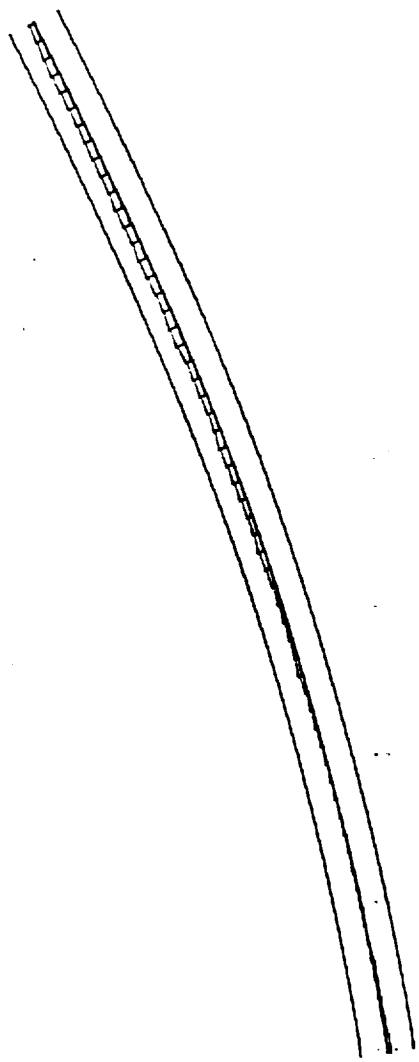

0.0100 **0.5000** +3deg PARABOLA	Z, X 4.9 : 1 07/26/1989 14.57 h (inch)

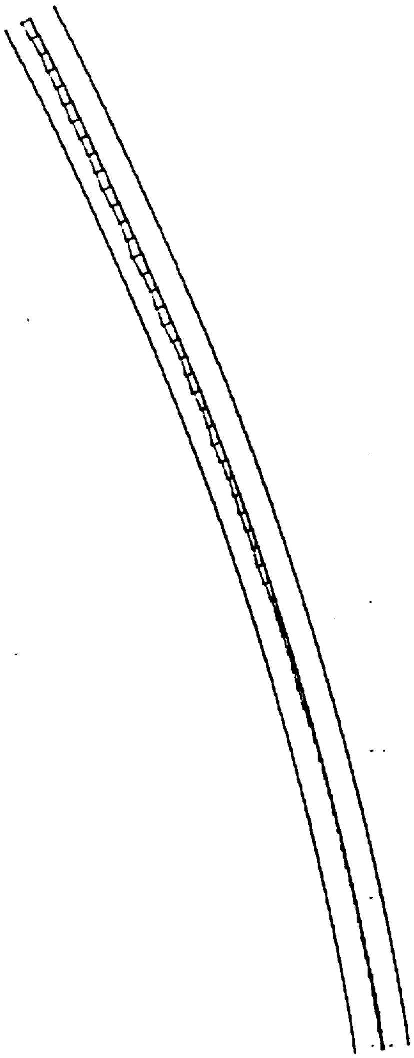

0.0100 0.5000 +6deg PARABOLA	Z, X 4.9 : 1 07/26/1989 15.02 h (inch)

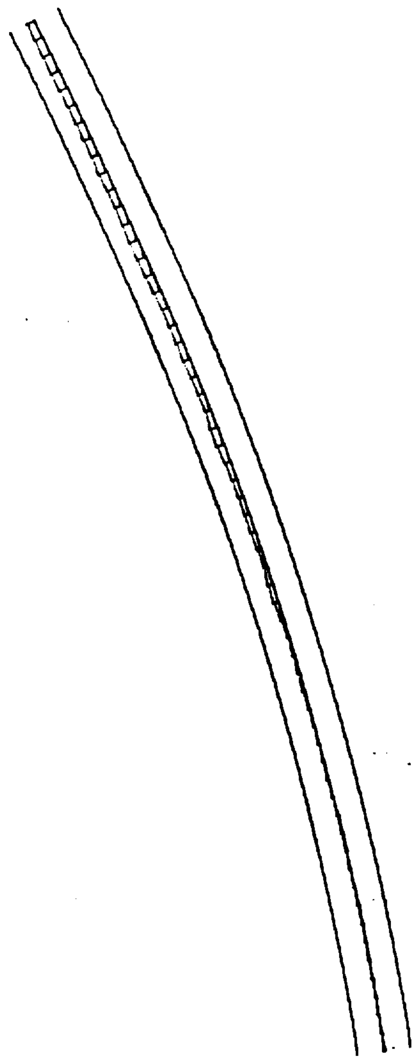

0.0100 **0.5000** +9deg PARABOLA	Z, X 4.9 : 1 07/26/1989 15.07 h (inch)

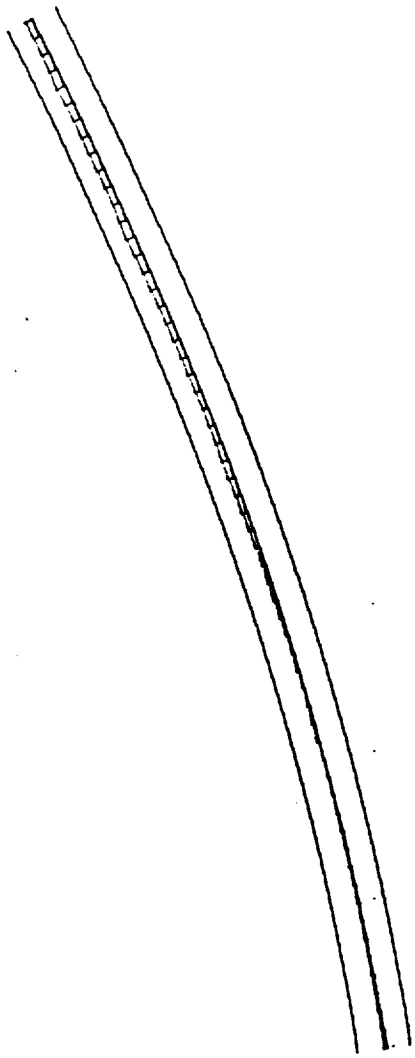

0.0100 0.5000 +11.25deg PARABOLA	Z, X 4.9 : 1 07/26/1989 15.12 h (inch)

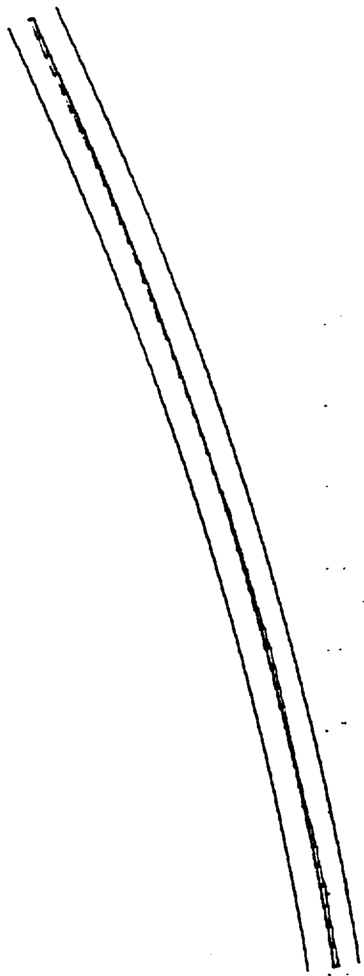

0.0100 0.5000 +16deg PARABOLA	Z, X 5.4 : 1 07/26/1989 15.20 h (inch)

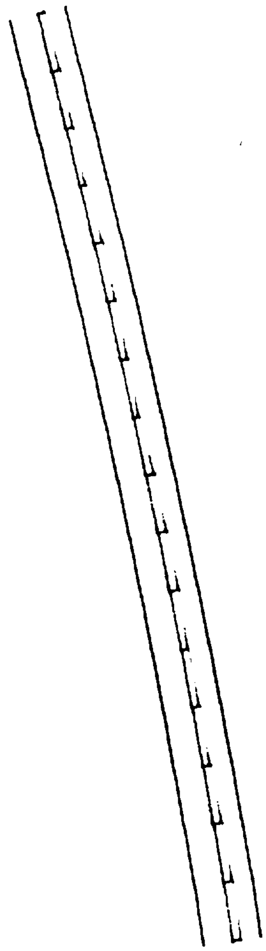

0.0100 0.5000 +30deg PARABOLA	Z, X 15.7 : 1 07/26/1989 15.25 h (inch)

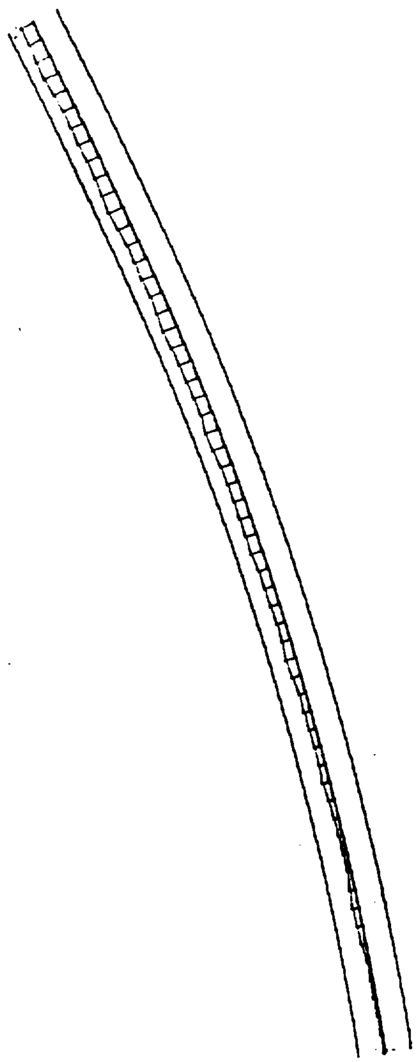

0.0100 **0.5000** -3deg PARABOLA	Z, X 4.9 : 1 07/26/1989 15.00 h (inch)

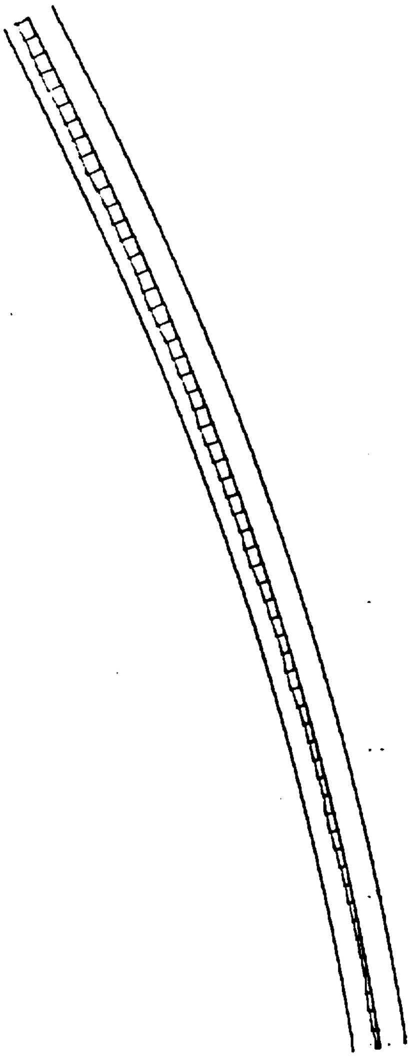

0.0100 0.5000 -6deg PARABOLA	Z, X 4.9 : 1 07/26/1989 15.05 h (inch)

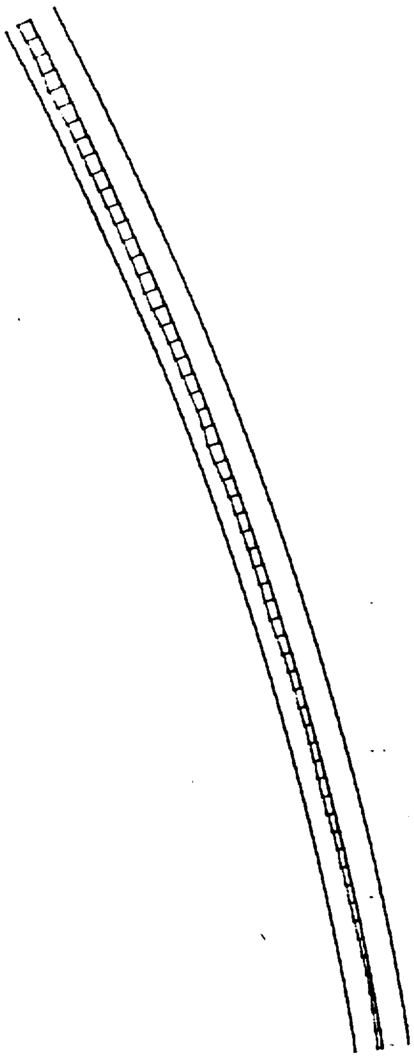

0.0100 0.5000 -9deg PARABOLA	Z, X 4.9 : 1 07/26/1989 15.10 h (inch)

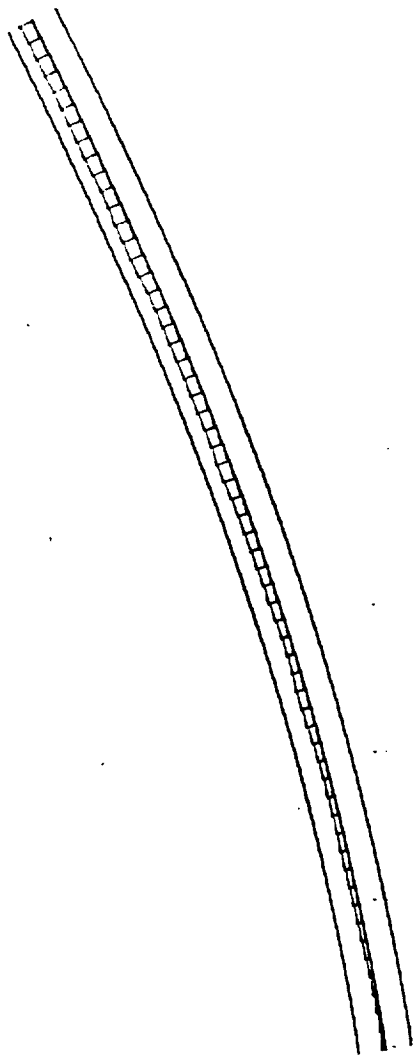

0.0100 0.5000 -11.25deg PARABOLA	Z, X 4.9 : 1 07/26/1989 15.14 h (inch)

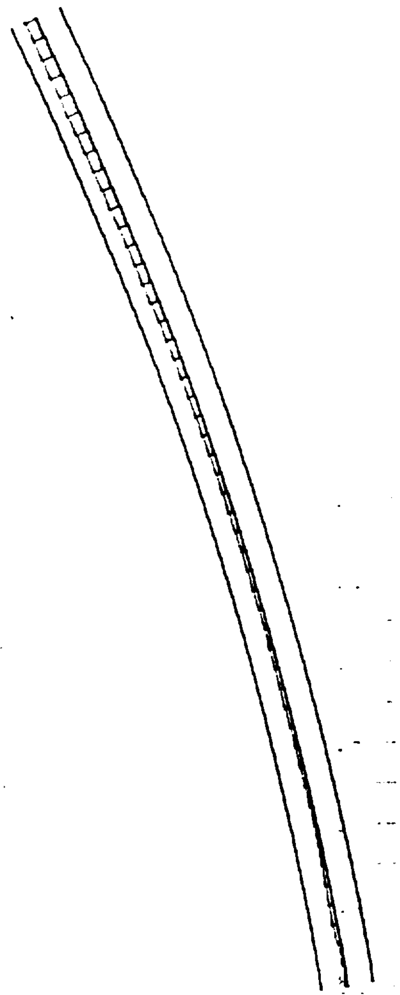

0.0100 0.5000 -16deg PARABOLA	Z, X 5.4 : 1 07/26/1989 15.22 h (inch)

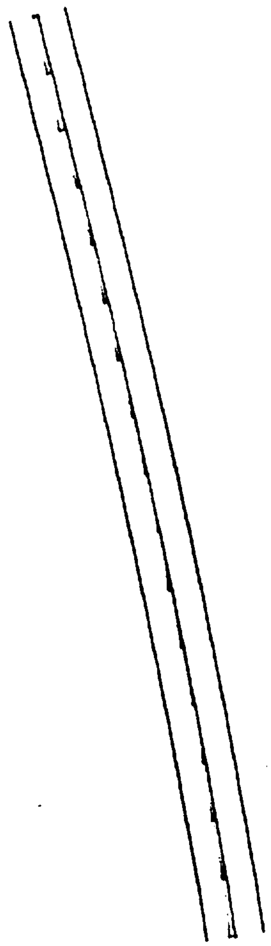

0.0100 0.5000 -30deg PARABOLA	Z, X 15.6 : 1 07/26/1989 15.27 h (inch)

intout of Comparison 07/26/1989 14.55 h

ne :APPEX

↖ 0°

	Nominal Coord. Z	Nominal Coord. X	Delta Coord. Z	Delta Coord. X	Total
1	-0.8712	11.7143	-0.0005	-0.0001	0.0005
2	-0.9463	12.2086	-0.0007	-0.0001	0.0007
3	-1.0244	12.7025	-0.0007	-0.0001	0.0007
4	-1.1056	13.1959	-0.0005	-0.0001	0.0005
5	-1.1897	13.6887	-0.0005	-0.0001	0.0005
6	-1.2768	14.1811	-0.0006	-0.0001	0.0006
7	-1.3669	14.6729	-0.0007	-0.0001	0.0008
8	-1.4600	15.1641	-0.0006	-0.0001	0.0006
9	-1.5560	15.6548	-0.0006	-0.0001	0.0006
10	-1.6549	16.1450	-0.0009	-0.0002	0.0010
11	-1.7568	16.6345	-0.0012	-0.0003	0.0012
12	-1.8616	17.1234	-0.0009	-0.0002	0.0009
13	-1.9693	17.6116	-0.0009	-0.0002	0.0009
14	-2.0798	18.0993	-0.0010	-0.0002	0.0010
15	-2.1932	18.5862	-0.0010	-0.0002	0.0011
16	-2.3095	19.0725	-0.0010	-0.0002	0.0011
17	-2.4286	19.5581	-0.0011	-0.0003	0.0012
18	-2.5505	20.0430	-0.0013	-0.0003	0.0013
19	-2.6753	20.5272	-0.0011	-0.0003	0.0012
20	-2.8028	21.0107	-0.0012	-0.0003	0.0013
21	-2.9330	21.4934	-0.0013	-0.0004	0.0014
22	-3.0660	21.9754	-0.0014	-0.0004	0.0015
23	-3.2018	22.4566	-0.0014	-0.0004	0.0014
24	-3.3403	22.9371	-0.0018	-0.0005	0.0019
25	-3.4814	23.4167	-0.0015	-0.0005	0.0016
26	-3.6253	23.8956	-0.0014	-0.0004	0.0014
27	-3.7718	24.3736	-0.0017	-0.0005	0.0018
28	-3.9209	24.8509	-0.0016	-0.0005	0.0016
29	-4.0727	25.3273	-0.0016	-0.0005	0.0017
30	-4.2271	25.8029	-0.0018	-0.0006	0.0019
31	-4.3841	26.2776	-0.0019	-0.0006	0.0020
32	-4.5436	26.7514	-0.0018	-0.0006	0.0019
33	-4.7057	27.2244	-0.0019	-0.0007	0.0020
34	-4.8703	27.6966	-0.0020	-0.0007	0.0022
35	-5.0375	28.1678	-0.0020	-0.0007	0.0022
36	-5.2071	28.6381	-0.0022	-0.0008	0.0023
37	-5.3792	29.1076	-0.0021	-0.0008	0.0022
38	-5.5538	29.5761	-0.0020	-0.0007	0.0021
39	-5.7308	30.0437	-0.0021	-0.0008	0.0022
40	-5.9102	30.5104	-0.0021	-0.0008	0.0023
41	-6.0920	30.9762	-0.0021	-0.0008	0.0023
42	-6.2762	31.4410	-0.0022	-0.0009	0.0024
43	-6.4628	31.9049	-0.0023	-0.0009	0.0025
44	-6.6517	32.3679	-0.0021	-0.0009	0.0023
45	-6.8429	32.8298	-0.0022	-0.0009	0.0023
46	-7.0365	33.2909	-0.0022	-0.0009	0.0024
47	-7.2323	33.7509	-0.0022	-0.0009	0.0024
48	-7.4304	34.2100	-0.0022	-0.0010	0.0024
49	-7.6307	34.6681	-0.0023	-0.0010	0.0025
50	-7.8333	35.1252	-0.0023	-0.0010	0.0026
51	-8.0381	35.5814	-0.0022	-0.0010	0.0024
52	-8.2450	36.0365	-0.0022	-0.0010	0.0024
53	-8.4542	36.4907	-0.0023	-0.0011	0.0025
[illegible]	[illegible]	[illegible]	-0.0022	-0.[illegible]	0.0024

55	-8.8788	37.3960	-0.0023	-0.0011	0.0025
56	-9.0944	37.8472	-0.0022	-0.0010	0.0024
57	-9.3120	38.2974	-0.0023	-0.0011	0.0025
58	-9.5317	38.7465	-0.0022	-0.0011	0.0024
59	-9.7535	39.1946	-0.0021	-0.0010	0.0023
60	-9.9773	39.6418	-0.0019	-0.0010	0.0022

intout of Comparison
ıme :+3deg

07/26/1989 14.57 h

	Nominal Coord. Z	Nominal Coord. X	Delta Coord. Z	Delta Coord. X	Total
1	-0.8712	11.7143	0.0007 ✓	0.0001	0.0007
2	-0.9463	12.2086	0.0005	0.0001	0.0005
3	-1.0244	12.7025	0.0004	0.0001	0.0004
4	-1.1056	13.1959	0.0004	0.0001	0.0004
5	-1.1897	13.6887	0.0004	0.0001	0.0004
6	-1.2768	14.1811	0.0004	0.0001	0.0004
7	-1.3669	14.6729	0.0001	0.0000	0.0001
8	-1.4600	15.1641	0.0001	0.0000	0.0001
9	-1.5560	15.6548	0.0003	0.0001	0.0003
10	-1.6549	16.1450	0.0003	0.0001	0.0003
11	-1.7568	16.6345	0.0002	0.0000	0.0002
12	-1.8616	17.1234	0.0002	0.0000	0.0002
13	-1.9693	17.6116	0.0002	0.0000	0.0002
14	-2.0798	18.0993	0.0001	0.0000	0.0001
15	-2.1932	18.5862	-0.0001	-0.0000	0.0001
16	-2.3095	19.0725	-0.0001	-0.0000	0.0001
17	-2.4286	19.5581	-0.0001	-0.0000	0.0001
18	-2.5505	20.0430	-0.0002	-0.0001	0.0002
19	-2.6753	20.5272	-0.0003	-0.0001	0.0003
20	-2.8028	21.0107	-0.0004	-0.0001	0.0004
21	-2.9330	21.4934	-0.0004	-0.0001	0.0004
22	-3.0660	21.9754	-0.0008	-0.0002	0.0008
23	-3.2018	22.4566	-0.0006	-0.0002	0.0006
24	-3.3403	22.9371	-0.0005	-0.0002	0.0006
25	-3.4814	23.4167	-0.0006	-0.0002	0.0006
26	-3.6253	23.8956	-0.0006	-0.0002	0.0006
27	-3.7718	24.3736	-0.0006	-0.0002	0.0006
28	-3.9209	24.8509	-0.0009	-0.0003	0.0009
29	-4.0727	25.3273	-0.0010	-0.0003	0.0011
30	-4.2271	25.8029	-0.0009	-0.0003	0.0009
31	-4.3841	26.2776	-0.0009	-0.0003	0.0009
32	-4.5436	26.7514	-0.0010	-0.0003	0.0010
33	-4.7057	27.2244	-0.0011	-0.0004	0.0011
34	-4.8703	27.6966	-0.0012	-0.0004	0.0012
35	-5.0375	28.1678	-0.0013	-0.0004	0.0013
36	-5.2071	28.6381	-0.0010	-0.0004	0.0011
37	-5.3792	29.1076	-0.0009	-0.0003	0.0010
38	-5.5538	29.5761	-0.0011	-0.0004	0.0011
39	-5.7308	30.0437	-0.0011	-0.0004	0.0011
40	-5.9102	30.5104	-0.0010	-0.0004	0.0011
41	-6.0920	30.9762	-0.0014	-0.0006	0.0015
42	-6.2762	31.4410	-0.0015	-0.0006	0.0016
43	-6.4628	31.9049	-0.0012	-0.0005	0.0013
44	-6.6517	32.3679	-0.0012	-0.0005	0.0013
45	-6.8429	32.8298	-0.0014	-0.0006	0.0015
46	-7.0365	33.2909	-0.0015	-0.0006	0.0017
47	-7.2323	33.7509	-0.0013	-0.0005	0.0014
48	-7.4304	34.2100	-0.0014	-0.0006	0.0015
49	-7.6307	34.6681	-0.0015	-0.0006	0.0016
50	-7.8333	35.1252	-0.0013	-0.0006	0.0014
51	-8.0381	35.5814	-0.0013	-0.0006	0.0014
52	-8.2450	36.0365	-0.0013	-0.0006	0.0014
53	-8.4542	36.4907	-0.0013	-0.0006	0.0014
54	-8.6654	36.9439	-0.0013	-0.0006	0.0013

55	-8.8788	37.3960	-0.0013	-0.0006	0.0014
56	-9.0944	37.8472	-0.0013	-0.0006	0.0015
57	-9.3120	38.2974	-0.0014	-0.0007	0.0015
58	-9.5317	38.7465	-0.0013	-0.0006	0.0014
59	-9.7535	39.1946	-0.0011	-0.0005	0.0012
60	-9.9773	39.6418	-0.0009	-0.0005	0.0010